# Elucidating the pathogenesis underlying bicuspid aortic valve disease using new disease models

Vera van de Pol

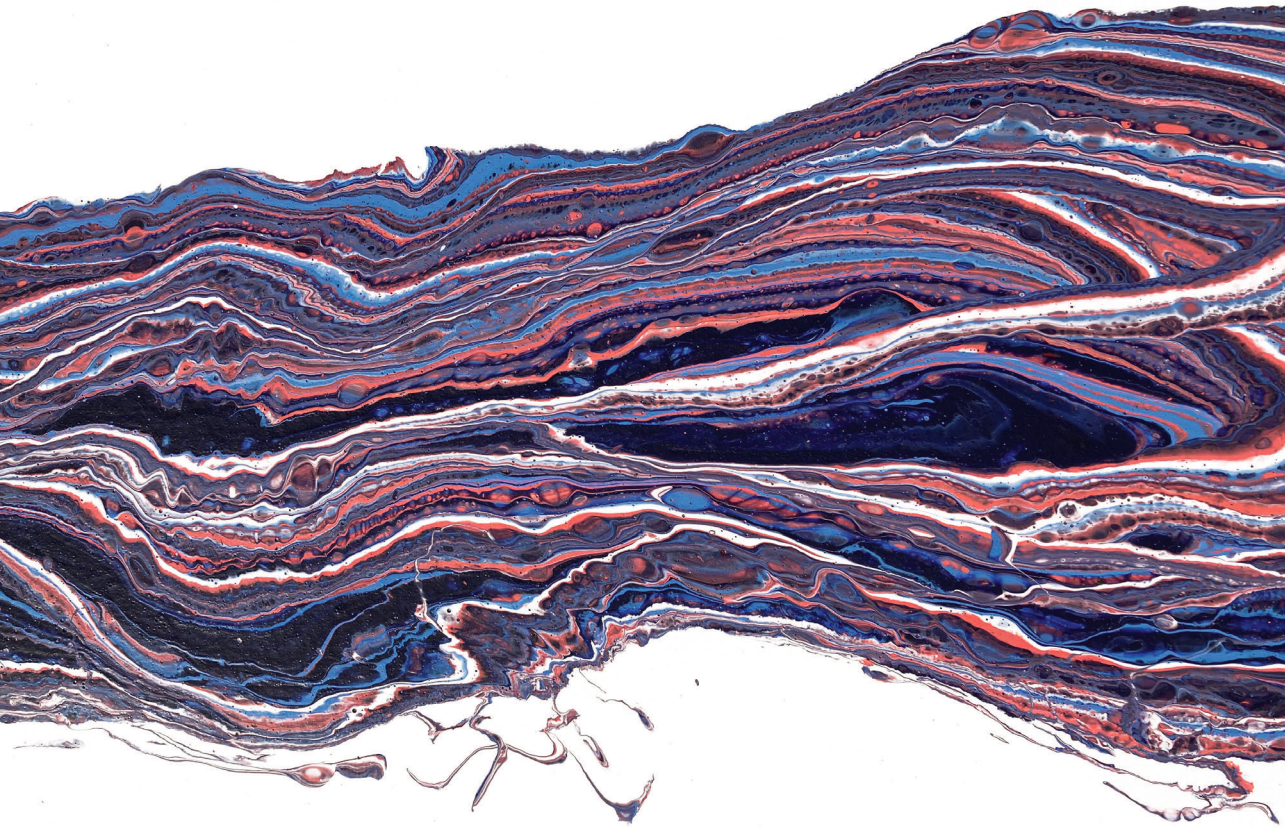

Elucidating the pathogenesis
underlying bicuspid aortic valve
disease using new disease models

**Vera van de Pol**

ISBN: 978-94-6416-919-5
Provided by thesis specialist Ridderprint, ridderprint.nl
Printing: Ridderprint
Layout and design: Erwin Timmerman, persoonlijkproefschrift.nl
Cover design: Vera van de Pol

Financial support by the Dutch Heart Foundation for the publication of this thesis is gratefully acknowledged. The research described in this thesis was supported by a grant of the Dutch Heart Foundation (2013T093).

# Elucidating the pathogenesis underlying bicuspid aortic valve disease using new disease models

**Proefschrift**

ter verkrijging van
de graad van doctor aan de Universiteit Leiden
op gezag van rector magnificus prof.dr.ir. H. Bijl,
volgens besluit van het college voor promoties
te verdedigen op woensdag 12 januari 2022
klokke 15:00 uur

door

**Vera van de Pol**

**Promotores:**
Prof. dr. M.J.T.H. Goumans
Prof. dr. M.C. de Ruiter

**Co-Promotor:**
Dr. K.B. Kurakula

**Promotiecommissie:**

| | |
|---|---|
| Prof. dr. B. Loeys | Universiteit van Antwerpen |
| Prof. dr. P.H.A. Quax | |
| Prof. dr. J.W. Roos-Hesselink | Erasmus Universiteit Rotterdam |
| Prof. dr. C.J.M. de Vries | Universiteit van Amsterdam |

## Table of contents

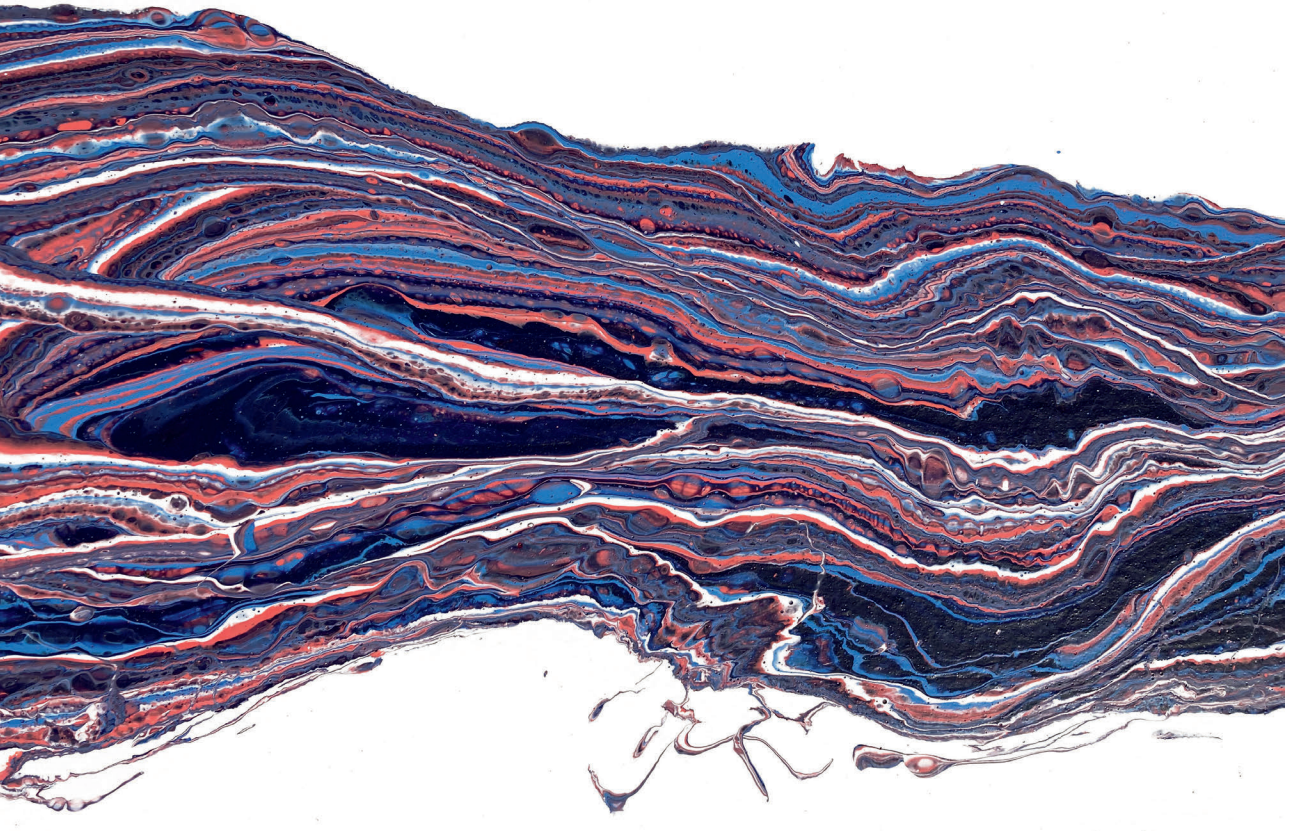

# Chapter 1

## General introduction

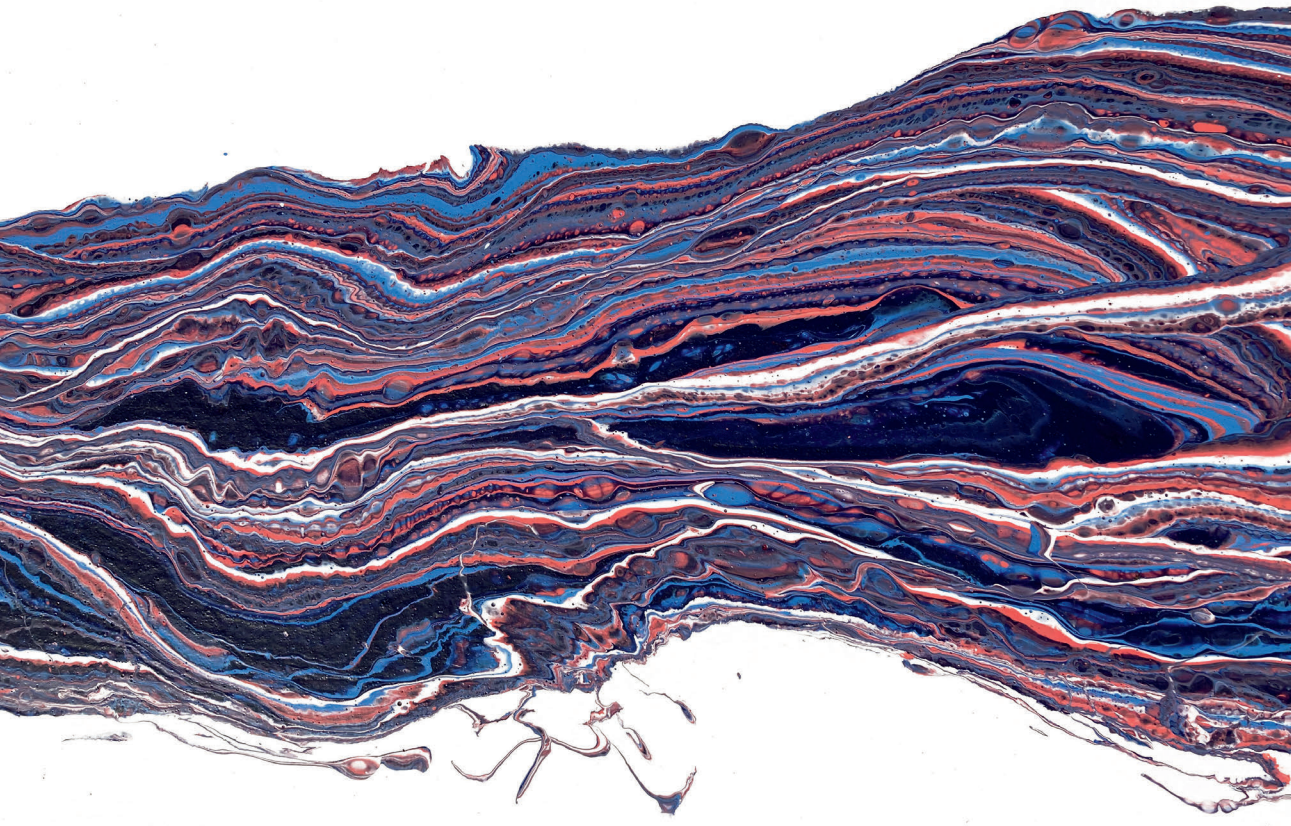

## Introduction

In 1-2% of the adult population two instead of the usual three aortic valve leaflets are present, a congenital cardiac defect known as a bicuspid aortic valve (BAV) [1]. Although a BAV can function normally, BAV patients develop aortic valve stenosis earlier in life and more often than people with a tricuspid aortic valve (TAV) [2]. Moreover, patients with a BAV have an increased risk of developing thoracic aortic aneurysm and rupture [3]. To date, there is no consensus on the etiology of this defect nor on the pathogenesis of the associated pathologies. This chapter will describe the different aspects involved in BAV and the associated aortic dilation and valvular stenosis. Let's start at the beginning: the embryonic development.



### Development of the aortic valves

The primitive heart tube consists of two layers. The outer layer of this tube is the myocardium which is covered on the inside by the endocardium. The myocardium secretes cardiac jelly, consisting of extracellular matrix, hyaluronic acid, glycosaminoglycans and proteoglycans, as a layer between the myocardium and the endocardium [4,5]. The myocardium of the outflow tract secretes increased amounts of cardiac jelly, forming local bulges. Moreover, it secretes bone morphogenetic protein 2 (BMP2) into the cardiac jelly, locally stimulating the endothelial cells (ECs) to undergo endothelial-to-mesenchymal transition (EndoMT) [5-9]. EndoMT is the transition of ECs with an epithelial phenotype into mesenchymal cells during which the cells gain a fibroblast-like phenotype [7]. The formed fibroblast-like cells migrate into the cardiac jelly. Once the bulges of cardiac jelly become populated with cells, they are defined as cardiac cushions [5,8,9]. Additional cells from both the neural crest lineage and the second heart field migrate into the cardiac cushions contributing to the developing cardiac valves [10-12]. After separation of the outflow tract into the aorta and pulmonary trunk, the cell-filled cardiac cushions mature into three separate valve leaflets in both the aortic and the pulmonary orifices. In the aorta, the three semilunar leaflets together form the TAV [6]. Cells in the mature valvular leaflets are referred to as valvular interstitial cells (VICs).

Considering these developmental processes, there are two theories describing how a BAV arises. The main accepted theory is that initially the three valve leaflets are properly formed but two of the three leaflets fuse later during development or postnatally [13,14]. A recent theory is that, instead of a fusion process, a BAV can also arise due to an incomplete separation of the non-coronary and right leaflet from one cardiac cushion [11]. Since ECs play an important role during the embryonic development of the aortic valves, it is not surprising that

disruption of normal EC function can have a major impact on aortic valve formation. This is, amongst others, demonstrated by multiple mouse models with an endothelial specific mutation that have been shown to develop a BAV, such as the *Tie2-cre*$^{+}$*Gata5*$^{fl/fl}$ mice [15,16].

**The aortic valves**

The aortic valve is situated in the aortic root between the left ventricle and the aorta [17].The three leaflets of the aortic valve are named according to the location of the coronary arteries. The two anteriorly situated leaflets are named by the origin of the right and left coronary arteries: the right and left coronary leaflets (R and L). The third, posterior leaflet is the non-coronary leaflet (N) because no coronary artery originates from the sinus of Valsalva connected to this leaflet in the majority of humans (Figure 1). Because of variation in the coronary position, the non-coronary leaflet is also known as the non-facing leaflet.

A BAV can have different morphologies. In the majority of patients (90%) a BAV has one large leaflet and one smaller leaflet, in which different morphologies are named after the TAV leaflets that seem to form the bigger leaflet: a RL BAV (80%), RN BAV (17%) or LN BAV (2%) (Figure 1) [18]. These morphologies can present with or without a raphe (the remnant of a fused commissure). In addition, "pure" bicuspid valves have two equally large leaflets in which the leaflet nomenclature derived from TAV anatomy cannot be applied.

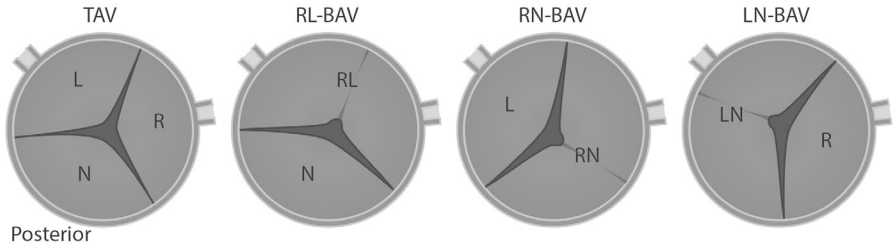


**Figure 1. Superior view TAV and BAV fusion patterns.** (R=right coronary leaflet, L=left coronary leaflet, N=non-coronary leaflet).

A valvular leaflet consists of three layers, the ventricularis, the spongiosa and the fibrosa (Figure 2) [19-21]. The ventricularis is the outer layer facing the ventricle and mainly consists of a dense network of elastin fibers. This sophisticated sheet of fibers provides elasticity to the leaflet [22]. The fibrosa is the outer layer of the leaflet facing the aortic lumen and mainly contains collagen fibers. These collagen fibers are oriented radially and thereby give the leaflet strength and

structure, while not impeding the longitudinal elasticity [23-25]. The spongiosa, the layer in between the ventricularis and fibrosa, is rich in glycosaminoglycans and proteoglycans with a meshwork of elastin weaving through it. Moreover, collagen fibers cross the layer to connect the elastin in the ventricularis to the collagen in the fibrosa. These components make the spongiosa a buffering layer that lubricates the shear between the outer layers, combining strength and elasticity into one structure [22-24]. These combined characteristics provide the motility and plasticity required by the valves to allow blood flow unidirectionally and without leakage back into the heart.



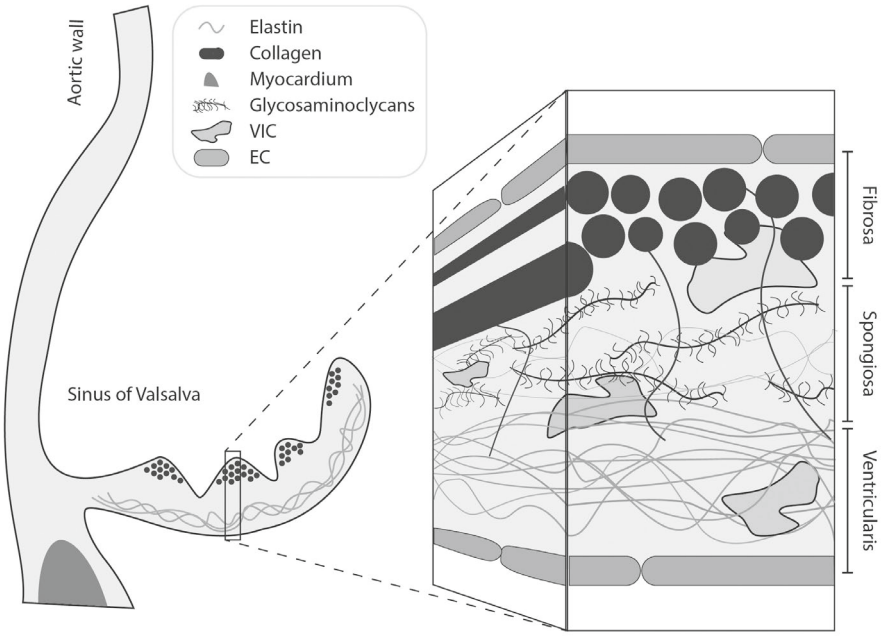


**Figure 2. Layers of the aortic valve.**

### Ossification and calcification processes in the aortic valve

BAV patients have a high risk of developing aortic valve stenosis, the final, most severe stage of calcific aortic valve disease (CAVD) [26-28]. CAVD is a pathology in which the aortic valve leaflets increase in thickness, lose their structural organization and form calcifying nodules on the aortic side of the leaflets, increasing the stiffness of the valves. Ultimately CAVD will limit the opening and closing of the valve leaflets, called valvular stenosis, which can lead to irreversible and life-threatening left ventricle hypertrophy [28]. It is estimated that 50% of the

CAVD patients have a BAV [29,30]. Furthermore, calcification of a BAV often requires surgery 5 to 10 years earlier than in case of a calcified TAV [31,32].

**Osteogenic calcificaton**

Endochondral ossification is the calcification process that normally occurs during development in which cartilage formation precedes bone formation [33]. In the aortic valve leaflet two processes have been described in the pathogenesis of valvular stenosis, differing in the location where the calcification occurs as well as the signaling pathway via which the calcification is initiated and sustained (Figure 3). One form of calcification that can be observed in the leaflets is osteogenic calcification [34]. Osteogenic calcification resembles endochondral ossification, because during both processes osteogenic genes such as BMP2, RUNX2, NOTCH1, COX2 and osteopontin are expressed [35-39]. In addition, cartilage formation has also been observed during osteogenic calcification Osteogenic calcification primarily occurs in the sinus wall and the aortic hinge points of the leaflets (intrinsic) and sporadically in the valve leaflets (nodular) [39].

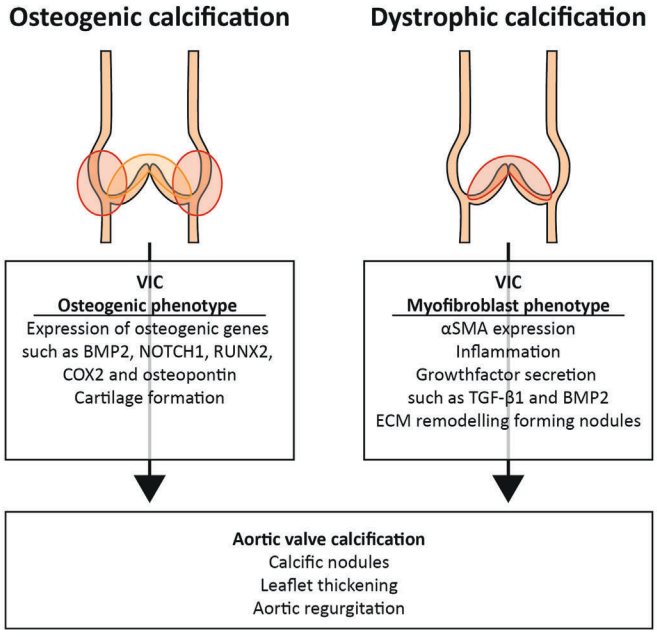


**Figure 3. Dystrophic and osteogenic calcification.** The orange and red shapes show where the calcification is most commonly located. In osteogenic differentiation the red shape indicates intrinsic calcification and the orange shape indicates nodular calcification.

It is hypothesized that osteogenic calcification is associated with repair of microfractures in the aortic valves and is therefore considered an abnormal healing response [39]. Interestingly, *NOTCH1* mutations in humans and *Notch*$^{+/-}$ in *Nos3*$^{-/-}$ mice can result in CAVD development as well as BAV formation, indicating the importance of osteogenic signaling pathways in both BAV and CAVD formation [40,41].

**Dystrophic calcification**

The other process of calcification observed in CAVD is dystrophic calcification. Whereas endochondral ossification in the valves is considered an abnormal healing response, dystrophic calcification is considered a pathological breakdown of tissue structures [42-44]. Mechanical stresses can trigger dystrophic calcification and result in endothelial activation and damage promoting lipid infiltration and inflammation [45,46]. Disturbed flow can also stimulate valvular ECs to secrete increased levels of inflammatory cytokines and pro-calcification signaling molecules [47]. The inflammation and lipid accumulation cause VICs to adopt a myofibroblast-like phenotype, demonstrated by the expression of $\alpha$-smooth muscle actin ($\alpha$SMA) [48]. The myofibroblast-like VICs secrete growth factors, such as transforming growth factor-β1 (TGF-β1) and BMP2, stimulating VICs to alter the extracellular fibronectin organization in the valves, initiating the local formation of nodules [49,50]. In addition, TGF-β1 and BMP2 stimulate alkaline phosphatase activity, apoptosis and increased matrix metalloproteinase 9 (MMP9) expression in these nodules, promoting the deposition of calcium minerals in nodules without a preceding phase of cartilage formation [42,43,48,50,51]. The aortic and ventricular side of the aortic valve leaflets experience different mechanical stresses, such as laminar shear stress at the ventricular side and oscillatory shear stress and pressure at the aortic side of the leaflets. The stresses at the aortic side have been hypothesized to be more detrimental, since the calcified nodules are mostly present at the aortic side of the valve leaflets [52-54].

To date, the understanding of mechanisms underlying the increased pathogenesis of valvular stenosis in BAV is hampered by the limited availability of tissue. When aortic valves do become available for research, they are isolated at the end-stage of disease and are therefore not suitable for studying the initial stages and progression of CAVD. *In vivo* studies to understand the pathology of CAVD in mice have been hampered by the difficulty of inducing calcification in the leaflets of wild-type mice [55-57]. The local (micro)environment of the aortic valve leaflets consists of multiple specific conditions that are known to have an impact on the calcification process, such as flow, tissue stiffness and the interactions between different cell types and between cells and the extracellular

matrix (ECM) [58-60]. The loss of this microenvironment *in vitro* makes CAVD a difficult disease to accurately model *in vitro* [55-57,61].

**The aorta**

The aortic wall consists of three layers: the intima, the media and the adventitia (Figure 4). The inner layer of the aortic wall, the intima, is composed of ECs on top of a small layer of connective tissue. The ECs sense the flow and biochemical composition of blood and communicate with both circulating cells in the blood and cells in the media. In a healthy vessel wall, the endothelium is a quiescent, tight layer that acts as a protective border for the underlying medial layer. The intima is separated from the media by the internal elastic lamina (IEL), a thick sheet composed of elastic fibers. The media is organized like lasagna, where layers of vascular smooth muscle cells (vSMCs) are alternating with elastic sheets called elastic lamellae. The vSMCs respond to signals from the ECs and secrete ECM required to maintain the elastic lamellae [62-65]. The composition of the ECM and elastic lamellae support the high pressure and pressure differences involved in the cardiac cycle. The elastic lamellae provide the compliance necessary to transiently expand when the left ventricle pumps blood into the aorta and buffer the blood volume [66]. This enables the conversion of a pulsatile flow into a continuous flow. The collagen fibers in the ECM limit the maximal expansion of the aorta, providing the stiffness to prevent overexpansion and damage [66]. Moreover, the ECM binds and stores many different growth factors and cytokines produced by the vSMCs, such as latent TGFβ and pro-MMPs [67,68]. Aside from an increased production of these proteins upon damage, the stored latent

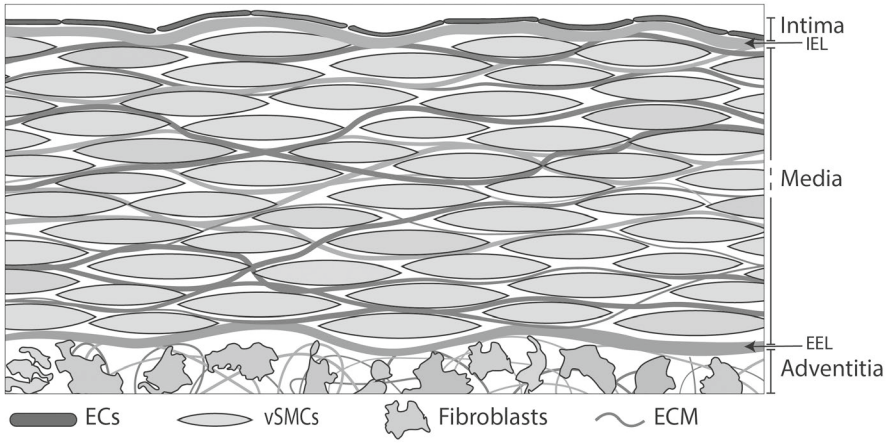


**Figure 4. Graphic representation of the different layers of the aorta.**

proteins are enzymatically cut and thereby activated when the ECM is degraded, enabling a quick response to the damage [69,70]. The media and adventitia are separated by the external elastic lamina (EEL). The adventitia consists of connective tissue mainly filled with blood vessels (the vasa vasorum). Its primary function is to supply the aortic media with nutrients and oxygen. Therefore, the adventitial vessels also protrude into the medial layer of the aorta.

**vSMCs in the aorta**



In a healthy aorta, the vSMCs in the media have a contractile phenotype, expressing proteins that are part of the contractile apparatus, such as $\alpha$SMA, smooth muscle myosin heavy chain (SM-MHC), h1-calponin and SM22$\alpha$ [71]. If the vessel wall is damaged, for example during surgery or due to hypertension, a healing response is required to restore proper functioning. This healing response is called vascular regeneration. Vascular regeneration is also responsible for continued maintenance of the vessel wall. It is initiated by a combination of many growth factors, such as TGFβ and PDGF-BB, secreted by platelets and vascular cells in areas of damage. The secretion of these growth factors is stimulated by, for example, loss of EC-vSMC contact, damage of ECM, contact with inflammatory cells, etc. [71-73]. These growth factors cause the contractile vSMCs to undergo a phenotypic switch and adopt a so-called synthetic phenotype (Figure 5). The synthetic vSMCs have a migratory, proliferative phenotype, decrease the expression of contractile proteins and increase expression of proteins such as collagen I, PDGF-A and ICAM-1. In addition, they start to secrete matrix degrading enzymes like extracellular matrix metalloproteases (MMPs). These MMPs break down the elastic lamellae allowing the vSMCs to migrate to the damaged site [74,75]. Synthetic vSMCs proliferate to replace lost vSMCs or to support remodeling vasculature in response to, for example, a high blood pressure.

To finish the vascular regeneration process, the synthetic vSMCs return to a contractile state. An important factor in inducing and maintaining this contractile phenotype is the transcription factor serum response factor (SRF) [73,76]. SRF recognizes and binds to CArG boxes, which are conserved cis-acting elements present in numerous promotor regions. Many promotors of genes that contribute to a contractile vSMC phenotype have multiple CArG boxes [71,77]. When SRF is bound to myocardin, a cardiac and SMC specific transcriptional co-activator, SRF induces targeted expression of the contractile genes in vSMCs [78].

Not only myocardin but also the scaffold protein four-and-a-half LIM-domain (FHL2) is highly involved in vSMC phenotypic switching. The scaffolding function of FHL2 allows it to bind to many proteins, regulating signaling cascades such as inflammation and proliferation. FHL2 has been shown to stimulate or

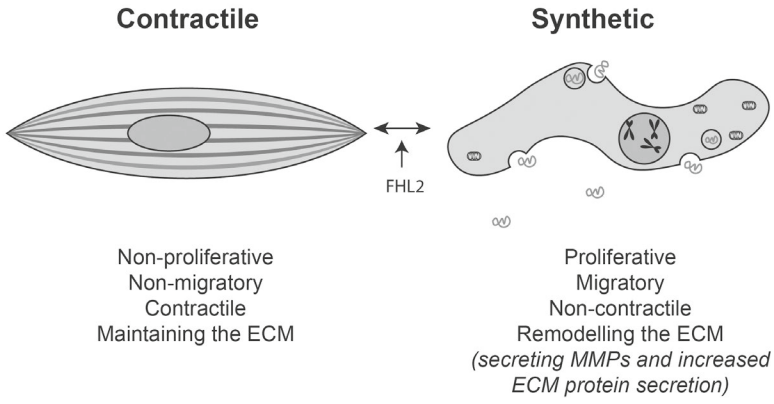


**Figure 5. vSMC phenotypes.**

inhibit a contractile vSMC phenotype, depending on the local microenvironment [79]. Intervention studies have shown the involvement of FHL2 in vascular remodeling, however its role in human aortic remodeling and aortic aneurysm development have not yet been studied [80,81]. Although FHL2 also impacts the calcification process as indicated by the osteopenia in FHL2$^{-/-}$ mice, its role in cardiovascular calcification is unknown [82].

**ECs in the aorta**

Although the media forms the bulk of the aortic tissue, the covering endothelium plays an important part in maintaining a healthy vessel wall homeostasis and a contractile vSMC phenotype [83]. ECs are able to sense differences in shear stress via mechanosensors and by movement of the primary cilium, a structure protruding from the membrane through the glycocalyx at the apical side of the EC into the vessel lumen [84,85]. Based on changes in blood flow and composition, the ECs orchestrate vascular homeostasis by appropriate signaling to other cell types such as vSMCs and mononuclear cells. For example, ECs can produce nitric oxide (NO) to locally regulate blood flow. NO diffuses through the plasma membrane into the underlying vSMCs, binds guanylyl cyclase resulting in vSMC relaxation and thereby a decrease in blood pressure [86-88]. In resting homeostasis, TGFβ and NO signaling by the ECs stimulate vSMC to adopt and maintain a contractile phenotype. Not only do ECs play a direct role in vSMC function, the endothelium acts as an active, impermeable protective border for the underlying media, selectively transporting molecules such as glucose into the media. In addition, ECs are crucial in processes such as inflammation, wound healing and atherogenesis/vasculogenesis.

**Aortic dilation in BAV**

Patients with a BAV have a higher risk of ascending aortic dilation than the general population. Estimates of ascending aortic dilation in BAV range from 9% to a staggering 79% [89-92]. Because aortic dilation could lead to a life-threatening rupture of the aorta, BAV patients require regular clinical check-ups to monitor the increase in the aortic diameter [93]. To prevent rupture, the aorta is surgically replaced if the diameter exceeds 55 mm or when the dilation rate becomes too high [93]. Ascending aortic dilation is caused by a loss of structural integrity due to medial degeneration. Medial degeneration is a pathology involving the phenotypic switching of vSMCs towards the synthetic phenotype as well as fragmentation of the elastic lamellae and breakdown of the ECM [94]. One of the underlying signaling cascades described in aortic dilation is the TGFβ pathway. TGFβ activates downstream signaling via two main pathways: the canonical- and non-canonical pathway [95]. Canonical signaling occurs by phosphorylation of SMAD proteins that translocate into the nucleus and bind DNA, whereas non-canonical signaling occurs via SMAD-independent signaling pathways, such as activation of PI3K/AKT, JNK, and ERK. Non-canonical PI3K/AKT signaling stimulates a contractile signaling whereas non-canonical signaling via ERK promotes a synthetic phenotype [96-98]. The effect of signaling via canonical cascades on different cellular processes is a more intricate balance, able to stimulate and inhibit vSMC phenotypic switching. Therefore, it can be difficult to predict the effect of a change (such as a mutation) in this canonical signaling [98].

Despite the known role of ECs in the developing aortic valves and the vascular homeostasis, the prominent medial degeneration in aortic dilation has been the focus of the majority of BAV research. Therefore, little research so far has focussed on the role of ECs in aortic dilation in BAV patients and a possible role for ECs in aortic aneurysm formation is only recently hypothesised. The study towards the characteristics of aortic ECs is hampered by the difficulty of obtaining "healthy" aortic tissue samples from both patients with a BAV and people with a TAV. The discovery of endothelial-colony-forming-cells (ECFCs) has facilitated research towards EC function in many different diseases such as diabetes, arthritis and pulmonary arterial hypertension [99-102]. ECFCs are a type of endothelial progenitor cells that can be isolated from peripheral blood [99]. *In vitro* they mimic the characteristics of ECs and they are able to integrate into the vasculature *in vivo* and contribute to vascular regeneration [99,103].

**Table 1.** Genes associated with BAV

| Gene | Human/ mouse |
|---|---|
| *ACTA2* [114] | Human |
| *AXIN1/PDIA2* [115] | Human |
| *EGFR* [116] | Human |
| *ELN* [117] | Human |
| *ENG* [115,116] | Human |
| *FBN1* [118,119] | Human |
| *FLNA* [120] | Human |
| *GATA4* [121] | Human |
| *GATA5* [15,122] | Both |
| *GATA6* [123,124] | Both |
| *Hoxa1* [125] | Mouse |
| *Hoxa3 * Fgf8* [126] | Mouse |
| *LOX* [127] | Human |
| *MAT2A* [128] | Human |
| *Nkx2.5 * Frs2* [129] | Mouse |
| *Nkx2.5* [130] | Mouse |
| *Nos3* [16] | Mouse |
| *NOTCH1* [108,131] | Both |
| *NR2F2* [132] | Human |
| *ROBO4* [133] | Both |
| *SMAD3* [134,135] | Human |
| *SMAD6* [136] | Human |
| *TBX20* [104] | Human |
| *TGFB2* [137] | Human |
| *TGFBR1* [138] | Human |
| *TGFBR2* [139] | Human |
| *TIMP1* [140] | Human |
| *TIMP3* [140] | Human |
| *Tbx1* [141] | Mouse |
| *45 × 0 karyotype* [142] | Human |

**Genetics involved in BAV**

To date, it is unclear what triggers the vessel wall structures to become compromised or why valvular calcification occurs earlier and more often in people with a BAV compared to a TAV. Furthermore, BAV and its associated pathologies present differently between different patients. Little is known about the cause of this variation between BAV patients, hampering accurate and patient specific prognoses and treatment.

Studying familial BAV gave the first insights into the genes contributing to BAV formation. Moreover, mutations found in patients with a hereditary BAV support the genetic hypothesis. Currently, mutations in over 20 genes have been directly or indirectly linked to BAV, amongst which are SMAD6, NOTCH1, GATA5 and TBX20 [40,104-109]. In addition, there are multiple mutations known that cause a BAV in mice [15,16,110]. However, only a hand full of mutations observed in BAV patients, is causally related to BAV in mice. Table 1 shows an overview of mutations associated with BAV.

One of the underlying signaling cascades described in aortic dilation for which multiple genes have been found mutated is the TGFβ pathway (Table 2) [111,112]. Furthermore, not only mutations but also changes in the expression of the canonical signaling protein SMAD3 has been associated with aortic dilation [113].

Also for CAVD and BAV mutations have been found that could help explain why aortic valve stenosis occurs earlier and more often in patients with a BAV. For example, mutations in the *NOTCH1* gene highly correlate to BAV and CAVD

[156]. NOTCH1 represses protein expression of BMP2, a potent osteogenic factor. Therefore, mutations in *NOTCH1* can impact the BMP2 signaling pathway and thereby dysregulate the calcification process [157]. *NOTCH1* mutations are present in approximately 6% of the BAV patients and could explain why some BAV patients are more prone to developing aortic valve stenosis [158,159]. However, most of the mutations are found in isolated BAV patients, only a few families have been identified in which *NOTCH1* is mutated [156]. In addition, for many of the mutations found in BAV patients the impact on the disease processes remain unknown. So far, in the majority of BAV patients no mutations are found [160].



**Table 2.** TGFβ family members in which mutations have been associated to aortic aneurysms

| Gene | Protein | BAV |
|---|---|---|
| *LTBP1* [143] | Latent TGF-β binding protein 1 | No |
| *LTBP3* [144] | Latent TGF-β binding protein 3 | No |
| *SMAD2* [145,146] | SMAD2 | No |
| *SMAD3* [134,135,147] | SMAD3 | Yes |
| *SMAD4* [148-150] | SMAD4 | No |
| *SMAD6* [136] | SMAD6 | Yes |
| *TGFB2* [137,151,152] | TGF-β2 | Yes |
| *TGFB3* [153] | TGF-β3 | No |
| *TGFBR1* [154,155] | TGF-β receptor type I | Yes |
| *TGFBR2* [154,155] | TGF-β receptor type II | Yes |

**Flow in BAV**

Not only genetics, but also flow is involved in BAV pathology. The altered leaflet morphology in a BAV results in a disturbed blood flow in the aorta and over the valvular leaflets [161-164]. In the past decade, the impact of altered flow in the BAV aorta has become an important research topic. Different types of altered flow have been described in BAV, such as a helical flow, a jet flow directed towards the outer curve of the aortic wall and an oscillatory flow on the inner curve of the vessel [164,165]. While a laminar blood flow is atheroprotective, oscillatory flow induces EC activation and is pro-atherogenic [166-169]. Illustrating the role of flow and the detrimental effect of oscillatory flow on ECs and the underlying media, are the vascular branchpoints, well known for the initiation of atherosclerotic plaques [170]. Not only oscillatory flow, but also changes in the vascular homeostasis such as damage, altered flow, inflammation and blood composition, can activate the ECs. The activated endothelium stimulates a response to the changed homeostasis. Upon activation, ECs start to secrete

pro-inflammatory cytokines, chemokines, increase their proliferation rate and can undergo EndoMT. [171-174]. The activated endothelium enables mononuclear cells to adhere, role and infiltrate the vessel wall [175]. In the meantime, the activated endothelium no longer supports a contractile phenotype of the underlying vSMCs, enabling the vSMCs to switch phenotype in response to the changes in homeostasis [176].

The observation that flow influences the aortic wall directly or indirectly has resulted in the flow hypothesis which postulates that altered blood flow around the BAV and in the aorta also causes the calcification of the aortic valves and the aortic dilation in BAV patients [161]. Multiple correlations between leaflet morphology, flow and aortic dilation have been described: aortic root (type 1) and distal ascending (type 3) aortic dilation are more prevalent in RN-BAV, whereas dilation in the middle of the ascending aorta (type 2) is more common in RL-BAV [177-181]. Additionally, altered shear stress experienced by the valvular leaflets is implicated in the etiology of CAVD in BAV patients [182,183]. Incongruently, several studies have reported progressive aortic dilation even after surgical replacement of the BAV [184,185].

## Scope of this thesis

The general aim of this thesis is to study the underlying pathogenesis of aortic valve calcification and aortic dilation in BAV patients and increase understanding of the role of ECs in these processes.

Although ECs play a major role in the homeostasis of the cardiovascular system, the role of ECs has not been a priority in BAV research. Therefore, the second chapter of this thesis is a literature review where the current knowledge on the role of endothelial cells in BAV pathology is discussed. To gain more insight into the functioning of ECs in BAV patients, chapters 3 and 4 are focused on the role of flow on ECs in BAV aorta (chapter 3) and the endothelial characteristics of BAV patients *in vitro* using ECFCs (chapter 4). As EndoMT is proposed to play a role in BAV pathogenesis, chapter 5 is aimed at gaining more insight into the role EndoMT plays in aortic ECs and vascular calcification.

To be able to understand valvular calcification, proper *in vitro*, *in vivo* and *ex vivo* models are imperative. Therefore, in chapter 6 we characterized and compared two different valvular calcification methods using *in vitro* and *ex vivo* culture. One of the methods developed in chapter 6 is used in chapter 7 to investigate the role of FHL2 in valvular calcification.

Since FHL2 also plays a major role in vSMC differentiation, a study investigating the role of FHL2 in aortic dilation is described in chapter 8. Finally, since inflammation in BAV aortic dilation is decreased compared to TAV aortic dilation

and FHL2 not only plays a role in vSMC phenotypic switching but also in inflammation, the role of FHL2 in inflammation and vSMC phenotypic switching is studied in chapter 9. In chapter 10 the results of this thesis are summarized and discussed.

## References


1. Larson, EW, et al. (1984). Risk factors for aortic dissection: A necropsy study of 161 cases. *Am J Cardiol*
2. Roberts, WC, et al. (2005). Frequency by decades of unicuspid, bicuspid, and tricuspid aortic valves in adults having isolated aortic valve replacement for aortic stenosis, with or without associated aortic regurgitation.
3. Michelena, HI, et al. (2011). Incidence of aortic complications in patients with bicuspid aortic valves. *Jama*
4. Manasek, FJ. (1968). Embryonic development of the heart. I. A light and electron microscopic study of myocardial development in the early chick embryo.
5. Sugi, Y, et al. (2004). Bone morphogenetic protein-2 can mediate myocardial regulation of atrioventricular cushion mesenchymal cell formation in mice. *Developmental Biology*
6. Wirrig, EE, et al. (2014). Conserved transcriptional regulatory mechanisms in aortic valve development and disease.
7. Kovacic, JC, et al. (2012). Epithelial-to-mesenchymal and endothelial-to-mesenchymal transition: From cardiovascular development to disease. *Circulation*
8. Eisenberg, LM, et al. (1995). Molecular regulation of atrioventricular valvuloseptal morphogenesis.
9. Kisanuki, YY, et al. (2001). Tie2-cre transgenic mice: A new model for endothelial cell-lineage analysis in vivo. *Develop Biol*
10. Eley, L, et al. (2018). A novel source of arterial valve cells linked to bicuspid aortic valve without raphe in mice. *eLife*
11. Peterson, JC, et al. (2018). Bicuspid aortic valve formation: Nos3 mutation leads to abnormal lineage patterning of neural crest cells and the second heart field. *Dis Model Mech*
12. Nakamura, T, et al. (2006). Neural crest cells retain multipotential characteristics in the developing valves and label the cardiac conduction system. *Circ Res*
13. Fernández, B, et al. (2009). Bicuspid aortic valves with different spatial orientations of the leaflets are distinct etiological entities. *Journal of the American College of Cardiology*
14. Théron, A, et al. (2016). Krox20 heterozygous mice: A model of aortic regurgitation associated with decreased expression of fibrillar collagen genes. *Archives of Cardiovascular Diseases*
15. Laforest, B, et al. (2011). Loss of gata5 in mice leads to bicuspid aortic valve. *J Clin Invest*
16. Lee, TC, et al. (2000). Abnormal aortic valve development in mice lacking endothelial nitric oxide synthase. *Circ*
17. Loukas, M, et al. (2014). The anatomy of the aortic root. *Clin Anat*

18. Sievers, HH, et al. (2014). Toward individualized management of the ascending aorta in bicuspid aortic valve surgery: The role of valve phenotype in 1362 patients. *J Thorac Cardiovasc Surg*
19. Schoen, FJ. (1997). Aortic valve structure-function correlations: Role of elastic fibers no longer a stretch of the imagination. *J Heart Valve Dis*
20. Schoen, FJ. (2008). Evolving concepts of cardiac valve dynamics: The continuum of development, functional structure, pathobiology, and tissue engineering. *Circulation*
21. Sauren, AA, et al. (1980). Aortic valve histology and its relation with mechanics-preliminary report. *J Biomech*
22. Buchanan, RM, et al. (2014). Interlayer micromechanics of the aortic heart valve leaflet. *Biomech mod mechanobiol*
23. Sacks, MS, et al. (2009). On the biomechanics of heart valve function. *Journal of biomechanics*
24. Stella, JA, et al. (2007). On the biaxial mechanical properties of the layers of the aortic valve leaflet. *J Biomech Eng*
25. Chen, J-H, et al. (2011). Cell–matrix interactions in the pathobiology of calcific aortic valve disease. *Circulation Research*
26. Li, Y, et al. (2017). Prevalence and complications of bicuspid aortic valve in chinese according to echocardiographic database. *Am J Cardiol*
27. Wang, Y, et al. (2020). Distribution patterns of valvular and vascular complications in bicuspid aortic valve. *Int Heart J*
28. Towler, DA. (2013). Molecular and cellular aspects of calcific aortic valve disease. *Circulation research*
29. Sabet, HY, et al. (1999). Congenitally bicuspid aortic valves: A surgical pathology study of 542 cases (1991 through 1996) and a literature review of 2,715 additional cases. *Mayo Clinic Proceedings*
30. Subramanian, R, et al. (1984). Surgical pathology of pure aortic stenosis: A study of 374 cases. *Mayo Clinic Proceedings*
31. Mautner, GC, et al. (1993). Clinical factors useful in predicting aortic valve structure in patients >40 years of age with isolated valvular aortic stenosis. *The American Journal of Cardiology*
32. Cozijnsen, L, et al. (2019). Differences at surgery between patients with bicuspid and tricuspid aortic valves. *Netherlands heart journal*
33. Dutta, P, et al. (2018). Calcific aortic valve disease: A developmental biology perspective. *Curr Cardiol Rep*
34. Gomez-Stallons, MV, et al. (2019). Calcification and extracellular matrix dysregulation in human postmortem and surgical aortic valves. *Heart*
35. Wirrig, EE, et al. (2011). Differential expression of cartilage and bone-related proteins in pediatric and adult diseased aortic valves. *Journal of molecular and cellular cardiology*

36. Passmore, M, et al. (2015). Osteopontin alters endothelial and valvular interstitial cell behaviour in calcific aortic valve stenosis through hmgb1 regulation. *Eur J Cardiothorac Surg*
37. Wirrig, EE, et al. (2015). Cox2 inhibition reduces aortic valve calcification in vivo. *Arterioscl thromb vasc biol*
38. Acharya, A, et al. (2011). Inhibitory role of notch1 in calcific aortic valve disease. *PloS one*
39. Mohler, ER, et al. (2001). Bone formation and inflammation in cardiac valves.
40. Garg, V, et al. (2005). Mutations in notch1 cause aortic valve disease. *Nature*
41. Bosse, K, et al.(2013).Endothelial nitric oxide signaling regulates notch1 in aortic valve disease.*J mol cell cardiol*
42. Otto, CM, et al. (1994). Characterization of the early lesion of 'degenerative' valvular aortic stenosis. Histological and immunohistochemical studies. *Circulation*
43. Jian, B, et al. (2003). Progression of aortic valve stenosis: Tgf-beta1 is present in calcified aortic valve cusps and promotes aortic valve interstitial cell calcification via apoptosis. *Ann Thorac Surg*
44. Cote, N, et al. (2013). Inflammation is associated with the remodeling of calcific aortic valve disease. *Inflamm*
45. Lee, YS, et al. (1997). Endothelial alterations and senile calcific aortic stenosis: An electron microscopic observation. *Proc Natl Sci Counc Repub China B*
46. Constantinescu, E, et al. (2002). An ex vivo model to study the monocyte-endothelial cell interaction in the prelesional stage of experimentally-induced atherogenesis in hamster. *J Submicrosc Cytol Pathol*
47. Fernández Esmerats, J, et al. (2016). Shear-sensitive genes in aortic valve endothelium. *Antiox redox signal*
48. Rutkovskiy, A, et al. (2017). Valve interstitial cells: The key to understanding the pathophysiology of heart valve calcification. *J Am Heart Assoc*
49. Walker, GA, et al. (2004). Valvular myofibroblast activation by transforming growth factor-beta: Implications for pathological extracellular matrix remodeling in heart valve disease. *Circ Res*
50. Osman, L, et al. (2006). Role of human valve interstitial cells in valve calcification and their response to atorvastatin. *Circulation*
51. Clark-Greuel, JN, et al. (2007). Transforming growth factor-beta1 mechanisms in aortic valve calcification: Increased alkaline phosphatase and related events. *Ann Thorac Surg*
52. Peiffer, V, et al. (2013). Does low and oscillatory wall shear stress correlate spatially with early atherosclerosis? A systematic review. *Cardiovascular research*

53. Simmons, CA, et al. (2005). Spatial heterogeneity of endothelial phenotypes correlates with side-specific vulnerability to calcification in normal porcine aortic valves. *Circ Res*
54. Gould, ST, et al. (2013). Hemodynamic and cellular response feedback in calcific aortic valve disease. *Circ Res*
55. van der Valk, DC, et al. (2018). Engineering a 3d-bioprinted model of human heart valve disease using nanoindentation-based biomechanics. *Nanomaterials (Basel)*
56. van der Ven, CFT, et al. (2017). In vitro 3d model and mirna drug delivery to target calcific aortic valve disease. *Clinical science (London, England : 1979)*
57. Halevi, R, et al. (2018). A new growth model for aortic valve calcification. *J Biomech Eng*
58. Balachandran, K, et al. (2011). Hemodynamics and mechanobiology of aortic valve inflammation and calcification. *Int J Inflam*
59. Yip, CY, et al. (2009). Calcification by valve interstitial cells is regulated by the stiffness of the extracellular matrix. *Arterioscler Thromb Vasc Biol*
60. Butcher, JT, et al. (2006). Valvular endothelial cells regulate the phenotype of interstitial cells in co-culture: Effects of steady shear stress. *Tissue Eng*
61. Bowler, MA, et al. (2015). In vitro models of aortic valve calcification: Solidifying a system. *Cardiovascular pathology : the official journal of the Society for Cardiovascular Pathology*
62. Shin, WS, et al. (1996). Nitric oxide attenuates vascular smooth muscle cell activation by interferon-gamma. The role of constitutive nf-kappa b activity. *J Biol Chem*
63. Rateri, DL, et al. (2011). Endothelial cell-specific deficiency of ang ii type 1a receptors attenuates ang ii-induced ascending aortic aneurysms in ldl receptor-/- mice. *Circ Res*
64. Lilly, B. (2014). We have contact: Endothelial cell-smooth muscle cell interactions. *Physiology (Bethesda)*
65. Lin, CH, et al. (2014). Notch signaling governs phenotypic modulation of smooth muscle cells. *Vascul Pharmacol*
66. Belz, GG. (1995). Elastic properties and windkessel function of the human aorta. *Cardiovasc Drugs Ther*
67. Horiguchi, M, et al. (2012). Matrix control of transforming growth factor-β function. *Journal of biochemistry*
68. Jacob, MP. (2003). Extracellular matrix remodeling and matrix metalloproteinases in the vascular wall during aging and in pathological conditions. *Biomed Pharmacother*
69. Xu, J, et al. (2014). Vascular wall extracellular matrix proteins and vascular diseases. *Biochit biophys acta*
70. Majesky, MW, et al. (1991). Production of transforming growth factor beta 1 during repair of arterial injury. *J Clin Invest*

71. Owens, GK, et al. (2004). Molecular regulation of vascular smooth muscle cell differentiation in development and disease.
72. Campbell, JH, et al. (1986). Endothelial cell influences on vascular smooth muscle phenotype. *Annu Rev Physiol*
73. Owens, GK. (2007). Molecular control of vascular smooth muscle cell differentiation and phenotypic plasticity. *Novartis Found Symp*
74. Bendeck, MP, et al. (1996). Inhibition of matrix metalloproteinase activity inhibits smooth muscle cell migration but not neointimal thickening after arterial injury. *Circ Res*
75. Bendeck, MP, et al. (1994). Smooth muscle cell migration and matrix metalloproteinase expression after arterial injury in the rat. *Circ Res*
76. Mack, CP. (2011). Signaling mechanisms that regulate smooth muscle cell differentiation.
77. Sobue, K, et al. (1999). Expressional regulation of smooth muscle cell-specific genes in association with phenotypic modulation. *Mol Cell Biochem*
78. Chen, J, et al. (2002). Myocardin: A component of a molecular switch for smooth muscle differentiation. *J Mol Cell Cardiol*
79. Tran, MK, et al. (2016). Protein-protein interactions of the lim-only protein fhl2 and functional implication of the interactions relevant in cardiovascular disease. *Biochim Biophys Acta*
80. Kurakula, K, et al. (2014). The lim-only protein fhl2 reduces vascular lesion formation involving inhibition of proliferation and migration of smooth muscle cells. *PLoS One*
81. Neuman, NA, et al. (2009). The four-and-a-half lim domain protein 2 regulates vascular smooth muscle phenotype and vascular tone. *J Biol Chem*
82. Gunther, T, et al.(2005).Fhl2 deficiency results in osteopenia due to decreased activity of osteoblasts. *Embo j*
83. van Buul-Wortelboer, MF, et al. (1986). Reconstitution of the vascular wall in vitro: A novel model to study interactions between endothelial and smooth muscle cells. *Experimental Cell Research*
84. Luu, VZ, et al. (2018). Role of endothelial primary cilia as fluid mechanosensors on vascular health. *Atheroscl*
85. Givens, C, et al. (2016). Endothelial mechanosignaling: Does one sensor fit all? *Antioxid Redox Signal*
86. Furchgott, RF, et al. (1980). The obligatory role of endothelial cells in the relaxation of arterial smooth muscle by acetylcholine. *Nature*
87. Palmer, RMJ, et al. (1987). Nitric oxide release accounts for the biological activity of endothelium-derived relaxing factor. *Nature*
88. Rubanyi, GM, et al. (1986). Flow-induced release of endothelium-derived relaxing factor.

89. Tzemos, N, et al. (2008). Outcomes in adults with bicuspid aortic valves. *JAMA*
90. Michelena, HI, et al. (2008). Natural history of asymptomatic patients with normally functioning or minimally dysfunctional bicuspid aortic valve in the community. *Circulation*
91. Hahn, RT, et al. (1992). Association of aortic dilation with regurgitant, stenotic and functionally normal bicuspid aortic valves. *J Am Coll Cardiol*
92. Ferencik, M, et al. (2003). Changes in size of ascending aorta and aortic valve function with time in patients with congenitally bicuspid aortic valves. *The American Journal of Cardiology*
93. Nishimura, RA, et al. (2014). 2014 aha/acc guideline for the management of patients with valvular heart disease: A report of the american college of cardiology/american heart association task force on practice guidelines. *The Journal of Thoracic and Cardiovascular Surgery*
94. Rabkin, SW. (2017). The role matrix metalloproteinases in the production of aortic aneurysm. *Prog Mol Biol Transl Sci*
95. Goumans, MJ, et al. (2003). Controlling the angiogenic switch: A balance between two distinct tgf-b receptor signaling pathways. *Trends Cardiovasc Med*
96. Pedroza, AJ, et al. (2020). Divergent effects of canonical and non-canonical tgf-beta signalling on mixed contractile-synthetic smooth muscle cell phenotype in human marfan syndrome aortic root aneurysms. *J Cell Mol Med*
97. Muto, A, et al. (2007). Smooth muscle cell signal transduction: Implications of vascular biology for vascular surgeons. *Journal of Vascular Surgery*
98. Goumans, MJ, et al. (2017). Tgf-beta signaling in control of cardiovascular function. *Cold Spring Harb Perspect Biol*
99. Ingram, DA, et al. (2004). Identification of a novel hierarchy of endothelial progenitor cells using human peripheral and umbilical cord blood. *Blood*
100. Langford-Smith, AWW, et al. (2019). Diabetic endothelial colony forming cells have the potential for restoration with glycomimetics. *Sci Rep*
101. Smits, J, et al. (2018). Blood outgrowth and proliferation of endothelial colony forming cells are related to markers of disease severity in patients with pulmonary arterial hypertension. *Int J Mol Sci*
102. Wilde, B, et al. (2016). Endothelial progenitor cells are differentially impaired in anca-associated vasculitis compared to healthy controls. *Arthritis Res Ther*
103. Yoder, MC, et al. (2006). Redefining endothelial progenitor cells via clonal analysis and hematopoietic stem/progenitor cell principals. *Blood*
104. Luyckx, I, et al. (2019). Copy number variation analysis in bicuspid aortic valve-related aortopathy identifies tbx20 as a contributing gene. *Eur J Hum Genet*
105. Luyckx, I, et al. (2019). Confirmation of the role of pathogenic smad6 variants in bicuspid aortic valve-related aortopathy. *Eur J Hum Genet*

106. Alonso-Montes, C, et al. (2018). Variants in cardiac gata genes associated with bicuspid aortic valve. *Eur J Clin Invest*
107. Park, JE, et al. (2019). A novel smad6 variant in a patient with severely calcified bicuspid aortic valve and thoracic aortic aneurysm. *Mol Genet Genomic Med*
108. McKellar, SH, et al. (2007). Novel notch1 mutations in patients with bicuspid aortic valve disease and thoracic aortic aneurysms. *The Journal of Thoracic and Cardiovascular Surgery*
109. Giusti, B, et al. (2017). Genetic bases of bicuspid aortic valve: The contribution of traditional and high-throughput sequencing approaches on research and diagnosis. *Frontiers in physiology*
110. Fernández, B, et al. (2020). Bicuspid aortic valve in 2 model species and review of the literature. *Vet Pathol*
111. Faggion Vinholo, T, et al. (2019). Genes associated with thoracic aortic aneurysm and dissection: 2019 update and clinical implications. *Aorta (Stamford, Conn.)*
112. Takeda, N, et al. (2018). Tgf-β signaling-related genes and thoracic aortic aneurysms and dissections. *Int J Mol Sci*
113. Nataatmadja, M, et al. (2013). Angiotensin ii receptor antagonism reduces transforming growth factor beta and smad signaling in thoracic aortic aneurysm. *Ochsner J*
114. Guo, DC, et al. (2007). Mutations in smooth muscle alpha-actin (acta2) lead to thoracic aortic aneurysms and dissections. *Nat Genet*
115. Wooten, EC, et al. (2010). Application of gene network analysis techniques identifies axin1/pdia2 and endoglin haplotypes associated with bicuspid aortic valve. *PLoS One*
116. Dargis, N, et al. (2016). Identification of gender-specific genetic variants in patients with bicuspid aortic valve. *The American Journal of Cardiology*
117. Callewaert, B, et al. (2011). New insights into the pathogenesis of autosomal-dominant cutis laxa with report of five eln mutations. *Human mutation*
118. Pepe, G, et al. (2014). Identification of fibrillin 1 gene mutations in patients with bicuspid aortic valve (bav) without marfan syndrome. *BMC medical genetics*
119. Nistri, S, et al. (2012). Association of marfan syndrome and bicuspid aortic valve: Frequency and outcome. *International Journal of Cardiology*
120. Pilop, C, et al. (2009). Proteomic analysis in aortic media of patients with marfan syndrome reveals increased activity of calpain 2 in aortic aneurysms.
121. Li, RG, et al. (2018). Gata4 loss-of-function mutation and the congenitally bicuspid aortic valve. *Am J Cardiol*
122. Shi, LM, et al. (2014). Gata5 loss-of-function mutations associated with congenital bicuspid aortic valve. *Int J Mol Med*
123. Xu, YJ, et al. (2018). Gata6 loss-of-function mutation contributes to congenital bicuspid aortic valve. *Gene*

124. Gharibeh, L, et al. (2018). Gata6 regulates aortic valve remodeling, and its haploinsufficiency leads to right-left type bicuspid aortic valve. *Circulation*
125. Makki, N, et al. (2012). Cardiovascular defects in a mouse model of hoxa1 syndrome. *Hum Mol Genet*
126. Macatee, TL, et al. (2003). Ablation of specific expression domains reveals discrete functions of ectoderm- and endoderm-derived fgf8 during cardiovascular and pharyngeal development. *Development*
127. Guo, D-c, et al. (2016). Lox mutations predispose to thoracic aortic aneurysms and dissections. *Circ res*
128. Guo, D-c, et al. (2015). Mat2a mutations predispose individuals to thoracic aortic aneurysms. *Am j hum gen*
129. Zhang, J, et al. (2008). Frs2alpha-deficiency in cardiac progenitors disrupts a subset of fgf signals required for outflow tract morphogenesis. *Development*
130. Biben, C, et al. (2000). Cardiac septal and valvular dysmorphogenesis in mice heterozygous for mutations in the homeobox gene nkx2-5. *Circ Res*
131. Proost, D, et al. (2015). Performant mutation identification using targeted next-generation sequencing of 14 thoracic aortic aneurysm genes. *Hum Mutat*
132. Wang, J, et al. (2019). Nr2f2 loss-of-function mutation is responsible for congenital bicuspid aortic valve. *International Journal of Molecular Medicine*
133. Gould, RA, et al. (2019). Robo4 variants predispose individuals to bicuspid aortic valve and thoracic aortic aneurysm. *Nat Genet*
134. van der Linde, D, et al. (2012). Aggressive cardiovascular phenotype of aneurysms-osteoarthritis syndrome caused by pathogenic smad3 variants. *J Am Coll Cardiol*
135. van de Laar, IM, et al. (2012). Phenotypic spectrum of the smad3-related aneurysms-osteoarthritis syndrome. *J Med Genet*
136. Gillis, E, et al. (2017). Candidate gene resequencing in a large bicuspid aortic valve-associated thoracic aortic aneurysm cohort: Smad6 as an important contributor. *Front Physiol*
137. Lindsay, ME, et al. (2012). Loss-of-function mutations in tgfb2 cause a syndromic presentation of thoracic aortic aneurysm. *Nat Genet*
138. Loeys, BL, et al. (2005). A syndrome of altered cardiovascular, craniofacial, neurocognitive and skeletal development caused by mutations in tgfbr1 or tgfbr2. *Nature Genetics*
139. Girdauskas, E, et al. (2011). Transforming growth factor-beta receptor type ii mutation in a patient with bicuspid aortic valve disease and intraoperative aortic dissection. *Ann Thorac Surg*
140. Corbitt, H, et al. (2018). Timp3 and timp1 are risk genes for bicuspid aortic valve and aortopathy in turner syndrome. *PLoS Genet*

141. Jerome, LA, et al. (2001). Digeorge syndrome phenotype in mice mutant for the t-box gene, tbx1. *Nat Genet*
142. Gøtzsche, CO, et al. (1994). Prevalence of cardiovascular malformations and association with karyotypes in turner's syndrome. *Archives of disease in childhood*
143. Quiñones-Pérez, B, et al. (2018). Three-generation family with novel contiguous gene deletion on chromosome 2p22 associated with thoracic aortic aneurysm syndrome. *Am J Med Genet A*
144. Guo, DC, et al. (2018). Ltbp3 pathogenic variants predispose individuals to thoracic aortic aneurysms and dissections. *Am J Hum Genet*
145. Micha, D, et al. (2015). Smad2 mutations are associated with arterial aneurysms and dissections. *Hum Mutat*
146. Zhang, W, et al. (2017). Exome sequencing identified a novel smad2 mutation in a chinese family with early onset aortic aneurysms. *Clin Chim Acta*
147. Tan, CK, et al. (2013). Smad3 deficiency promotes inflammatory aortic aneurysms in angiotensin ii-infused mice via activation of inos. *J Am Heart Assoc*
148. Zhang, P, et al. (2016). Smad4 deficiency in smooth muscle cells initiates the formation of aortic aneurysm. *Circ Res*
149. Heald, B, et al. (2015). Prevalence of thoracic aortopathy in patients with juvenile polyposis syndrome-hereditary hemorrhagic telangiectasia due to smad4. *Am J Med Genet A*
150. Wain, KE, et al. (2014). Appreciating the broad clinical features of smad4 mutation carriers: A multicenter chart review. *Genet Med*
151. Boileau, C, et al. (2012). Tgfb2 mutations cause familial thoracic aortic aneurysms and dissections associated with mild systemic features of marfan syndrome. *Nat Genet*
152. Renard, M, et al. (2013). Thoracic aortic-aneurysm and dissection in association with significant mitral valve disease caused by mutations in tgfb2. *Int J Cardiol*
153. Bertoli-Avella, AM, et al. (2015). Mutations in a tgf-β ligand, tgfb3, cause syndromic aortic aneurysms and dissections. *J Am Coll Cardiol*
154. Gallo, EM, et al. (2014). Angiotensin ii-dependent tgf-β signaling contributes to loeys-dietz syndrome vascular pathogenesis. *J Clin Invest*
155. Jondeau, G, et al. (2016). International registry of patients carrying tgfbr1 or tgfbr2 mutations: Results of the mac (montalcino aortic consortium). *Circ Cardiovasc Genet*
156. Debiec, R, et al. (2017). Genetic insights into bicuspid aortic valve disease.
157. Nigam, V, et al. (2009). Notch1 represses osteogenic pathways in aortic valve cells. *J Mol Cell Cardiol*
158. Foffa, I, et al. (2013). Sequencing of notch1, gata5, tgfbr1 and tgfbr2genes in familial cases of bicuspid aortic valve. *BMC Medical Genetics*

159. Mohamed, SA, et al. (2006). Novel missense mutations (p.T596m and p.P1797h) in notch1 in patients with bicuspid aortic valve. *Biochem Biophys Res Commun*
160. Prakash, SK, et al. (2014).A roadmap to investigate the genetic basis of bicuspid aortic valve and its complications:Insights from the international bavcon(bicuspid aortic valve consortium).*J Am Coll Cardiol*
161. Uretsky, S, et al. (2014). Nature versus nurture in bicuspid aortic valve aortopathy: More evidence that altered hemodynamics may play a role. *Circulation*
162. Ha, H, et al. (2016). The influence of the aortic valve angle on the hemodynamic features of the thoracic aorta. *Scientific Reports*
163. Lorenz, R, et al. (2014). 4d flow magnetic resonance imaging in bicuspid aortic valve disease demonstrates altered distribution of aortic blood flow helicity. *Magn Reson Med*
164. Barker, AJ, et al. (2012). Bicuspid aortic valve is associated with altered wall shear stress in the ascending aorta. *Circ Cardiovasc Imaging*
165. Hope, MD, et al. (2010). Bicuspid aortic valve: Four-dimensional mr evaluation of ascending aortic systolic flow patterns. *Radiology*
166. Zhou, J, et al. (2014). Shear stress-initiated signaling and its regulation of endothelial function. *Arterioscler Thromb Vasc Biol*
167. Krüger-Genge, A, et al. (2019). Vascular endothelial cell biology: An update. *Int J Mol Sci*
168. Nerem, RM, et al. (1998). The study of the influence of flow on vascular endothelial biology. *Am J Med Sci*
169. Chien, S. (2008). Effects of disturbed flow on endothelial cells. *Ann Biomed Eng*
170. Baeyens, N, et al. (2016). Endothelial fluid shear stress sensing in vascular health and disease. *J Clin Invest*
171. Phelps, JE, et al. (2000). Spatial variations in endothelial barrier function in disturbed flows in vitro. *Am J Physiol Heart Circ Physiol*
172. DePaola, N, et al. (1992). Vascular endothelium responds to fluid shear stress gradients. *Arterioscler Thromb*
173. Tardy, Y, et al. (1997). Shear stress gradients remodel endothelial monolayers in vitro via a cell proliferation-migration-loss cycle. *Arterioscler Thromb Vasc Biol*
174. Nagel, T, et al. (1999). Vascular endothelial cells respond to spatial gradients in fluid shear stress by enhanced activation of transcription factors. *Arterioscler Thromb Vasc Biol*
175. Gimbrone, MA, Jr., et al. (2016). Endothelial cell dysfunction and the pathobiology of atherosclerosis. *Circulation research*
176. Hergenreider, E, et al. (2012). Atheroprotective communication between endothelial cells and smooth muscle cells through mirnas. *Nature Cell Biology*

177. Dux-Santoy, L, et al. (2019). Increased rotational flow in the proximal aortic arch is associated with its dilation in bicuspid aortic valve disease. *Eur Heart J Cardiovasc Imaging*
178. Bissell, MM, et al. (2013). Aortic dilation in bicuspid aortic valve disease: Flow pattern is a major contributor and differs with valve fusion type. *Circulation. Cardiovascular imaging*
179. Mahadevia, R, et al. (2014). Bicuspid aortic cusp fusion morphology alters aortic three-dimensional outflow patterns, wall shear stress, and expression of aortopathy. *Circulation*
180. Della Corte, A, et al. (2014). Towards an individualized approach to bicuspid aortopathy: Different valve types have unique determinants of aortic dilatation. *Eur J Cardiothorac Surg*
181. Burris, NS, et al. (2015). Bicuspid valve-related aortic disease: Flow assessment with conventional phase-contrast mri. *Acad Radiol*
182. Barker, AJ, et al. (2010). Quantification of hemodynamic wall shear stress in patients with bicuspid aortic valve using phase-contrast mri. *Annals of biomedical engineering*
183. Chandra, S, et al. (2012). Computational assessment of bicuspid aortic valve wall-shear stress: Implications for calcific aortic valve disease. *Biomech Model Mechanobiol*
184. Girdauskas, E, et al. (2015). Aortic events after isolated aortic valve replacement for bicuspid aortic valve root phenotype: Echocardiographic follow-up study. *Eur J Cardiothorac Surg*
185. Yasuda, H, et al. (2003). Failure to prevent progressive dilation of ascending aorta by aortic valve replacement in patients with bicuspid aortic valve: Comparison with tricuspid aortic valve. *Circulation*

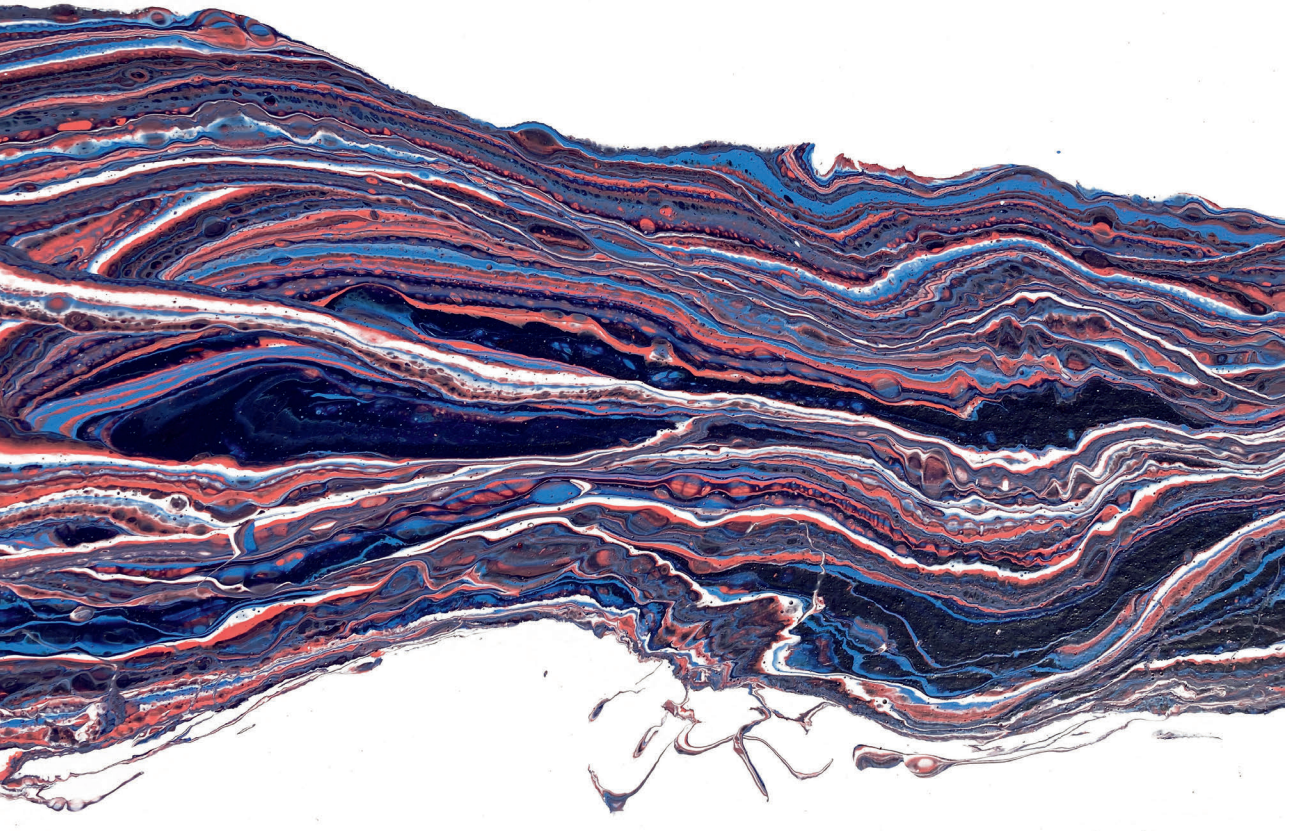

# Chapter 2

## Thoracic aortic aneurysm development in patients with bicuspid aortic valve: What is the role of endothelial cells?

**Vera van de Pol[1], Konda Babu Kurakula[1], Marco C. DeRuiter[2], Marie-José Goumans[1]**

[1] Department of Molecular Cell Biology, Leiden University Medical Center, Leiden, The Netherlands
[2] Department of Anatomy and Embryology, Leiden University Medical Center, Leiden, The Netherlands

*Published: Frontiers in Physiology, 2017 | 8: p. 938*

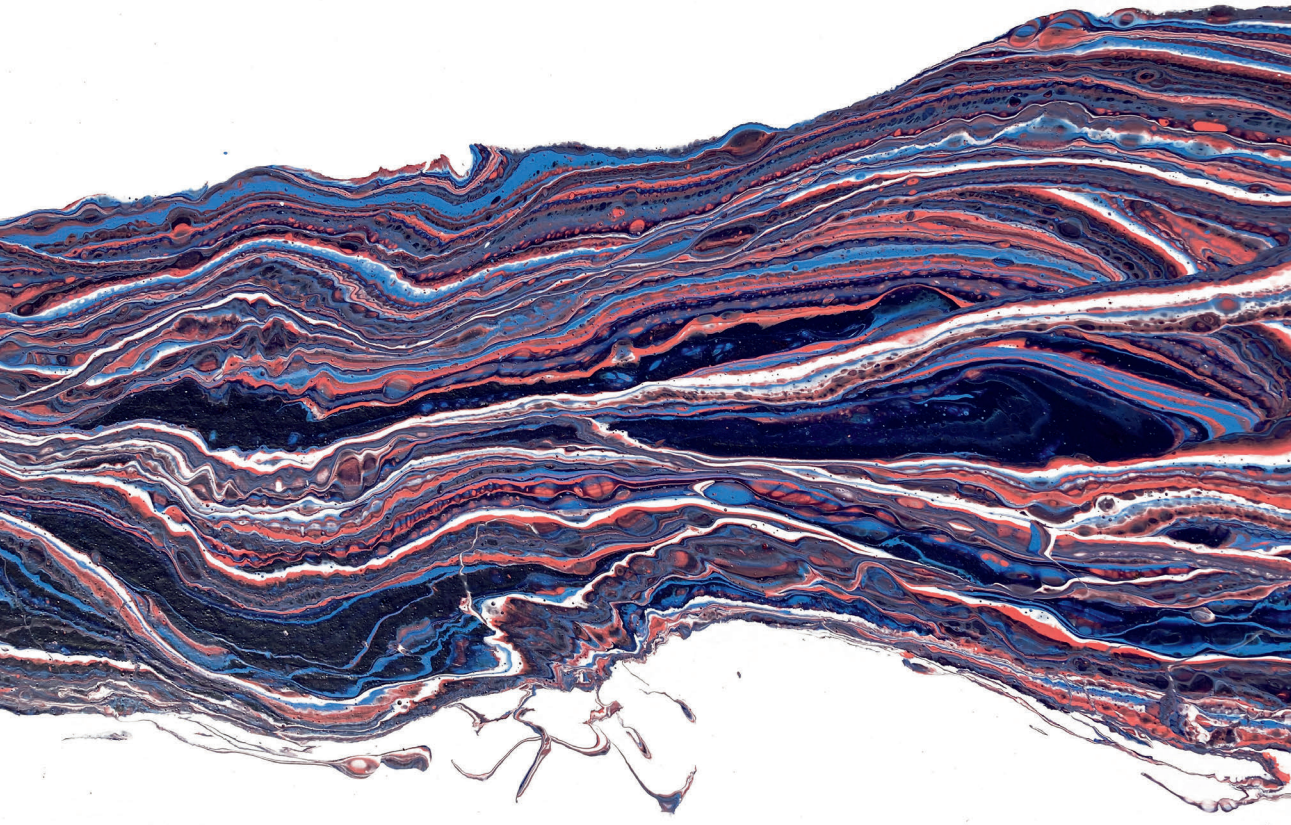

## Abstract

Bicuspid aortic valve (BAV) is the most common type of congenital cardiac malformation. Patients with a BAV have a predisposition for the development of thoracic aortic aneurysm (TAA). This pathological aortic dilation may result in aortic rupture, which is fatal in most cases. The abnormal aortic morphology of TAAs results from a complex series of events that alter the cellular structure and extracellular matrix (ECM) composition of the aortic wall. Because the major degeneration is located in the media of the aorta, most studies aim to unravel impaired smooth muscle cell (SMC) function in BAV TAA. However, recent studies suggest that endothelial cells play a key role in both the initiation and progression of TAAs by influencing the medial layer. Aortic endothelial cells are activated in BAV mediated TAAs and have a substantial influence on ECM composition and SMC phenotype, by secreting several key growth factors and matrix modulating enzymes. In recent years there have been significant advances in the genetic and molecular understanding of endothelial cells in BAV associated TAAs. In this review, the involvement of the endothelial cells in BAV TAA pathogenesis is discussed. Endothelial cell functioning in vessel homeostasis, flow response and signaling will be highlighted to give an overview of the importance and the under investigated potential of endothelial cells in BAV-associated TAA.

## Introduction

Bicuspid aortic valve (BAV) is the most common congenital cardiovascular malformation with a prevalence of 0.5–1.5% in the general population and a male predominance of about 3:1 [1,2]. In this anomaly, the aortic valve consists of 2 leaflets instead of the regular 3 leaflets. The BAV usually exhibits normal function at birth and during early life, however in adulthood BAV patients can develop several serious complications such as valvular stenosis and/or regurgitation, aortic dilation and thoracic aortic aneurysms (TAA). Although TAAs occur both in tricuspid aortic valves (TAV) and BAV, it has been estimated that 50%–70% of BAV patients develop aortic dilation and approximately 40% of BAV patients develop TAAs [3,4]. Moreover, patients with a BAV have a 9-fold higher risk for aortic dissection compared to the general population [5]. To monitor dilation progression in BAV patients the aortic diameter is regularly measured using echocardiography. However, no treatment options are available to prevent dilation or impact on the remodeling aortic wall. Surgical intervention with the aim to prevent rupture is therefore currently the only therapy for TAAs.



### Thoracic aortic aneurysm

While smooth muscle cells (SMCs) in the healthy media have a contractile phenotype, they are not terminally differentiated. This ensures the ability to regenerate the vessel wall after injury. This flexible change between cellular phenotypes is called "phenotypic switching", with the contractile and synthetic SMCs on opposite sides of the spectrum. After phenotypic switching the synthetic SMCs can migrate towards a wounded area by secreting proteinases to break down the ECM. Synthetic SMCs also proliferate and produce ECM to repair the wall. When the vessel wall is repaired, synthetic SMCs will re-differentiate towards a contractile phenotype. TAA is characterized by phenotypic switching of contractile to synthetic SMCs and fragmentation of elastic lamellae (Figure 1). The BAV aorta is more prone to TAA development, possibly due to differences in vascular homeostasis. For example, it has been shown that non-dilated BAV aorta, like the dilated TAV aorta, has an increased collagen turnover [6]. Moreover, orientation, fiber thickness and collagen crosslinking is altered in the dilated BAV aorta compared to the TAV aorta [7]. Additionally, decreased expression levels of lamin A/C, $\alpha$-smooth muscle actin ($\alpha$-SMA), calponin and smoothelin were not only found in dilated, but also in non-dilated BAV aorta [8]. Abdominal aortic aneurysms (AAA) share some common features with TAA, but differ in that atherosclerosis plays a major role in AAA, whereas medial degeneration is characteristic of TAA [9].

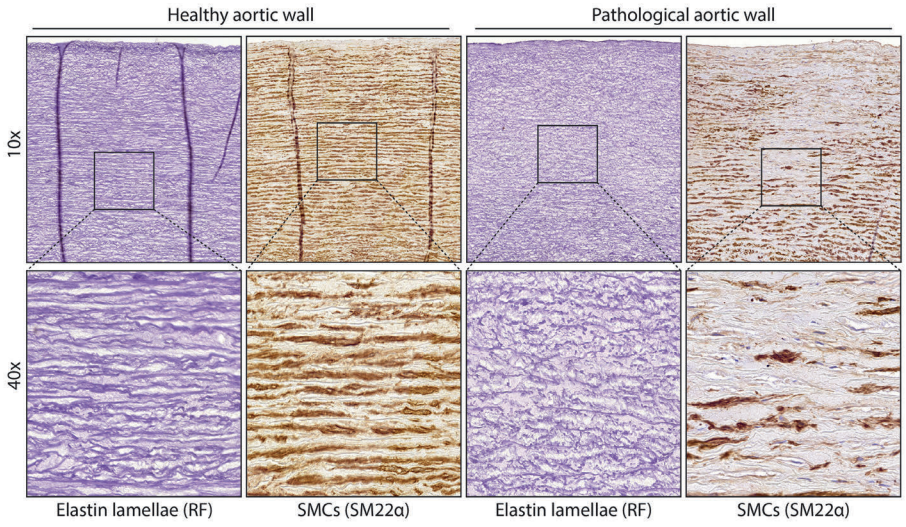


**Figure 1. Structure of normal and diseased aortic wall.** Images of aortic tissue showing elastic lamellae (stained with RF) or smooth muscle cells (SM22 staining). On the left is normal aortic tissue, the right image shows aortic tissue with fragmentation of the lamellae or loss of contractile SMCs.

The mechanism initiating thoracic aortic dilation is thus far unknown, however, the two main hypotheses are that either an altered flow greatly impacts vessel wall homeostasis (flow hypothesis) or that an intrinsic cellular defect contributes to the formation of BAV as well as to the dilation of the aorta in these patients (genetic hypothesis) [10]. Several genes related to structural proteins have been found mutated in BAV patients, such as *ACTA2, MYH11.* Furthermore, in BAV patients multiple mutations have also been found in genes related to signaling proteins such as *NOTCH1* and genes related to the TGFβ signaling pathway [11-13]. In addition to isolated cases, BAV has also been demonstrated to occur within families [14,15]. Interestingly, 32% of the first-degree relatives of BAV patients with a TAV also develop aortic root dilation, suggesting that the genetic predisposition for BAV and TAA overlap or may be identical in these families [16]. However, a clear inheritance pattern remains to be found. TAAs are also observed in patients with other syndromes such as Marfan, Loeys–Dietz and Ehler–Danlos, but contrastingly, BAV seldom occurs in these syndromes [17,18]. For an overview of genetic variation associated with BAV and the effect on endothelial functioning see Table 1.

**Table 1.** Consequences of genetics associated with BAV on cardiac malformations and endothelial cell functioning

| Pathway | Mutation | Effect | Other cardiovascular malformations | BAV occurrence | Effect of mutation on endothelial function |
|---|---|---|---|---|---|
| TGFb | *GATA5*$^{cre}$*ALK2*$^{fl/fl\ b}$ [127] | ALK2 deletion in cushion mesenchyme | not/under developed non-coronary leaflet | 78-83% | Constitutively active ALK2 induces EndoMT and is required for HDL induced EC survival and protection from calcification [128,129] |
| | *ENG*[a] [101] | Conservative peptide shift | HHT | Increased haplotype in BAV with an OR of 2,79 | Flow and ligand induced EC migration is disrupted increased proliferation and responsiveness to TGFβ1 [130,131] |
| | *TGFBR2*[a] [11,132] | Missense/nonsense/ splicing mutations | LDS, Marfan, TAA | 7% of the cohort | Maintenance of vascular integrity [133] |
| | SMAD6[a][12] | Loss of function | AoS, AoC and aortic calcification | 3/436 patients, 0/829 controls | Increases SMAD6, inhibits TGFβ signaling [134] |
| | *ADAMTS5*$^{-/-}$*SMAD2*$^{+/-b}$ [135] | Loss of function for Adamts5 and SMAD2 | Myxomatous valves, BPV | 75% Non-coronary with either left or right coronary cusp | Embryonic vascular instability, SMAD2 increases eNOS expression [136] |
| Other | *IFT88*$^{fl/fl}$*NFATC*$^{Cre\ b}$[23] | Endothelial specific loss of primary cillia | - | 68% BAV right/non-coronary fusion | ECs without primary cilia undergo EndoMT upon shear stress [22] |
| | *eNOS*$^{-/-\ b}$[83] | No functional eNOS | - | 42% BAV right/non-coronary fusion | Decreased EndoMT [137] |
| | *GATA5*[a] /*TIE2*$^{cre}$*GATA5*$^{fl/fl\ b}$ [138,139] [140] | Reduced Gata5 activity Gata5[a] / Gata5 deletion in ECs[b] | VSD, aortic stenosis[a] / LV hypertrophy, AS[b] | autosomal dominant BAV inheritance[a] / 25%[b] | Altered PKA and NO signaling [141] |

**Table 1.** Consequences of genetics associated with BAV on cardiac malformations and endothelial cell functioning *(continued)*

| Pathway | Mutation | Effect | Other cardiovascular malformations | BAV occurrence | Effect of mutation on endothelial function |
|---|---|---|---|---|---|
| | *NOTCH1*[a][64] | Autosomal dominant mutant notch1 | CAVD and other cardiac malformations | Autosomal dominant inheritance with complete penetrance | NOTCH1 increases calcification, oxidative stress and inflammation, when exposed to shear stress [142] |
| | *NKX2.5*[a][143] | Loss of function | ASD, PFO, AS and conduction defects | One family with an autosomal dominant inheritance | - |
| | *ACTA2*[a][144] | Missense mutation | Family with FTAAD | 3/18 patients with TAAD and mutation | - |
| | *FBN1*[a][132] | Diverse | Marfan, TAA | 4% of the cohort | - |

[a] found in human, [b] found in mice, OR= Odds ratio, AoC= Aortic coarctation, AoS= Aortic valve stenosis, AS= Aortic stenosis, ASD= Atrial septal defect, BPV= Bicuspid pulmonary valve, CAVD= calcific aortic valve disease, HHT= Hereditary hemorrhagic telangiectasia, LDS= Loeys-Dietz syndrome, LV= Left ventricle, PFO= Patent foramen ovale

**Endothelial cells in vessel homeostasis**

Due to the obvious medial degeneration in the aortic wall, research in the past decades has focussed on characterizing the organization and SMC phenotype of the aortic media during dilation and aneurysm [17,19,20]. Therefore, despite their main regulatory function, endothelial cells have so far taken the back seat in research towards understanding and treating aortic dilation. However, there is growing evidence that endothelial cells play an important role in the development and progression of aortic dilation.

Endothelial cells line the lumen of the aorta which, together with some ECM and the internal elastic lamella, form the intima. As the layer between the blood (flow) and the main structural component of the aorta (the media) the function of endothelial cells is to communicate the signal between these two layers. Upon flow and stimuli such as inflammatory cytokines, signaling pathways like TGFβ, angiotensin and nitric oxide (NO) allow endothelial cells to directly target the contraction status of SMCs or indirectly target the SMC contractile phenotype to influence vessel wall functioning (Figure 2). Primary cilia on the luminal surface of the endothelial cells enable mechanosensing and signaling

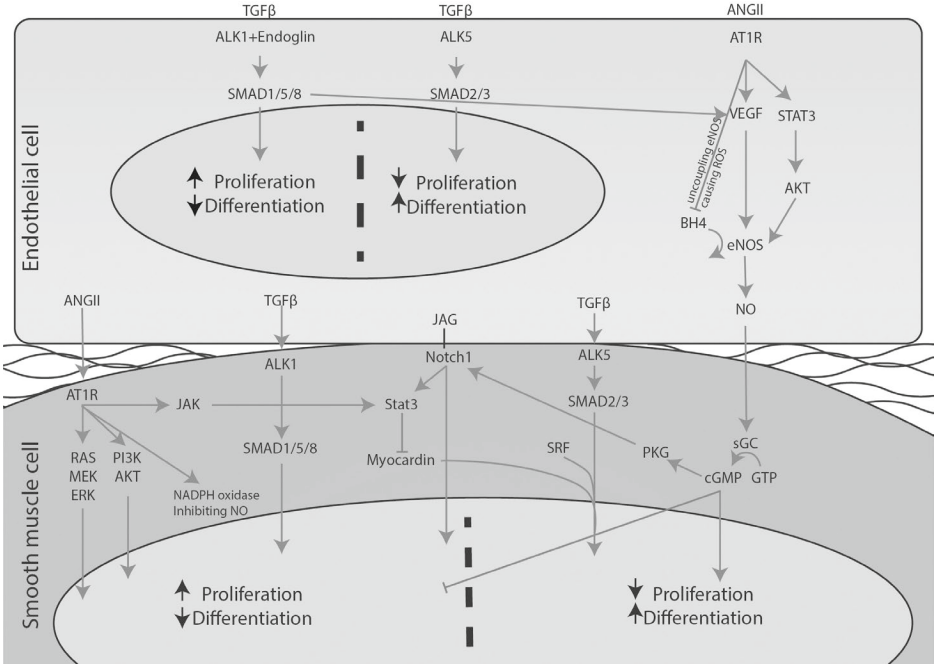


**Figure 2. Schematic overview of signaling pathways between endothelial cells and SMCs.** A simplified overview on the communication between endothelial cells and SMCs is depicted. Extensive crosstalk between pathways such as Notch1, ANGII, TGFβ, and NO can influence proliferation and differentiation of SMCs and affect the phenotypic switch of SMCs.

[21]. Endothelial cells lacking cilia change towards a mesenchymal phenotype, a process called endothelial to mesenchymal transformation (EndoMT) in which endothelial specific genes such as VE-cadherin and PECAM1 are down-regulated, whereas mesenchymal genes such as αSMA and fibronectin are up-regulated [22]. Intriguingly, a recent study demonstrated that *Ift88*$^{fl\text{-}fl}$ mice crossed with *Nfatc*$^{Cre}$, thereby lacking a primary cilium specifically in endothelial cells, display a highly penetrant BAV [23] (Table 1).

**The influence of flow on endothelial functioning and vessel homeostasis**

The flow pattern of blood from the heart into the aorta is altered by a BAV [24]. This difference between TAV and BAV hemodynamics in the aorta can be beautifully demonstrated using 4D MRI. Compared to a TAV, BAV generate a high velocity 'jet' propelling at an angle against the wall in the BAV aorta. This jet stream also causes an increase in peak shear stress on the endothelial cells [24]. As mentioned above, aside from the genetic hypothesis, the altered flow is also hypothesized to cause the aortic dilation in BAV.

It has been long known that adjusting flow induces remodeling of the vessel wall. Already, more than 30 years ago it was published that by decreasing blood flow in the carotid artery of rabbits by 70%, the lumen size of the vessel was decreased by 21% to compensate for the decreased blood flow [25]. Vascular remodeling is induced by increased shear stress on endothelial cells to restore original shear forces on the wall [26]. That flow greatly impacts endothelial functioning is also portrayed by the localization of fatty streaks and atherosclerosis at branch points and curves of arteries [26]. The turbulent flow at these locations causes dysfunctional endothelium: endothelial cells undergo apoptosis or exhibit increased proliferation. Moreover, permeability is increased, allowing LDL penetration into the intima as well as inflammatory cell adhesion and infiltration. Laminar flow induces the opposing quiescent endothelial phenotype characterized by a low turnover, alignment in the direction of the flow, decreased expression of inflammatory adhesion molecules like I-CAM and a low permeability caused by increased cell-cell adhesion molecules such as N-CAM and E-cadherin [27]. Experiments using co-culture of endothelial cells and SMCs revealed that flow on endothelial cells can also impact the phenotype of the underlying SMCs. Laminar shear stress on endothelial cells induces a contractile phenotype in synthetic SMCs, shown with both co-culture experiments of endothelial cells under flow with SMCs, as by adding conditioned medium from flow exposed endothelial cells to SMCs [28,29]. Upon laminar flow, endothelial cells signal towards SMCs using, for example, microRNA (miR)-126, prostacyclin, TGFβ3 and NO [28-31] MiR-126 in endothelial microparticles (EMPs) decreases

SMC proliferation and neointima formation [32]. Interestingly, EMP secretion is elevated in BAV associated TAA [33]. It is believed that EMPs are formed when endothelial cells are trying to avoid undergoing apoptosis, possibly explaining the association of elevated levels of EMPs with vascular diseases such as diabetes, congestive heart failure and acute coronary syndrome [34-36].

MiR-126 is only one means by which endothelial cells can impact on the vascular homeostasis. The main signaling pathways involved in BAV TAA and endothelial cells will be discussed in the next paragraphs.

**Angiotensin II signaling in TAA**



One of the major signaling pathways disturbed in aortic dilation is the Renin-Angiotensin-Aldosterone-System (RAAS), which is important for maintaining blood pressure. By constriction/relaxation of blood vessels and altering water retention of the kidneys, the blood pressure is regulated. The juxtaglomerular cells in the kidney and baroreceptors in vessel wall can sense arterial blood pressure. Upon a drop in pressure, renin is released by the juxtaglomerular cells and renin then converts angiotensinogen into angiotensin I (ANGI), which in turn is converted by angiotensin converting enzyme (ACE) into angiotensin II (ANGII). Amongst others, ANGII can cause contraction of the SMCs to increase blood pressure. This contraction is caused by the binding of ANGII to the angiotensin II type 1 receptor (AT1) on the SMCs, which in a cascade via $Ca^{+}$/calmodulin, activates the myosin light chain (MLC) kinase and rapidly phosphorylates MLC, causing contraction of SMCs. In addition, ANGII stimulates the cortex of the adrenal gland to secrete aldosterone, which increases water resorption in the kidney.

Aside from this direct vasoconstrictive effect, prolonged RAAS activation has diverse pathological effects. Aldosterone has been shown to cause endothelial dysregulation as well as a synthetic phenotype in SMCs [37]. Chronic infusion of ANGII in *ApoE*$^{-/-}$ mice demonstrated to cause progressive TAAs and AAAs [38,39]. The administration of ANGII in these mice decreased $\alpha$SMA and calponin expression in the mouse aortas [40,41]. Moreover, ACE2 expression was increased in mouse aortas after ANGII infusion as well as in dilated aortas of BAV patients [42]. ACE insertion/deletion polymorphisms were also identified as risk factor for the development of TAA in BAV patients [43]. Furthermore, a correlation was found between chronic elevated levels of ANGII and endothelial cell dysfunction in patients with hyperaldosteronism, underlining the importance of the RAAS system and endothelial functioning [44].

A seminal study performed by Rateri and colleagues, displayed the importance of endothelial cell functioning in the ANGII aneurysm model [45]. Interestingly, mice with specific deletion of *AT1* in SMCs or monocytes still developed

aortic aneurysms following a chronic ANGII infusion, while endothelial specific knock-out of *AT1*, did not exhibit dilation of the thoracic aorta. This study indicates that the primary target cell for ANGII in this model is the endothelial cell, which in turn influences the SMCs, causing the aortic structure to break down. How exactly this ANGII-endothelial cell signaling affects the SMC phenotype remains a crucial and intriguing question to be investigated. The same group one year later showed that AAA are not inhibited in the endothelial cell specific *AT1* knock-out, elegantly demonstrating that indeed there is a difference in pathogenesis between TAA and AAA [46]. This difference might be explained by a more prominent role for the adventitia than the intima in AAA development, or the developmentally different origin of SMCs in different parts of the aorta [47-50].

Aside from studies to understand the pathogenesis of TAA, ANGII treatment to model aortic aneurysm in mice is also used in the search of new treatment options. A recent study displayed that by treating ANGII infused mice with a combination therapy of Rosuvastatin and Bexarotene (retinoid X receptor-$\alpha$ ligand), aneurysm development was inhibited [51]. Moreover, they showed that this combination therapy affected endothelial cell proliferation, migration and signaling. In addition, upon ANGII treatment the VEGF secretion by endothelial cells *in vitro* was decreased [51]. Culture of SMCs from BAV patients exhibited an increase in AT1R expression, which was reduced to the levels of control SMCs by treatment using losartan [52]. Interestingly, antagonizing TGFβ by blocking the AT1 receptor using Losartan in a Marfan disease model mouse (*FBN1* mutation) demonstrated promising results for preventing and even reversing aortic dilation [53]. Furthermore, several clinical studies in Marfan patients reveal similar exciting results. However, a meta-analysis of clinical studies towards Losartan in Marfan patients did not show a reduction of aortic dilation in Losartan treated patients [54]. Losartan treatment in BAV patients has not been investigated yet. A clinical study was initiated, but recently terminated due to low enrolment.* Therefore, the effect of Losartan on BAV TAA still needs to be determined.

**Notch1 signaling in TAA**

Notch signaling plays an important role in cardiovascular development [55]. In contrast to many signaling pathways, Notch signaling is cell-cell contact dependent. There are 4 Notch homologues of which Notch1 is the best known. Binding of Notch1 ligands Jagged1, Jagged2 and/or Delta expressed in one cell induces cleavage of the receptor and nuclear translocation of the intracellular domain in the other cell causing transcription of, amongst others, the HES/HEY gene family, key regulators in EndoMT [56]. Notch1 signaling induces EndoMT in

endothelial cells and promotes a contractile phenotype in SMCs [57]. Moreover, Notch1 signaling is required for angiogenesis [58].

Notch signaling was displayed to be crucial for normal development of the aortic valve and outflow tract amongst others, as determined in *NOTCH1*$^{-/-}$ mice [59]. Specifically in the neural crest cells, Notch signaling is important. It was found that disruption of endothelial Jagged1 signaling to Notch on neural crest cells, inhibits SMC differentiation [60]. The Notch signaling pathway, as well as the TGFβ signaling pathway, is involved in EndoMT occurring in the outflow tract cushions, where endothelial cells change to populate the developing cardiac valves [61]. Thereby EndoMT is a crucial part of aortic valve development. Previous studies hypothesised that EndoMT may also play a role in the pathogenesis of BAV. Additionally, genes involved in this process such as *NOTCH1, TGFBR2* and *SMAD6*, have been found to cause BAV in mouse models, as well as being linked to BAV in human studies [11-13,62-64]. Mice with *NOTCH1* missense alleles have been characterized with multiple outflow tract and EndoMT defects [65]. Recently, it was demonstrated that specifically endothelial Notch1 signaling is required for normal outflow tract and valve development [66]. Moreover, a *NOTCH1* mutation was found in a family with BAV, underscoring Notch1 as an important signaling pathway in BAV [64]. These mutations have been associated with an increased risk of calcific aortic valve disease (CAVD), explained by the normally repressive function of Notch on calcification in valvular cells [64,67,68]. Additionally, one study reported severely calcified valves in BAV patients with Cornelia de Lange syndrome, a disease caused by dysfunctional Notch signaling [69].

Aside from the role of Notch signaling in valve formation, proper Notch signaling is also important for the homeostasis of the aorta, as illustrated by several studies. The non-dilated aorta of BAV patients showed increased Notch signaling and EndoMT marker expression based on proteomic analysis [70]. Furthermore, a study using endothelial cells isolated from BAV aorta demonstrated decreased *Notch1*, *Notch4* and *DLL4* mRNA levels compared to TAV non-aneurysmal tissue [71]. Moreover, upon TGFβ stimulation, there was a defective Notch dependent EndoMT response. Endothelial marker proteins such as VWF and PECAM, were unchanged between BAV and TAV endothelial cells. However, EndoMT markers HES1 and SLUG were significantly less upregulated in BAV endothelial cells compared to TAV endothelial cells. In addition, *JAG1* expression is normally upregulated upon Notch1 signaling and acts as a positive feedback-loop. This upregulation of Jagged1 was decreased in BAV endothelial cells, explaining at least part of the dysfunctional Notch signaling in BAV patients with TAA [71].

Interestingly, Notch1 plasma levels in combination with TNF$\alpha$-converting enzyme were shown to correlate highly with the presence of AAA [72]. Furthermore, studies demonstrated that *NOTCH1*haploinsufficiency or Notch1 inhibition can prevent or reduce the formation of AAA in ANGII infused mice [73,74]. However, the similarity in Notch signaling between AAA and TAA is debatable, as it has been displayed that in descending TAA tissue, in contrast to the ascending TAA, the SMCs exhibit a decreased Notch1 signaling, emphasizing the importance of the local environment in the aortic aneurysm formation [75].

**eNOS signaling in TAA**

Nitric oxide (NO) is produced when NO synthase (NOS) converts arginine into citrulline, releasing NO in the process. NOS was originally discovered in neurons (nNOS/NOS1), after which inducible NOS (iNOS/NOS2) and endothelial NOS (eNOS/NOS3) were found. eNOS phosphorylation increases NO production and is induced by factors such as shear stress, acetylcholine and histamine. NO has a very short half-life of a few seconds, making it a local and timely signal transducer. Endothelial secreted NO diffuses into the SMC where it relaxes the cell by increasing the calcium uptake into the sarcoplasmic reticulum by stimulating the sarco/endoplasmic reticulum ATPase (SERCA), thereby decreasing cytoplasmic $Ca^{+}$ levels. Additionally, NO has also been revealed to regulate gene transcription by reacting with NO sensitive transcription factors [76]. Finally NO has been shown to impact the SMC inflammatory status, however more research is required to fully understand the effect of NO on SMC phenotype [77]. Uncoupled eNOS causes free oxygen radicals to be formed, which damages proteins and DNA.

Multiple studies have identified an important role for dysregulated endothelial NO signaling in aneurysm development. For example, it has been demonstrated that the oxidative stress is increased in the media of the aortas of BAV patients compared to TAV aortas [78]. Interestingly, a mouse model with uncoupled eNOS (HPH-1 mice) rapidly developed AAA and aortic rupture upon ANGII infusion, whereas wild-type (WT) mice did not display this phenotype [79]. Re-coupling of eNOS by infusion of folic acid, inhibited AAA formation [79]. A study investigating the effect of iNOS deletion in an elastase infusion mouse model of experimentally induced AAA did not demonstrate any substantial exacerbation of the aneurysm phenotype, indicating the importance of endothelial NO in aneurysm formation [80]. Intriguingly, a follow-up study identified plasma and tissue levels of the eNOS co-factor tetrahydrobiopterin, necessary for coupling of eNOS, correlate with aneurysm development in *ApoE*$^{-/-}$ mice and HPH-1 mice [81]. In line with these studies, it was shown that endothelial specific

expression of reactive oxygen species, by an endothelial specific overexpression of NOX2, can cause dissection in WT mice upon ANGII infusion [82]. Moreover, eNOS knockout mice develop BAV, underlining the importance of endothelial dysfunction in the formation of BAV and the related TAA [83].

In patients with a TAV and TAA, profiling of the aortic tissue revealed that eNOS phosphorylation was increased via a miR-21 dependent mechanism [84]. MiR-21 is specifically upregulated by shear stress and causes PTEN mRNA degradation, allowing an increase in eNOS phosphorylation [85]. Furthermore, BAV TAA patient aortic samples displayed increased eNOS expression and activation compared to TAV TAA controls [86]. These studies indicate an increased eNOS activity in TAA formation in BAV patients. Contrastingly, decreased eNOS expression has been found in 72,7% aortic samples of BAV patients (N=22) [87]. In addition, a negative correlation between eNOS expression levels and aortic dilation in BAV patients was reported [88].

In conclusion, multiple studies have investigated eNOS in the BAV aorta, with contrasting outcomes [86-89]. These discrepancies may be caused by differences between patient populations, location of the aortic sample used, stage of aortic aneurysm formation and the use of different control samples for comparison. Nonetheless, all these studies indicate that normal levels of coupled eNOS are necessary to maintain a healthy aortic wall.

**TGFβ signaling in TAA**

TGFβ signaling is mediated by binding of the ligand TGFβ to the TGFβ type 2 receptor, which recruits and phosphorylates a TGFβ type 1 receptor. While there is only one type 2 receptor, TGFβ can signal via two TGFβ type 1 receptors, Activin-like kinase (ALK)1 and ALK5. Upon ligand binding, ALK5 can phosphorylate SMAD2 or SMAD3 and ALK1 can phosphorylate SMAD1, SMAD5 or SMAD8. The phosphorylated SMADs translocate into the nucleus with SMAD4 to induce the canonical signaling pathway. TGFβ can also signal via non-canonical pathways by activating PI3K/AKT, MAPK or NF-kB. Via the canonical and non-canonical pathways, TGFβ influences cell cycle arrest, apoptosis, inflammation, proliferation and more.

In endothelial cells, TGFβ signaling can either inhibit or stimulate the cell growth and function depending on the context [90]. TGFβ signaling via ALK1 induces proliferation and migration, whereas ALK5 signaling promotes plasminogen activator inhibitor 1 (PAI1) expression, decreasing the breakdown of the ECM necessary for maturation of the vessel wall [91,92]. The two opposing effects of TGFβ signaling enable the initial growth of vessels followed by stabilization of the ECM and attraction of SMCs. Moreover, endothelial TGFβ signaling

in concert with platelet derived growth factor-BB is crucial for attracting and differentiating pre-SMCs during vasculogenesis [93]. Because of these crucial functions of TGFβ during embryonic development, loss of TGFβ signaling in the vascular system, either total knockout or SMC or endothelial cell specific deletion is embryonically lethal [90]. In SMCs TGFβ induces a contractile phenotype, and dysregulation of TGFβ therefore can have a major impact on SMC phenotype [94]. The importance of endothelial TGFβ signaling on SMC differentiation is illustrated by co-culture of endothelial cells and SMCs. Cultured alone, the SMCs have a synthetic phenotype, but when co-cultured with endothelial cells, they differentiate into contractile SMCs via the PI3K/AKT signaling pathway [95].

The TGFβ Type III receptor endoglin (*ENG*) is highly expressed by endothelial cells and plays a role in the ALK1 and ALK5 signaling balance [96]. In fact, without endoglin, endothelial cells stop proliferating as a result of decreased ALK1 signaling [97]. In addition, knock-out of *ENG* in mice causes embryonic lethality due to impaired angiogenesis, whereas vasculogenesis remains intact [98,99]. This exemplifies the pivotal role for TGFβ signaling in endothelial cells for proper angiogenesis. As mentioned above, TGFβ signaling, like Notch signaling, is important for the process of EndoMT necessary for the developing cardiac valves. Chimera research using $ENG^{-/-}$ mice embryonic stem cells, added to WT mice morulae highlighted the indispensable role of endoglin for EndoMT in the developing cardiac valves [100]. These chimeric mice showed contribution of the $ENG^{-/-}$ cells to the endothelium. However, no $ENG^{-/-}$ cells participated in populating the atrio-ventricular (AV) mesenchyme of the developing AV cushions. Intriguingly, a single-nucleotide polymorphism in *ENG* was found in BAV patients, indicating that in BAV patients endothelial TGFβ signaling might be altered, potentially promoting a phenotypic switch in the underlying SMCs [101].

Many studies using *in vitro*, *ex vivo* and histological methods, also indicate a role for TGFβ signaling in TAA formation in BAV. Unstimulated, cultured BAV and TAV SMCs did not demonstrate any difference in gene expression in basal conditions, however after TGFβ stimulation, 217 genes were found differentially expressed between BAV and TAV SMCs demonstrating a difference in TGFβ signaling [102]. Moreover, induced pluripotent stem cells (iPSCs) derived from BAV patients with a dilated aorta exhibited decreased TGFβ signaling compared with iPSCs from TAV controls without aortic dilation (Jiao et al., 2016). Conversely, a hypothesis-free analysis of the secretome of BAV TAA indicated a highly activated TGFβ signaling pathway in the aortic wall of BAV patients when compared to the secretome of TAV aneurysmal aortic tissue [103]. This study showed, using mass spectrometry on all proteins in conditioned medium of the aortic samples, a 10-fold increase of latent TGFβ binding protein 4 (LTBP4) in the BAV samples

[103]. Histological analysis identified that, compared to normal aortic tissue, BAV dilated aortic tissue had an increase in SMAD3 and TGFβ in the tunica media [52]. However, when compared to dilated TAV aorta, the expression of SMAD 2/3 was higher in the TAV dilated aorta than the BAV dilated aorta [103]. Furthermore, it has been shown that the circulating TGFβ levels in BAV patient are elevated, which is in agreement with studies showing increased TGFβ signaling [104,105].

Multiple studies have demonstrated that antagonizing TGFβ signaling in aneurysm mouse models prevents and even reverses aneurysm formation [53,106,107]. The positive effects of TGFβ antagonism on aneurysm formation were shown in using a neutralizing TGFβ-antibody or by blocking the AT1 receptor using Losartan, which also decreases TGFβ signaling. In different mice models, Fibrillin-1 deficient, Fibulin-4 deficient and ANGII treated mice, the TGFβ inhibition prevented and reversed aortic aneurysm, making it a promising target for therapy [53,106,107]. A study using cultured SMCs revealed that Losartan treatment decreased intracellular TGFβ protein levels and nuclear SMAD3 localization [52]. BAV derived SMCs displayed a decrease in endoglin expression upon Losartan treatment [108]. Furthermore, serum TGFβ levels decreased when mice were treated with Losartan. The same was also seen in Marfan patients on Losartan, validating the study results obtained in mice [53,109]. However, as mentioned above, so far Losartan treatment does not seem to decrease or prevent aneurysm formation in a clinical setting. Given the recent success of specific TGFβ blockers in other vascular disorders such as pulmonary arterial hypertension (PAH) and restenosis, targeting the TGFβ pathway more directly could be a strategy for developing new treatment modalities for TAA [110,111].



**Endothelial dysfunction in other diseases: implications for BAV-TAA?**

Many cardiovascular disorders have highlighted the importance of normal endothelial functioning for maintaining homeostasis across the vessel wall, such as atherosclerosis, brain aneurysms, PAH and hereditary haemorrhagic telangiectasia (HHT). PAH and HHT are 2 major genetic diseases in which the role of the endothelial cells is well recognized. Two recent advances in these research fields worth mentioning for future perspectives in BAV TAA research, will be discussed in the next paragraphs.

PAH is an incurable fatal disease caused by remodeling of the pulmonary arteries. Proliferation of the pulmonary artery smooth muscle cells (PASMCs) causes narrowing and occlusion of the lumen, leading to an increased pressure in the lungs and increased load of the right ventricle [112]. While originally defined

as a SMC disorder, over the past years dysfunction of the endothelial cells has become of interest in the pathogenesis of PAH [112-114]. The application of conditioned medium from normal endothelial cells to PASMCs resulted in an increase in PASMC proliferation rate [115]. This effect is exaggerated when adding conditioned medium of endothelial cells from PAH patients. Complementary, PASMCs from PAH patients showed an increased proliferation to both endothelial cell conditioned media, compared with control PASMCs. Two of the major players identified within the conditioned medium are miR-143 and miR-145. These miRs have been demonstrated to highly impact the SMC phenotypic switch, inducing a contractile phenotype [116]. Expression of these two miRs is regulated by TGFβ and they have been shown to be secreted in exosomes [117,118]. Intriguingly, in PAH mouse models as well as patient lung tissue and cultured SMCs, miR-143-3p expression is increased. Furthermore, miR-143$^{-/-}$ mice developed pulmonary hypertension, a phenotype that was rescued by restoring miR-143 levels [118].

Interestingly, signaling from endothelial cells to SMCs concerning miR-143 and miR-145 has also been investigated in atherosclerosis research [119]. Transduction of HUVECs with the shear-responsive transcription factor KLF2, or exposure of HUVECS to flow caused an increase in miR-143 and miR-145, indicating a flow responsiveness of the miR-143 and miR-145 expression [119]. Additionally, endothelial cells secreted miR-143 and miR-145 in microvesicles and targeted gene expression in SMCs. Moreover, when treating *ApoE*$^{-/-}$ mice with endothelial secreted vesicles containing, amongst others, miR-143 and miR-145, the mice developed less atherosclerosis [120]. The SMCs of the knockout mice displayed increased migration and proliferation. Analyses of the mouse aortas showed EMC degradation in the miR-143 and miR-145 deficient mice. These results support the findings of a role for miR-143 and miR-145 in inducing a contractile SMC phenotype [120]. Furthermore, in TAA miR-143 and miR-145 were found to be decreased compared to non-dilated samples [120]. The impact these miRs have on SMC phenotype, the expression regulation by flow and their secretion by endothelial cells as well as the decrease in TAA, makes them relevant and interesting for BAV TAA research. The first study towards BAV and miR-143 and miR-145 was recently published, describing a local decrease of miR-143 and miR-145 in the inner curve of the BAV aorta compared to the outer curve. Moreover, they also found altered miR expression affecting mechanotransduction [121].

Intriguingly, mechanotransduction has also been of interest in HHT research. HHT, a vascular haploinsufficiency disease characterized by frequent severe bleedings due to fragile and tortuous blood vessels. Disturbed TGF-beta signaling plays a major role in the development of these malformed blood vessels. 80% of HHT patients have a mutation in *ENG* (HHT1) or *ALK1* (HHT2) [122]. The

endothelial cell-SMC communication is disrupted in HHT, and recruiting and differentiation of SMCs falters causing improperly formed vessels. Disturbed mechanotransduction in endothelial cells has been shown to impact BMP/Smad1/5 signaling as well as vessel stabilization in HHT [123]. By subjecting endothelial cells to shear stress, SMAD1 was activated. Moreover, decreasing either ALK1 or endoglin both inhibited the SMAD1 activation in response to flow. Interestingly, when co-cultured with pericytes, both ALK1 and endoglin were found to be crucial for endothelial shear stress induced migration and proliferation of these pericytes [123]. It would be highly interesting to investigate if BAV endothelial cells also have an intrinsic mechanotransduction defect causing the aorta to be prone to TAA development. The study by Albinsson and colleagues showing the altered miR related to mechanotransduction in BAV aorta samples is an important first step to lead the BAV TAA research field towards relevant studies on mechanotransduction defects possibly explaining (part of the) BAV TAA pathogenesis.



## Conclusions and future perspectives

BAV is a common congenital cardiac malformation and the majority of BAV patients develop TAA over time. Although the last decade has witnessed the discovery of several key findings in the field of BAV-associated TAAs, the cellular and molecular mechanisms in BAV-associated TAAs that drive the degeneration of media of the vessel wall are still largely unknown. Many studies have focussed on changes in the signaling pathways in SMCs, however the importance of endothelial cells and their contribution to the initiation and progression of BAV-associated TAAs has not been appreciated in detail.

Under normal physiological conditions, endothelial cells and SMCs communicate with each other for optimal function of the vessel wall in order to maintain homeostasis in the circulatory system. Dysregulation of this communication can lead to medial degeneration and aortic aneurysm, clearly demonstrated in animal models using ANGII infusion or eNOS uncoupling. Interestingly, blocking TGFβ signaling is a possible treatment option to prevent TAA formation, as evidenced by multiple animal studies mentioned before. Patient samples also indicate a pivotal role for these pathways as revealed by the dysregulation of eNOS, Notch1 and TGFβ signaling proteins in the BAV aortic tissue. The involvement of these pathways is validated by the mutations that have been shown to cause BAV and/or TAA in mouse models and the finding of mutations in these genes in patients with BAV and TAA. In addition to these observations made *in vivo*, *in vitro* studies using patient derived endothelial cells indicate an EndoMT defect in cultured cells from BAV patients. In conclusion, all studies to date indicate great

potential of an underexplored research field concerning the endothelial-smooth muscle cell communication in the BAV TAA formation.

While hardly studied in BAV, the importance of endothelial functioning for vessel homeostasis has been elucidated in other vascular disorders such as PAH, HHT and atherosclerosis. In line with the latest research in these fields, it would be very interesting to investigate if the mechanotransduction and/or microvesicle secretion is altered in endothelial cells of BAV TAA patients. Unfortunately, research towards endothelial cell contribution in BAV TAA pathogenesis has been hampered by the difficulty of obtaining non-end stage study material. The discovery of circulating endothelial progenitor cells (EPCs) and endothelial colony forming cells (ECFCs) will, however, provide a new study model, facilitating patient specific analysis of the endothelial contribution to the disease [124,125]. Thus far, one study was published using these circulatory cells from BAV patients. An impaired EPC migration and colony formation potential was shown when the cells were isolated from BAV patients with a dysfunctional valve compared to BAV patients with a normal functioning valve [126]. Currently, the cause and effect of impaired EPCs is unknown, and more research is required to understand the full potential of circulating endothelial progenitor cells in BAV TAA pathogenesis and their use as a biomarker for patient stratification.

Although few studies on the role of endothelium in BAV disease and its associated TAAs have been performed in the last decade, some seminal papers have been published. In this review, we have created an overview of the recent studies implicating endothelial cells as a pivotal player of vascular homeostasis, and their underappreciated role in TAA pathogenesis in patients with a BAV. Figure 3 schematically depicts the different factors and processes involved in BAV TAA development as discussed throughout this review. Up to date, we are still unable to stratify and cure these patients. Therefore, further research is required to understand the role of endothelial cells and comprehend the interplay between endothelial cells and SMCs in BAV-associated TAA. In conclusion, appreciation of the role of endothelium is crucial for a better understanding of BAV TAA pathogenesis, which is necessary in development of new therapeutic strategies for the BAV-associated TAAs.

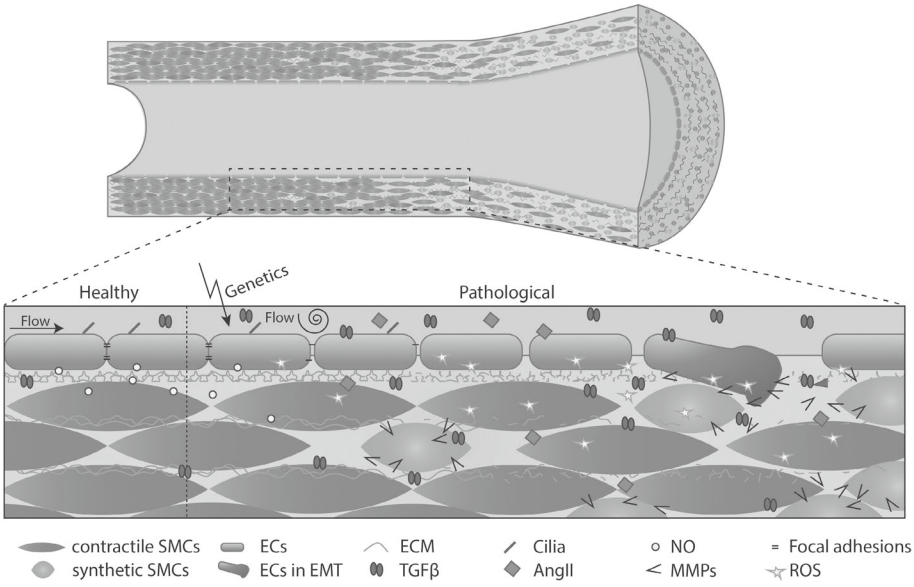


**Figure 3. Schematic overview of events in development of aortic dilation.** Schematic overview of an aorta over time. Initiation by flow and/or genetics causes endothelial cell dysfunction, affecting the aortic structure i.e. causing synthetic SMCs and lamellar fragmentation.

**Acknowledgements**

We acknowledge support from the Netherlands CardioVascular Research Initiative: the Dutch Heart Foundation, Dutch Federation of University Medical Centers, the Netherlands Organization for Health Research and Development, and the Royal Netherlands Academy of Sciences Grant CVON-PHAEDRA (CVON 2012-08) and the Dutch heart foundation grant number 2013T093 awarded to the BAV consortium.

## References


1. Basso, C, et al. (2004). An echocardiographic survey of primary school children for bicuspid aortic valve. *Am J Cardiol*
2. Roberts, WC. (1970). The congenitally bicuspid aortic valve. A study of 85 autopsy cases. *Am J Cardiol*
3. Saliba, E, et al. (2015). The ascending aortic aneurysm: When to intervene? *IJC Heart & Vasculature*
4. Yuan, SM, et al. (2010). The bicuspid aortic valve and its relation to aortic dilation. *Clinics (Sao Paulo)*
5. Lewin, MB, et al. (2005). The bicuspid aortic valve: Adverse outcomes from infancy to old age. *Circulation*
6. Wagsater, D, et al. (2013). Impaired collagen biosynthesis and cross-linking in aorta of patients with bicuspid aortic valve. *J Am Heart Assoc*
7. Tsamis, A, et al. (2016). Extracellular matrix fiber microarchitecture is region-specific in bicuspid aortic valve-associated ascending aortopathy. *J Thorac Cardiovasc Surg*
8. Grewal, N, et al. (2014). Ascending aorta dilation in association with bicuspid aortic valve: A maturation defect of the aortic wall. *J Thorac Cardiovasc Surg*
9. Guo, DC, et al. (2006). Pathogenesis of thoracic and abdominal aortic aneurysms. *Ann N Y Acad Sci*
10. Girdauskas, E, et al. (2011). Is aortopathy in bicuspid aortic valve disease a congenital defect or a result of abnormal hemodynamics? A critical reappraisal of a one-sided argument. *Eur J Cardiothorac Surg*
11. Girdauskas, E, et al. (2011). Transforming growth factor-beta receptor type ii mutation in a patient with bicuspid aortic valve disease and intraoperative aortic dissection. *Ann Thorac Surg*
12. Tan, HL, et al. (2012). Nonsynonymous variants in the smad6 gene predispose to congenital cardiovascular malformation. *Hum Mutat*
13. Andelfinger, G, et al. (2016). A decade of discovery in the genetic understanding of thoracic aortic disease. *Can J Cardiol*
14. Huntington, K, et al. (1997). A prospective study to assess the frequency of familial clustering of congenital bicuspid aortic valve. *J Am Coll Cardiol*
15. Calloway, TJ, et al. (2011). Risk factors for aortic valve disease in bicuspid aortic valve: A family-based study. *Am J Med Genet A*
16. Biner, S, et al. (2009). Aortopathy is prevalent in relatives of bicuspid aortic valve patients. *J Am Coll Cardiol*
17. Ruddy, JM, et al. (2013). Pathophysiology of thoracic aortic aneurysm (taa): Is it not one uniform aorta? Role of embryologic origin. *Prog Cardiovasc Dis*
18. El-Hamamsy, I, et al. (2009). Cellular and molecular mechanisms of thoracic aortic aneurysms. *Nat Rev Cardiol*

19. Wolinsky, H. (1970). Comparison of medial growth of human thoracic and abdominal aortas. *Circ Res*
20. Halloran, BG, et al. (1995). Localization of aortic disease is associated with intrinsic differences in aortic structure. *J Surg Res*
21. Egorova, AD, et al. (2012). Primary cilia as biomechanical sensors in regulating endothelial function. *Differentiation*
22. Egorova, AD, et al. (2011). Lack of primary cilia primes shear-induced endothelial-to-mesenchymal transition. *Circ Res*
23. Toomer, KA, et al. (2017). A role for primary cilia in aortic valve development and disease.
24. Barker, AJ, et al. (2012). Bicuspid aortic valve is associated with altered wall shear stress in the ascending aorta. *Circ Cardiovasc Imaging*
25. Langille, BL, et al. (1986). Reductions in arterial diameter produced by chronic decreases in blood flow are endothelium-dependent. *Science*
26. Baeyens, N, et al. (2016). Endothelial fluid shear stress sensing in vascular health and disease. *J Clin Invest*
27. Chistiakov, DA, et al. (2017). Effects of shear stress on endothelial cells: Go with the flow. *Acta Physiol (Oxf)*
28. Tsai, MC, et al. (2009). Shear stress induces synthetic-to-contractile phenotypic modulation in smooth muscle cells via peroxisome proliferator-activated receptor alpha/delta activations by prostacyclin released by sheared endothelial cells. *Circ Res*
29. Zhou, J, et al. (2013). Regulation of vascular smooth muscle cell turnover by endothelial cell-secreted microrna-126: Role of shear stress. *Circ Res*
30. Noris, M, et al. (1995). Nitric oxide synthesis by cultured endothelial cells is modulated by flow conditions. *Circ Res*
31. Walshe, TE, et al. (2013). The role of shear-induced transforming growth factor-beta signaling in the endothelium. *Arterioscler Thromb Vasc Biol*
32. Jansen, F, et al. (2017). Intercellular transfer of mir-126-3p by endothelial microparticles reduces vascular smooth muscle cell proliferation and limits neointima formation by inhibiting lrp6. *J Mol Cell Cardiol*
33. Alegret, JM, et al. (2016). Circulating endothelial microparticles are elevated in bicuspid aortic valve disease and related to aortic dilation. *Int J Cardiol*
34. Bernal-Mizrachi, L, et al. (2003). High levels of circulating endothelial microparticles in patients with acute coronary syndromes. *Am Heart J*
35. Rossig, L, et al. (2000). Congestive heart failure induces endothelial cell apoptosis: Protective role of carvedilol. *J Am Coll Cardiol*
36. Tramontano, AF, et al. (2010). Circulating endothelial microparticles in diabetes mellitus. *Mediators Inflamm*

37. Hashikabe, Y, et al. (2006). Aldosterone impairs vascular endothelial cell function. *J Cardiovasc Pharmacol*
38. Daugherty, A, et al. (2000). Angiotensin ii promotes atherosclerotic lesions and aneurysms in apolipoprotein e-deficient mice. *J Clin Invest*
39. Daugherty, A, et al. (2010). Angiotensin ii infusion promotes ascending aortic aneurysms: Attenuation by ccr2 deficiency in apoe-/- mice. *Clin Sci (Lond)*
40. Leibovitz, E, et al. (2009). Aldosterone induces arterial stiffness in absence of oxidative stress and endothelial dysfunction. *J Hypertens*
41. Chou, CH, et al. (2015). Aldosterone impairs vascular smooth muscle function: From clinical to bench research. *J Clin Endocrinol Metab*
42. Patel, VB, et al. (2014). Angiotensin-converting enzyme 2 is a critical determinant of angiotensin ii-induced loss of vascular smooth muscle cells and adverse vascular remodeling. *Hypertension*
43. Foffa, I, et al. (2012). Angiotensin-converting enzyme insertion/deletion polymorphism is a risk factor for thoracic aortic aneurysm in patients with bicuspid or tricuspid aortic valves. *J Thorac Cardiovasc Surg*
44. Matsumoto, T, et al. (2015). Effect of aldosterone-producing adenoma on endothelial function and rho-associated kinase activity in patients with primary aldosteronism. *Hypertension*
45. Rateri, DL, et al. (2011). Endothelial cell-specific deficiency of ang ii type 1a receptors attenuates ang ii-induced ascending aortic aneurysms in ldl receptor-/- mice. *Circ Res*
46. Rateri, DL, et al. (2012). Depletion of endothelial or smooth muscle cell-specific angiotensin ii type 1a receptors does not influence aortic aneurysms or atherosclerosis in ldl receptor deficient mice. *PLoS One*
47. Police, SB, et al. (2009). Obesity promotes inflammation in periaortic adipose tissue and angiotensin ii-induced abdominal aortic aneurysm formation. *Arterioscler Thromb Vasc Biol*
48. Tieu, BC, et al. (2009). An adventitial il-6/mcp1 amplification loop accelerates macrophage-mediated vascular inflammation leading to aortic dissection in mice. *J Clin Invest*
49. Tanaka, H, et al. (2015). Hypoperfusion of the adventitial vasa vasorum develops an abdominal aortic aneurysm. *PLoS One*
50. Sawada, H, et al. (2017). Smooth muscle cells derived from second heart field and cardiac neural crest reside in spatially distinct domains in the media of the ascending aorta-brief report. *Arterioscler Thromb Vasc Biol*

51. Escudero, P, et al. (2015). Combined treatment with bexarotene and rosuvastatin reduces angiotensin-ii-induced abdominal aortic aneurysm in apoe(-/-) mice and angiogenesis. *Br J Pharmacol*
52. Nataatmadja, M, et al. (2013). Angiotensin ii receptor antagonism reduces transforming growth factor beta and smad signaling in thoracic aortic aneurysm. *Ochsner J*
53. Habashi, JP, et al. (2006). Losartan, an at1 antagonist, prevents aortic aneurysm in a mouse model of marfan syndrome. *Science*
54. Gao, L, et al. (2016). The effect of losartan on progressive aortic dilatation in patients with marfan's syndrome: A meta-analysis of prospective randomized clinical trials. *Int J Cardiol*
55. Niessen, K, et al. (2008). Notch signaling in cardiac development. *Circ Res*
56. Noseda, M, et al. (2004). Notch activation results in phenotypic and functional changes consistent with endothelial-to-mesenchymal transformation. *Circ Res*
57. Tang, Y, et al. (2010). Notch and transforming growth factor-beta (tgfbeta) signaling pathways cooperatively regulate vascular smooth muscle cell differentiation. *J Biol Chem*
58. Krebs, LT, et al. (2000). Notch signaling is essential for vascular morphogenesis in mice. *Genes Dev*
59. High, FA, et al. (2009). Murine jagged1/notch signaling in the second heart field orchestrates fgf8 expression and tissue-tissue interactions during outflow tract development. *J Clin Invest*
60. High, FA, et al. (2008). Endothelial expression of the notch ligand jagged1 is required for vascular smooth muscle development. *Proc Natl Acad Sci U S A*
61. Niessen, K, et al. (2008). Slug is a direct notch target required for initiation of cardiac cushion cellularization. *J Cell Biol*
62. Koenig, SN, et al. (2017). Genetic basis of aortic valvular disease. *Curr Opin Cardiol*
63. Gillis, E, et al. (2017). Candidate gene resequencing in a large bicuspid aortic valve-associated thoracic aortic aneurysm cohort: Smad6 as an important contributor. *Front Physiol*
64. Garg, V, et al. (2005). Mutations in notch1 cause aortic valve disease. *Nature*
65. Koenig, SN, et al. (2015). Evidence of aortopathy in mice with haploinsufficiency of notch1 in nos3-null background. *J Cardiovasc Dev Dis*
66. Koenig, SN, et al. (2016). Endothelial notch1 is required for proper development of the semilunar valves and cardiac outflow tract. *J Am Heart Assoc*
67. Nigam, V, et al. (2009). Notch1 represses osteogenic pathways in aortic valve cells. *J Mol Cell Cardiol*
68. Kent, KC, et al. (2013). Genotype-phenotype correlation in patients with bicuspid aortic valve and aneurysm. *J Thorac Cardiovasc Surg*

69. Oudit, GY, et al. (2006). Calcific bicuspid aortic valve disease in a patient with cornelia de lange syndrome: Linking altered notch signaling to aortic valve disease. *Cardiovasc Pathol*
70. Maleki, S, et al. (2016). Mesenchymal state of intimal cells may explain higher propensity to ascending aortic aneurysm in bicuspid aortic valves. *Sci Rep*
71. Kostina, AS, et al. (2016). Notch-dependent emt is attenuated in patients with aortic aneurysm and bicuspid aortic valve. *Biochim Biophys Acta*
72. Wang, YW, et al. (2015). Combining detection of notch1 and tumor necrosis factor-alpha converting enzyme is a reliable biomarker for the diagnosis of abdominal aortic aneurysms. *Life Sci*
73. Hans, CP, et al. (2012). Inhibition of notch1 signaling reduces abdominal aortic aneurysm in mice by attenuating macrophage-mediated inflammation. *Arterioscler Thromb Vasc Biol*
74. Cheng, J, et al. (2014). Pharmacological inhibitor of notch signaling stabilizes the progression of small abdominal aortic aneurysm in a mouse model. *J Am Heart Assoc*
75. Zou, S, et al. (2012). Notch signaling in descending thoracic aortic aneurysm and dissection. *PLoS One*
76. Bogdan, C. (2001). Nitric oxide and the regulation of gene expression. *Trends Cell Biol*
77. Shin, WS, et al. (1996). Nitric oxide attenuates vascular smooth muscle cell activation by interferon-gamma. The role of constitutive nf-kappa b activity. *J Biol Chem*
78. Billaud, M, et al. (2017). Elevated oxidative stress in the aortic media of patients with bicuspid aortic valve. *J Thorac Cardiovasc Surg*
79. Gao, L, et al. (2012). Role of uncoupled endothelial nitric oxide synthase in abdominal aortic aneurysm formation: Treatment with folic acid. *Hypertension*
80. Lee, JK, et al. (2001). Experimental abdominal aortic aneurysms in mice lacking expression of inducible nitric oxide synthase. *Arterioscler Thromb Vasc Biol*
81. Siu, KL, et al. (2014). Circulating tetrahydrobiopterin as a novel biomarker for abdominal aortic aneurysm. *Am J Physiol Heart Circ Physiol*
82. Fan, LM, et al. (2014). Endothelial cell-specific reactive oxygen species production increases susceptibility to aortic dissection. *Circulation*
83. Lee, TC, et al. (2000). Abnormal aortic valve development in mice lacking endothelial nitric oxide synthase. *Circulation*
84. Licholai, S, et al. (2016). Unbiased profile of microrna expression in ascending aortic aneurysm tissue appoints molecular pathways contributing to the pathology. *Ann Thorac Surg*
85. Weber, M, et al. (2010). Mir-21 is induced in endothelial cells by shear stress and modulates apoptosis and enos activity. *Biochem Biophys Res Commun*
86. Kotlarczyk, MP, et al. (2016). Regional disruptions in endothelial nitric oxide pathway associated with bicuspid aortic valve. *Ann Thorac Surg*

87. Kim, YH, et al. (2016). Clinical implication of aortic wall biopsy in aortic valve disease with bicuspid valve pathology. *Korean J Thorac Cardiovasc Surg*
88. Aicher, D, et al. (2007). Endothelial nitric oxide synthase in bicuspid aortic valve disease. *Ann Thorac Surg*
89. Mohamed, SA, et al. (2012). Locally different endothelial nitric oxide synthase protein levels in ascending aortic aneurysms of bicuspid and tricuspid aortic valve. *Cardiol Res Pract*
90. Goumans, MJ, et al. (2017). Tgf-beta signaling in control of cardiovascular function. *Cold Spring Harb Perspect Biol*
91. Goumans, MJ, et al. (2002). Balancing the activation state of the endothelium via two distinct tgf-beta type i receptors. *Embo j*
92. Watabe, T, et al. (2003). Tgf-beta receptor kinase inhibitor enhances growth and integrity of embryonic stem cell-derived endothelial cells. *J Cell Biol*
93. Hirschi, KK, et al. (1998). Pdgf, tgf-beta, and heterotypic cell-cell interactions mediate endothelial cell-induced recruitment of 10t1/2 cells and their differentiation to a smooth muscle fate. *J Cell Biol*
94. Guo, X, et al. (2012). Transforming growth factor-beta and smooth muscle differentiation. *World J Biol Chem*
95. Brown, DJ, et al. (2005). Endothelial cell activation of the smooth muscle cell phosphoinositide 3-kinase/akt pathway promotes differentiation. *J Vasc Surg*
96. Goumans, MJ, et al. (2003). Activin receptor-like kinase (alk)1 is an antagonistic mediator of lateral tgfbeta/alk5 signaling. *Mol Cell*
97. Lebrin, F, et al. (2004). Endoglin promotes endothelial cell proliferation and tgf-beta/alk1 signal transduction. *Embo j*
98. Li, DY, et al. (1999). Defective angiogenesis in mice lacking endoglin. *Science*
99. Arthur, HM, et al. (2000). Endoglin, an ancillary tgfbeta receptor, is required for extraembryonic angiogenesis and plays a key role in heart development. *Dev Biol*
100. Nomura-Kitabayashi, A, et al. (2009). Endoglin is dispensable for angiogenesis, but required for endocardial cushion formation in the midgestation mouse embryo. *Dev Biol*
101. Wooten, EC, et al. (2010). Application of gene network analysis techniques identifies axin1/pdia2 and endoglin haplotypes associated with bicuspid aortic valve. *PLoS One*
102. Paloschi, V, et al. (2015). Aneurysm development in patients with a bicuspid aortic valve is not associated with transforming growth factor-beta activation. *Arterioscler Thromb Vasc Biol*
103. Rocchiccioli, S, et al. (2017). Hypothesis-free secretome analysis of thoracic aortic aneurysm reinforces the central role of tgf-beta cascade in patients with bicuspid aortic valve. *J Cardiol*

104. Rueda-Martinez, C, et al. (2017). Increased blood levels of transforming growth factor beta in patients with aortic dilatation. *Interact Cardiovasc Thorac Surg*
105. Hillebrand, M, et al. (2014). Total serum transforming growth factor-beta1 is elevated in the entire spectrum of genetic aortic syndromes. *Clin Cardiol*
106. Ramnath, NW, et al. (2015). Fibulin-4 deficiency increases tgf-beta signalling in aortic smooth muscle cells due to elevated tgf-beta2 levels. *Sci Rep*
107. Chen, X, et al. (2016). Tgf-beta neutralization enhances angii-induced aortic rupture and aneurysm in both thoracic and abdominal regions. *PLoS One*
108. Lazar-Karsten, P, et al. (2016). Generation and characterization of vascular smooth muscle cell lines derived from a patient with a bicuspid aortic valve. *Cells*
109. Matt, P, et al. (2009). Circulating transforming growth factor-beta in marfan syndrome. *Circulation*
110. Yao, EH, et al. (2009). A pyrrole-imidazole polyamide targeting transforming growth factor-beta1 inhibits restenosis and preserves endothelialization in the injured artery. *Cardiovasc Res*
111. Yung, LM, et al. (2016). A selective transforming growth factor-beta ligand trap attenuates pulmonary hypertension.
112. Morrell, NW, et al. (2009). Cellular and molecular basis of pulmonary arterial hypertension. *J Am Coll Cardiol*
113. Xu, W, et al. (2011). Endothelial cell energy metabolism, proliferation, and apoptosis in pulmonary hypertension. *Compr Physiol*
114. Sakao, S, et al. (2009). Endothelial cells and pulmonary arterial hypertension: Apoptosis, proliferation, interaction and transdifferentiation. *Respir Res*
115. Eddahibi, S, et al. (2006). Cross talk between endothelial and smooth muscle cells in pulmonary hypertension: Critical role for serotonin-induced smooth muscle hyperplasia. *Circulation*
116. Boettger, T, et al. (2009). Acquisition of the contractile phenotype by murine arterial smooth muscle cells depends on the mir143/145 gene cluster. *J Clin Invest*
117. Climent, M, et al. (2015). Tgfbeta triggers mir-143/145 transfer from smooth muscle cells to endothelial cells, thereby modulating vessel stabilization. *Circ Res*
118. Deng, L, et al. (2015). Microrna-143 activation regulates smooth muscle and endothelial cell crosstalk in pulmonary arterial hypertension. *Circ Res*
119. Hergenreider, E, et al. (2012). Atheroprotective communication between endothelial cells and smooth muscle cells through mirnas. *Nat Cell Biol*
120. Elia, L, et al. (2009). The knockout of mir-143 and -145 alters smooth muscle cell maintenance and vascular homeostasis in mice: Correlates with human disease. *Cell Death Differ*
121. Albinsson, S, et al. (2017). Patients with bicuspid and tricuspid aortic valve exhibit distinct regional microrna signatures in mildly dilated ascending aorta.

122. McDonald, J, et al. (2015). Hereditary hemorrhagic telangiectasia: Genetics and molecular diagnostics in a new era. *Front Genet*
123. Baeyens, N, et al. (2016). Defective fluid shear stress mechanotransduction mediates hereditary hemorrhagic telangiectasia. *J Cell Biol*
124. Asahara, T, et al. (1997). Isolation of putative progenitor endothelial cells for angiogenesis. *Science*
125. Ingram, DA, et al. (2004). Identification of a novel hierarchy of endothelial progenitor cells using human peripheral and umbilical cord blood. *Blood*
126. Vaturi, M, et al. (2011). Circulating endothelial progenitor cells in patients with dysfunctional versus normally functioning congenitally bicuspid aortic valves. *Am J Cardiol*
127. Thomas, PS, et al. (2012). Deficient signaling via alk2 (acvr1) leads to bicuspid aortic valve development. *PLoS One*
128. Yao, Y, et al. (2008). High-density lipoproteins affect endothelial bmp-signaling by modulating expression of the activin-like kinase receptor 1 and 2. *Arterioscler Thromb Vasc Biol*
129. Medici, D, et al. (2010). Conversion of vascular endothelial cells into multipotent stem-like cells. *Nat Med*
130. Pece-Barbara, N, et al. (2005). Endoglin null endothelial cells proliferate faster and are more responsive to transforming growth factor beta1 with higher affinity receptors and an activated alk1 pathway. *J Biol Chem*
131. Jin, Y, et al. (2017). Endoglin prevents vascular malformation by regulating flow-induced cell migration and specification through vegfr2 signalling.
132. Attias, D, et al. (2009). Comparison of clinical presentations and outcomes between patients with tgfbr2 and fbn1 mutations in marfan syndrome and related disorders. *Circulation*
133. Allinson, KR, et al. (2012). Endothelial expression of tgfbeta type ii receptor is required to maintain vascular integrity during postnatal development of the central nervous system. *PLoS One*
134. Topper, JN, et al. (1997). Vascular mads: Two novel mad-related genes selectively inducible by flow in human vascular endothelium. *Proc Natl Acad Sci U S A*
135. Dupuis, LE, et al. (2013). Insufficient versican cleavage and smad2 phosphorylation results in bicuspid aortic and pulmonary valves. *J Mol Cell Cardiol*
136. Itoh, F, et al. (2012). Smad2/smad3 in endothelium is indispensable for vascular stability via s1pr1 and n-cadherin expressions. *Blood*
137. Forstermann, U, et al. (2006). Endothelial nitric oxide synthase in vascular disease: From marvel to menace. *Circulation*
138. Shi, LM, et al. (2014). Gata5 loss-of-function mutations associated with congenital bicuspid aortic valve. *Int J Mol Med*

139. Bonachea, EM, et al. (2014). Rare gata5 sequence variants identified in individuals with bicuspid aortic valve. *Pediatr Res*
140. Laforest, B, et al. (2012). Genetic insights into bicuspid aortic valve formation. *Cardiol Res Pract*
141. Messaoudi, S, et al. (2015). Endothelial gata5 transcription factor regulates blood pressure.
142. Theodoris, CV, et al. (2015). Human disease modeling reveals integrated transcriptional and epigenetic mechanisms of notch1 haploinsufficiency. *Cell*
143. Qu, XK, et al. (2014). A novel nkx2.5 loss-of-function mutation associated with congenital bicuspid aortic valve. *Am J Cardiol*
144. Guo, DC, et al. (2007). Mutations in smooth muscle alpha-actin (acta2) lead to thoracic aortic aneurysms and dissections. *Nat Genet*

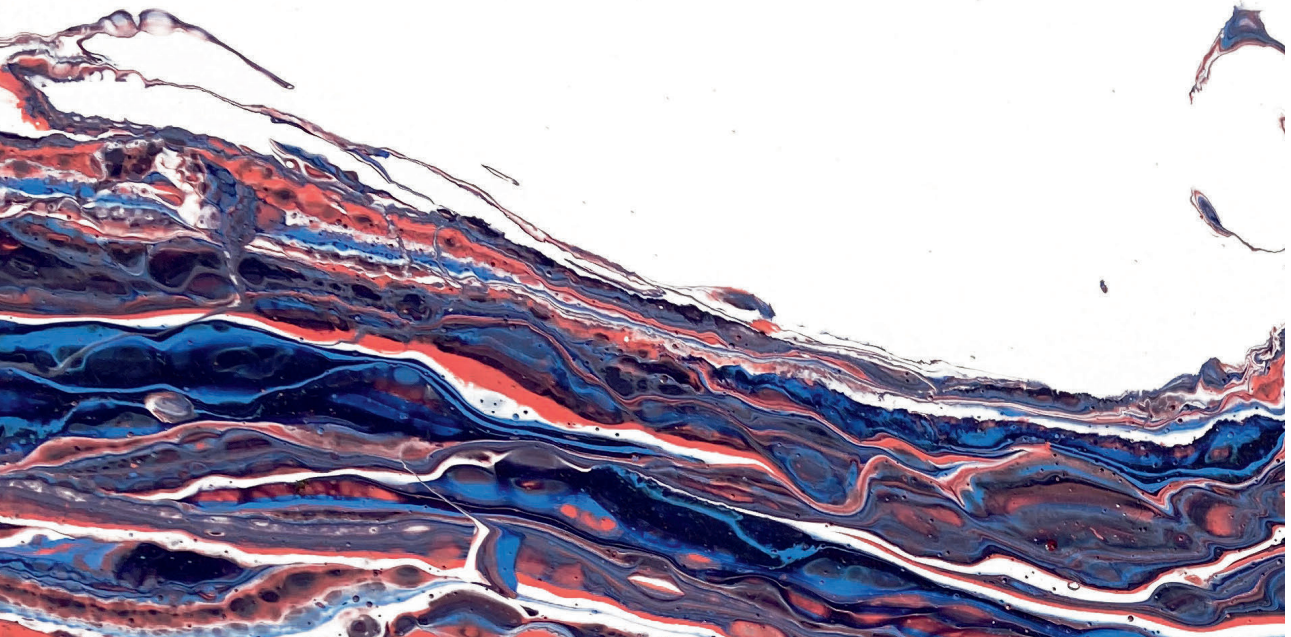

# Chapter 3

## Higher expression of inflammatory and EndoMT markers in endothelial cells in the inner aortic curve of bicuspid aortic valve patients

**Vera van de Pol[1], Zuzana Miranovova[1], Nimrat Grewal[2], Adri C. Gittenberger-de Groot[3,4], Evaldas Girdauskas[5], Marie-José Goumans[1], Marco C. DeRuiter[3]**

[1] Department of Cell and Chemical Biology, Leiden University Medical Center, Leiden, The Netherlands
[2] Department of Cardiothoracic Surgery, Leiden University Medical Center, Leiden, The Netherlands
[3] Department of Anatomy and Embryology, Leiden University Medical Center, Leiden, The Netherlands
[4] Department of Cardiology, Leiden University Medical Center, Leiden, The Netherlands
[5] Department of Cardiac Surgery, Heart Center, Zentralklinik Bad Berka, Germany

*Study in progress*

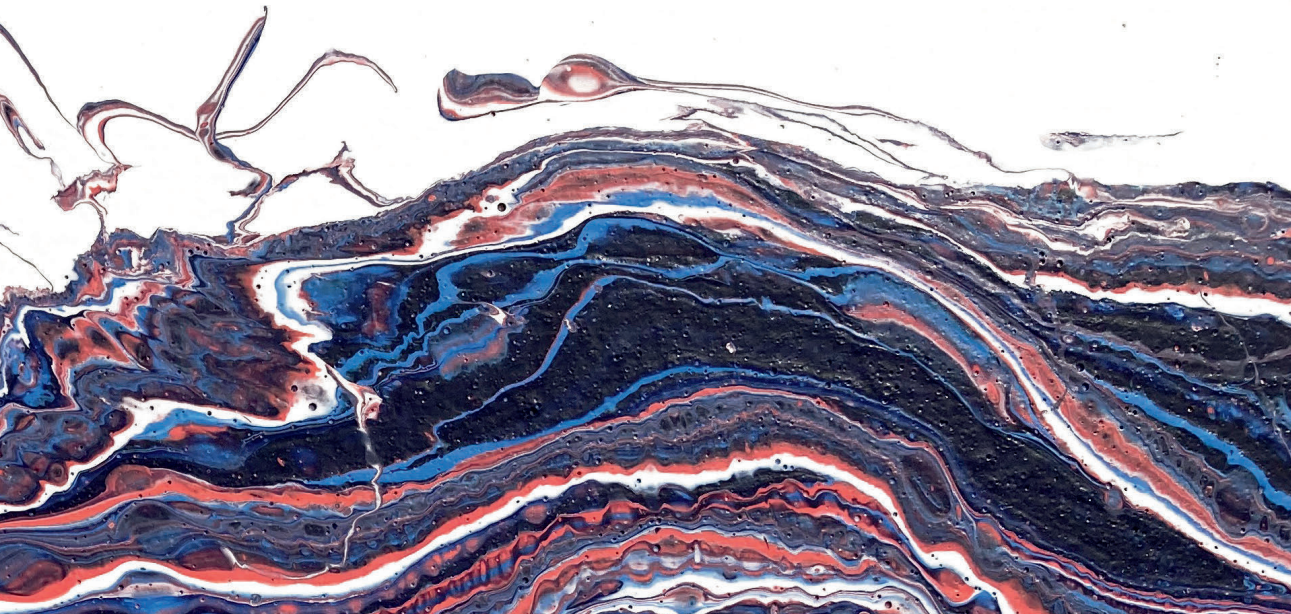

## Abstract

Bicuspid aortic valve (BAV), in which the aortic valve consists of two leaflets instead of the usual three, is the most common congenital heart defect. The shape of a BAV causes a different blood flow within the ascending aorta compared to a tricuspid aortic valve, exposing one side of the aortic wall to an increased blood flow velocity ("jet side") and the opposing side to an oscillatory flow ("non-jet side"). Different types of flow can affect the endothelium and thereby vessel wall homeostasis, but it is not known whether the altered flow in BAV affects endothelial cell (EC) phenotype in the aorta. Therefore, the aim of this study was to investigate if these flow differences in BAV patients activate the endothelium.

Aortic samples from the two opposing sides of the aorta were collected during surgery and the intima and inner media were histologically examined. The structural organization was assessed measuring the amount of elastin and the intimal thickness while the activation was studied with a staining for von Willebrand Factor (vWF). In addition, markers of endothelial-to-mesenchymal-transition (EndoMT) (SNAI1), proliferation (KI67) and inflammation (p50) were investigated in $PECAM^+$ ECs.

Whereas there were no observable differences in $elastin^+$ surface area in the intima and inner media between jet and non-jet side, we observed a significantly larger area of tissue containing deposited vWF at the jet side of the aorta of BAV patients compared to the non-jet side. In contrast, the $PECAM^+$ ECs showed a trend towards higher expression of SNAI1, KI67 and p50 at the non-jet side compared to the jet side, indicating increased endothelial activation at the non-jet side. In conclusion, the endothelium at the jet site of the BAV aorta shows a different protein expression of activation markers compared to the non-jet side of the aorta.

## Introduction

Bicuspid aortic valve (BAV), a congenital defect in which the aortic valve consists of two leaflets instead of the usual three, is the most common congenital heart defect occurring in approximately 1-2% of the population. Although a BAV can function normally, BAV patients have an increased prevalence of thoracic aortic aneurysm and rupture, as well as aortic valve regurgitation and stenosis [1].

The thoracic aorta in BAV patients dilates because of a loss of structural integrity in the medial layer of the aorta called medial degeneration. Medial degeneration is the process during which elastic lamellae become fragmented (by elastases produced by smooth muscle cells (SMCs) and inflammatory cells or decreased elastin turnover) and SMCs undergo phenotypic switching from a contractile to an activated synthetic phenotype [2-5]. Despite extensive research, it is not well understood how medial degeneration is initiated.



Using 4D MRI it is shown that the disturbed/malformed opening of the BAV alters the blood flow causing a focussed 'jet' that hits the aortic wall, thereby locally increasing wall shear stress [6,7]. Conversely, the opposing side of the aorta is subjected to turbulent flow. The flow-hypothesis is based on these observations and states that the aortic dilation in BAV patients is caused by the altered flow. Supporting this hypothesis are, amongst others, results showing that local differences in flow patterns relate to the underlying histopathological logical features [8-12].

Different types of flow are known to highly affect endothelial function, which in turn affects vessel wall homeostasis. Laminar flow maintains a quiescent EC state, promoting vessel wall homeostasis, whereas turbulent flow can activate the endothelium, stimulating vascular remodeling. Activated ECs are part of a normal vascular healing response but also of many different cardiovascular diseases. Activated ECs are characterized by an increased proliferation rate, expression of inflammatory markers and secretion of Von Willebrand factor [13-15]. To date, little research has been performed to elucidate the role of endothelial cells in the pathogenesis of BAV related aortic aneurysm.

To study the effect of flow differences on the aortic structure, we made use of a collection of aortic samples from the jet and non-jet side of the aorta from BAV patients. A previous study using these specimens demonstrated a dispersion of the elastic lamellae and decreased $\alpha$-smooth muscle actin ($\alpha$SMA) expression in the media located at the jet side of the aorta [12]. To relate the vessel wall structure to endothelial activation, we investigated elastin morphology in the vessel wall located directly underneath the endothelium. Moreover, we focused on endothelial activation caused by flow differences within the aortas of BAV patients by measuring vWF deposition and the expression of the inflammatory

marker p50, the proliferation marker KI-67 and the EndoMT marker SNAI1 in ECs at the jet and non-jet side of the BAV aortic wall.

## Results

### More vWF deposition at the jet side of the BAV aorta

To study the intima/inner media organization and vWF secretion, samples from the jet and non-jet side of the aorta of 17 BAV patients were analysed (Table 1). The gender distribution and prevalence of type 1 and type 2 BAV of these patients reflect the known population distributions [16,17].

**Table 1.** Patient information

| | BAV patients (n=17) |
|---|---|
| Age at time of operation, years (SD) | 55.5 (9.8) |
| Female gender | 23.5% |
| Aortic diameter, mm (SD) | 44.6 (7.8) |
| Type I fusion | 82.4% |
| Type II fusion | 17.6% |

Since activated ECs can secrete vWF, not only in the blood but also into the tissue, the expression of vWF is not limited to the ECs but can also be identified in the subendothelial extracellular matrix. Before quantifying the VWF expression we noticed that the areas positive for vWF show large variation between patients as well as within the aortic wall of one patient. Because of spatial differences within the tissue samples, both the average (A) percentage of vWF positive area per aortic wall sample and the area with the lowest (L) and highest (H) percentage positive for vWF were used for the analysis. All three approaches to analyse the expression showed significantly higher areas positive for vWF at the jet side compared to the non-jet side (jet: M=16.6% (A) | 11.7% (L)| 22.7% (H), SEM=2.7% (A)| 2.2%(L)| 3.7% (H), non-jet: M=9.5% (A)| 6.1% (L)| 12.6% (H), SEM=1.5% (A)| 1.3% (L)| 2.2% (H), p=0.035 (A)| 0.013 (L)| 0.046 (H)) (Figure 1A,B and Supplemental figure 1A,B).

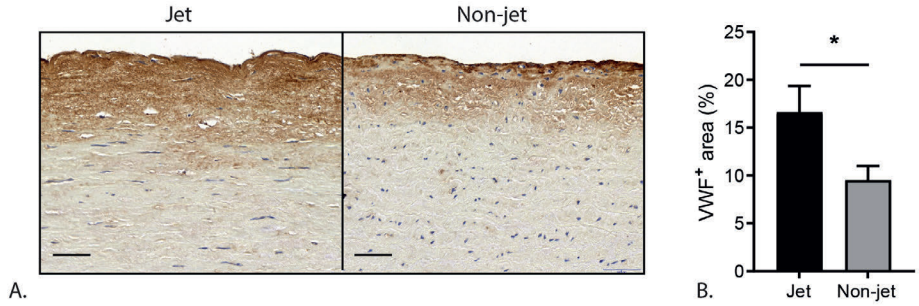


**Figure 1. Intimal and inner medial expression of vWF in jet and non-jet aortic wall samples of BAV patients.** A. Representative pictures of the vWF staining in jet and non-jet aortic wall samples from BAV patients. B. Quantification of the average vWF$^+$ area in jet and non-jet aortic wall samples as % of the surface area of the inner media (500 $\mu$m). Bar indicates 50 $\mu$m. *p>0.05.



## Amount of elastin fibers and intimal thickness do not differ between jet and non-jet side

Taking a closer look at the elastin morphology, we observed thick and thin elastin fibers (Figure 2A). Resorcin-Fuchsin (RF) staining was used to visualize the elastic fibers. To determine whether differences in the amount of elastin co-occurred with differences in flow, the RF$^+$ surface area was quantified. However, there were no differences in the RF$^+$ surface area between jet and non-jet side (Figure 2B). To study intimal growth the thickness of the intimal layer up to the first elastic lamella was measured. No differences between jet and non-jet intimal thickness was observed (Figure 2C).

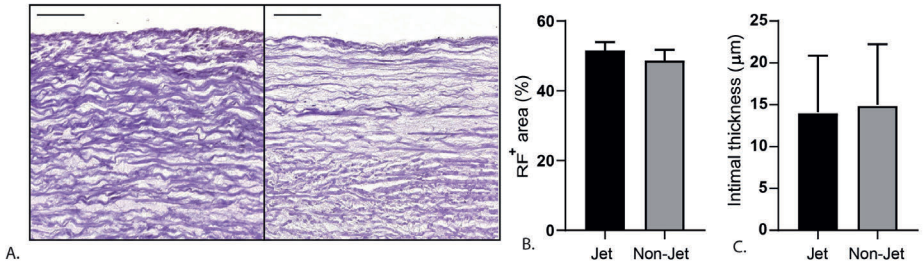


**Figure 2. Intimal and inner media analysis on jet and non-jet side of BAV patient aortas.** A. Representative pictures of the RF staining showing thick (left) and thin (right) elastic lamellae. B. Graph showing data of RF quantification. C. Thickness of layer up to the first elastic lamella in jet and non-jet side of BAV patients. Bar indicates 50 $\mu$m. *p>0.05.

### Trends towards higher activation at the non-jet side

Because immunohistochemistry for vWF can indicate both secreted vWF and vWF present in ECs, vWF expression in tissue is a limited indicator for EC activation. Therefore, we used patient specimens in which PECAM$^+$ ECs could be detected to further study endothelial activation. Due to the fragile nature of the endothelium, only limited samples still contained PECAM$^+$ ECs (n=6, Table 2). No significant differences were observed in the patient characteristics between the total sample population and the selected samples with ECs (data not shown).

**Table 2.** Patient information selection for PECAM$^+$ ECs

| | BAV patients (n=6) |
|---|---|
| Age at time of operation*, years (SD) | 55.8 (12.8) |
| Female gender*, | 16.7% |
| Aortic diameter*, mm (SD) | 52.5 (4.8) |
| Type I fusion | 83% |
| Type II fusion | 17% |

To standardize the area in which the ECs were quantified, the location with the least structured organization and αSMA and elastic lamellae in the inner media was selected for analysis. In order to assess the state of inflammation in the aortic endothelium, a co-staining for both PECAM and p50, a subunit of NFκB, was performed (Figure 3A,B). Although an increase of p50$^+$ PECAM$^+$ ECs in the non-jet side was observed, this difference did not reach significance. Signaling pathways for proliferation (ki67) and EndoMT (SNAI1) showed the same trend towards higher expression in PECAM$^+$ ECs of the non-jet side when compared to the jet side of BAV aorta (Figure 3C-F).

Because KLF2 and KLF4 have been shown to be important flow-responsive transcription factors, we determined their expression [18]. Although KLF2 and KLF4 positive ECs were present in multiple samples, at the location with the least structured organization and αSMA and elastic lamellae in the inner media no KLF2/KLF4 expression was observed (Supplemental figure 2A/B and data not shown).

## Discussion

The usual laminar flow in the aorta is altered in BAV patients due to the different leaflet morphology. Instead, the aortic wall is exposed to a high velocity jet flow on one side and an oscillatory flow on the opposing side in BAV patients. This study focussed on the effect of both the high velocity jet flow and oscillatory

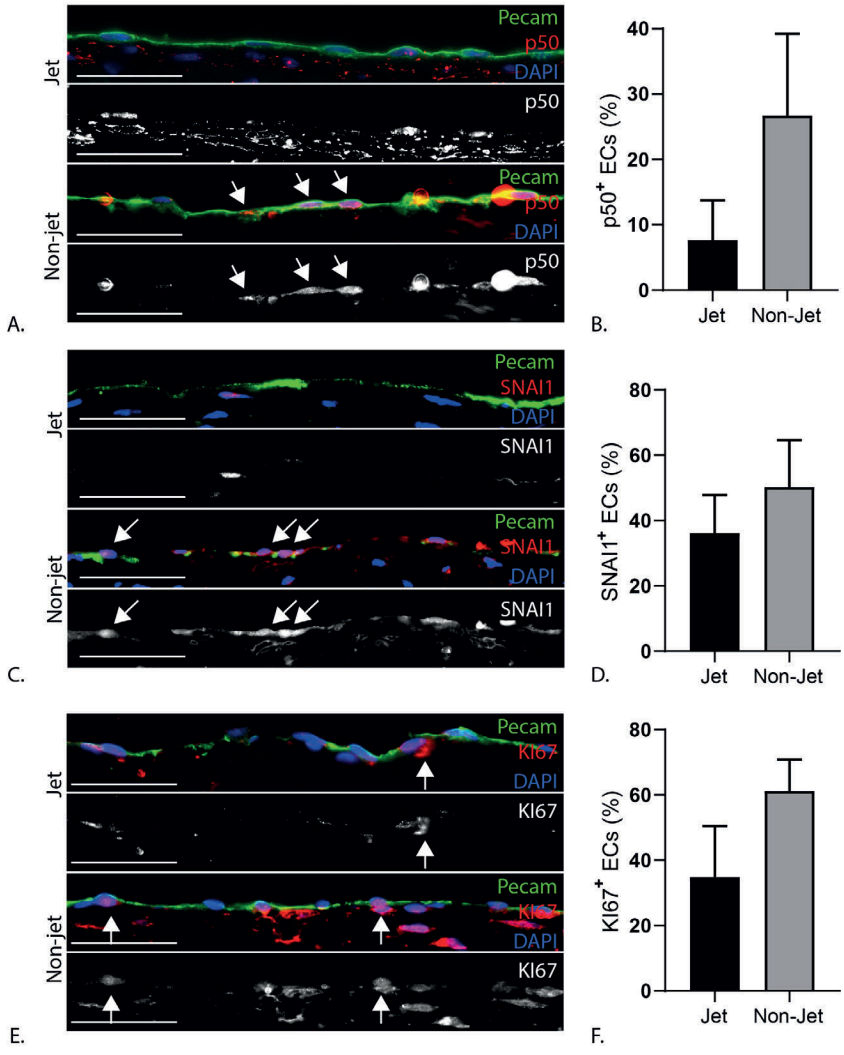


**Figure 3. Endothelial activation in the jet and non-jet side of BAV aorta.** A,C,E. Representative images showing Pecam staining combined with p50 (A), SNAI1 (B) and KI67 (E) in BAV tissue from jet and non-jet side. B,D,F. Quantifications of the p50 (B), SNAI1 (E) and KI67 (F) positive ECs on jet vs non-jet side. Bar indicates 50 $\mu$m. Arrows indicate double positive cells.

flow on endothelial activation in the aorta of BAV patients. Samples from aortas of BAV patients showed a higher amount of vWF expression in the intima and inner media at the jet side of the aorta compared to the non-jet side. In contrast, a trend towards increased expression of inflammatory, EndoMT and proliferation pathways in was observed in PECAM$^+$ECs exposed to oscillatory flow at the non-

jet side. The flow responsive proteins KLF2 and KLF4 were only sporadically expressed in these dilated aortic walls.

ECs are able to regulate vWF secretion and secrete vWF both under basal conditions and in an activated state [19,20]. Flow and wall shear stress are important determinants in vWF biochemistry and secretion. Since an increased wall shear stress has been shown to stimulate vWF function and secretion, our results could indicate a higher activation of the endothelium at the jet side compared to the non-jet side [21]. Most knowledge on vWF concerns vWF secreted in the blood while only little is known on the function and biochemistry of vWF deposited within the tissue. vWF can be secreted when endothelial cells are activated, but the diverse conditions in which vWF is secreted are not fully known. In addition, it is unclear how long secreted vWF remains detectable in tissue. Therefore, the cause of vWF deposition is difficult to conclude from a staining, limiting direct conclusions on the pathological endothelial activation based solely on vWF secretion in the aortic tissue. Interestingly, it has been shown that vWF secretion can cause an increase of EndoMT in osteosarcoma derived ECs *in vitro [22]*. However, in our data no relation between $vWF^+$ area and $SNAI1^+$ ECs was observed. This may be explained by a separation of these different processes by time or could be caused by the limited sample numbers.

In contrast to previous results obtained by studying the media of these samples, we did not find differences in elastin surface area in the intima and inner media between the jet and non-jet side [23]. A previous study by Guzzardi et al. reported that increased wall shear stress correlates with decreased elastin content in BAV aorta [24]. However, our results are obtained by focussing specifically on the inner 250 $\mu$m of the aorta (inner media/intima) whereas Guzzardi et al. used the elastin content of the entire vessel wall. These differences could indicate that the degenerative processes locate mainly in the middle of the vessel wall.

To study the endothelial protein expression in relation to laminar jet and oscillatory flow, ECs were labelled with an antibody against $PECAM^+$. Only limited samples were available in which both the jet and non-jet side of the aorta had enough $PECAM^+$ ECs to analyse. The characteristics of the patients of which the samples qualified do not significantly differ from the total population. Therefore, the lack of ECs in the majority of the samples is likely due to the fragile nature of the intima and the damage it sustains during surgical removal of the tissue.

Endothelial were shown to upregulate gene expression of pathways such as proliferation and organization of the cytoskeleton upon altered flow [25]. Prolonged exposure to a new flow speed or direction will cause adaptation of the ECs and reduce the activation of these pathways back to baseline [26]. Constantly changing oscillatory flow however, causes a chronically activated and patho-

logical phenotype [27]. The results in this study support the hypothesis that this activated EC state is caused by the oscillatory flow conditions in the BAV aorta at the non-jet side, but not by the constant laminar jet flow at the opposing side.

The BAV samples show a trend towards a higher endothelial p50 expression at the non-jet side compared to the jet side. This result is in line with previous studies on inflammation and oscillatory flow, showing an increased inflammatory response in ECs when there are exposed to oscillatory flow [13,28,29]. The role of inflammation in medial degeneration of BAV the aorta remains disputed [30,31]. However, no study thus far has focussed on the endothelial expression of inflammatory markers in the aorta. Previously we have shown that, after exposure to the inflammatory stimulus TNF$\alpha$, TAV endothelial colony forming cells (ECFCs) upregulate the expression of phosphate transporter 2 (PiT2), whereas BAV ECFCs did not increase the expression of PiT2 at all [32]. Therefore, it would be of future interest to study how an increase in the NFκB signaling pathway, will affect the aortic EC response and the underlying vascular remodeling in BAV patients.



Research has shown that oscillatory flow can cause an increase of SNAI1 in endothelial cells [33]. Consistent with this, our data indicates a trend towards increased expression of SNAI1 in endothelial cells at the non-jet side of BAV aortas, indicating an activated phenotype. Interestingly, we observed SNAI1 expression in adventitial vessels in both the jet and non-jet samples. This observation suggests ongoing EndoMT in the adventitia, but requires further evaluation. In addition, a trend towards higher KI67$^+$ ECs at the BAV non-jet side could be observed. However, although proliferation is associated with an activated EC phenotype *in vitro*, it is unclear what a normal proliferative rate is *in vivo* and therefore requires further research [34].

Vasoprotective transcription factors KLF2 and KLF4 have been reported to be upregulated by laminar shear stress [35,36]. Since the analysis in this study focussed on the location with the most severe morphology, the lack of KLF2 and KLF4 in the endothelium studied can be a result of a life long exposure to these flow conditions and/or advanced pathogenesis. This hypothesis is supported by the presence of endothelial expression of KLF2 and KLF4 at distant locations, where the vascular remodeling was less severe.

These results together support the hypothesis that in BAV patients the ECs at the non-jet side of the aorta have an activated phenotype. However, since vWF$^+$ area is higher in the jet side and EC proliferation, inflammation and EndoMT are higher at the non-jet side, further research should be performed to relate activation of ECs to expression vWF expression.

## Methods

### Patient material

For this study, sample collection and handling were carried out according to the official guidelines of the Medical Ethical Committee of the Central Hospital Bad Berka [12]. All patients gave written informed consent. Aortic samples from BAV (n=23) patients were collected during aortic and aortic valve replacement surgery with or without concomitant proximal aortic replacement. Jet-side and non-jet side of the ascending aorta were determined based on preoperative MRI analysis. A valve was considered a BAV if only two commissures were present. Patients with genetic disorders (e.g. Marfan syndrome) were excluded. Aortic valve stenosis and regurgitation were defined according to the valvular guidelines [37]. The diameter of the proximal aorta was measured preoperatively by means of transthoracic echocardiography and MRI. Dilation was defined by reaching an ascending aortic wall diameter of 45 mm or more [38]. Samples were fixed in 4% formalin (24 hours) and decalcified in a formic acid-formate buffer (120 hours) prior to embedding in paraffin. Transverse sections (5 $\mu$m) were mounted on Starfrost slides (Klinipath, Radnor, PA, USA).

### Elastin visualization

Sections were deparaffinised, rehydrated and incubated with Weigert's resorcin fuchsin (RF, Klinipath) according to the manufacturer's protocol to study the elastin morphology of the vessel wall.

### Immunohistochemistry

To stain for vWF, a staining based on DAB was used. To this end, sections were deparaffinised, rehydrated and endogenous peroxidase activity was inhibited by exposure to 0.3% $H_2O_2$ for 20 min before antigen retrieval by heating the sections to 97°C in sodium citrate buffer (pH 6.0) for 11 minutes. Subsequently, sections were incubated o/n at rt with the primary antibodies diluted in PBS-Tween-20 (PBST) containing 1% bovine serum albumin (BSA, A8022; Sigma-Aldrich, St Louis, MO, USA, 1%BSA-PBST, polyclonal rabbit anti-vWF antibody (A 0082). A list of all primary antibodies can be found in Supplemental Table 1. The following day, the sections were incubated with a biotin-conjugated secondary antibody in PBST containing 1,5% normal goat serum for 60 minutes, followed by a 75 minute incubation with the ABC-cocktail (1:100 compound A and 1:100 compound B, Vector Laboratories, Burlingame, Calif; PK610) after a pre-incubation of the cocktail of at least 45 minutes. For visualization, slides were incubated with 400mg/ml 3,30-diaminobenzidine tetrachloride (Sigma-Aldrich Chemie,

Buchs, Switzerland; D5637) dissolved in Tris-maleate buffer with 20 ml of H2O2 for 5 minutes. Counterstaining was performed using 0,1% haematoxylin (Merck, Darmstadt, Germany) for 5 seconds. After dehydration, the sections were mounted using Entellan (Merck).

For the immunofluorescent stainings, sections were deparaffinised, rehydrated and antigen retrieval was performed as described above. Sections were incubated o/n at room temperature with the primary antibodies diluted in 1%BSA-PBST before incubating the with the secondary antibodies diluted in 1%BSA-PBST for 40 minutes and 4',6-Diamidine-2'-phenylindole dihydrochloride (DAPI, D3571 Life Technologies 1:1000) for 5 minutes to stain for nuclei. Sections were mounted using Prolong Gold (Invitrogen, Carlsbad, CA, USA; P36934) Between the staining steps, all sections were rinsed in PBS (2x) and PBST (1x). All sections used for quantitative analysis were stained at the same time.



**Sample selection for double positive analysis**

Sections from all of the patients were stained for PECAM and $\alpha$-SMA and scanned with Panoramic 250 Slidescanner (3DHISTECH Ltd.) at 40x magnification. Additionally, only the patient samples containing continuous a endothelial layer on both the jet side and non-jet side were selected for further examination.

**Quantification of images**

No images were taken from areas with ruptured intimal tissue. To quantify the $vWF^+$ positive area the surface area positive for vWF the stained sections were scanned with a Panoramic 250 Slidescanner. A representative number of images of the intima and media (up to 500 $\mu$m from the intimal edge) were taken randomly divided over the section. The number of images varied based on the size of the tissue but was at least 2 per sample. The area of vWF was calculated by determining threshold appropriate to each individual image in a blinded manner using ImageJ2. The percentage of $vWF^+$ area per image was calculated. An average of all images per tissue as well as the images with the lowest and highest percentages were used in the analysis.

To quantify the thickness of the intima, the inner elastic lamellae up to the lumen was measured every 100 $\mu$m. There were at least 2 measurements per sample. EC positive for PECAM and ECs double positive for PECAM and either p50, SNAI1 or ki67 were quantified. To standardize the area in which the ECs were quantified, the location with the least structured SMC and elastic lamellar organization in the inner media was selected. All subsequent analysis was focused on endothelium in the selected location. Images were made using a Leica DM500 microscope and the 40x magnification lens. The positive ECs in

the images were manually counted twice by two different, blinded observers. Discrepancies in the observations were studied until a consensus was achieved.

**Statistical analysis**

A paired sample t-test was performed to assess the flow induced differences between the two aortic wall sides. Statistical analysis was performed using the GraphPad Prism 7 (GraphPad Software, Inc.), applying a significance level of $p < 0.05$. Graphs are depicted with standard error of the mean (SEM).

**Acknowledgements**

We gratefully thank dr. R. Fontijn for providing the KLF2 antibody.

**Funding**

This work is supported by the Dutch Heart Foundation (BAV consortium grant 31190).

## Supplementals

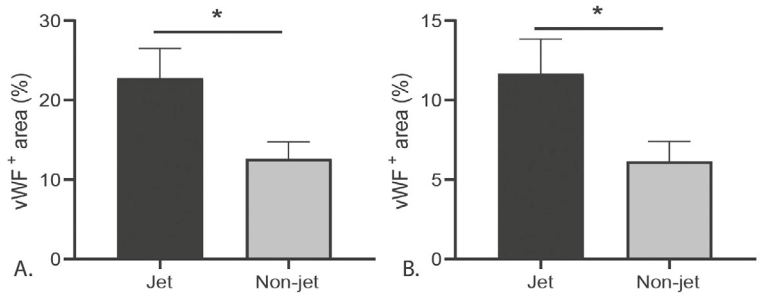


**Supplemental figure 1. Quantification of intimal and inner media vWF+area on jet and non-jet side of BAV patient aortas.** A,B. Quantification using the highest measurement of vWF+ area per sample (A) or the lowest measurement of vWF+ area per sample (B) as % of the surface area of the inner media (500 $\mu$m). *p>0.05.



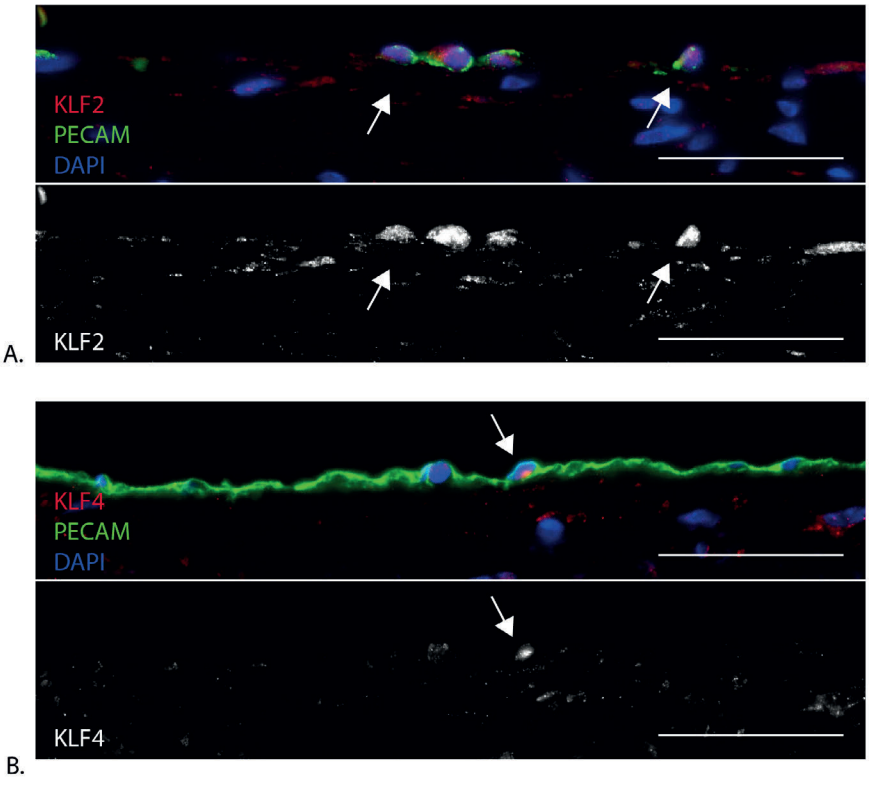


**Supplemental figure 2. Pictures of KLF2/4 staining.** A. KLF2 positive ECs in a remote area. B. KLF4 positive ECs in a remote area. Bar indicates 50 $\mu$m. Arrows indicate KLF2/4 -PECAM positive cells.

**Supplemental table 1.** List of primary antibodies

| Target | Host | Supplier | Reference | Concentration |
|---|---|---|---|---|
| PECAM-1 | Rabbit | Santa Cruz | SC-1506-R | 1:500 |
| PECAM-1 | Goat | R&D Systems | AF3628 | 1:1000 |
| SNAI1 | Goat | R&D Systems | AF3639 | 1:100 |
| NFκB p50 | Mouse | Santa Cruz | SC-7386 | 1:200 |
| α-SMA | Mouse | Sigma-Aldrich | A2547 | 1:10.000 |
| KI-67 | Rabbit | ABcam | AB15580 | 1:300 |
| KLF2 | Rabbit | Manufactured at VUmc | * | 1:200 |
| KLF4 | Rabbit | ABcam | AB34814 | 1:200 |

## References


1. Ward, C. (2000). Clinical significance of the bicuspid aortic valve. *Heart*
2. Wang, X, et al. (2005). Decreased expression of fibulin-5 correlates with reduced elastin in thoracic aortic dissection. *Surgery*
3. Tsamis, A, et al. (2013). Elastin and collagen fibre microstructure of the human aorta in ageing and disease: A review. *Journal of the Royal Society, Interface*
4. Cohen, JR, et al. (1992). Smooth muscle cell elastase, atherosclerosis, and abdominal aortic aneurysms. *Ann Surg*
5. Nathan, CF. (1987). Secretory products of macrophages. *J Clin Invest*
6. Barker, AJ, et al. (2010). Quantification of hemodynamic wall shear stress in patients with bicuspid aortic valve using phase-contrast mri. *Annals of biomedical engineering*
7. Barker, AJ, et al. (2012). Bicuspid aortic valve is associated with altered wall shear stress in the ascending aorta. *Circ Cardiovasc Imaging*
8. Cotrufo, M, et al. (2005). Different patterns of extracellular matrix protein expression in the convexity and the concavity of the dilated aorta with bicuspid aortic valve: Preliminary results. *J Thorac Cardiovasc Surg*
9. Bissell, MM, et al. (2013). Aortic dilation in bicuspid aortic valve disease: Flow pattern is a major contributor and differs with valve fusion type. *Circ Cardiovasc Imaging*
10. Mahadevia, R, et al. (2014). Bicuspid aortic cusp fusion morphology alters aortic three-dimensional outflow patterns, wall shear stress, and expression of aortopathy. *Circulation*
11. Atkins, SK, et al. (2014). Etiology of bicuspid aortic valve disease: Focus on hemodynamics. *World J Cardiol*
12. Grewal, N, et al. (2017). The effects of hemodynamics on the inner layers of the aortic wall in patients with a bicuspid aortic valve. *Integr Mol Med*
13. Chatzizisis, YS, et al. (2007). Role of endothelial shear stress in the natural history of coronary atherosclerosis and vascular remodeling: Molecular, cellular, and vascular behavior. *J Am Coll Cardiol*
14. Wang, C, et al. (2013). Endothelial cell sensing of flow direction. *Arterioscler Thromb Vasc Biol*
15. Wagner, DD, et al. (2008). The vessel wall and its interactions. *Blood*
16. Sievers, HH, et al. (2014). Toward individualized management of the ascending aorta in bicuspid aortic valve surgery: The role of valve phenotype in 1362 patients. *J Thorac Cardiovasc Surg*
17. Kong, WKF, et al. (2020). Sex differences in bicuspid aortic valve disease. *Progr Cardiovasc Dis*
18. Nayak, L, et al. (2011). "Go with the flow": How krüppel-like factor 2 regulates the vasoprotective effects of shear stress. *Antioxid Redox Signal*

19. Brott, DA, et al. (2014). Evaluation of von willebrand factor and von willebrand factor propeptide in models of vascular endothelial cell activation, perturbation, and/or injury. *Toxicol Pathol*
20. Lenting, PJ, et al. (2015). Von willebrand factor biosynthesis, secretion, and clearance: Connecting the far ends. *Blood*
21. Gogia, S, et al. (2015). Role of fluid shear stress in regulating vwf structure, function and related blood disorders. *Biorheology*
22. Ling, J, et al. (2019). Feedback modulation of endothelial cells promotes epithelial-mesenchymal transition and metastasis of osteosarcoma cells by von willebrand factor release. *J Cell Biochem*
23. Grewal, N, et al. (2019). The role of hemodynamics in bicuspid aortopathy: A histopathologic study. *Cardiovasc Pathol*
24. Guzzardi, DG, et al. (2015). Valve-related hemodynamics mediate human bicuspid aortopathy: Insights from wall shear stress mapping. *J Am Coll Cardiol*
25. Peters, DG, et al. (2002). Genomic analysis of immediate/early response to shear stress in human coronary artery endothelial cells. *Physiol Genomics*
26. Takahashi, M, et al. (1997). Mechanotransduction in endothelial cells: Temporal signaling events in response to shear stress. *J Vasc Res*
27. Chatzizisis, YS, et al. (2007). Role of endothelial shear stress in the natural history of coronary atherosclerosis and vascular remodeling: Molecular, cellular, and vascular behavior. *Journal of the American College of Cardiology*
28. Zamboni, P, et al. (2016). Oscillatory flow suppression improves inflammation in chronic venous disease. *J Surg Res*
29. Wang, F, et al. (2019). Oscillating flow promotes inflammation through the tlr2-tak1-ikk2 signalling pathway in human umbilical vein endothelial cell (huvecs). *Life Sci*
30. Tobin, SW, et al. (2019). Novel mediators of aneurysm progression in bicuspid aortic valve disease. *J Mol Cell Cardiol*
31. Grewal, N, et al. (2016). Histopathology of aortic complications in bicuspid aortic valve versus marfan syndrome: Relevance for therapy? *Heart and vessels*
32. van de Pol, V, et al. (2019). Endothelial colony forming cells as an autologous model to study endothelial dysfunction in patients with a bicuspid aortic valve. *Int J Mol Sci*
33. Bjorck, HM, et al. (2018). Altered DNA methylation indicates an oscillatory flow mediated epithelial-to-mesenchymal transition signature in ascending aorta of patients with bicuspid aortic valve. *Sci Rep*
34. Li, Y-SJ, et al. (2005). Molecular basis of the effects of shear stress on vascular endothelial cells. *Journal of Biomechanics*
35. Dekker, RJ, et al. (2006). Klf2 provokes a gene expression pattern that establishes functional quiescent differentiation of the endothelium. *Blood*

36. Villarreal, G, Jr., et al. (2010). Defining the regulation of klf4 expression and its downstream transcriptional targets in vascular endothelial cells. *Biochem Biophys Res Commun*
37. Baumgartner, H, et al. (2009). Echocardiographic assessment of valve stenosis: Eae/ase recommendations for clinical practice. *J Am Soc Echocardiogr*
38. Hiratzka, LF, et al. (2016). Surgery for aortic dilatation in patients with bicuspid aortic valves: A statement of clarification from the american college of cardiology/american heart association task force on clinical practice guidelines. *J Am Coll Cardiol*

# Chapter 4

## Endothelial colony forming cells as an autologous model to study endothelial dysfunction in patients with a bicuspid aortic valve

**Vera van de Pol[1], Lidia R. Bons[2], Kirsten Lodder[1], Konda Babu Kurakula[1], Gonzalo Sanchez-Duffhues[1], Hans-Marc J. Siebelink[3], Jolien W. Roos-Hesselink[2], Marco C. DeRuiter[4], Marie José Goumans[1,*]**

[1]Department of Cell and Chemical Biology, Leiden University Medical Center, Leiden, The Netherlands
[2]Department of Cardiology, Erasmus Medical Center, Rotterdam, The Netherlands
[3]Department of Cardiology, Leiden University Medical Center, Leiden, The Netherlands
[4]Department of Anatomy and Embryology, Leiden University Medical Center, Leiden, The Netherlands

*Published: International journal of Molecular Sciences, 2019 | 20: p. 3251*

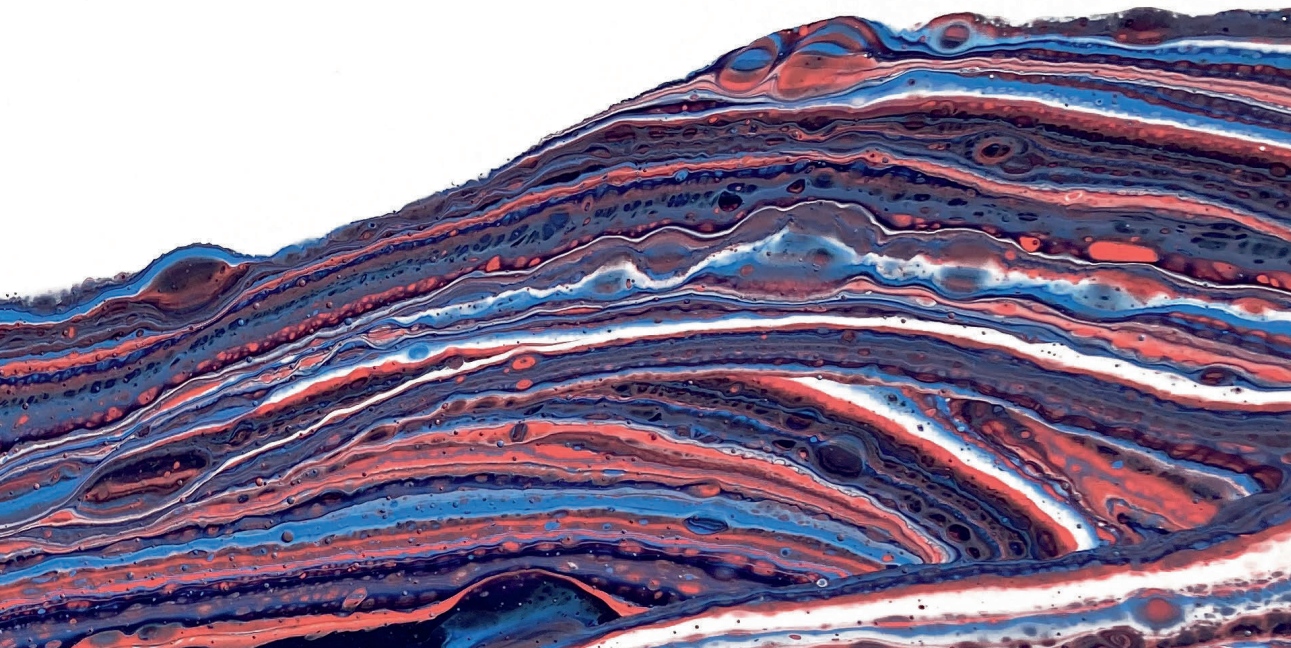

## Abstract

Bicuspid aortic valve (BAV), the most common congenital heart defect, is associated with an increased prevalence of aortic dilation, aortic rupture and aortic valve calcification. Endothelial cells (ECs) play a major role in vessel wall integrity. Little is known regarding EC function in BAV patients, due to lack of patient derived primary ECs. Endothelial colony forming cells (ECFCs) have been reported to be a valid surrogate model for several cardiovascular pathologies, thereby facilitating an in vitro system to assess patient-specific endothelial dysfunction. Therefore, the aim of this study was to investigated cellular functions in ECFCs isolated from BAV patients. Outgrowth and proliferation of ECFCs from patients with BAV (n=34) and controls with a tricuspid aortic valve (TAV, n=10) was determined and related to patient characteristics. Interestingly, we were only able to generate ECFCs from TAV and BAV patients without aortic dilation and failed to isolate ECFC colonies from patients with a dilated aorta. Analyzing EC function showed that while proliferation, cell size and endothelial-to-mesenchymal transition were similar in TAV and BAV ECFCs, migration and the wound healing capacity of BAV ECFCs is significantly higher compared to TAV ECFCs. Furthermore, calcification is blunted in BAV compared to TAV ECFCs. Our results reveal ECs dysfunction in BAV patients and future research is required to unravel the underlying mechanisms and to further validate ECFCs as a patient-specific in vitro model for BAV.

## Introduction

Bicuspid aortic valve (BAV) is the most common congenital heart defect, present in 1-2% of the adult population worldwide. While a normal aortic valve consists of three leaflets (tricuspid aortic valve, TAV), a BAV has only two free moveable/floating leaflets either with or without a raphe. BAV can occur sporadically or can be inherited and mutations in e.g. *NOTCH1*, *TGFBR1* and *SMAD6*, have been reported to be associated with BAV [1,2]. Furthermore, there is a remarkable male preponderance of 3:1 in the total population. Patients with a BAV have an increased prevalence of dilation and even rupture of the ascending aorta, while also aortic valve regurgitation or stenosis can occur [3].

Aortic dilation can become a life threatening situation manifested by destructive changes in the aortic architecture, caused amongst others by dedifferentiation of contractile smooth muscle cells (SMCs) and elastic lamella fragmentation [4]. To understand the cellular and molecular mechanisms driving the pathogenesis in aortic dilation, research over the last decades has mainly focused on SMCs and the role of biochemical signals to steer their differentiation and extracellular matrix modulation within the media of the aorta [5]. Little is known about a possible role of the endothelium in aortic dilation in BAV patients. Recently, the endothelial cells (ECs) have become of increased interest in BAV pathology (reviewed in [6]). Interestingly, altered EC migration, EC function and endothelial-to-mesenchymal transition (EndoMT) have been described in BAV patients [7,8]. Furthermore, mutations in *ROBO4* have recently been identified in BAV patients, which was shown to impair the barrier function of the ECs and induces EndoMT [9].

It is extremely difficult to obtain primary ECs from ascending aorta to study endothelial function, especially when matched controls are needed for comparison. Furthermore, patient-derived aortic ECs are a heterogeneous, non-proliferative population of ECs, derived from end-stage disease material [10]. Therefore, circulating endothelial progenitor cells have become an important tool to study EC function in different cardiovascular diseases.

There are 2 main types of circulating endothelial progenitor cells described, namely endothelial progenitor cells (EPCs) and endothelial colony forming cells (ECFCs). While EPCs express some EC markers such as PECAM1, von Willebrand Factor and VE-cadherin, it is now well established that these cells are $CD14^+$ circulating mononuclear cells, instead of true endothelial progenitors [11]. Previous studies have shown that the number of EPCs is reduced in BAV patients with or without aneurysms, when compared to TAV patients with or without aneurysms, respectively [12]. In addition, BAV patients with dysfunctional valves have reduced numbers of circulating EPCs when compared to BAV patients with

a normal functioning valve [13]. Moreover, EPCs exhibit a decreased migratory capacity in BAV patients with dysfunctional valves [13]. ECFCs, also known as blood outgrowth endothelial cells (BOECs), are the real circulating endothelial progenitor cells. ECFCs can be isolated from amongst others peripheral blood and give rise to a cell population indistinguishable from mature ECs [11,14]. These cells are able to contribute to vessel formation *in vivo* and have a high proliferative potential [11,15]. ECFCs have been used as a proxy to study EC function in diseases such as pulmonary arterial hypertension (PAH), diabetes and ischemic heart disease [16-19]. For example in PAH, it is reported that failure of ECFC outgrowth is associated with clinical worsening [20].

To date, there is no data available describing the function of ECFCs in BAV patients. Given the important role of EC function in vessel stability, in this study we aimed to investigate EC function in BAV patients. Because ECFCs resemble EC function very well and isolating ECs from aortic tissue is not feasible, studying these cells may provide a valuable insight into EC functioning in BAV patients. Therefore, we isolated ECFCs from BAV patients and participants with a TAV serving as healthy controls. The outgrowth and proliferation of ECFCs was quantified and related to patient characteristics. Moreover, migration and response to calcifying stimulation was assessed in the ECFCs. Our results demonstrate ECFC dysfunction in BAV patients compared to healthy TAV controls. We expect that this will encourage other researchers to further develop and characterize ECFCs as an *in vitro* model for BAV.

## Results

### No successful growth of ECFC colonies isolated from patients with a dilated aorta

We first investigated whether ECFCs can be isolated from BAV patients and TAV controls. To isolate ECFC colonies, peripheral blood derived mononuclear cells were collected from patients (n=34) and healthy participants (controls, n=10). There were no significant differences between the included control participants and the patients with regard to age, height, weight and gender (Table 1). The isolated mononuclear cells fractions were seeded and wells were monitored for colonies to appear after 2-5 weeks. In total, 74 colonies appeared, but not all colonies resulted in a successful ECFC patient-derived cell line. Growth of an ECFC colony was considered successful if they were able to proliferate for at least 8 passages. Unsuccessful ECFC isolations were those colonies that showed a decrease in proliferation rate, and adopted morphologically a senescent, mesenchymal phenotype (Figure 1A).

**Table 1.** Participant characteristics

| | TAV (10) | BAV (34) | |
|---|---|---|---|
| **Male sex, n (%)** | 5 (50) | 18 (52.9) | |
| **Age, year (stdev)** | 32.0 (10.5) | 38.4 (15.5) | |
| **Height, cm (stdev)** | 179.4 (15.8) | 176 (11.0) | |
| **Weight, kg (stdev)** | 74.8 (11.2) | 76.9 (14.5) | |
| **Valve types, n (%)[1]** | | | |
| Type 0 | - | 5 (14.7) | |
| Type 1 L-R | - | 17 (50) | |
| Type 1 R-N | - | 4 (11.8) | |
| Type 2 L-R, R-N | - | 2 (5.9) | |
| Unknown | - | 6 (17.6) | |
| **Dilation, yes (%)** | 0 (0) | 17 (50)* | |
| **Aortic size, mm (stdev)** | all | non-dilated | dilated |
| Aorta ascendens | 28.6 (3.0) | 30.2 (3.0) | 43.1 (5.5) |
| **Stenosis, n (%)** | | | |
| Severe | 0 (0) | 4 (11.8) | |
| Moderate | 0 (0) | 6 (17.6) | |
| Mild | 0 (0) | 15 (14.7) | |
| None | 10 (100) | 19 (55.9) | |
| **Insufficiency, n (%)** | | | |
| Moderate | 0 (0) | 10 (29.4) | |
| Mild | 0 (0) | 12 (35.3) | |
| None | 10 (100) | 17 (50) | |

[1]Valve classification according to Sievers[21].

There was no correlation between successful and unsuccessful ECFC isolations when comparing gender, age, length and weight between TAV control and BAV patients (Table 2). From the TAV control participants, 30% of the isolations lead to successful colony growth. For the isolations of BAV patients derived ECFCs there was a trend towards decrease in isolation efficiency with a success rate of 14,7% ($\chi 2(1)= 1.22$, $p=0.27$). Interestingly, all isolations from BAV patients that did result in an ECFC cell line were isolated from BAV patients without aortic dilation (non-dilated BAV: nBAV, n=17). We were unable to isolate stable ECFCs from BAV patients with aortic dilation (dilated BAV: dBAV, n=17). The decreased isolation efficiency observed in dBAV patients was significantly different compared to both TAV control samples and nBAV patients ($\chi 2(2)= 6.16$, $p=0.046$) (Figure 1B). When comparing patient characteristics, dBAV patients did have a significantly

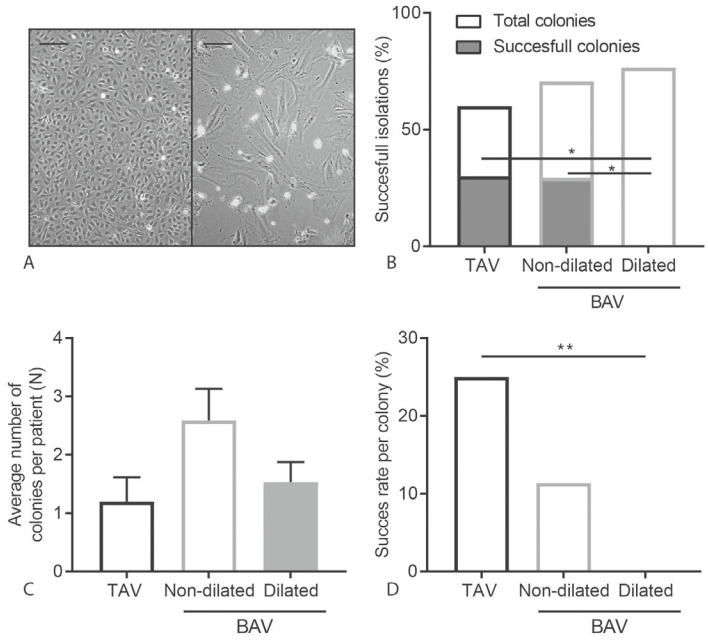


**Figure 1. Successful growth of ECFCs in TAV and BAV non-dilated patients.** A. Representative images of a successful (left) and an unsuccessful (right) ECFC colony. Scalebar is 200 $\mu$m. B. Graph showing the percentage of patient isolations resulting in a colony and the percentage of patient isolations resulting in a cell line. C. Graph indicating the average number of colonies per isolation. D. Graph showing the percentage of colonies resulting in a successful ECFC cell line. * $p<0.05$, ** $p<0.01$.

higher age and bodyweight (Supplementary Table A1). Interestingly, the observed decrease in successful ECFC isolations was not due to a decrease in total number of colonies that appeared after seeding of the mononuclear cells (Figure 1B) or the number of colonies observed per patient (Figure 1C). There was a significant decrease in success per colony after the first passage in colonies from dBAV patients compared to colonies from TAV patients ($\chi 2(1)= 7.075$, $p=0.008$) (Figure 1D). Our results demonstrate for the first time that the establishment of stable ECFCs cultures from BAV patients with an aortic dilation is compromised.

There was no correlation between successful and unsuccessful ECFC isolations when comparing gender, age, length and weight between TAV control and BAV patients (Table 2). From the TAV control participants, 30% of the isolations lead to successful colony growth. For the isolations of BAV patients derived ECFCs there was a trend towards decrease in isolation efficiency with a success rate of 14,7% ($\chi 2(1)= 1.22$, $p=0.27$). Interestingly, all isolations from BAV patients that did result in an ECFC cell line were isolated from BAV patients without

**Table 2.** Participant characteristics successful ECFC isolations

| | TAV (3 30,0%) | BAV (5, 14.7%) |
|---|---|---|
| **Male sex, n (%)** | 2 (66.7) | 3 (60) |
| **Age, year (stdev)** | 34.0 (12.2) | 25.8 (5.9) |
| **Height, cm (stdev)** | 186.3 (5.1) | 174.6 (14.0) |
| **Weight, kg (stdev)** | 77.7 (10.0) | 66.4 (10.3) |
| **Valve types, n (%)** | | |
| Type 0 | - | 2 (20) |
| Type 1 L-R | - | 2 (20) |
| Type 1 R-N | - | 0 (0) |
| Type 2 L-R, R-N | - | 0 (0) |
| Unknown | - | 1 (20) |
| **Dilation, yes (%)** | 0 (0) | 0 (0)* |
| **Aorta ascendens size, mm (stdev)** | 28 (2.0) | 29.8 (2.3) |
| **Stenosis, n (%)** | | |
| Severe | 0 (0) | 0 (0) |
| Moderate | 0 (0) | 1 (20) |
| Mild | 0 (0) | 1 (20) |
| None | 3 (100) | 3 (60) |
| **Insufficiency, n (%)** | | |
| Moderate | 0 (0) | 1 (20) |
| Mild | 0 (0) | 1 (20) |
| None | 3 (100) | 3 (60) |

aortic dilation (non-dilated BAV: nBAV, n=17). We were unable to isolate stable ECFCs from BAV patients with aortic dilation (dilated BAV: dBAV, n=17). The decreased isolation efficiency observed in dBAV patients was significantly different compared to both TAV control samples and nBAV patients ($\chi 2(2)= 6.16$, $p=0.046$) (Figure 1B). When comparing patient characteristics, dBAV patients did have a significantly higher age and bodyweight (Supplementary Table A1). Interestingly, the observed decrease in successful ECFC isolations was not due to a decrease in total number of colonies that appeared after seeding of the mononuclear cells (Figure 1B) or the number of colonies observed per patient (Figure 1C). There was a significant decrease in success per colony after the first passage in colonies from dBAV patients compared to colonies from TAV patients ($\chi 2(1)= 7.075$, $p=0.008$) (Figure 1D). Our results demonstrate for the first time that the establishment of stable ECFCs cultures from BAV patients with an aortic dilation is compromised.

**EndoMT response is similar in TAV and BAV ECFCs**

Recent studies demonstrate that EndoMT is altered in BAV patients compared to TAV controls [7,9,22,23]. To investigate this, we examined the ability of ECFCs to undergo EndoMT in response to TGFβ stimulation. After 48 hours of TGFβ stimulation, we determined the expression levels of the EndoMT associated genes *SNAI1* (encoding Snail), *Transgelin* (*TAGLN*, encoding SM22a) and *Fibronectin* (*FN1*) by qRT-PCR. As expected, an increase in mRNA expression of these EndoMT target genes was observed in both TAV and BAV ECFCs upon TGFβ stimulation. There was no difference TGFβ induced EndoMT between the TAV and BAV ECFCs (Supplementary figure 1).

**Proliferation and cell size are similar in TAV and BAV ECFCs**

During cell culture, we observed an apparent variation in cell size and proliferation between the different ECFC cell lines (Figure 2A). These differences were not depending on confluence of the wells since they were observed in both confluent and non-confluent situations. Next, cell surface area was determined to investigate a potential relationship between cell size and aortic valve morphology, but no significant difference in cell size was found between TAV and BAV ECFCs (p= 0.9387) (Figure 2B). To determine if the variation in cell size is caused by changes in cell growth, cell proliferation rate was measured and

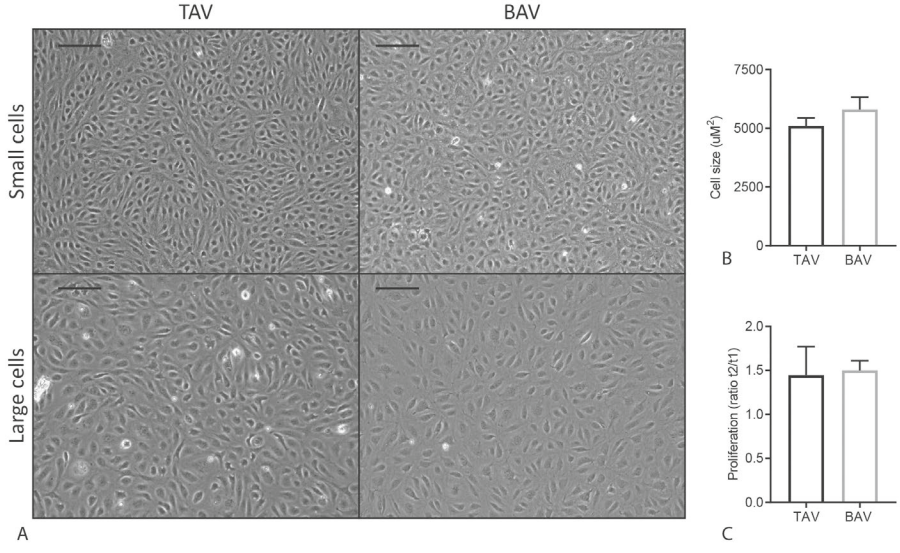


**Figure 2. ECFC proliferation rate and cell size in TAV and BAV.** A. Representative images of variation in cell size in TAV and BAV ECFCs. The scale bar is 200$\mu$m. B. Graph showing TAV and BAV ECFC cell size. C. Graph indicating TAV and BAV ECFC proliferation.

depicted as the difference in cell number 24 and 72 hours after seeding. As can be appreciated in Figure 2C, no difference in proliferation rate between TAV and BAV ECFCs was observed (p= 0.8407). In addition, the was no correlation between cell proliferation and cell size when comparing average proliferation rate and cell size per ECFC line (p=0.321, data not shown). Furthermore, since during epithelial-to-mesenchymal transition (EMT) an increase in size of epithelial cells in transition is observed [24], we next analyzed if there was a correlation between cell size and EndoMT gene transcription, but no significant differences were observed (data not shown).

**BAV ECFCs migrate faster compared to TAV ECFCs**

Previous studies have shown that poor cell migration of EPCs correlated with worse valvular function in BAV [13]. Therefore, we next determined migration of ECFCs using two different assays, transwell and scratch assay. In order to assess the intrinsic migratory potential of the ECFCs, we first performed a transwell assays using serum as a migratory stimulus, and visualized the migrated cells using crystal violet (Figure 3A). There was a remarkable significant increase in migration of BAV ECFCs compared to TAV ECFCs (TAV: M=87.2 SEM=13.6, BAV: M=193.9 SEM=22.0, p=0.0029) (Figure 3B). Next we performed a scratch (wound healing) assay. To determine the wound healing response we calculated the difference in surface area between 2 timepoints. The scratch assay confirmed the difference observed in the transwells. There was a significant increase in wound closure by BAV ECFCs compared to TAV ECFCs (TAV: M=6.73 SEM=0.56, BAV: M=10.03 SEM=0.82, p=0.020) (Figure 3C,D). Sempahorin3C (sema3C), a secreted guidance protein, regulates endothelial migration [25]. We therefore quantified *Sema3c* expression by qRT-PCR in TAV and BAV ECFCs, and observed a trend towards an increase in sema3C expression in BAV ECFCs compared to TAV ECFCs (Figure 3E). Taken together, we show that migration of cells is reduced in BAV ECFCs.

**Calcification is decreased in BAV ECFCs compared to TAV ECFCs**

Since valvular calcification is a serious complication in BAV patients, we studied the ability of the BAV and TAV ECFCs to calcify. After culturing ECFCs in osteogenic medium we stained the wells with Alizarin Red (Figure 4A). Interestingly, calcium deposits could already be detected in some of the samples after cultured for 18 days in growth medium. These deposits were more present in the BAV than the TAV ECFCs, however, the difference was not significant (TAV: M=0.35% SEM=0.24, BAV: M=0.97% SEM=0.41, p=0.31) (Figure 4A,B, Supplementary figure 2A). Culturing the cells osteogenic medium increased the amount of Alizarin

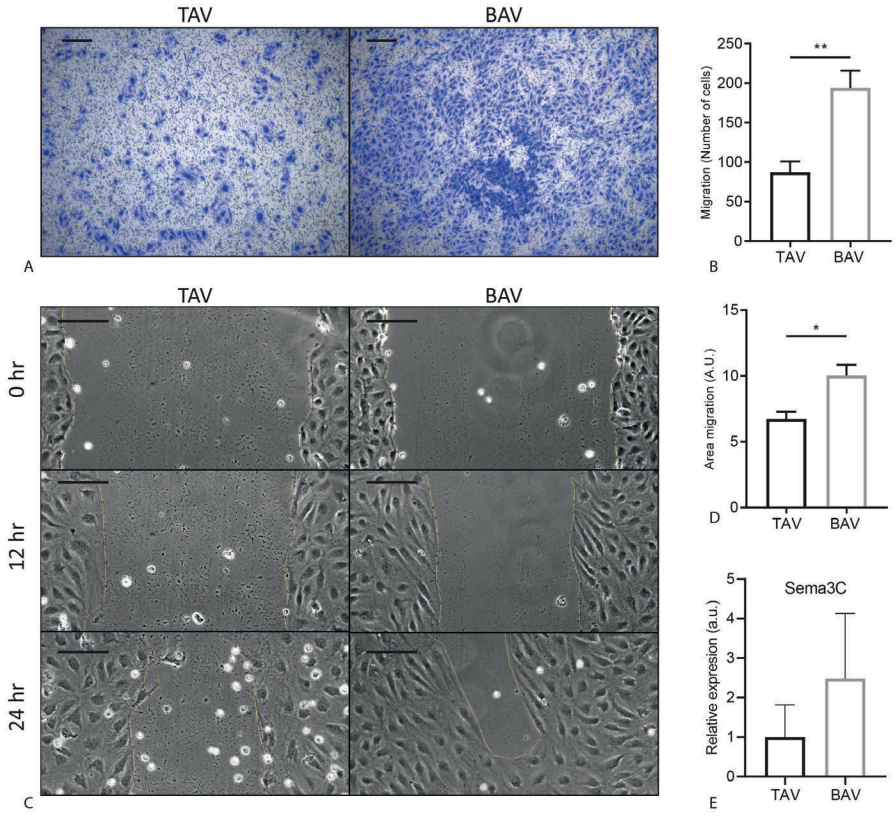


**Figure 3. Migration assay of TAV and BAV ECFCs.** A. Representative images of TAV and BAV ECFC transwell migration stained with crystal violet. B. Graph indicating TAV and BAV transwell migration, quantified by counting the number of ECFCs migrated in 24 hr.C. Representative images of three different timepoints in the scratch assay of TAV and BAV ECFCs. D. Graph showing TAV and BAV scratch migration quantification. Difference in area between 8hr and 12hr was measured. E. Graph indicating qPCR results for Semaphorin3C. Scalebar is 200 $\mu$m * $p<0.05$ ** $p<0.01$, a.u.= arbitrary units.

Red staining in the TAV and BAV ECFCs when compared to growth medium. Although both showed an increase in calcium deposition, this increase is less in BAV ECFCs when compared to TAV ECFCs when cultured in osteogenic medium (Figure 4A,B, Supplementary figure 2A).

Previously it has been shown that inorganic phosphate transporter 1 and 2 (PiT1 and PiT2) are expressed in progenitor cells during differentiation towards osteoblasts [26]. Furthermore, an increased expression of *PiT1* is related to increased mineralization and shown to be involved in SMC transdifferentiation into osteoblast-like cells [27,28]. Therefore, we determined whether PiT1 and PiT2 may play a role in ECFC calcification and found a trend towards increased

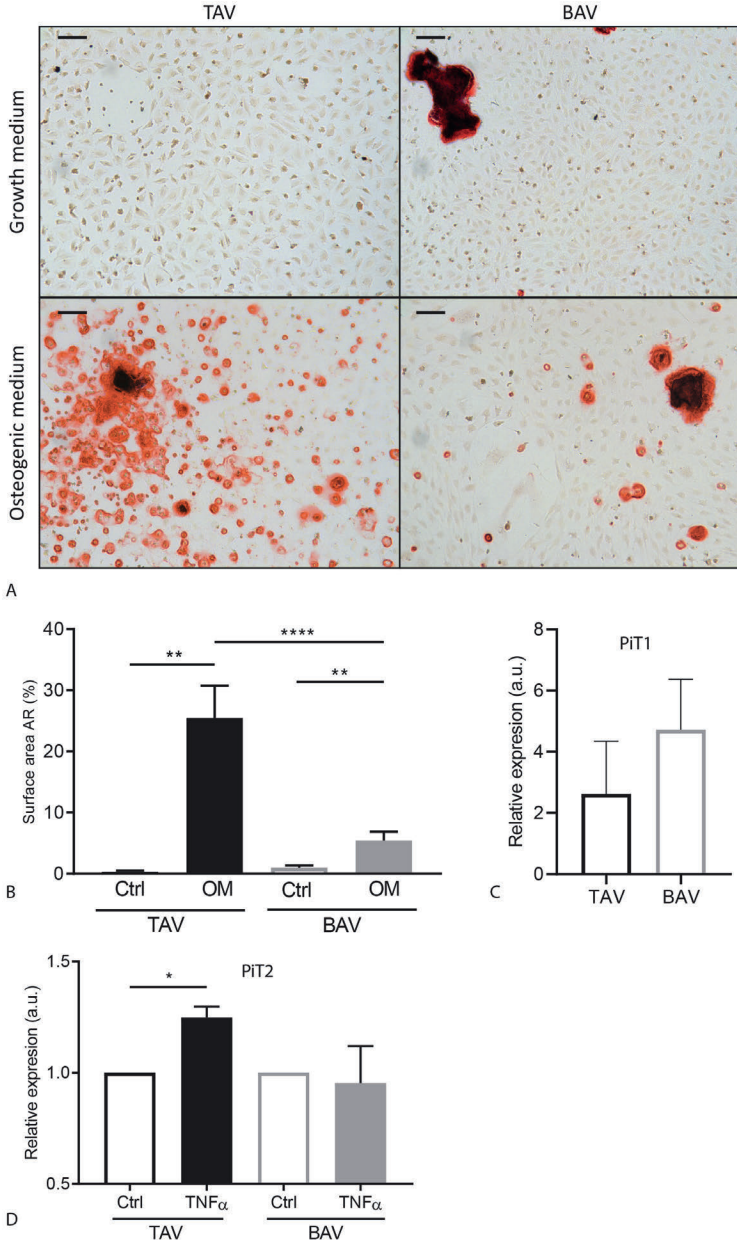


**Figure 4. TAV and BAV ECFC calcification results.** A. Representative images of an Alizarin Red staining of TAV and BAV ECFCs after 18 days of culture in growth medium or osteogenic medium. B. Graph of TAV and BAV calcification measured using picture analysis measuring surface area of Alizarin Red. C. Graph indicating *PiT1* gene expression in BAV and TAV ECFCs under normal culture conditions. D. Graph showing *PiT2* gene expression levels upon ECFC stimulation with TNFα. Scalebar is 100 μm. * p<0.05 ** p<0.01 **** p<0.001.

expression of both *PiT1* and *PiT2* in BAV ECFCs compared to TAV ECFCs under normal culture conditions (Figure 4C, Supplementary figure 2B).

Inflammatory stimulation using tumor necrosis factor (TNF)-$\alpha$ has been reported to sensitize ECFCs for calcification [29]. Therefore, we stimulated ECFCs with TNF$\alpha$ for 48 hours and determined the expression levels of *PiT1* and *PiT2*. Interestingly, *PiT2* expression upon TNF$\alpha$ significantly increased in TAV ECFCs (p=0.0157, 24,8%, SEM=0.05) but not in BAV ECFCs (p=0.788, -4,5%, SEM=0.166) (Figure 4D). In addition, the expression of *PiT1* showed a similar trend (Supplemenrary figure 2C). In summary, ECFCs from BAV patients exhibit a reduced capacity to calcify when compared to TAV derived ECFCs and TNF-$\alpha$ stimulation specifically induced the expression of PiT2 in TAV ECFCs, but not in BAV ECFCs.

## Discussion

In this study, we isolated ECFCs from BAV patients and TAV controls to study EC function, and observed a striking decrease in efficiency of successful ECFC isolation in BAV patients with a dilated aorta. In the ECFCs that were successfully isolated, proliferation rate and cell size were similar but, there was a decrease in migratory behavior of ECFCs from BAV patients when compared to TAV patients. While no differences were detected in their response to TGFβ induced EndoMT, we did observe a reduced calcification response in BAV ECFCs compared to TAV ECFCs.

Normal endothelial function is pivotal for a healthy cardiovascular function. In the past years, research to understand bicuspid aortic valve disease has suggested that endothelial dysfunction might play a role [7,9,30]. *In vitro* characterization of ECs isolated from aneurysmal aortic tissue show a decreased proliferation rate in BAV aortic ECs compared to TAV control and TAV aneurysmal ECs [31]. Unfortunately, primary ECs isolated from aortic tissue are heterogeneous, have very limited proliferative capacity and can only be obtained from end stage disease surgical material, hampering progress in our understanding of the impact of the endothelium in BAV. Therefore, we took the approach to generate ECFC cell lines from BAV patients to study EC function. ECFCs not only provide an *in vitro* cell model for patient specific endothelial functioning, but *in vivo* they contribute to endothelial wound healing [14-16]. Therefore, altered function of ECFCs might contribute to endothelial dysfunction when e.g. repairing the endothelial layer damaged due to years of altered wall shear stress [32]. Although the behavior of ECFCs might not fully recapitulate the ECs present in the aortic wall, these cells can not be obtained from healthy matched controls. ECFCs are an EC source that does most closely resemble mature ECs obtained using a minimal invasive isolation protocol [11,14], Peripheral ECs can also be isolated to study

patient specific EC functioning, but they have been reported to have clear different characteristics from aortic ECs, and would cause a higher isolation burden. Therefore we decided to use ECFCs to study patient specific EC function [33].

The isolation efficiency of ECFCs from BAV patients with a non-dilated aorta was similar to TAV control. Interestingly, we were unable to isolate ECFCs from BAV patients with an aortic dilation. This observation might suggest a possible biomarker role of ECFCs in BAV aortic dilation. A recent study analyzing EPCs reported a reduced number of EPCs in BAV patients with a dysfunctional aortic valve when compared to a normal functioning BAV [13]. A decrease in circulating progenitor cells in BAV patients with additional cardiovascular pathologies, could explain the lack of successful ECFC isolations from dBAV patients. Incongruently, we were able to successfully isolate ECFCs from patients with valvular dysfunction. Moreover, we did not observe a difference between the number of colonies that appeared in isolations from BAV patients with or without aortic dilation compared to TAV ECFCs. We did observe a difference in the proliferative capacity of the different colonies. All colonies isolated from dBAV patients stopped proliferating soon after appearing and gained a senescent/mesenchymal morphology. Recent studies have shown that there was an increase in EndoMT gene expression profile associated with a BAV [7,9,22,23]. Increased EndoMT could be the cause of an increased amount of BAV colonies to gain a mesenchymal phenotype. Moreover, as epithelial cell size has been correlated to EMT, the different cell sizes observed in the ECFC culture could be related to an EndoMT phenotype [24]. However, in the BAV ECFCs we did not observe a difference in upregulation of expression of EndoMT related genes upon TGFβ stimulation between TAV and BAV ECFC cell lines. Moreover, we did not observe a correlation between cell size and the expression of different EndoMT related target genes. Although increased age has been reported to impair ECFC isolation [34], but we did not observe a significant age difference when comparing successful and non-successful isolations in this study. There was, however, a significant increase in age of patients with a dilated aorta compared to BAV patients without a dilated aorta.

To study EC behavior, migration of the ECFCs was investigated. Our data shows that migration is increased in BAV ECFCs when compared to TAV ECFCs. Moreover, BAV ECFCs show an increase in *Sema3C* expression, a secreted protein that regulates EC function and enhances migration. Reduced EC migration *in vitro* has been found in many different diseases, e.g. in ECFCs derived from patients with diabetes or preeclampsia [35,36], and related to the functionality of the patient specific ECs. In contrast to diabetes and preeclampsia, we observed an increase in migration of ECFCs derived from BAV patients, leaving

to speculate how this affects the function *in vivo*. Migratory behavior has been studied using aortic SMCs from BAV patients with an aortic aneurysm. When comparing them to TAV non-aneurysmal aortic SMCs, these BAV SMCs show a decreased migration rate [31]. Either no difference, or reduced migration has been observed in SMC migration from BAV aneurysmal aorta when compared to TAV aneurysmal aorta. Since no SMCs were isolated from BAV with a non-dilated aorta it is difficult to draw any conclusion if SMC migration in BAV patients is already altered prior to vessel dilation. Finally, a decrease in migration of BAV EPCs was related to increased dysfunction in aortic valves [13], but unfortunately, our study is not sufficiently powered to be able to relate patient characteristics to aortic valve dysfunction.

Because valvular calcification is a common problem in a subpopulation of patients with a BAV, we studied calcification of the ECFCs. Interestingly, BAV ECFCs cultured in a well for 18 days on growth medium show more calcium deposits compared to TAV. Moreover, expression of *PiT1*, a gene shown to be involved in calcification, shows a modest increase in BAV ECFCs [26-28]. Since patients with a BAV have a high chance to develop calcific aortic valve disease (CAVD), we expected BAV ECFCs to calcify more than TAV ECFCs. However, upon osteogenic stimulation, BAV ECFCs showed a much smaller increase in calcium deposition than TAV ECFCs did. This unexpected result might be explained by differences between *in vitro* and *in vivo* cell function, and/or the calcifying stimulation *in vivo* in BAV is different from our experimental set-up. It does however confirm that the calcification response in BAV ECFCs is altered compared to TAV ECFCs. Inflammatory stimulation using TNF$\alpha$ has been shown to sensitize ECFCs for calcification [29]. Moreover, a recent study on a large CAVD cohort showed that inflammatory markers were increased in CAVD BAV patients compared to CAVD TAV patients [37]. Therefore, we stimulated the ECFCs with TNF$\alpha$, which caused significant increase in mRNA expression of *PiT2* in TAV ECFCs but not in BAV ECFCs. This lack of increase in PiT2 could explain the reduced response of BAV ECFCs to osteogenic medium.

In this study we have for the first time characterized ECFCs from BAV patients. Our data suggests that EC dysfunction is present in these patients, and future research should focus on the role of endothelial dysfunction in the pathogenesis of BAV and the related aortic valve calcification and aortic dilation, taking into account the role of BAV related genes that are known to affect cell migration, proliferation, EndoMT, and calcification such as *SMAD6*, *NOTCH1* or *TGF$\beta$R1* [1,2] [38-41]. Altogether, we expect that this study will stimulate the use of ECFCs as a surrogate model to determine endothelial function in BAV

## Materials and Methods

Ethical approval for this study was obtained from the Medical Ethical Committee from the Leiden University Medical Center, Leiden, The Netherlands (P15.377). The included patients were 18 years of age or older, had a bicuspid aortic valve and were invited to participate during routine visit to the outpatient clinic. Patients were excluded if they had undergone aortic valve surgery or intervention. Control participants were age and gender matched to the average of the patient population and a TAV was confirmed. The ascending aortic diameter was measured with echocardiography using the leading edge-to-leading edge technique [42]. An ascending thoracic aortic diameter equal to or larger than 40 mm was considered dilated. After obtaining written informed consent, peripheral blood (60ml) was drawn from BAV patients and TAV control participants. To isolate the mononuclear cell fraction, the blood was diluted 1:1 with PBS and centrifuged using a ficoll gradient. In detail, the sample was divided in fractions of 25 ml which were gently pipetted in a 50ml tube on top of 12,5 ml Ficoll Paque Plus (GE Healthcare, 17-1440-03). The tubes were centrifuged at 750 G for 30 minutes without brake. The plasma layer was aspirated and the buffy coat of the mononuclear cell fraction was transferred to a new 50 ml tube. The cells were washed 3x with PBS supplemented with PenStrep (100U/ml, Gibco) by adding 25 ml PBS to the tube, centrifuging 5 minutes at 230 G and aspirating the supernatant. The pellet was resuspended in 12,5 ml growth medium (EGM-2 (Lonza, CC-3162)) supplemented with 8% extra fetal bovine serum (FBS) and PenStrep (100U/ml, Gibco). 48-Well plates were coated with 50ug/ml purified bovine collagen (Advanced Biomatrix, #5005) in MQ, 250 $\mu$l per well and were incubated 2 hours at 37°C and washed 3x using PBS before plating the resuspended cells. The medium was replaced for the first time after 3 days using growth medium, after which the medium was replaced 2 times per week. Colonies that appeared 2 to 5 weeks after isolation were passaged when covering approximately 25% of the well. Cells were dissociated by incubating the ECFCs for 1 minute with EDTA (0,5mM, Sigma) followed by incubation with Trypsin 0,25%/EDTA (1:1 Serva and USH products) for approximately 5 minutes until cells were dissociated from the well. This dissociation was confirmed using a microscope after which they were resuspended and reseeded 1:2 onto collagen coated wells. The ECFCs were checked for expression of PECAM1 (qRT-PCR and Western blot) and VE-Cadherin (qRT-PCR) expression and absence of the lymphocyte marker CD45 was confirmed.

### Protein isolation and Western blot

To isolate protein, ECFCs were grown to confluence, washed with PBS and lysed in Giordano buffer (50nM Tris-HCl (pH7,4), 250mM NaCl, 0,1% Triton X-100 and 5mM EDTA) with 15% glycerol and protease inhibitors. Protein concentration was determined using Bradford Reagent (Biorad, 500-0006). Equal amounts of protein were loaded and separated by SDS-PAGE and transferred to Immobilon-P PVDF membranes (Merck, IPVH00010). Membranes were blocked in Tris-buffered saline, 0.2% Tween-20 (TBST) containing 10% dry milk and incubated overnight with Pecam1 antibody (Santa Cruz, sc-1506-r, clone M-20) diluted 1:1000 in 5% BSA in TBST. Membranes were washed 3 times with TBST and incubated with a horseradish peroxidase-conjugated goat-anti-rabbit antibody (Thermo, 31458) diluted 1:10,000 in 10% dry milk in TBST. Membranes were washed with TBST again after which protein expression was detected using enhanced chemiluminescence (WesternBright Quantum, Advanstra) and visualized on x-ray film (Fuji film).

### mRNA isolation and quantitative RT-PCR

RNA was isolated using the ReliaPrep RNA cell miniprep kit (Promega, Z6012) according to the manufacturer's protocol. RevertAid First Strand cDNA Synthesis (ThermoFisher Scientific, K1622) was used to generate cDNA according to the manufacturer's protocol, after which qRT-PCR was performed using GoTaq qPCR Master Mix (Promega, A6001). *GAPDH* and *ARP* were used as housekeeping genes. Primer sequences used are detailed in the supplemental methods.

**Supplemental table 1. Primer sequences for qPCR**

| gene | forward* | reverse* |
|---|---|---|
| GAPDH | AGCCACATCGCTCAGACAC | GCCCAATACGACCAAATCC |
| ARP | CACCATTGAAATCCTGAGTGATGT | TGACCAGCCGAAAGGAGAAG |
| PECAM1 | ATCGGTTGTTCAATGCGTCC | CCTTCAGGATTTGGTACATGACA |
| VE-Cadherin | CTGCATCCTCACCATCACAG | ACCGACACATCGTAGCTGGT |
| Transgelin | TTCAAGCAGATGGAGCAGGT | TGCCATGTCTTTGCCTTCAA |
| Fibronectin | CGTCATAGTGGAGGCACTGA | CAGACATTCGTTCCCACTCA |
| SNAI1 | GAGGACAGTGGGAAAGGCTC | TGGCTTCGGATGTGCATCTT |
| PiT1 | GTTCGTGCATTCATCCTCCAT | TGGTACCCCACAGAGGAAGTTT |
| PiT2 | TCTCATGGCTGGGGAAGTTAGT | TTGCGACCAGTGAGAATCCTAT |
| CD45 | ATAGTCTGCCACGCCTCTG | AGTGTGAAGCGGCCAATG |

* 5'end to 3'end

### Cell size

To measure cell size, pictures were acquired from confluent areas. In these pictures, the number of cells was counted in an area of 2 $mm^2$ from which an

average cell surface area was calculated. Then the average cell surface area was calculated (2 $mm^2$/number of cells).

**Proliferation**

Cell proliferation was determined by calculating the increase in cell number in 48 hours. To this end, 15.000 cells were seeded per $cm^2$ in growth medium which did not reach confluency before the end of the experiment. To quantify proliferation, cells were dissociated to single cells 24 and 72 hours after seeding and automatically counted 3 times using a TC20 automated cell counter (Bio-Rad). The ratio between the number of cells of day 3 and day 1 was used as indication for proliferation rate.

**MTT and PrestoBlue assays**

MTT and PrestoBlue assays were used to determine proliferation rate. For both assays 3000 cells/well were seeded in 96-well plates in a final volume of 100µl/well. For the MTT assay, the growth medium was replaced by growth medium supplemented with 0,5mg/ml 3-(4,5-Dimethylthiazol-2-yl)-2,5-diphenyltetrazolium bromide (MTT, Sigma M5655) for 3 hours at 37 °C, 16 (t1) and 40 hours (t2) after seeding. The absorbance was measured at 595 nm as described previously [43]. For the PrestoBlue assay, the growth medium was replaced with growth medium supplemented with 4% PrestoBlue Cell Viability Reagent (ThermoFisher, A13261). After 3 hours of incubation at 37 °C, fluorescence was measured at 590 nm as a read out for mitochondrial respiration on a victor3V multilabel reader (Perkin Elmer). Three technical replicates were included in each experiment and assays were repeated at least 2 times.

**EndoMT assay**

To induce EndoMT, growth medium supplemented with 5ng/ml TGFβ3 was added to a 6-wells well of ECFCs with a confluency of 60%. After 48 hours, the cells were washed with PBS and RNA was isolated as described above.

**Transwell migration**

To measure migration towards a stimulus, a transwell migration assay was performed. A transwell insert with 5$\mu$m pores (Corning, CLS3421-48EA) was coated using 50ug/ml bovine-collagen. Next, 10.000 ECFCs in 100 $\mu$l EGM2 (2%FBS) were seeded into the transwell insert. The bottom well contained 600 $\mu$l growth medium (10% FBS). After 24hr, the inserts were washed with PBS and fixated for 10 minutes with 4% paraformaldehyde (PFA) before staining the membrane with 4% Crystal violet (Sigma, C0775) in methanol. The ECFCs that did not migrate

through the membrane were removed before taking pictures. Migrated ECFCs were counted from the pictures taken (5 images per transwell).

**Scratch migration**

A scratch assay was performed as an *in vitro* model for wound healing. The scratch assay was performed in a 24 well with a confluent layer of cells. Cells were scraped using a 200 $\mu$l tip after which they were automatically imaged for 24 hours. To calculate the migration rate, the open area was measured at 8 and 12 hours after making the scratch. The difference in area between the timepoints was determined to calculate the migration speed.

**Calcification assay**

To study calcification, ECFCs were seeded in triplo in 48-wells plates. When reaching confluency, the ECFCs were incubated with osteogenic medium (growth medium supplemented with 2,7 mM $CaCl_2$ and 2,5 mM $NaH_2PO_4$) which was replaced twice-weekly. After 18 days, the ECFCs were fixated using 4% PFA for 10 minutes, washed with MQ and incubated with 2% Alizarin Red (Sigma, TMS-008-C, pH 4.2) in MQ for 3 minutes. The plates were washed again 2x with MQ before imaging. Surface area of AR in the images was automatically measured using Fiji [44]. Finally the alizarin red was dissolved by replacing the MQ with 150 $\mu$l cetylperidiumchloride for 3hr at 37C, after which the absorbance was measured in duplo at 595nm. To study the effect of inflammation on calcification, ECFCs were stimulated with 10 ng/ml TNF$\alpha$ (Peprotech, 300-01A) for 48 hours before isolating RNA as described above and studying gene expression by qRT-PCR.

**Statistics**

All results were obtained in at least 4 independent experiments. The isolation and initial culture, as well as the first round of experiments were performed while blinded. Statistical assays were performed using Graph Pad Prism (version 7). Correlations were tested using Pearson correlation. All other statistical tests were performed using Students t-test, except from the number of colonies per patients which was analyzed using Fischer's exact test and one-way ANOVA for the % of successful colony growth. qRT-PCR results from the experiments with TNF$\alpha$ and TGF$\beta$ stimulation are related to the non-stimulated control per cell line. P-values < 0.05 (*), 0.01 (**), 0.001(****) were considered significantly different.

**Author Contribution**

Conceptualization, Vera van de Pol, Jolien Roos-Hesselink, Marco C. DeRuiter and Marie-José Goumans; Formal analysis, Vera van de Pol and Kirsten Lodder; Funding acquisition, Jolien Roos-Hesselink, Marco C. DeRuiter and Marie-José Goumans; Investigation, Vera van de Pol, Lidia R. Bons and Kirsten Lodder; Methodology, Vera van de Pol, Lidia R. Bons, Konda Babu Kurakula, Gonzalo Sanchez-Duffhues, Hans-Marc J. Siebelink, Jolien Roos-Hesselink, Marco C. DeRuiter and Marie-José Goumans; Supervision, Jolien Roos-Hesselink, Marco C. DeRuiter and Marie-José Goumans; Writing – original draft, Vera van de Pol; Writing – review & editing, Vera van de Pol, Lidia R. Bons, Kirsten Lodder, Konda Babu Kurakula, Gonzalo Sanchez-Duffhues, Hans-Marc J. Siebelink, Jolien Roos-Hesselink, Marco C. DeRuiter and Marie-José Goumans.

**Funding**

This research is supported by the Dutch Heart Foundation (BAV consortium grant 31190).

**Acknowledgments**

The TGFβ3 was a kind gift of Dr. K. Iwata. Moreover, we are grateful for the services of the nurses of the Cardiology departments of the Erasmus Medical Center and the Leiden University Medical Center. Most importantly, this research would not have been possible without the gracious participation of the patient and control participants.

**Conflicts of Interest**

The authors declare no conflict of interest.

### Abbreviations

| | |
|---|---|
| BAV | Bicuspid aortic valve |
| CAVD | Calcific aortic valve disease |
| ECFC | Endothelial Colony Forming Cells |
| EC | Endothelial cell |
| EPC | Endothelial Progenitor Cells |
| EndoMT | Endothelial-to-Mesenchymal transition |
| FBS | Fetal Bovine Serum |
| TAV | Tricuspid aortic valve |
| TGFβ | Transforming growth factor β |
| TNFα | Tumor necrosis factor α |

## Supplemental tables/figures

**Supplementary table A1.** BAV patient characteristics with/without aortic dilation

| | Non-dilated aorta (17) | Dilated aorta (17) |
|---|---|---|
| **Male sex,** n (%) | 7 (41.2) | 11 (64.7) |
| **Age,** year (stdev) | 28.9 (7.8) | 47.9 (15.7)# |
| **Height,** cm (stdev) | 173.9 (11.8) | 178.4 (9.9) |
| **Weight,** kg (stdev) | 69.5 (12.5) | 84.2 (12.9)** |
| **Valve types,** n (%) | | |
| Type 0 | 4 (23.5) | 1 (5.9) |
| Type 1 L-R | 8 (47.1) | 9 (52.9) |
| Type 1 R-N | 1 (5.9) | 3 (17.6) |
| Type 2 L-R, R-N | 1 (5.9) | 1 (5.9) |
| Unknown | 3 (17.6) | 3 (17.6) |
| **Aortic size**, mm (stdev) | 30.2 (3.0) | 43.1 (5.5) |
| **Stenosis,** n (%) | | |
| Severe | 2 (11.8) | 1 (5.9) |
| Moderate | 3 (17.6) | 4 (23.5) |
| Mild | 2 (11.8) | 3 (17.6) |
| None | 10 (58.8) | 9 (52.9) |
| **Insufficiency,** n ( %) | | |
| Moderate | 2 (11.8) | 7 (41.2) |
| Mild | 3 (17.6) | 4 (23.5) |
| Trace | 4 (23.5) | 2 (11.8) |
| None | 8 (47.1) | 4 (23.5) |

** p<0.01 , #=P<0.0001.

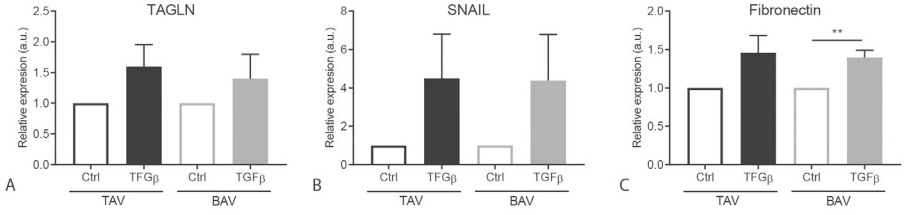


**Supplementary figure 1. EndoMT related gene expression in TAV and BAV ECFCs upon TGFβ stimulation.** A-C. Graphs showing the relative increase in expression upon TGFβ stimulation compared to not stimulated cells of TAGLN (A), SNAIL (B) and Fibronectin (C). ** p<0.01.

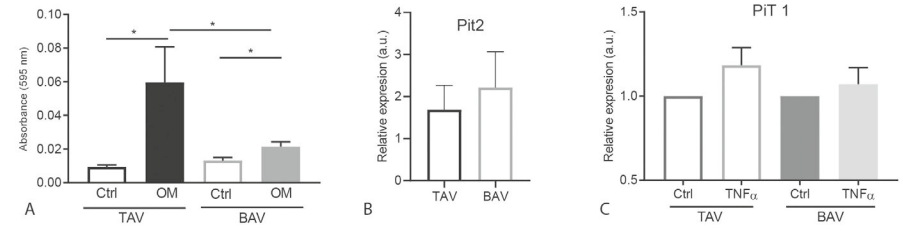


**Supplementary figure 2. Calcification results of TAV and BAV ECFCs.** A. Graph of TAV and BAV calcification measured using absorbance after dissolving alizarin red. B. Graph indicating Pi2 gene expression in BAV and TAV ECFCs under normal culture conditions. C. Graph showing PiT1 gene expression levels upon ECFC stimulation with TNFα. * p<0.05.

## References


1. Gillis, E, et al. (2017). Candidate gene resequencing in a large bicuspid aortic valve-associated thoracic aortic aneurysm cohort: Smad6 as an important contributor. *Front Physiol*
2. Debiec, R, et al. (2017). Genetic insights into bicuspid aortic valve disease. *Cardiol Rev*
3. Ward, C. (2000). Clinical significance of the bicuspid aortic valve. *Heart*
4. Halushka, MK, et al. (2016). Consensus statement on surgical pathology of the aorta from the society for cardiovascular pathology and the association for european cardiovascular pathology: Ii. Noninflammatory degenerative diseases - nomenclature and diagnostic criteria. *Cardiovasc Pathol*
5. Girdauskas, E, et al. (2013). Comparison of aortic media changes in patients with bicuspid aortic valve stenosis versus bicuspid valve insufficiency and proximal aortic aneurysm. *Interact Cardiovasc Thorac Surg*
6. van de Pol, V, et al. (2017). Thoracic aortic aneurysm development in patients with bicuspid aortic valve: What is the role of endothelial cells? *Front Physiol*
7. Bjorck, HM, et al. (2018). Altered DNA methylation indicates an oscillatory flow mediated epithelial-to-mesenchymal transition signature in ascending aorta of patients with bicuspid aortic valve. *Sci Rep*
8. Ali, OA, et al. (2014). Interactions between inflammatory activation and endothelial dysfunction selectively modulate valve disease progression in patients with bicuspid aortic valve. *Heart*
9. Gould, RA, et al. (2019). Robo4 variants predispose individuals to bicuspid aortic valve and thoracic aortic aneurysm. *Nat Genet*
10. Leclercq, A, et al. (2015). A methodology for concomitant isolation of intimal and adventitial endothelial cells from the human thoracic aorta. *PloS one*
11. Chopra, H, et al. (2018). Insights into endothelial progenitor cells: Origin, classification, potentials, and prospects. *Stem Cells Int*
12. Balistreri, CR, et al. (2018). Deregulation of notch1 pathway and circulating endothelial progenitor cell (epc) number in patients with bicuspid aortic valve with and without ascending aorta aneurysm. *Sci Rep*
13. Vaturi, M, et al. (2011). Circulating endothelial progenitor cells in patients with dysfunctional versus normally functioning congenitally bicuspid aortic valves. *Am J Cardiol*
14. Tura, O, et al. (2013). Late outgrowth endothelial cells resemble mature endothelial cells and are not derived from bone marrow. *Stem Cells*
15. Critser, PJ, et al. (2010). Endothelial colony-forming cell role in neoangiogenesis and tissue repair. *Curr Opin Organ Transplant*

16. Paschalaki, KE, et al. (2018). Recent advances in endothelial colony forming cells toward their use in clinical translation. *Front Med (Lausanne)*
17. Dauwe, D, et al. (2016). Neovascularization potential of blood outgrowth endothelial cells from patients with stable ischemic heart failure is preserved. *J Am Heart Assoc*
18. Ingram, DA, et al. (2008). In vitro hyperglycemia or a diabetic intrauterine environment reduces neonatal endothelial colony-forming cell numbers and function. *Diabetes*
19. Toshner, M, et al. (2009). Evidence of dysfunction of endothelial progenitors in pulmonary arterial hypertension. *Am J Respir Crit Care Med*
20. Smits, J, et al. (2018). Blood outgrowth and proliferation of endothelial colony forming cells are related to markers of disease severity in patients with pulmonary arterial hypertension.
21. Sievers, HH, et al. (2007). A classification system for the bicuspid aortic valve from 304 surgical specimens. *J Thorac Cardiovasc Surg*
22. Maleki, S, et al. (2019). The mir-200 family regulates key pathogenic events in ascending aortas of individuals with bicuspid aortic valves. *J Intern Med*
23. Maleki, S, et al. (2016). Mesenchymal state of intimal cells may explain higher propensity to ascending aortic aneurysm in bicuspid aortic valves. *Sci Rep*
24. Lamouille, S, et al. (2007). Cell size and invasion in tgf-beta-induced epithelial to mesenchymal transition is regulated by activation of the mtor pathway. *J Cell Biol*
25. Banu, N, et al. (2006). Semaphorin 3c regulates endothelial cell function by increasing integrin activity. *Faseb j*
26. Nielsen, LB, et al. (2001). Expression of type iii sodium-dependent phosphate transporters/retroviral receptors mrnas during osteoblast differentiation. *Bone*
27. Suzuki, A, et al. (2006). Enhanced expression of the inorganic phosphate transporter pit-1 is involved in bmp-2-induced matrix mineralization in osteoblast-like cells. *J Bone Miner Res*
28. Giachelli, CM. (2003). Vascular calcification: In vitro evidence for the role of inorganic phosphate. *J Am Soc Nephrol*
29. Sanchez-Duffhues, G, et al. (2019). Inflammation induces endothelial-to-mesenchymal transition and promotes vascular calcification through downregulation of bmpr2. *J Pathol*
30. Alegret, JM, et al. (2016). Circulating endothelial microparticles are elevated in bicuspid aortic valve disease and related to aortic dilation. *Int J Cardiol*
31. Malashicheva, A, et al. (2016). Phenotypic and functional changes of endothelial and smooth muscle cells in thoracic aortic aneurysms. *Int J Vasc Med*
32. Barker, AJ, et al. (2010). Quantification of hemodynamic wall shear stress in patients with bicuspid aortic valve using phase-contrast mri. *Ann Biomed Eng*

33. Craig, LE, et al. (1998). Endothelial cells from diverse tissues exhibit differences in growth and morphology. *Microvasc Res*
34. Scheubel, RJ, et al. (2003). Age-dependent depression in circulating endothelial progenitor cells in patients undergoing coronary artery bypass grafting. *J Am Coll Cardiol*
35. Langford-Smith, AWW, et al. (2019). Diabetic endothelial colony forming cells have the potential for restoration with glycomimetics. *Sci Rep*
36. von Versen-Hoynck, F, et al. (2014). Vitamin d antagonizes negative effects of pre-eclampsia on fetal endothelial colony forming cell number and function. *PLoS One*
37. Song, J, et al. (2019). Predictive roles of neutrophil-to-lymphocyte ratio and c-reactive protein in patients with calcific aortic valve disease. *Int Heart J*
38. Noseda, M, et al. (2004). Notch activation results in phenotypic and functional changes consistent with endothelial-to-mesenchymal transformation. *Circ Res*
39. Schlereth, K, et al. (2018). The transcriptomic and epigenetic map of vascular quiescence in the continuous lung endothelium.
40. Ramasamy, SK, et al. (2014). Endothelial notch activity promotes angiogenesis and osteogenesis in bone. *Nature*
41. Lebrin, F, et al. (2005). Tgf-beta receptor function in the endothelium. *Cardiovasc Res*
42. Lang, RM, et al. (2015). Recommendations for cardiac chamber quantification by echocardiography in adults: An update from the american society of echocardiography and the european association of cardiovascular imaging. *J Am Soc Echocardiogr*
43. Kurakula, K, et al. (2011). Fhl2 protein is a novel co-repressor of nuclear receptor nur77. *J Biol Chem*
44. Schindelin, J, et al. (2012). Fiji: An open-source platform for biological-image analysis. *Nat Methods*

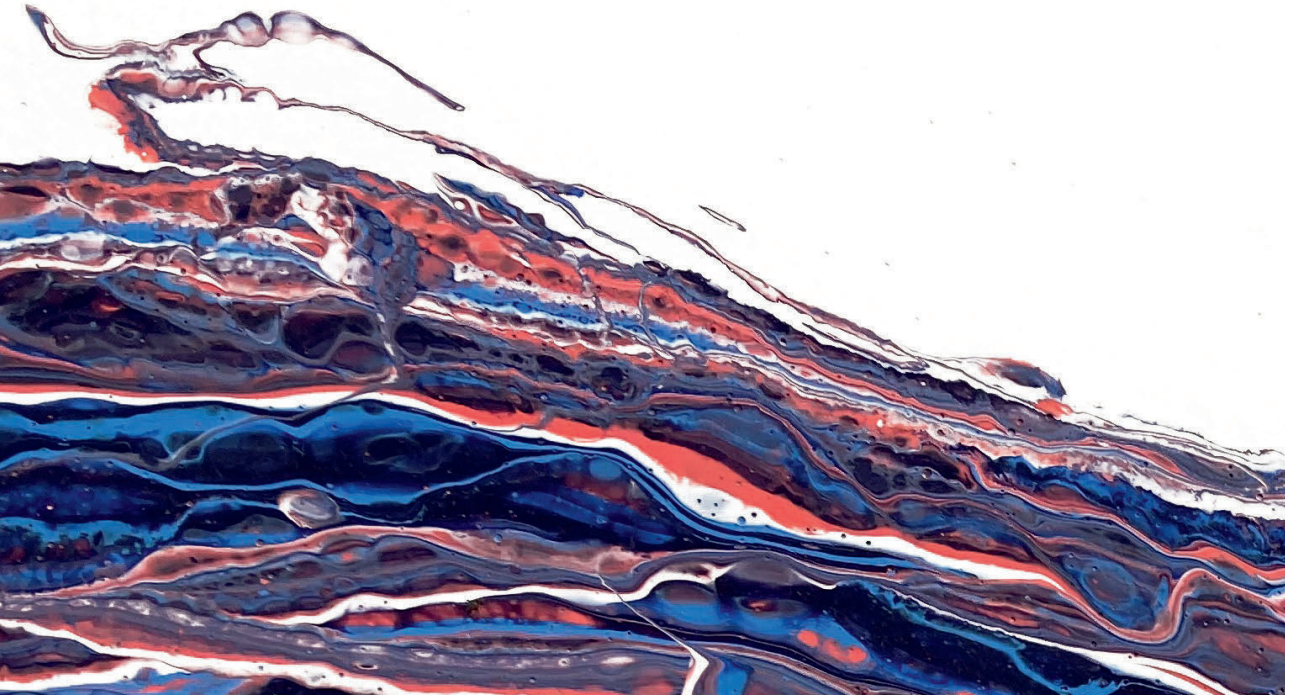

# Chapter 5

## Inflammation induces endothelial-to-mesenchymal transition and promotes vascular calcification through down regulation of BMPR2

**Gonzalo Sánchez-Duffhues[1], Amaya García de Vinuesa[1], Vera van de Pol[1], Marlieke E. Geerts[2], Margreet R. de Vries[2], Stef G. T. Janson[1], Hans van Dam[1], Jan Lindeman[2], Marie-José Goumans[1], Peter ten Dijke[1]**

[1]Department of Cell and Chemical Biology, Oncode Institute. Leiden University Medical Center, Leiden, The Netherlands.
[2]Department of Vascular Surgery. Leiden University Medical Center, Leiden, The Netherlands.

*Published: Journal of Pathology, 2019 | 3: p. 333*

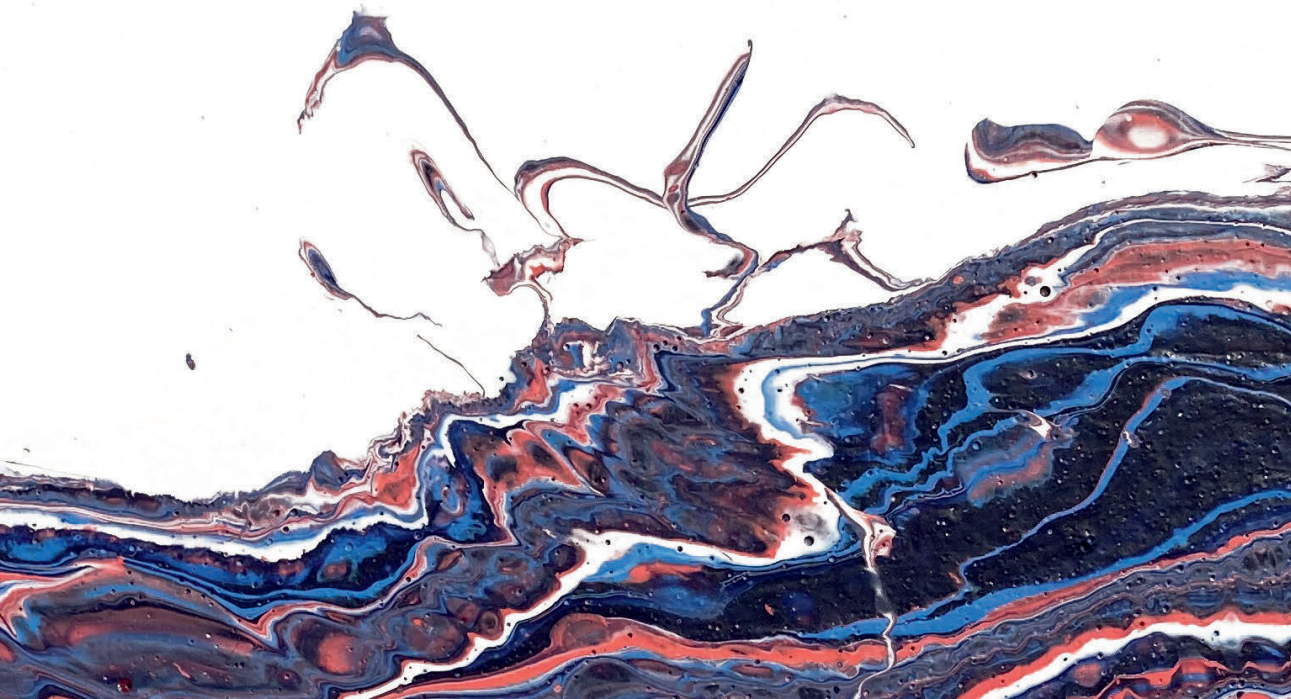

## Abstract

Endothelial-to-mesenchymal transition (EndMT) has been unveiled as a common cause for a multitude of human pathologies, including cancer and cardiovascular disease. Vascular calcification is a risk factor for ischemic vascular disorders and slowing calcification may reduce mortality in affected patients. The absence of early biomarkers hampers the identification of patients at risk. EndMT and vascular calcification are induced upon cooperation between distinct stimuli, including inflammatory cytokines and Transforming growth factor (TGF)-β family growth factors. However, how these signaling pathways interplay to promote cell differentiation, and eventually, vascular calcification is not well understood. Using in vitro and ex vivo analysis in animal models and patient-derived tissues, we have identified that the proinflammatory cytokines tumor necrosis factor (TNF)-α and interleukin (IL)-1β induce EndMT in human primary aortic endothelial cells, thereby sensitizing them for BMP-9-induced osteogenic differentiation. Down regulation of the BMP type II receptor BMPR2 is key event in this process. Rather than compromising BMP canonical signal transduction, loss of BMPR2 results in decreased JNK signaling in ECs, thus enhancing BMP-9-induced mineralization. Altogether, our results point at the BMPR-JNK signaling axis as a key pathway regulating inflammation-induced EndMT and contributing to calcification.

## Introduction

Vascular calcification is a prevalent feature in cardiovascular diseases associated with elevated risk of mortality. The underlying cellular and molecular mechanisms involved have been an area of intense study in recent decades. Mineralization of blood vessels occurs through a coordinated crosstalk between different cell types and cytokines, but ultimately relies on osteoblast lineage cells for the actual synthesis and mineralization of the calcified matrix [1]. We and others have shown that endothelial cells (ECs) can function as an additional source of osteogenic progenitors in vascular calcification [2-4]. ECs can undergo a process known as Endothelial-to-Mesenchymal transition (EndMT), which involves loss of endothelial features and acquisition of a fibroblast-like phenotype, eventually leading to cells with osteogenic potential. EndMT is modulated by different extracellular growth factors (i.e., Transforming growth factor (TGF)-β family ligands, inflammatory cytokines, fibroblast growth factors), and conditions (i.e., mechanical stress, hypoxia) (reviewed in [5]). Noteworthy, during the onset and progression of calcified plaques in aorta, both inflammatory cytokines, such as tumor necrosis factor (TNF)-$\alpha$ and interleukin (IL)-1β [6], and TGF-β family ligands, including the bone morphogenetic proteins (BMPs) [7,8], coincide in the affected area. Whereas BMP-2 and BMP-4 mainly have a paracrine function, BMP-9 and BMP-6 are found in systemic circulation [9]. BMP-9 has been shown to regulate vascular homeostasis, by regulating proliferation [10], angiogenesis [11], permeability [12] and monocyte recruitment [13]. Interestingly, BMP-9 has been shown capable of inducing heterotopic ossification when expressed ectopically using adenovirus [14]. Noteworthy, administration of BMP antagonists prevents experimental atherosclerosis in preclinical animal models [15,16], highlighting the relevance of this pathway in the context of atherosclerosis.

TGF-β signaling is initiated with the oligomerization of receptor complexes at the cell membrane upon ligand binding. BMPs signal via complexes consisting of a type I receptor named Activin receptor-like kinase (ALK)1/2/3/6; and one of three possible type-II receptors: BMPR2, activin type II receptor A and B (ACVR2A, ACVR2B) [17]. Receptor activation induces the phosphorylation of SMAD1/5/8, which form heteromeric complexes with SMAD4 and translocate into the nucleus to regulate the expression of genes. In osteogenic cells, BMPs induce the transcription of genes related with osteoblast differentiation and activation [18]. In addition to this so-called canonical SMAD signaling pathway, TGF-β family ligands modulate the activity of different mitogen activated protein (MAP) kinases, including ERK (Extracellular signal-Regulated Kinases), p38 kinases and JNK (c-JUN N-terminal protein Kinase) in a cell specific and context-dependent fashion [19,20]. Furthermore, how BMP signaling is fine-tuned

by inflammation in EndMT-derived cells and cells with osteogenic potential is yet to be determined. Whereas it has been suggested that inflammatory stimuli inhibit BMP signaling and osteoblast differentiation and activation [21,22], others have shown that inflammation is needed for osteogenesis [23,24].

In this manuscript, we investigate the interplay between inflammation and BMP signaling in ECs. We found that TNF-$\alpha$ and IL-1$\beta$ induce EndMT in primary ECs, which become prone to undergo osteogenic differentiation in response to BMP-9. We identified BMPR2 down regulation as a key event in this process, which leads to decreased JNK activation, thereby enhancing BMP-9 induced mineralization. Finally, we supported our findings in a preclinical animal model of atherogenesis, as well as patient derived tissues from atherosclerotic donors. Our results provide a better understanding on the molecular mechanisms underlying EndMT and vascular calcification and may have broad implications for other human inflammatory pathologies involving BMP signaling.

## Materials and methods

### Cell culture and reagents

Human aortic endothelial cells (HAoECs, CC-2535, Batch number 0000316662), pulmonary aortic endothelial cells (PAEC, CC-2530) and coronary microvascular endothelial cells (cMVECs, CC-7030) were purchased from Lonza. Human skin microvascular endothelial cells (HMECs) were described elsewhere [25]. All cells were cultured in complete EBM-2 medium (Lonza) on 1% w/v gelatin coated wells. Endothelial colony forming cells (ECFCs) were isolated as previously described [26] and cultured in complete EBM-2 medium. All experiments were performed with cells grown to near confluency between passage 6-8. 2H-11 cells are derived from endothelial cells isolated from lymph nodes of adult C3H/HeJ mice transformed using SV40 and have been reported previously [27,28]. These cells were grown on 1% w/v gelatin coated dishes (Merck) in DMEM medium (Invitrogen) supplemented with 4.5 g/L D-glucose (Invitrogen), 110 mg/L sodium pyruvate (Invitrogen), non-essential amino acids (Invitrogen), 10% (v/v) heat inactivated Fetal Bovine Serum (Sigma-Aldrich Chemie), 0.5% (v/v) antibiotic/antimyotic solution (Invitrogen) and 2mM L- glutamine (Invitrogen).

### EndMT assays

HAoECs were seeded confluently in 12 wells plates (for qPCR analysis), or Lab-Tek II chamber slides (for immunofluorescent labeling) in EBM2 complete medium containing 2% FBS. Next day, the cells were stimulated with the indicated ligands for 24 hours in EBM2 complete medium containing 10% FBS.

Subsequently, expression of endothelial and mesenchymal specific markers was analyzed by quantitative RT-PCR or immunofluorescent labeling.

**Osteoblast differentiation assays**

To study osteoblast differentiation, formation of calcium and phosphate deposits was analyzed by Alizarin Red Solution staining. The cells were seeded in 48 wells plates confluently. For HAoECs, the cells were pretreated with TNF-$\alpha$ (10 ng/mL) or TGF-$\beta_3$ (5 ng/mL) for 4 days in EBM2 containing 10% of FBS. Next, the medium was replaced by osteogenic medium (DMEM containing 10% FBS, $10^{-8}$ mol/L dexamethasone, 0.2 mmol/L ascorbic acid and 10 mmol/L β-glycerol-phosphate) in the presence of BMP-9 (10 ng/mL) for 14 days. For 2H-11 cells, they were incubated with the aforementioned osteogenic medium containing both TNF-$\alpha$ (10 ng/mL) and BMP-9 (10 ng/mL) for 14 days. The medium was refreshed every 4 days. Afterwards cells were washed twice with PBS and fixed with 3.7% formaldehyde for 5 minutes. Next, cells were washed twice with distilled water and measurement of calcium deposition was performed by Alizarin Red Staining (ARS), as previously described [29]. Precipitates originated from 3 independent ARS assays were dissolved using 10% cetylpyridinium chloride and absorbance was measured at 570 nm. Representative pictures were obtained using a Leica DMIL LED microscope with 10 times magnification.



**Quantitative RT-PCR**

Total RNA extraction was performed using NucleoSpin RNA II (MACHEREY-NAGEL). 500 ng of RNA were retro-transcribed using RevertAid First Strand cDNA Synthesis Kits (Fermentas), and real-time reverse transcription-PCR experiments were performed using SYBR Green (Bio-Rad) and a Bio-Rad machine. The primers used in this study are indicated as online supplemental information. *Gapdh* was used for normalization.

**Immunofluorescent labeling on cultured cells**

HAoECs grown on coverslips were fixed with 4% formaldehyde for 30 minutes at room temperature, washed with glycine for 5 minutes, permeabilized with 0.2% Triton X-100 and blocked in PSB containing 5% BSA for one hour. Next, the cells were incubated overnight at 4C in blocking solution containing primary antibody with gentle shaking. Next day, the cells were washed 5 times in washing buffer (PBS containing 0.05% Tween-20 and 1% BSA) and incubated with secondary antibody (Alexa Fluor FITC goat anti-mouse IgG, Alexa-Fluor 555 anti-rabbit IgG (Invitrogen, 1:200) or Phalloidin-488 (1:100) in PBS with 0.5% BSA for one hour. Finally, the cells were washed 5 times in washing buffer and

mounted in Prolong Gold containing DAPI (Invitrogen). After careful drying, the preparations were imaged in a Leica SP5 confocal scanning laser microscope. A representative picture from each staining is shown (n = 3). The antibodies used are described in online supplemental information.

**Western Blotting**

Cells were seeded into 12-well plates and cultured till they reached confluence. Next, cells were stimulated as indicated and then washed with cold PBS. Cells were lysed in 2x sample buffer as previously described [30]. A more complete protocol description and the antibodies used can be found in online supplemental information.

**Lentiviral production and transduction**

Lentiviral vectors were produced in HEK293T cells as described before [29]. Lentiviral vectors expressing specific shRNAs were obtained from Sigma (MISSION® shRNA). The shRNA constructs used in this study can be found at Online Supplement. Lentiviral vectors to over-express mMKP-1 have been described before [31].

**Vein graft procedure**

Vein grafts were performed as reported elsewhere [32]. A detailed explanation of the method can be found in online supplemental information.

**Immunostaining on tissues**

In short, immuno-fluorescent and -histochemical stainings on human and murine aortic tissues were performed as previously described [3]. Detailed protocols and list of antibodies used can be found in online supplemental information. 4 μm human aortic sections were prepared from each donor and classified according to the revised classification of the American Heart Association (AHA), as proposed by Virmani et al., by two independent observers with no knowledge of the donor characteristics [33,34]. Sample collection and handling was performed in accordance with the guidelines of the Medical and Ethical Committee in Leiden, Netherlands and the code of conduct of the Dutch Federation of Biomedical Scientific Societies.

**Transfections, luciferase assays and DNA constructs**

For luciferase reporter assays, cells were seeded in 24-well plates and transfected with DharmaFECT Duo (Thermo Fisher Scientific), following the recommendations of the manufacturer. 48 hours after transfection the cells were harvested

and lysed. Luciferase activity was measured using the luciferase reporter assay system from Promega) by a Perkin Elmer luminometer Victor$^3$ 1420. Each transfection mixture was equalized with empty vector when necessary and every experiment was performed in triplicate. The BRE-Luc reporter has been reported elsewhere [35]. The expression vector encoding the constitutively active fusion protein MKK7-JNK3 and its characterization has been previously described [36].

**Iodination and ligand affinity labeling of cell surface receptors.**

Iodination of BMP9 was performed according to the chloramine T method and cells were subsequently affinity labelled with the radioactive ligand as described before [37]. Cell lysates were immunoprecipitated with specific antibodies against ALK1, ALK2, BMPR2 and ACVR2A. The generation and characterization of these antibodies have been previously published [38][39][40]. Image quantification was performed by densitometry using Image J analysis.

**Statistical analysis**

Student's *t*-test was used for statistical analysis and * $P < 0.05$; ** $P < 0.01$; *** $P < 0.001$ was considered significant. All experiments were performed at least three independent times. The results are shown as the mean ± SD of the mean of three independent experiments. Reproducible results were obtained, and representative data are shown in the figures.



## Results

**TNF-α and IL-1β induce EndMT in HAoECs, thereby enhancing BMP-induced-mineralization in HAoECs**

In order to determine the mechanisms by which ECs contribute to the generation of atherosclerotic plaques, we used primary human coronary aortic endothelial cells (HAoECs) stimulated with the indicated pro-inflammatory cytokines and members of the TGF-β superfamily of growth factors. After 24 hours, TNF-α and IL-1β induced a decrease in the expression of the endothelial markers *CDH5* (encoding for VE-CADHERIN) and *Pecam-1*, and an up-regulation of the mesenchymal genes *CDH2* (encoding for N-CADHERIN) and *Fibronectin* (Figure 1A). Accordingly, these two cytokines significantly up-regulated the expression of *SNAI1* and *TWIST1* (Figure S1). This correlated with the loss of the typical endothelial cobblestone-like phenotype, as seen by cytoskeletal staining with Phalloidin, and the down regulation of VE-CADHERIN, PECAM-1 and TIE2, and increase in N-CADHERIN, αSMA and VIMENTIN (Figure 1B). Furthermore, pretreatment with TNF-α sensitized HAoECs to become osteoblast-like

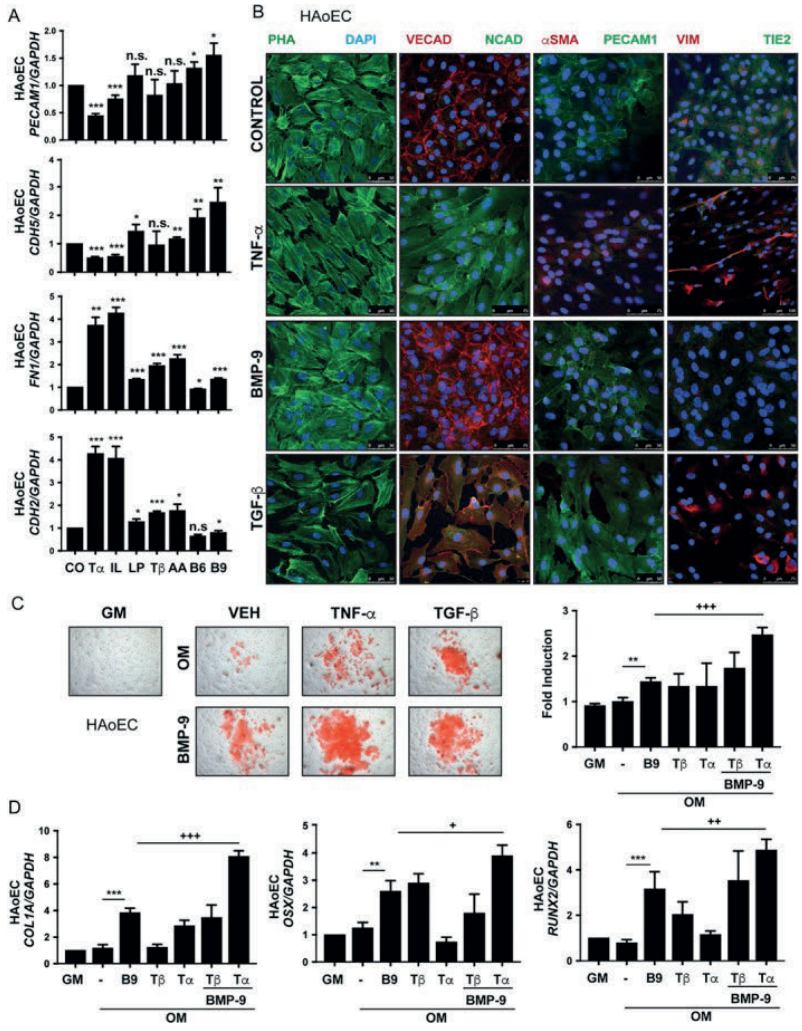


**Figure 1. The pro-inflammatory cytokine TNF-α induces EndMT in HAoECs, priming them for BMP-9-induced osteogenic differentiation.** A. Gene expression of analysis of the genes Cdh5 (encoding for VE-CADHERIN), Pecam1, Fibronectin and Cdh2 (encoding for N-CADHERIN) in HAoECs stimulated for 24 hours with the indicated cytokines and growth factors. CO: control; Tα: TNF-α (10 ng/mL); IL: IL-1β (10 ng/mL); LP: LPS (10 ng/mL); Tβ: TGF-$\beta_3$ (5 ng/mL); AA: activin A (50 ng/mL); B6: BMP-6 (50 ng/mL); B9: BMP-9 (10 ng/mL). B. Immunofluorescent staining on HAoECs stimulated with TNF-α, BMP-9 or TGF-$\beta_3$ as previously mentioned. PHA (Phalloidin), VECAD (VE-CADHERIN), NCAD (N-CADHERIN), αSMA, PECAM-1, VIM (Vimentin) and TIE2. C. Alizarin Red Solution staining and corresponding quantification on HAoECs incubated with BMP-9 for 21 days under osteogenic conditions, after induction of EndMT with TNF-α or TGF-β. Quantification is shown at the right side. GM: Growth medium; OM: osteogenic medium. D. qPCR analysis of the osteogenic genes Collagen-1-alpha-1 (Col1a1), Osterix (Osx) and Runx2 in HAoECs subjected to osteogenic differentiation.

cells in response to BMP-9, more potently than TGF-β, as shown by Alizarin Red Solution (ARS) staining (Figure 1C), and the enhanced expression of the osteogenic genes *Collagen 1 alpha 1* (Col1a), *Runx2* and *Osterix* (Osx) (Figure 1D). We found that TNF-α alone induced the expression of *BMP7* and the combination of BMP-9 and TNF-α induced the up-regulation of the osteogenic *BMP2*, and *BMP4* (Figure S2). These results show that the pro-inflammatory cytokine TNF-α induces EndMT in HAoECs and that EndMT derived cells exhibit an enhanced osteogenic response to BMP-9.

**BMPR2 down-regulation is necessary and sufficient for TNF-α to induce EndMT in HAoECs**

BMP-9 signaling in ECs is mediated by two possible type I receptors ALK1 and or ALK2, and three type II receptors, BMPR2, ACVR2A and ACVR2B [41]. We investigated whether the expression of the BMP type II receptors is modified by stimuli inducing EndMT, thereby enhancing the osteogenic response of BMP-9. As shown in Figure 2A, the two potent EndMT inducers TNF-α and IL-1β triggered a clear down regulation of BMPR2, whereas ACVR2A and ACVR2B were not affected. This effect correlated with a decreased mRNA expression of *BMPR2* (Figure S3), and was not exclusive of HAoECs, as endothelial colony forming cells (ECFCs) and, to a lesser extent, human skin microvascular ECs (HMECs), displayed a similar response (Figure S4). Noteworthy, incubation with higher concentrations of TNF-α led to a reduced expression of all three BMP type II receptors (Figure S5). We next investigated whether BMPR2 down regulation is necessary for TNF-α to induce EndMT in HAoECs, using knockdown and overexpression experiments (Figure 2B). Knock down of *BMPR2* in HAoECs using two different shRNA constructs resulted in reduced *CDH5* and *Pecam-1*, and increased *CDH2* and *Fibronectin* gene expression and loss of endothelial morphology. In contrast, ectopic overexpression of a full length BMPR2 construct (BMPR2 FL) in HAoECs using lentiviral particles prior to TNF-α stimulation prevented TNF-α-induced EndMT, as shown by gene expression analysis (Figure 2C) and immunofluorescent labeling (Figure 2D,E). Altogether our results show that down-regulation of BMPR2 is required for TNF-α to induce EndMT in HAoECs, and BMPR2 over-expression can partially prevent EndMT.

BMPR2 is down-regulated in ApoE3Leiden mice in response to high fat diet We next aimed to validate our findings *in vivo* using an animal model of atherosclerosis. The contribution of EndMT to vascular calcification and atherosclerosis has been recently investigated in different animal models, including $LDLR^{-/-}$, ApoE deficient or $Ins^{Akita}$ mice [4,42,43]. The ApoE3Leiden mice constitute a valuable model of diet-induced atherosclerosis with a human-like lipoprotein

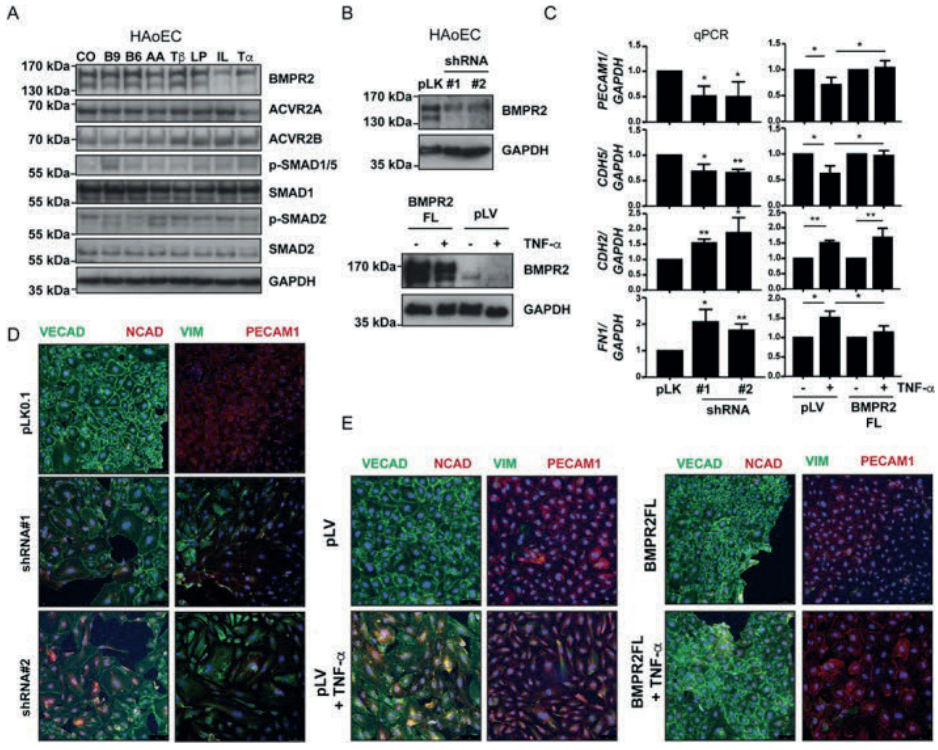


**Figure 2. TNF-α-induced down regulation of BMPR2 is necessary for HAoECs to undergo EndMT.** A. Western blot in HAoECs where EndMT has been induced for 24 hours as shown in Figure 1A. B. Western blot in HAoECs transduced with a control (pLK) lentivirus or two shRNA constructs (#1 and #2) against BMPR2 (upper panel) or with lentivirus encoding a full-length version of BMPR2 (BMPR2 FL) and treated with TNF-α for 24 hours (lower panel). C-E. EndMT analysis by qPCR (C) and Immunofluorescent staining (Ve-Cadherin, N-Cadherin, Vimentin, Pecam-1) (D and E) in HAoECs knocked-down for BMPR2 or over-expressing BMPR2 FL.

profile, when fed with a high fat diet [30,39]. Furthermore, this model is currently considered one the animal models of native atherosclerosis closest to the human pathology. Although some aspects of this model have been characterized already (e.g., a strong inflammatory infiltrate potentiates plaque's development), the contribution of EndMT to plaque formation is not known yet. Therefore, we performed immunofluorescent co-stainings for Pecam-1 and αSMA on sections from control animals (7 days normal diet vein grafts) and high hypercholesterolemic diet (high fat diet, HFD)-induced atherosclerosis animals (after 7, 14 and 28 days). As previously reported [32], the luminal endothelial layer of the aorta of HFD fed mice down-regulated Pecam-1 expression after 7 days, in contrast to control animals (Figure 3A, low magnification). This was accompanied by evident neointimal thickening. Interestingly, we observed Pecam-1 and αSMA

double positive cells migrating from the luminal layer into the neointima area (Figure 3A, high magnification). Such phenomenon was visible from day 7-28 in HFD fed animals, with a progressive increase in the expression of αSMA in the neointima. Consistent with our *in vitro* findings, BMPR2 expression was markedly reduced in the aorta at the onset of atherosclerosis, as early as 7 days of administration of HFD (Figure 3B).

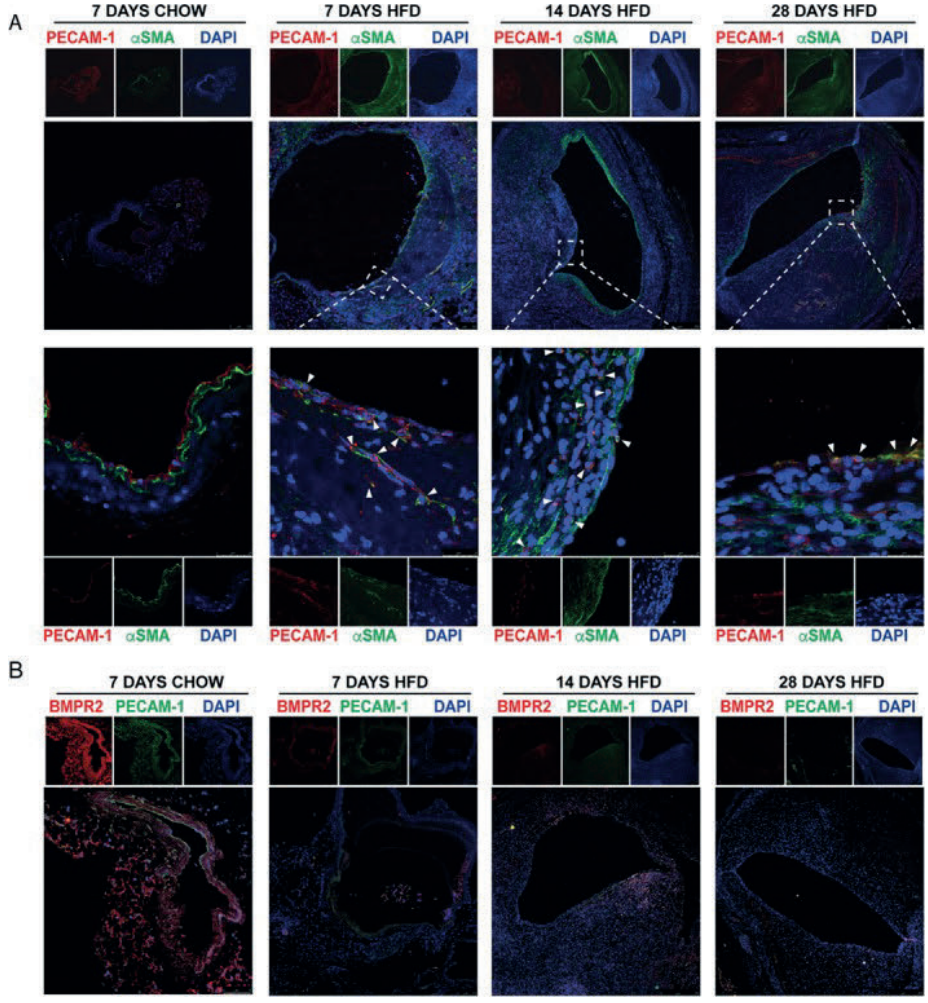


**Figure 3. BMPR2 is downregulated in the aorta of ApoE3Leiden mice developing atherosclerotic disease.** Aortic sections from ApoE3Leiden mice fed with a normal (Chow) or high fat diet (HFD) for 7, 14 or 28 days and stained for PECAM-1 and αSMA (A) or BMPR2 and PECAM-1 (B). A representative picture per condition is shown. White arrows point at PECAM-1/αSMA double positive cells, suggestive of EndMT.

**Down regulation of BMPR2 does not compromise BMP-induced canonical SMAD1/5 signaling**

In order to investigate the mechanisms by which loss of BMPR2 induced by TNF-$\alpha$ enhanced the osteogenic differentiation of ECs in response to BMP-9, we characterized an easy-to-culture EC line, the 2H-11 murine ECs. First, we demonstrated that, BMP-2, BMP-6, BMP-7 and BMP-9 effectively induce cell calcification in 2H-11 cells (Figure S6A), which can be blocked by coincubation with a BMP type I receptor kinase inhibitor (Figure S6B). Moreover, similar to primary HAoECs, knock-down of *BMPR2* (and not *ACVR2A* or *ACVR2B*) enhanced the osteogenic differentiation of 2H-11 cells induced by BMP-9 (Figure S7 and S8). On the contrary, stable overexpression of *BMPR2* FL partially prevented the osteogenic effect of BMP-9 (Figure S9). Since one of the main determinants of osteogenic differentiation is the induction of BMP canonical SMAD1/5 signal transduction, we first analyzed whether this was affected by TNF-$\alpha$. Although TNF-$\alpha$ pretreatment of 2H-11 cells resulted in a dose-dependent increase in osteogenic differentiation of BMP-9-induced 2H-11 cells (Figure 4A), the canonical BMP-9-induced transcriptional response (as measured using the BRE-LUC reporter construct, Figure 4B) was not increased by TNF-$\alpha$. Using a previously reported protocol for Iodination and ligand affinity labeling of cell surface receptors, we studied the high affinity receptors for BMP-9 in 2H-11 cells. As Figure 4C shows, while BMP-9 mainly forms a receptor complex including BMPR2 in control conditions, upon knock-down of *BMPR2*, BMP-9 recruits ACVR2A in a receptor signaling complex, together with ALK1/2 (Figure S10). To investigate whether this affects the canonical signaling response to BMP-9 in 2H-11 cells, we performed western blotting in stably knocked-down 2H-11 cells for *BMPR2*, *ACVR2A* or *ACVR2B*. As expected, single knock-down of any of the type II receptors failed to compromise BMP-9-induced p-SMAD1/5 response. Interestingly, pre-treatment with TNF-$\alpha$ blocked p-SMAD1/5 activation exclusively in cells knocked-down for ACVR2A (Figure 4D). These results suggest that loss of BMPR2 induced by TNF-$\alpha$, leads to an enhanced recruitment of ACVR2A in the signaling receptor complex, in order to balance downstream canonical signaling in ECs.

**Down regulation of BMPR2 decreases JNK pathway activation to fine tune EC mineralization**

Since the enhanced osteogenic response to BMP-9 of ECs lacking BMPR2 was not related to BMP-9 canonical signaling, we next tested the effect of different chemical inhibitors of non-canonical signaling on BMP-9-induced osteogenic differentiation. We used SP600125 to inhibit c-JUN N-terminal kinase (JNK), UO120

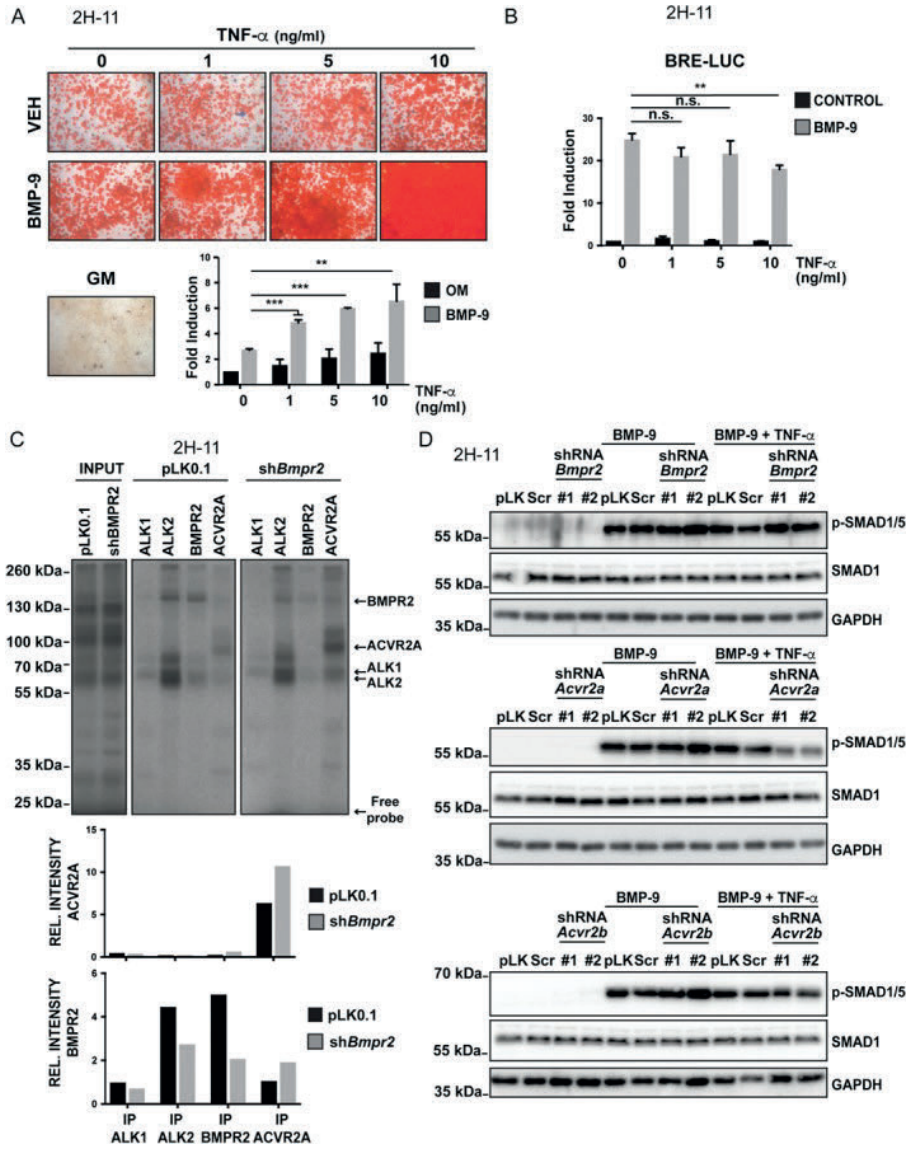


**Figure 4. TNF-α-induced loss of BMPR2 does not compromise BMP-9 canonical signaling in ECs.** A. Alizarin Red staining and quantification (lower figure) in 2H-11 cells incubated with BMP-9 (10 ng/ml) and increasing concentrations of TNF-α. GM: growth medium. Statistical significant difference with respect to control or BMP-9/TNF-α-treated cells (**, *** or non significant). B. BMP-9-induced canonical transcriptional response in 2H-11 cells stimulated with BMP-9 (10 ng/ml) upon pre-incubation with TNF-α. Fold induction of untreated control cells is shown. C. Ligand–receptor interaction assay in 2H-11 cells stably knocked down for BMPR2 or a control vector (pLK0.1). Quantification is shown below. D. Western blot of p-SMAD1/5 and total SMAD1 in 2H-11 cells stably knocked down for *Bmpr2, Acvr2A* or *Acvr2B* and treated with BMP-9 (10 ng/ml) and TNF-α (10 ng/ml).

against Extracellular signal related kinase (ERK), SB203580 for p38 kinase and PDTC (Ammonium pyrrolidinedithiocarbamate) to block Nuclear factor kappa B (NF-κB) signaling. We found that among all inhibitors used, only SP600125 enhanced the osteogenic differentiation of 2H-11 cells (Figure 5A). We confirmed this using a mutant version of the phosphatase MKP-1 (mMKP-1) [31]. 2H-11 cells transduced with mMKP-1 showed decreased activation of p-c-JUN, a downstream target of JNK, in response to BMP-9 (Figure S11). Next, we investigated the activation of p-c-JUN in 2H-11 cells stably knocked-down for BMPR2 or the other type II receptors. As Figure 5B shows, down regulation of *BMPR2,* and not ACVR2A or ACVR2B, by two different shRNA constructs decreased p-c-JUN in response to BMP-9. Furthermore, chemical inhibition of JNK in shBMPR2 2H-11 cells failed to enhance the calcifying effect of BMP-9, unlike control (pLK0.1), shACVR2A and shACVR2B stable cells (Figure 5C). This might suggest that BMPR2 functionally interacts with JNK in order to activate JNK signaling, as it has been previously suggested [44,45]. Accordingly, endogenous JNK was detected in GST pull down experiments performed with GST-BMPR2 (Figure S12). Finally, In order to determine the contribution of JNK signaling to the osteogenic differentiation of 2H-11 cells, we restored JNK signaling in cells with stable knock-down of *BMPR2* by over-expressing the MKK7-JNK3 fusion protein, which induces constitutive activation of JNK [36]. Ectopic over expression of MKK7-JNK3 increased the levels of phospho-c-JUN (Figure S13). Interestingly, this correlated with a partial inhibition of BMP-9-induced mineralization (Figure 5D). Taken together these data confirm that down-regulation of JNK activity in ECs favors their osteogenic differentiation in response to BMPs.

**ECs forming the *vasa vasora* in advanced human atherosclerosis exhibit reduced BMPR2 expression and JNK activation**

A unique characteristic of human atherosclerosis consists in the progressive ingrowth of micro capillaries from the adventitia towards the intima in the aorta. We have previously shown that ECs lining such capillaries (known as *vasa vasora*) increase the expression of the transcription factor Slug in early stages on atherosclerosis [3], suggesting that these cells may undergo EndMT and thereby contribute to a population of cells with osteogenic potential. To further extend these studies, we performed immunofluorescent labeling on sections of the human aorta corresponding to different stages of the atherosclerosis spectrum [34]. We observed an accumulation of αSMA positive cells and loss of luminal PECAM-1 in microcapillaries from sections corresponding to Fibrotic Calcified Plaque

(Advanced) (Figure 6A). Noteworthy, we found double positive PECAM-1 αSMA cells around the luminal endothelium, which is suggestive of EndMT.

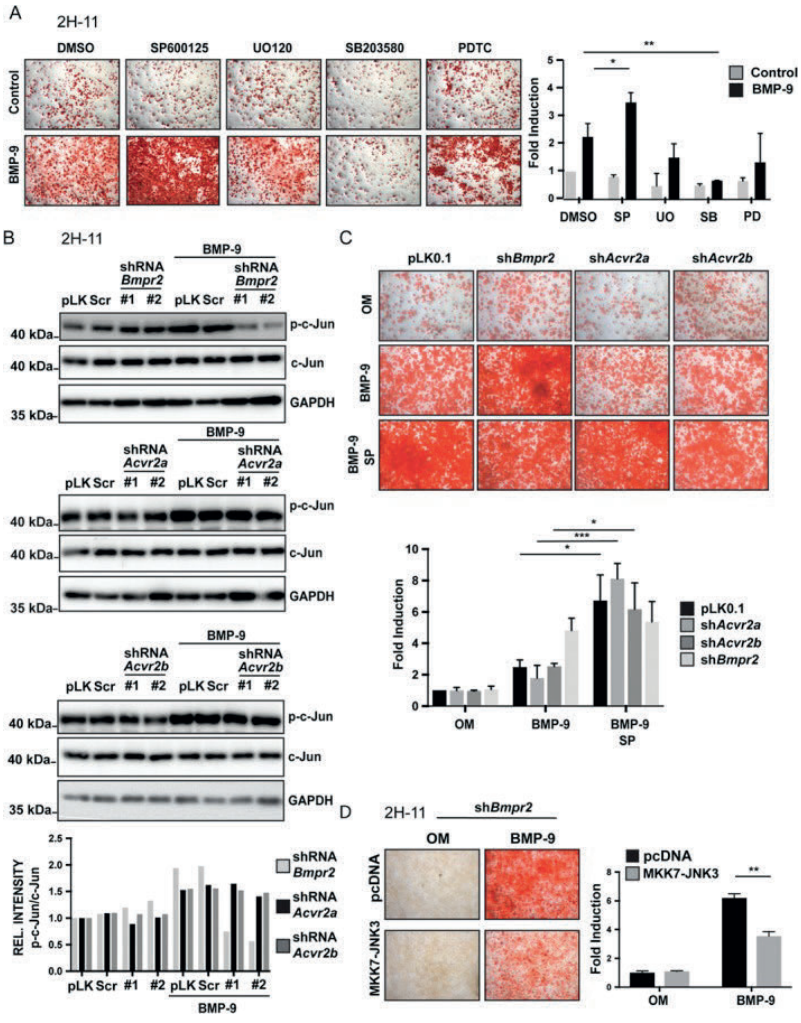


**Figure 5. Loss of BMPR2 decreases c-JUN activation, thereby enhancing BMP-9-induced osteogenic differentiation of ECs.** A. Alizarin Red Solution (ARS) staining and quantification on 2H-11 cells co-treated for 14 days with BMP-9 (10 ng/mL) and chemical inhibitors targeting the JNK (SP600125, 5 μmol/L), ERK (UO120, 10 μmol/L), p38 (SB203580, 10 μmol/L) and NF-κB (PDTC, 50 μmol/L) signaling pathways, incubated under osteogenic conditions. Fold induction of DMSO treated control cells is shown. B. Western blot of p-c-JUN and total c-JUN in 2H-11 cells stably knocked-down for *BMPR2*, *ACVR2A* or *ACVR2B* and stimulated with BMP-9 (10 ng/mL) for 45 mins. Quantification is shown below. C. ARS staining and quantification on 2H-11 cells stably knocked-down for BMPR2 (shRNA #1), ACVR2A (shRNA #1) or ACVR2B (shRNA #1) and stimulated for 14 days with BMP-9 (10 ng/mL) or BMP-9 and SP600125 (5 μmol/L) in osteogenic conditions. OM: Osteogenic medium. D. ARS staining and quantification in 2H-11 cells stably knocked-down for *BMPR2* and transfected with MKK7-JNK3 or an empty vector (pcDNA3), incubated with BMP-9 (10 ng/mL) under osteogenic conditions. Fold induction of pcDNA-transfected untreated cells is shown. OM: Osteogenic medium.

Furthermore, whereas BMPR2 was very potently expressed in ECs from capillaries of Normal and Early fibroatheroma (Early) sections (Figure 6B), ECs in Advanced lesions were very poorly stained for BMPR2 and PECAM-1. Finally, we analyzed the nuclear expression of p-SMAD1/5 and p-c-JUN in vasa vasorum ECs (Figure 6C,D). As Figure 6E shows, ECs expression of p-SMAD1/5 significantly augmented in Early and remained elevated in Advanced lesions. On the contrary, p-c-JUN expression peaked in Early stages, and dramatically dropped in Advanced lesions, in agree with the loss of BMPR2 expression. Altogether, these results support the mechanisms we have identified *in vitro*, and propose BMPR2 as a novel biomarker and druggable target for human atherosclerosis.

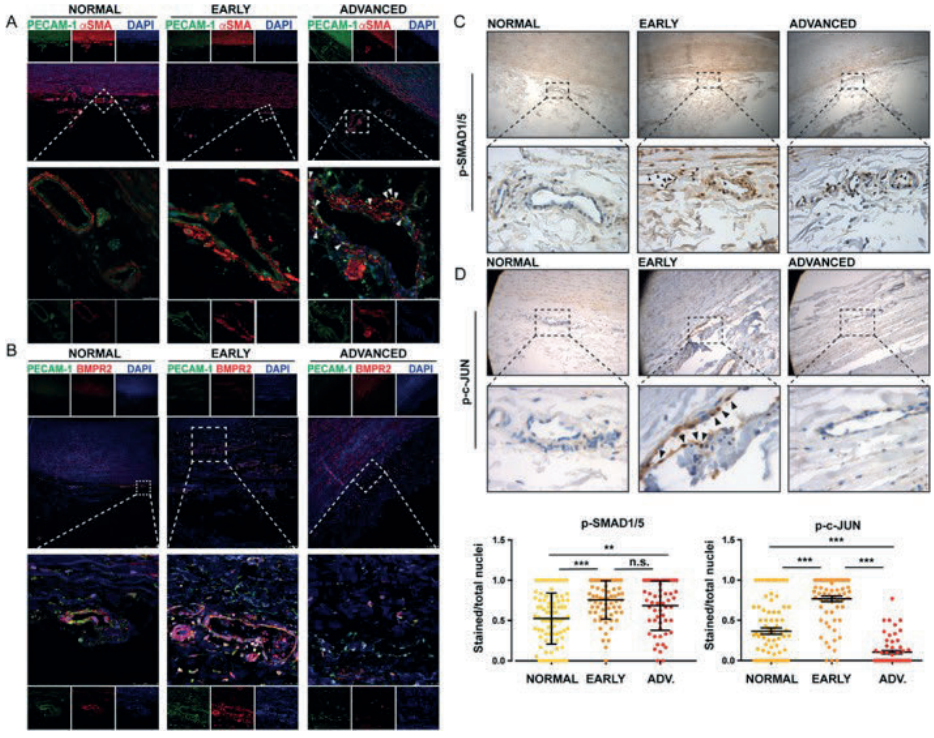


**Figure 6. BMPR2 is downregulated in ECs of advanced lesions of human atherosclerosis.** Immunofluorescent staining on aortic sections of control, Early Fibroatheroma (Early) or Fibrotic calcified plaque (FCP) donors. A representative picture per condition is shown. Zoomed images focus on microcapillaries in intimal and medial regions underneath the fibrotic core. A. Staining for PECAM-1 (green), αSMA (red) and DAPI (blue). White arrows point at PECAM-1 αSMA double positive cells. B. Staining for PECAM1 (green), BMPR2 (red) and DAPI (blue). Immunohistochemical staining for p-SMAD1/5 (C) or p-c-JUN (D) on the aforementioned sections. Black arrows point at positively stained cells. Low magnification (10X) and zoomed images (40X) are shown. E. Quantification of (C) and (D), based on number of p-SMAD1/5 or p-c-JUN positive ECs nuclei in one vessel/total nuclei in such vessel. A minimum of 55 vessels from 3 independent donors were considered per condition.

## Discussion

The identification of patients at increased risk of acute coronary events associated to vascular calcification, who may benefit from intensified preventative measures and for monitoring therapeutic efficacy is a major, ongoing challenge [46]. Recent publications have suggested that ECs directly contribute to vascular calcification through EndMT [2-4,42]. We have investigated the interplay between inflammatory cytokines and BMPs, a subfamily of the TGF-β family, in ECs. We found that the proinflammatory cytokine TNF-α induces EndMT in HAoECs, thereby enhancing their differentiation into osteoblast-like cells in response to BMP-9. TNF-α and IL-1β-induced EndMT in HAoECs, which results in BMPR2 down regulation. BMPR2 loss is sufficient and necessary for TNF-α to trigger EndMT in HAoECs. In addition, BMPR2 down regulation coincides with neointima formation and decrease of luminal PECAM1 positive cells in ApoE3Leiden mice subjected to high fat diet. Moreover, we showed that, in the absence of BMPR2, BMP-9 induces the formation of a receptor complex involving ACVR2A to induce downstream canonical signaling. Interestingly, we identified that BMPR2 down regulation leads to decreased JNK activation in ECs, as measured by phosphorylation of its downstream target c-JUN, and showed that JNK deactivation facilitates BMP-induced mineralization in ECs. Finally, we showed that adventitial microvessels (*vasa vasora*) in advanced atherosclerotic disease exhibit loss of luminal PECAM1 and BMPR2 expression and accumulation of PECAM1 αSMA double positive cells in layers underneath, which is suggestive of EndMT. Congruently, whereas p-SMAD1/5 activation increases in the *vasa vasora* ECs at early stages of atherosclerosis and remains sustained in advanced lesions, p-c-JUN activation dramatically drops in vessels in fibrotic calcified plaque lesions. These results point at a key role of BMPR2 as an integrator of TGF-β/BMP and inflammatory signaling in ECs, determining EndMT and subsequent calcification.

Endothelial cells with reduced BMPR2 expression displayed increased expression of inflammatory markers, such as ICAM and VCAM [47]. Interestingly, siRNA mediated knock-down of BMPR2 in human umbilical vein endothelial cells (HUVECs) led to reduced p-SMAD1/5 in response to BMP-4, although the authors did not test whether this effect was specific for BMPR2. BMP-9, unlike BMP-4, shows a high affinity for ALK1 in ECs [48] and BMPR2 [49], which may revert in a different contribution of BMPR2 in BMP-9 or BMP-4-induced receptor complexes. Furthermore, ALK1 (and not ALK2) was recently shown to mediate LDL uptake in ECs [50], and ECs exposed to an inflammatory cocktail lowered their LDL uptake capacity [51]. Whether BMPR2 deficiency alters the ALK1-LDL interaction is an interesting area of study.

BMPR2 deficiency leads to Pulmonary arterial hypertension (PAH), where heterozygous germ line mutations in the *BMPR2* gene are found in more than 70% of patients with hereditary PAH and 20% of patients with idiopathic PAH [52,53]. Several publications have pointed at EndMT as a causative factor for the vascular remodeling in the pulmonary arteries of PAH patients [54,55]. Furthermore, PAH patients display a higher tendency to develop calcified lesions within the pulmonary arteries [56], suggesting that BMPR2 may have a protective role inhibiting calcification in cells with osteogenic potential. In this sense, osteoblast specific knock out of *BMPR2* led to increased bone mass in transgenic mice [57]. Importantly, BMP-9 has been recently proposed as a therapeutic option for PAH [12]. Nevertheless, it remains to be determined whether systemic administration of BMP-9 may lead to calcification of the arteries under inflammatory conditions, such as those considered risk factors for atherosclerotic disease (renal disease, diabetes, hypertension or hyperlipidemia).

In summary, we have shown that aortic ECs undergo EndMT in response to inflammatory stimuli, which favour the calcification of ECs. The underlying mechanisms of such enhanced osteogenic potential point at non-canonical signal transduction, that fine tunes BMP-SMAD1/5 signaling (summarized in Figure S14). A hallmark of this process is the down regulation of BMPR2. Therefore, monitoring BMPR2 expression as a biomarker of calcification, or developing drugs specifically increasing BMPR2 expression to prevent EndMT in the arteries constitute an area of interest for future research.

**Acknowledgements**

We thank K. Iwata, S. Vukicevic and J. Nickel for reagents. We are grateful to Martijn Rabelink for shRNA lentiviral constructs. We thank Maarten van Dinther, Midory Thorikay, Kirsten Lodder and Karien Weismeijer for excellent technical assistance, and the entire group for scientific discussions. Research in the laboratory of PTD and MJG on TGF-β family is granted by the Netherlands Cardiovascular Research Initiative: the Dutch Heart Foundation, Dutch Federation of University Medical Centres, the Netherlands Organization for Health Research and Development, and the Royal Netherlands Academy of Sciences (PHAEDRA consortium) and by the gravitation program CancerGenomiCs.nl from the Netherlands Organization for Scientific Research (NWO). MJG and VP are supported by the BAV consortium (2013T093). GSD is supported by the RECONNECT consortium (belonging to the Netherlands Cardiovascular Research Initiative, as aforementioned) and a Postdoctoral Fellowship from AFM-Telethon. AGV would like to acknowledge the Dutch Arthritis Association (Reumafonds) for support.

**Statement of author contributions**

*Study design*: GSD, PtD, JL, MJG, MDV. *Data collection*: GSD, AGVA, VP, STGJ, MG. *Data analysis*: GSD, AGVA, VP, STGJ, MG. *Data interpretation*: GSD, PtD, JL, MJG, HVD, MDV. *Literature search*: GSD, PtD, JL, MJG, HVD, MDV. *Generation of figures*: GSD, AGVA, VP, STGJ. *Writing of the manuscript*: GSD, PtD, MJG, JL, HVD, MDV.

## References

*Cited only in Supplementary Information.


1. Libby P, Ridker PM, Hansson GK. Progress and challenges in translating the biology of atherosclerosis. *Nature* 2011; **473**: 317–325.
2. Evrard SM, Lecce L, Michelis KC, *et al*. Endothelial to mesenchymal transition is common in atherosclerotic lesions and is associated with plaque instability. *Nat Commun* 2016; **7**: 1–15.
3. Sánchez-Duffhues G, de Vinuesa AG, Lindeman JH, *et al*. SLUG is expressed in endothelial cells lacking primary cilia to promote cellular calcification. *Arterioscler Thromb Vasc Biol* 2015; **35**: 616–627.
4. Chen P-Y, Qin L, Baeyens N, *et al*. Endothelial-to-mesenchymal transition drives atherosclerosis progression. *J Clin Invest* 2015; **125**: 4514–4528.
5. Sánchez-Duffhues G, García de Vinuesa A, ten Dijke P. Endothelial to mesenchymal transition in cardiovascular diseases: Developmental signalling pathways gone awry. *Dev Dyn* 2018; **247**: 492-508.
6. Gisterå A, Hansson GK. The immunology of atherosclerosis. *Nat Rev Neph* 2017; **13**: 368-380.
7. Boström K, Watson KE, Horn S, *et al*. Bone morphogenetic protein expression in human atherosclerotic lesions. *J Clin Invest* 1993; **91**: 1800–1809.
8. Dhore CR, Cleutjens JP, Lutgens E, *et al*. Differential expression of bone matrix regulatory proteins in human atherosclerotic plaques. *Arterioscler Thromb Vasc Biol* 2001; **21**: 1998–2003.
9. Morrell NW, Bloch DB, ten Dijke P, *et al*. Targeting BMP signalling in cardiovascular disease and anaemia. *Nat Rev Cardiol* 2016; **13**: 106–120.
10. David L, Mallet C, Keramidas M, *et al*. Bone morphogenetic protein-9 is a circulating vascular quiescence factor. *Circ Res* 2008; **102**: 914–922.
11. van Meeteren LA, Thorikay M, Bergqvist S, *et al*. Anti-human activin receptor-like kinase 1 (ALK1) antibody attenuates bone morphogenetic protein 9 (BMP9)-induced ALK1 signaling and interferes with endothelial cell sprouting. *J Biol Chem* 2012; **287**: 18551–18561.
12. Long L, Ormiston ML, Yang X, *et al*. Selective enhancement of endothelial BMPR-II with BMP9 reverses pulmonary arterial hypertension. *Nat Med*. 2015; **21**:777–785.
13. Mitrofan C-G, Appleby SL, Nash GB, *et al*. Bone morphogenetic protein 9 (BMP9) and BMP10 enhance tumor necrosis factor-α-induced monocyte recruitment to the vascular endothelium mainly via activin receptor-like kinase 2. *J Biol Chem* 2017; **292**: 13714–13726.

14. Kang Q, Sun MH, Cheng H, *et al.* Characterization of the distinct orthotopic bone-forming activity of 14 BMPs using recombinant adenovirus-mediated gene delivery. *Gene Ther* 2004; **11**: 1312–1320.
15. Saeed O, Otsuka F, Polavarapu R, *et al.* Pharmacological suppression of hepcidin increases macrophage cholesterol efflux and reduces foam cell formation and atherosclerosis. *Arterioscler Thromb Vasc Biol* 2012; **32**: 299–307.
16. Derwall M, Malhotra R, Lai CS, *et al.* Inhibition of bone morphogenetic protein signaling reduces vascular calcification and atherosclerosis. *Arterioscler Thromb Vasc Biol* 2012; **32**: 613–622.
17. de Vinuesa AG, Abdelilah-Seyfried S, Knaus P, *et al.* BMP signaling in vascular biology and dysfunction. *Cytokine Growth Factor Rev* 2016; **27**: 65–79.
18. de Jong DS, Vaes BLT, Dechering KJ, *et al.* Identification of novel regulators associated with early-phase osteoblast differentiation. *J Bone Miner Res* 2004; **19**: 947–958.
19. Zhang YE. Non-Smad pathways in TGF-β signaling. *Cell Res* 2009; **19**: 128–139.
20. Mu Y, Gudey SK, Landström M. Non-Smad signaling pathways. *Cell Tissue Res* 2012; **347**: 11–20.
21. Gilbert L, He X, Farmer P, *et al.* Inhibition of osteoblast differentiation by tumor necrosis factor-alpha. *Endocrinology* 2000; **141**: 3956–3964.
22. Kaneki H, Guo R, Chen D, *et al.* Tumor necrosis factor promotes Runx2 degradation through up-regulation of Smurf1 and Smurf2 in osteoblasts. *J Biol Chem* 2006; **281**: 4326–4333.
23. Gerstenfeld LC, Cho TJ, Kon T, *et al.* Impaired fracture healing in the absence of TNF-alpha signaling: the role of TNF-alpha in endochondral cartilage resorption. *J Bone Miner Res* 2003; **18**: 1584–1592.
24. Chang J, Wang Z, Tang E, *et al.* Inhibition of osteoblastic bone formation by nuclear factor-κB. *Nat Med* 2009; **15**: 682–689.
25. De Boeck M, Cui C, Mulder AA, *et al.* Smad6 determines BMP-regulated invasive behaviour of breast cancer cells in a zebrafish xenograft model. *Sci Rep* 2016; **6**: 24968.
26. Tasev D, van Wijhe MH, Weijers EM, *et al.* Long-Term Expansion in Platelet Lysate Increases Growth of Peripheral Blood-Derived Endothelial-Colony Forming Cells and Their Growth Factor-Induced Sprouting Capacity. *PLoS ONE* 2015; **10**: e0129935.
27. O'Connell KA, Rudmann AA. Cloned spindle and epithelioid cells from murine Kaposi's sarcoma-like tumors are of endothelial origin. *J Invest Dermatol* 1993; **100**: 742–745.
28. O'Connell K, Landman G, Farmer E, *et al.* Endothelial cells transformed by SV40 T antigen cause Kaposi's sarcomalike tumors in nude mice. *Am J Pathol* 1991; **139**: 743–749.
29. Zhang J, Zhang X, Zhang L, *et al.* LRP8 mediates Wnt/β-catenin signaling and controls osteoblast differentiation. *J Bone Miner Res* 2012; **27**: 2065–2074.

30. van Dinther M, Visser N, de Gorter DJJ, *et al*. ALK2 R206H mutation linked to fibrodysplasia ossificans progressiva confers constitutive activity to the BMP type I receptor and sensitizes mesenchymal cells to BMP-induced osteoblast differentiation and bone formation. *J Bone Miner Res* 2010; **25**: 1208–1215.
31. Hamdi M, Kool J, Cornelissen-Steijger P, *et al*. DNA damage in transcribed genes induces apoptosis via the JNK pathway and the JNK-phosphatase MKP-1. *Oncogene* 2005; **24**: 7135–7144.
32. Lardenoye JHP, de Vries MR, Löwik CWGM, *et al*. Accelerated atherosclerosis and calcification in vein grafts: a study in APOE*3 Leiden transgenic mice. *Circ Res* 2002; **91**: 577–584.
33. Virmani R, Kolodgie FD, Burke AP, *et al*. Lessons from sudden coronary death: a comprehensive morphological classification scheme for atherosclerotic lesions. *Arterioscler Thromb Vasc Biol* 2000; **20**: 1262–1275.
34. van Dijk RA, Virmani R, Thüsen von der JH, *et al*. The natural history of aortic atherosclerosis: a systematic histopathological evaluation of the peri-renal region. *Atherosclerosis* 2010; **210**: 100–106.
35. Korchynskyi O, ten Dijke P. Identification and functional characterization of distinct critically important bone morphogenetic protein-specific response elements in the Id1 promoter. *J Biol Chem* 2002; **277**: 4883–4891.
36. Rennefahrt UEE, Illert B, Kerkhoff E, *et al*. Constitutive JNK activation in NIH 3T3 fibroblasts induces a partially transformed phenotype. *J Biol Chem* 2002; **277**: 29510–29518.
37. Scharpfenecker M, van Dinther M, Liu Z, *et al*. BMP-9 signals via ALK1 and inhibits bFGF-induced endothelial cell proliferation and VEGF-stimulated angiogenesis. *J Cell Sci* 2007; **120**: 964–972.
38. Rosenzweig BL, Imamura T, Okadome T, *et al*. Cloning and characterization of a human type II receptor for bone morphogenetic proteins. *Proc Natl Acad Sci USA* 1995; **92**: 7632–7636.
39. Ichijo H, Yamashita H, ten Dijke P, *et al*. Characterization of in vivo phosphorylation of activin type II receptor. *Biochem Biophys Res Commun* 1993; **194**: 1508–1514.
40. ten Dijke P, Yamashita H, Ichijo H, *et al*. Characterization of type I receptors for transforming growth factor-b and activin. *Science* 1994; **264**: 101–104.
41. Upton PD, Morrell NW. TGF-β and BMPR-II pharmacology--implications for pulmonary vascular diseases. *Curr Opin Pharmacol* 2009; **9**: 274–280.
42. Guihard PJ, Yao J, Blazquez-Medela AM, *et al*. Endothelial-Mesenchymal Transition in Vascular Calcification of Ins2Akita/+ Mice. Ushio-Fukai M, editor. *PLoS ONE* 2016; **11**: e0167936–12.
43. Wang L, Luo J-Y, Li B, *et al*. Integrin-YAP/TAZ-JNK cascade mediates atheroprotective effect of unidirectional shear flow. *Nature* 2016; **540**: 579–582.

44. Podkowa M, Zhao X, Chow C-W, *et al.* Microtubule stabilization by bone morphogenetic protein receptor-mediated scaffolding of c-Jun N-terminal kinase promotes dendrite formation. *Mol Cell Biol* 2010; **30**: 2241–2250.
45. Chen W-K, Yeap YYC, Bogoyevitch MA. The JNK1/JNK3 interactome--contributions by the JNK3 unique N-terminus and JNK common docking site residues. *Biochem Biophys Res Commun* 2014; **453**: 576–581.
46. Franco M, Cooper RS, Bilal U, *et al.* Challenges and Opportunities for Cardiovascular Disease Prevention. *Am J Med* 2011; **124**: 95–102.
47. Kim CW, Song H, Kumar S, *et al.* Anti-inflammatory and antiatherogenic role of BMP receptor II in endothelial cells. *Arterioscler Thromb Vasc Biol* 2013; **33**: 1350–1359.
48. Scharpfenecker M, van Dinther M, Liu Z, *et al.* BMP-9 signals via ALK1 and inhibits bFGF-induced endothelial cell proliferation and VEGF-stimulated angiogenesis. *J Cell Sci* 2007; **120**: 964–972.
49. Kraehling JR, Chidlow JH, Rajagopal C, *et al.* Genome-wide RNAi screen reveals ALK1 mediates LDL uptake and transcytosis in endothelial cells. *Nature Commun* 2016; **7**: 1–15.
50. Rieder F, Kessler SP, West GA, *et al.* Inflammation-induced endothelial-to-mesenchymal transition: a novel mechanism of intestinal fibrosis. *Am J Pathol* 2011; **179**: 2660–2673.
51. Brown MA, Zhao Q, Baker KA, *et al.* Crystal structure of BMP-9 and functional interactions with pro-region and receptors. *J Biol Chem* 2005; **280**: 25111–25118.
52. International PPH Consortium, Lane KB, Machado RD, *et al.* Heterozygous germline mutations in BMPR2, encoding a TGF-β receptor, cause familial primary pulmonary hypertension. *Nat Genet* 2000; **26**: 81–84.
53. Deng Z, Morse JH, Slager SL, *et al.* Familial primary pulmonary hypertension (gene PPH1) is caused by mutations in the bone morphogenetic protein receptor-II gene. *Am J Hum Genet* 2000; **67**: 737–744.
54. Ranchoux B, Antigny F, Rucker-Martin C, *et al.* Endothelial-to-Mesenchymal Transition in Pulmonary Hypertension. *Circulation* 2015; **131**: 1006-1018.
55. Qiao L, Nishimura T, Shi L, *et al.* Endothelial fate mapping in mice with pulmonary hypertension. *Circulation* 2014; **129**: 692–703.
56. Ruffenach G, Chabot S, Tanguay VF, *et al.* Role for Runt-related Transcription Factor 2 in Proliferative and Calcified Vascular Lesions in Pulmonary Arterial Hypertension. *Am J Respir Crit Care Med* 2016; **194**: 1273–1285.
57. Lowery JW, Intini G, Gamer L, *et al.* Loss of BMPR2 leads to high bone mass due to increased osteoblast activity. *J Cell Sci* 2015; **128**: 1308–1315.
*58. Nakao A, Imamura T, Souchelnytskyi S, *et al.* TGF-β receptor-mediated signalling through Smad2, Smad3 and Smad4. *EMBO J* 1997; **16**: 5353–5362.

*59. Zou Y, Dietrich H, Hu Y, *et al*. Mouse model of venous bypass graft arteriosclerosis. *Am J Pathol* 1998; **153**: 1301–1310.

*60. Hawinkels LJAC, Paauwe M, Verspaget HW, *et al*. Interaction with colon cancer cells hyperactivates TGF-β signaling in cancer-associated fibroblasts. *Oncogene* 2014; **33**: 97–107.

## Supplemental figures

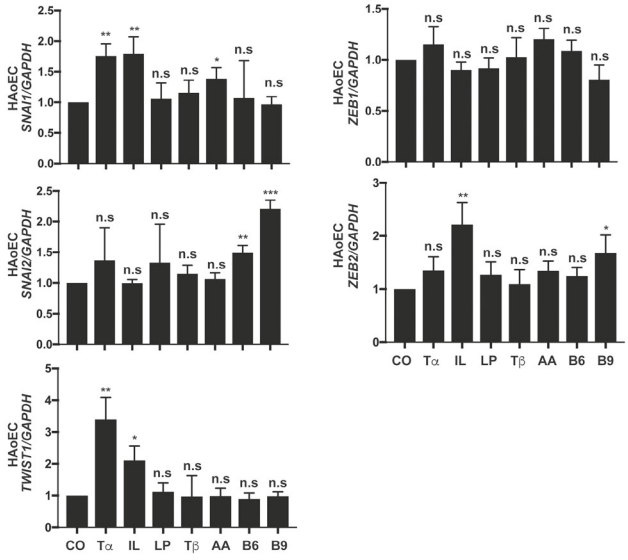


**Figure S1. TNF-α and IL-1β induce the up-regulation of EndMT factors in HAoECs.** Gene expression analysis of the genes SNAI1 (encoding SNAIL), SNAI2 (encoding SLUG), TWIST1, ZEB1 and ZEB2 in HAoECs stimulated for 24 h with the indicated cytokines and growth factors. CO: control; Tα: TNF-α (10 ng/ml); IL: IL-1β (10 ng/ml); LP: LPS (10 ng/ml); Tβ: TGF-β3 (5 ng/ml); AA: activin A (50 ng/ml); B6: BMP-6 (50 ng/ml); B9: BMP-9 (10 ng/ml).

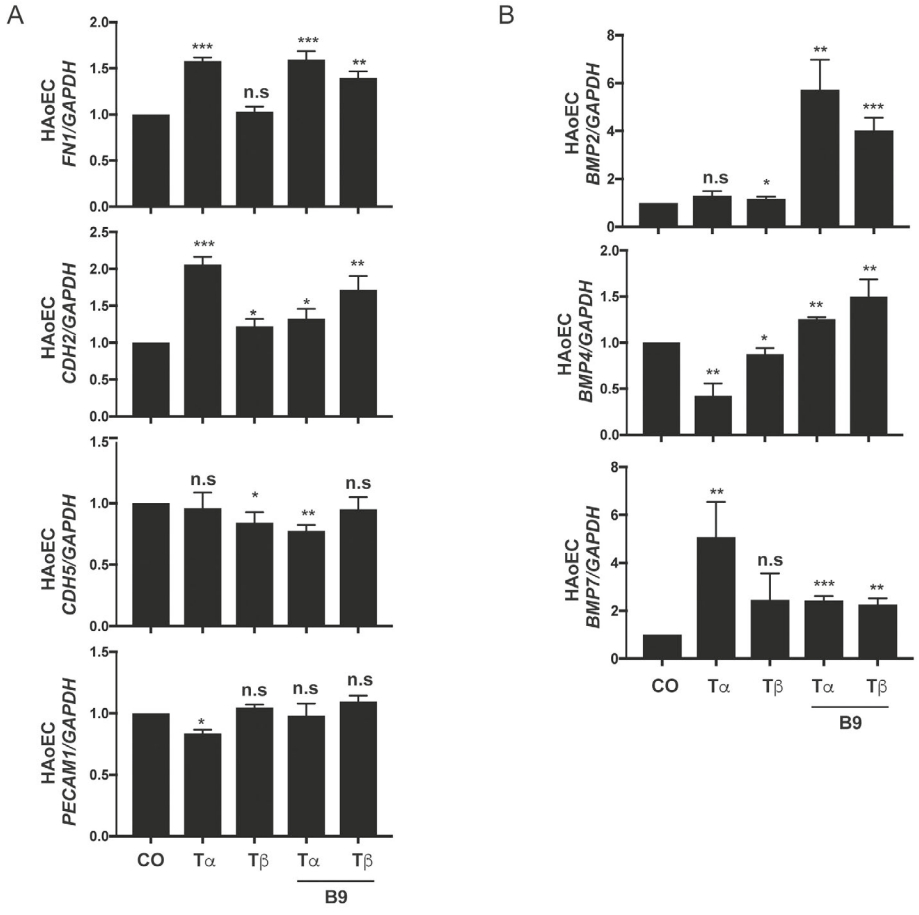


**Figure S2. Long term effect of TNF-α and TGF-β in HAoECs.** A. Gene expression analysis of FN (encoding Fibronectin), CDH2 (encoding N-CAHDERIN), CDH5 (encoding VE-CADHERIN) and PECAM1 in HAoECs stimulated for 4 days with TNF-α (Tα: 10 ng/ml) or TGF-β3 (Tβ: 5 ng/ml); followed by 24 h of BMP-9 (B9: 10 ng/ml). B. qPCR gene expression analysis of the BMP ligand encoding genes BMP2, BMP4 and BMP7, in HAoECs treated as indicated in (A).

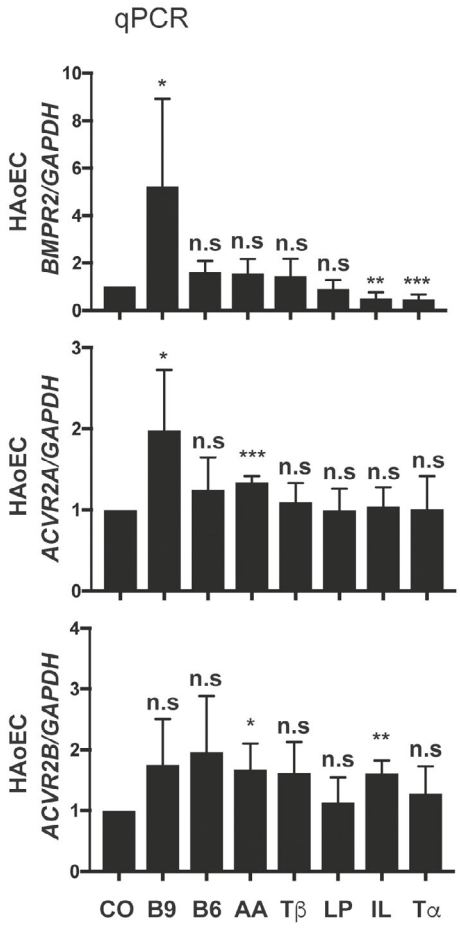


**Figure S3. TNF-α and IL-1β induce the down regulation of BMPR2 in HAoECs.** Gene expression analysis of the BMP type II receptors BMPR2, ACVR2A and ACVR2B in HAoECs incubated for 24 h with the indicated growth factors in the presence of 10% of serum.

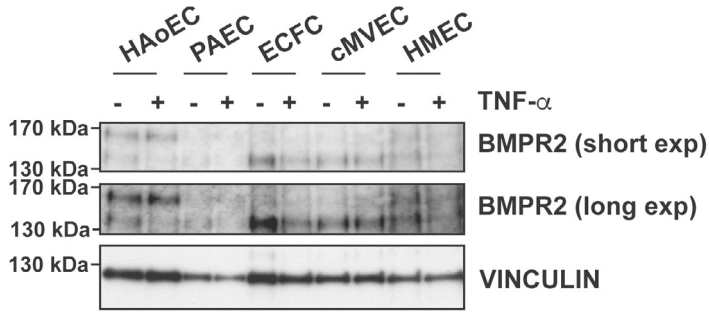


**Figure S4: TNF-α induces the up-regulation of BMPR2 in a cell type specific manner.** Western blot for BMPR2 (long and short exposures) in HAoEC, human pulmonary aortic ECs (PAEC), human endothelial colony forming cells (ECFC), human coronary microvascular EC (cMVEC) and human skin microvascular ECs (HMEC) treated for 24 h with TNF-α (10 ng/ml) in medium containing 10% serum.

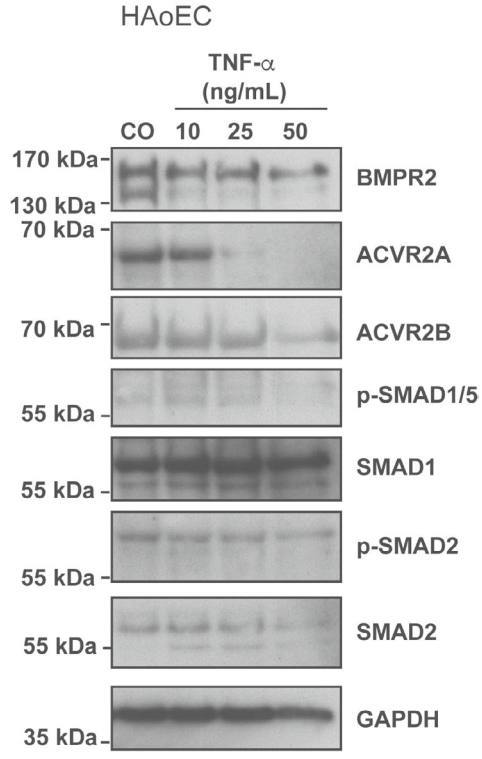


**Figure S5. TNF-α down regulates BMPR2 in a dose dependent manner.** Western blot in HAoECs treated for 24 h with increasing concentrations of TNF-α in medium containing 10% serum. CO: Control.

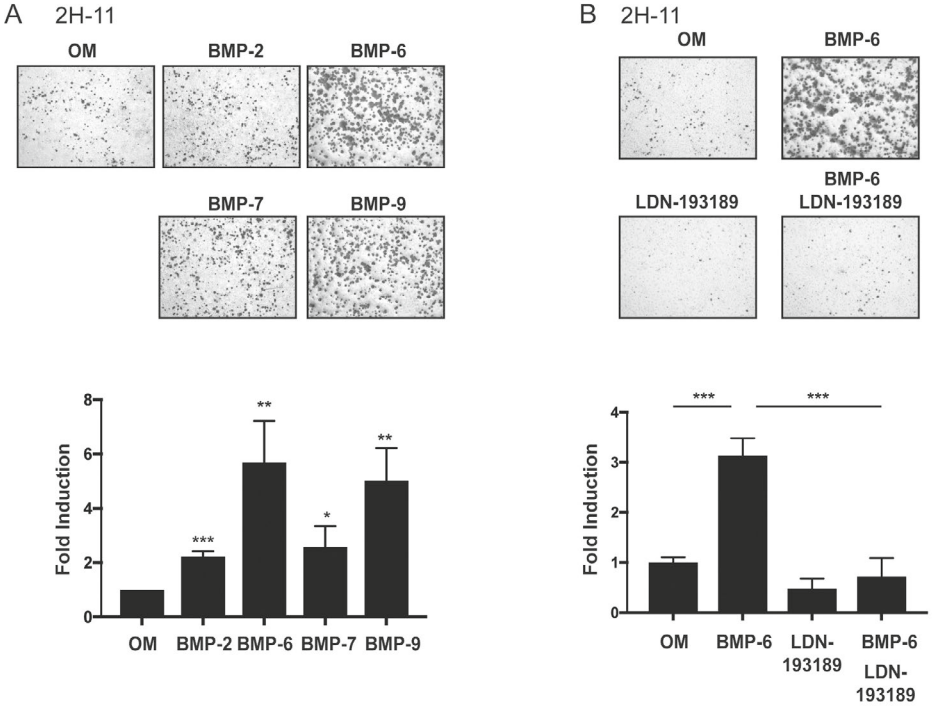


**Figure S6. BMP receptor activation is required to induce cell mineralization in 2H-11 endothelial cells.** A. Alizarin Red staining (ARS) of 2H-11 cells stimulated with either BMP-2, BMP-6 or BMP-7 (50 ng/ml) or BMP-9 (10 ng/ml) for 14 days under osteogenic culture conditions (OM). Quantification is shown below as fold induction of OM control cells. B. ARS of 2H-11 cells stimulated for 14 days with BMP-6 (50 ng/ml) and/or the BMP type I receptor kinase inhibitor LDN-193189 (120 nM). Quantification is shown below as fold induction of OM control cells.

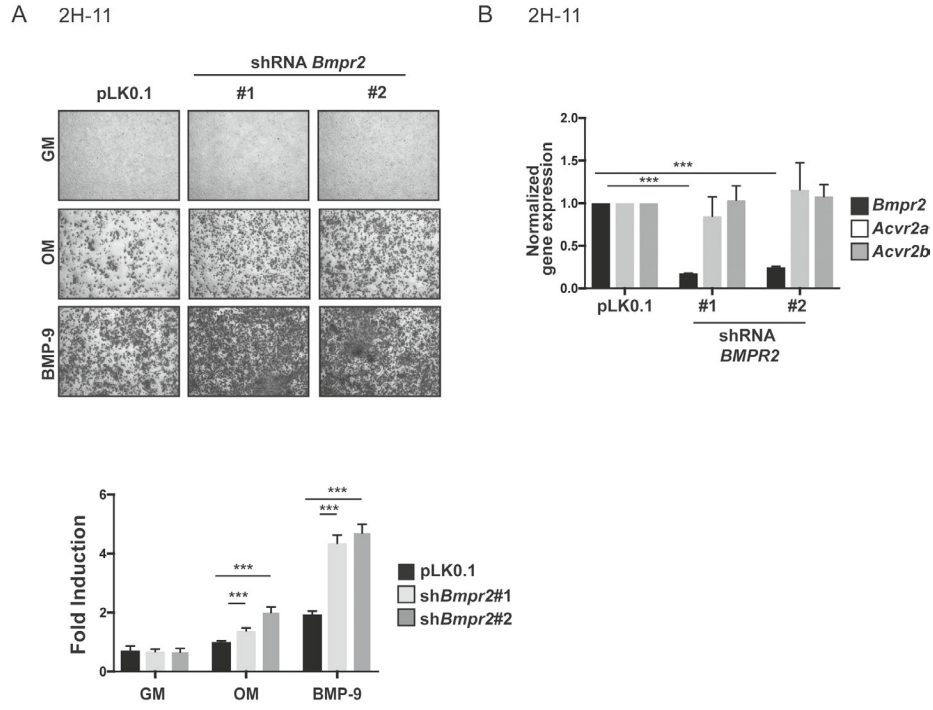


**Figure S7. BMPR2 knock-down enhances BMP-9 induced mineralization in 2H-11 cells.** A. Alizarin Red staining (ARS) of 2H-11 cells stably transduced with two independent shRNA constructs targeting BMPR2 (#1 and #2) or an empty vector (pLK0.1) and incubated with BMP-9 (10 ng/ml) for 14 days under osteogenic culture conditions (OM) or regular growth medium (GM). Quantification is shown below as fold induction of pLK0.1 stable cells in OM. B. qPCR analysis of BMPR2, ACVR2A and ACVR2B in 2H-11 cells knocked down for BMPR2.

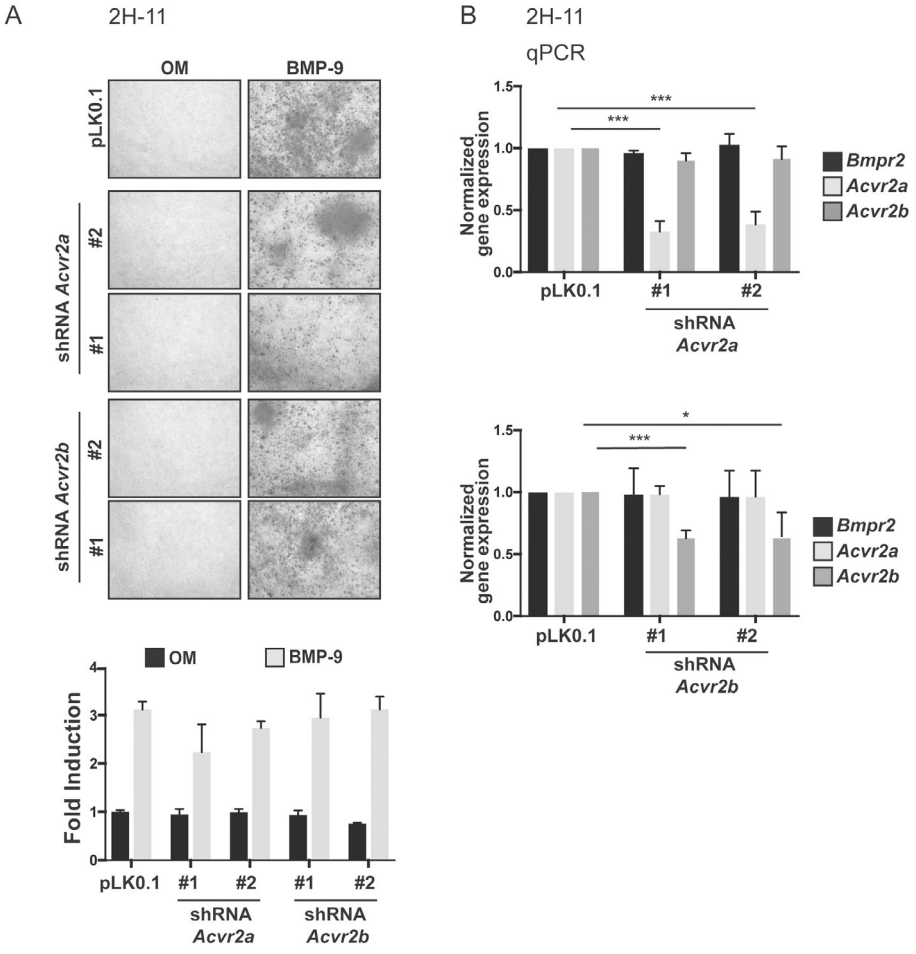


**Figure S8. Knock-down of ACVR2A or ACVR2B does not affect BMP-9 induced mineralization in 2H-11 cells.** A. ARS of 2H-11 cells stably transduced with two shRNA constructs targeting Acvr2A or Acvr2B (#1 and #2) or a control vector (pLK0.1) and incubated with BMP-9 (10 ng/ml) for 14 days under osteogenic culture conditions (OM) or regular growth medium (GM). Quantification is shown below as fold induction of pLK0.1 stable cells in OM. B. qPCR analysis of Bmpr2, Acvr2A and Acv2 in 2H-11 cells knocked down for AcvrA and Acvr2B.

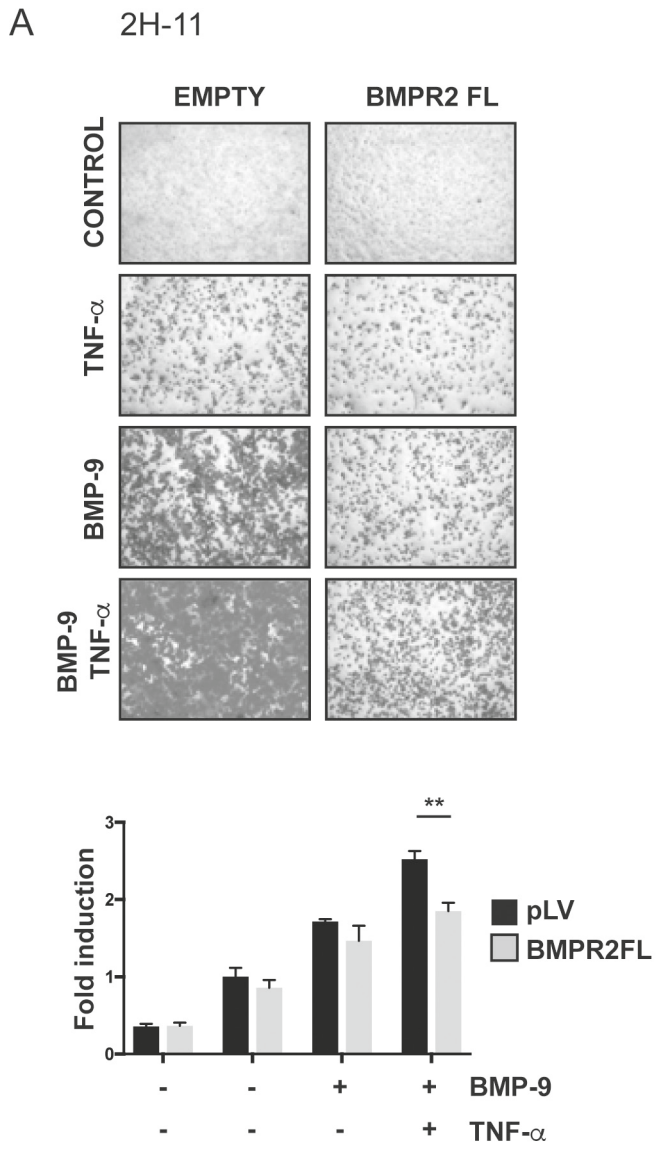


**Figure S9. BMPR2 over-expression partially prevents BMP-9 induced mineralization in 2H-11 cells.** ARS of 2H-11 cells stably over-expressing a BMPR2 full length construct (BMPR2 FL) or an empty vector (EMPTY, pLV) and stimulated with BMP-9 (10 ng/ml) and/or TNF-α (10 ng/ml) for 14 days under osteogenic conditions. Quantification is shown below as fold induction of pLV stable cells in OM.

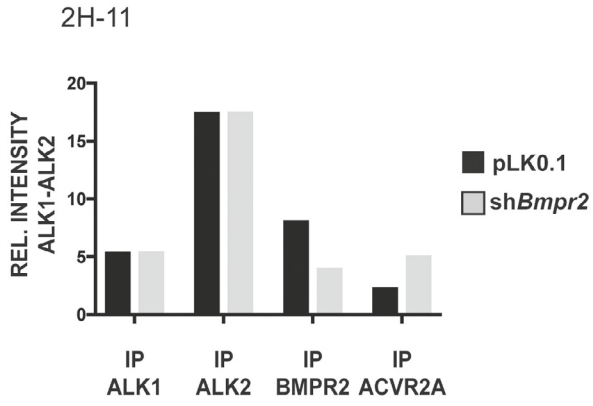


**Figure S10. Knock-down of BMPR2 does not compromise BMP-9 binding to ALK1 or ALK2.** Quantification by densitometry corresponding to a ligand-receptor interaction assay performed in 2H-11 stably infected with a control (pLK0.1) or BMPR2 knock-down (shBMPR2) lentivirus. ALK1-ALK2 intensity is shown. IP: Immunoprecipitation.



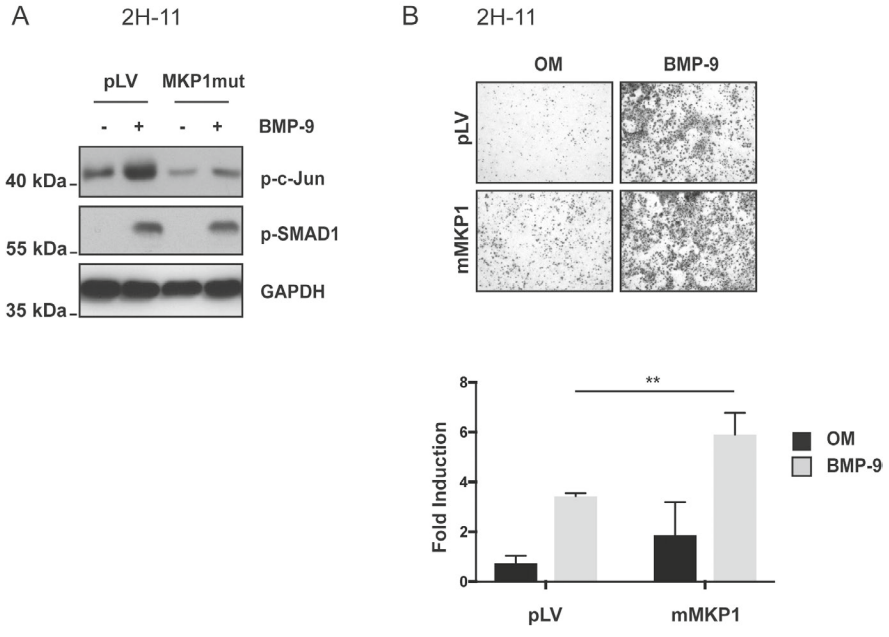


**Figure S11. Inhibition of c-Jun phosphorylation enhances BMP-9 induced mineralization in 2H-11 cells.** A. Western blot of 2H-11 cells transduced with lentivirus encoding for a c-Jun-specific mutant version of MKP1 (mMKP1) or an empty vector and stimulated with BMP-9 (10 ng/ml). B. ARS of 2H-11 cells infected with mMKP1 and stimulated with BMP-9 (10 ng/ml) under osteogenic culture conditions (OM). Calcium deposits were solubilized and measured by absorbance.

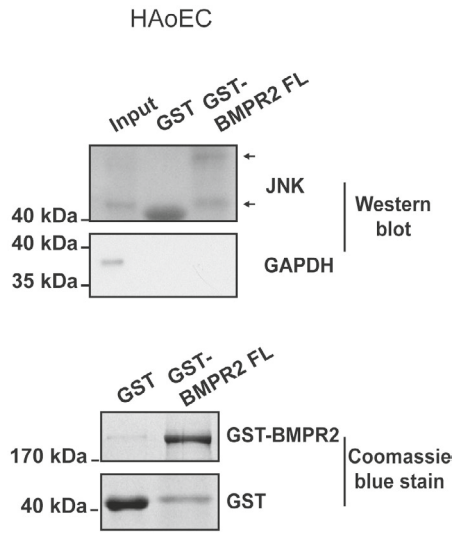


**Figure S12. *In vitro* protein interaction BMPR2-JNK.** JNK interacts with BMPR2 in GST-BMPR2 pull down assay on whole cell lysate of HAoECs. Endogenous JNK interacts *in vitro* with GST-BMPR2 FL, whereas GAPDH is only detected in the input.

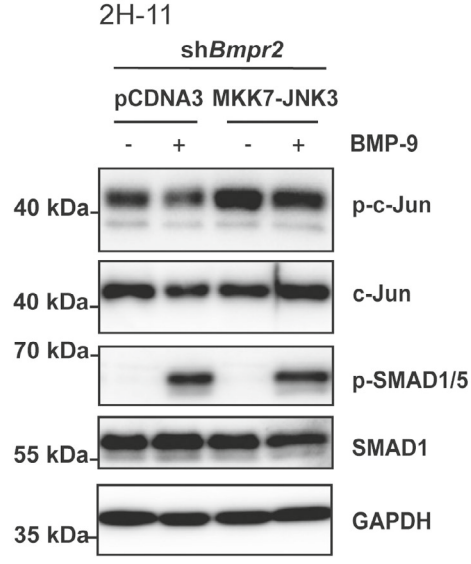


**Figure S13. MKK7-JNK3 over expression restores p-c-Jun in 2H-11 shBMPR2 cells.** Western blot of 2H-11 cells stably knocked-down for BMPR2 and transfected with a MKK7-JNK3 encoding construct or an empty vector (pcDNA3). Cells were serum starved for 16 h and stimulated for 45 min with BMP-9 (10 ng/ml).

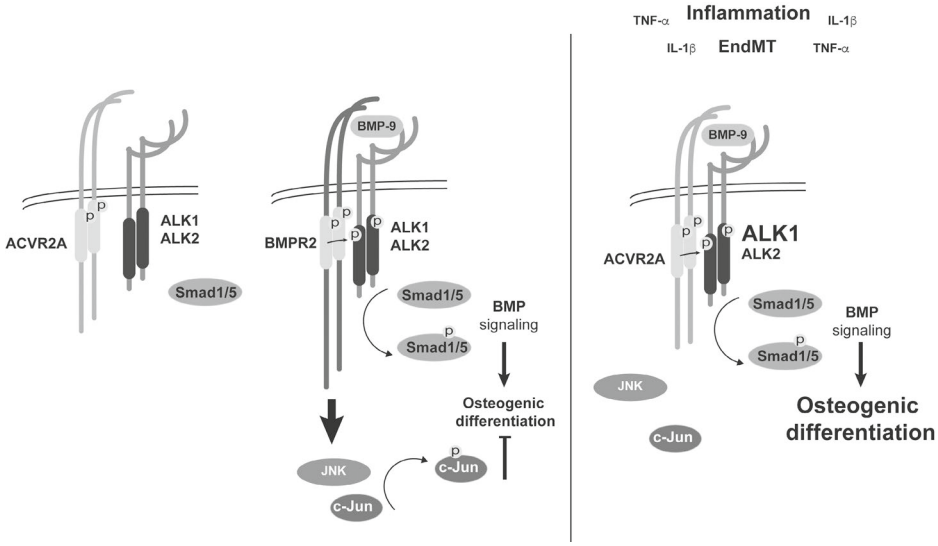


**Figure S14. Graphical summary.** In the presence of BMP-9, a heterotetrameric BMP membrane receptor complex is formed consisting of ALK1/2 and BMPR2 in ECs. This induces the downstream activation of canonical SMAD1/5 and non-canonical JNK signaling, leading to osteogenic differentiation and calcium deposition. Upon stimulation with TNF-α, ECs undergo EndMT and down-regulate BMPR2. BMP-9 now interacts with a receptor complex consisting of ALK1/2 and ACVR2A in ECs. This induces the phosphorylation of SMAD1/5, but does not activate p-c-Jun potently. As p-c-Jun acts as a negative regulator of EC calcification, EndMT-derived cells exhibit a higher osteogenic activity in response to BMP-9.

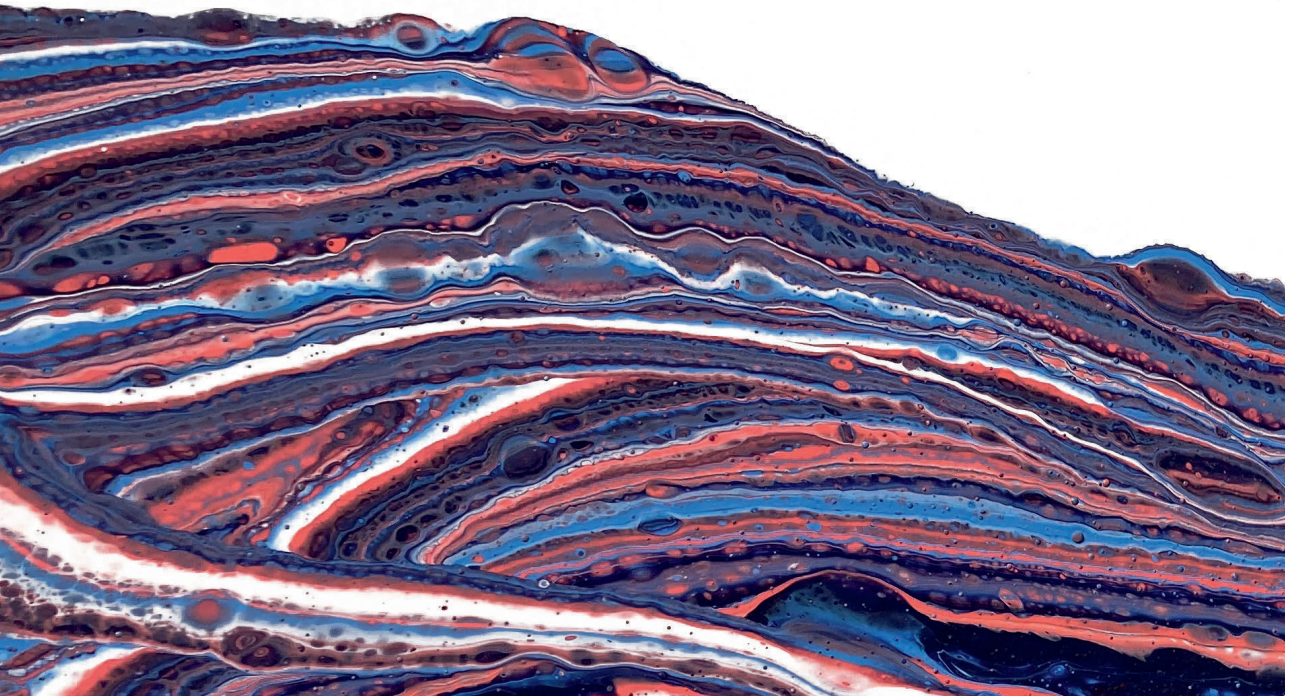

# Chapter 6

## New calcification model for intact murine aortic valves

**Vera van de Pol[1&], Boudewijn P.T. Kruithof[*1,2,4&] ,Tamara Los[1], Kirsten Lodder[1], Babak Mousavi Gourabi[3], Marco C. DeRuiter[3], Marie-José Goumans[1#], Nina Ajmone Marsan[2#]**

&,#: equally contributed

[1] Department of Molecular Cell Biology, Leiden University Medical Center, Leiden, The Netherlands
[2] Department of Cardiology, Leiden University Medical Center, Leiden, The Netherlands
[3] Department of Anatomy and Embryology, Leiden University Medical Center, Leiden, The Netherlands
[4] Netherlands Heart Institute, Utrecht, The Netherlands

*Published: Journal of Molecular and Cellular Cardiology, 2021 | 165: p.95*

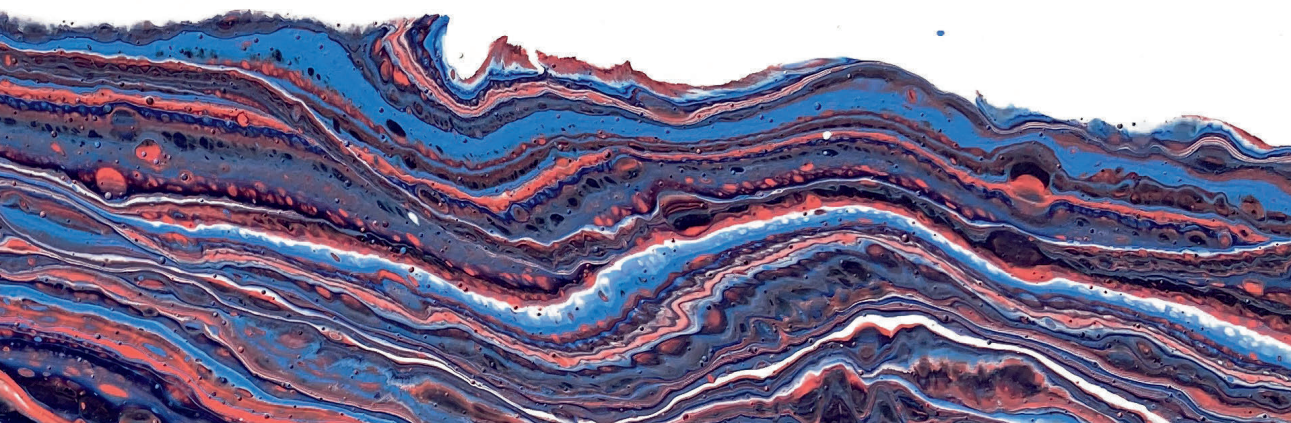

## Abstract

Calcific aortic valve disease (CAVD) is a common progressive disease of the aortic valves, for which no medical treatment exists and surgery represents currently the only therapeutic solution. The development of novel pharmacological treatments for CAVD has been hampered by the lack of suitable test-systems, which require the preservation of the complex valve structure in a mechanically and biochemical controllable system. Therefore, we aimed at establishing a model which allows the study of calcification in intact mouse aortic valves by using the Miniature Tissue Culture System (MTCS), an *ex vivo* flow model for whole mouse hearts. Aortic valves of wild-type mice were cultured in the MTCS and exposed to osteogenic medium (OSM, containing ascorbic acid, β-glycerophosphate and dexamethasone) or inorganic phosphates (PI). Osteogenic calcification occurred in the aortic valve leaflets that were cultured ex vivo in the presence of PI, but not of OSM. In vitro cultured mouse and human valvular interstitial cells calcified in both OSM and PI conditions, revealing in vitro-ex vivo differences. Furthermore, endochondral differentiation occurred in the aortic root of ex vivo cultured mouse hearts near the hinge of the aortic valve in both PI and OSM conditions. Dexamethasone was found to induce endochondral differentiation in the aortic root, but to inhibit calcification and the expression of osteogenic markers in the aortic leaflet, partly explaining the absence of calcification in the aortic valve cultured with OSM. The osteogenic calcifications in the aortic leaflet and the endochondral differentiation in the aortic root resemble calcifications found in human CAVD. In conclusion, we have established an ex vivo calcification model for intact wild-type murine aortic valves in which the initiation and progression of aortic valve calcification can be studied. The in vitro-ex vivo differences found in our studies underline the importance of ex vivo models to facilitate pre-clinical translational studies.

## Graphical abstract

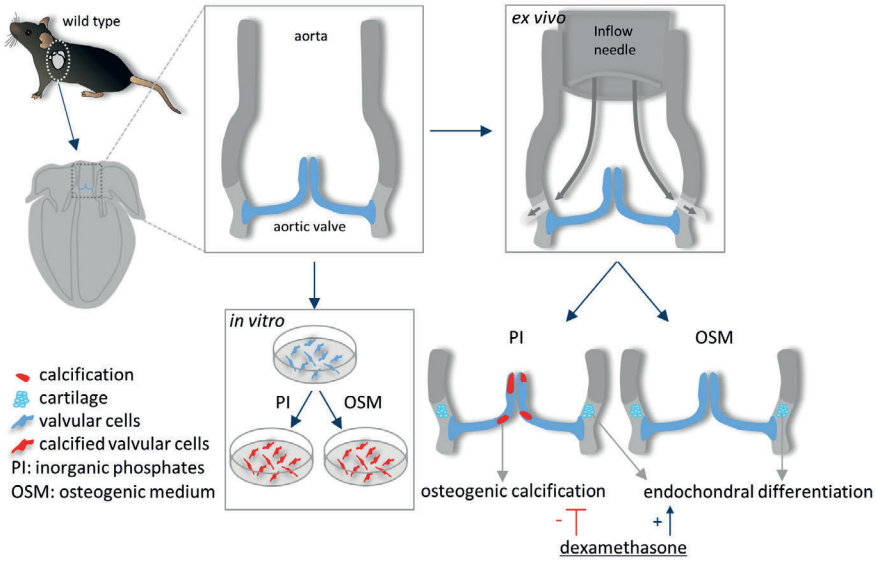

## Introduction

Calcific aortic valve disease (CAVD) is a common progressive disease, whose prevalence, and therefore health and financial burden, is expected to significantly increase with the ageing population [1]. Currently no pharmacological therapy has shown to be effective in CAVD and when severe aortic stenosis occurs surgical or percutaneous valve replacement is the only treatment option [2]. Full understanding of the pathogenesis of CAVD is therefore imperative to find new medical treatments and research is focused on finding accurate models to elucidate the pathological process behind CAVD [3-5].

Aortic valves have a highly organized structure consisting of 3 layers of extracellular matrix (ECM) rich in collagen (fibrosa), proteoglycans (spongiosa) and elastin (ventricularis). The leaflets are covered by valvular endothelial cells (VECs) and interspersed with valvular interstitial cells (VICs). VICs are responsible for the maintenance of the valvular structure by producing, degrading and organizing the ECM [6]. In CAVD, presence of calcification is the prominent feature together with inflammation, fibrosis and lipid deposition. Calcific mineral deposition can occur through dystrophic, osteogenic and endochondral calcification and involves the activation of VICs. During dystrophic calcification, VICs adopt a myofibroblast phenotype expressing alpha-smooth muscle actin (αSMA) and undergo apoptosis creating a substrate on which calcium deposits form [5,7-12]. During osteogenic calcification VICs adopt an osteogenic phenotype, demonstrated by the expression of proteins such as runt-related transcription factor 2 (RUNX2), alkaline phosphatase (ALP) and cyclo-oxygenase 2 (COX2), and produce calcium deposits [13-18]. During endochondral calcification, osteogenic calcification is preceded by cartilage formation [19]. These 3 types of calcification can occur simultaneously or independently in human aortic valves [9,18,20,21], where the calcifications have been described as “nodular” or “intrinsic”. Nodular calcifications have been mostly observed in the mid-tip of valve leaflets and are characterized by elastin fragmentation. “Intrinsic” calcifications have recently been described within the ECM in the hinge point of the aortic valves and are characterized by increased proteoglycan deposit as in endochondral calcification [9]. Both calcifications are motly located at regions with high mechanical stress and disturbed flow indicating that mechanical stress has an important role in activating VICs and propagating calcification [22,23].

To study aortic valve calcification, both *in vitro* and *in vivo* models have been explored. *In vitro*, the most commonly used protocol is culturing VICs in osteogenic media (OSM) which consists of ascorbic acid, β-glycerophosphate and dexamethasone [24]. Dexamethasone has been shown to induce expression of and activate RUNX2; ascorbic acid facilitates differentiation by altering the ECM

and β-glycerolphosphate provides phosphates used to create mineral depositions [25-28]. A different *in vitro* protocol induces calcification by addition of 3 mM inorganic phosphates to the medium (referred to as PI) mimicking mild hyperphosphatemia (healthy is up to 1.45 mM) [29,30]. Aside from the phosphates required to generate mineral depositions, inorganic phosphates have been shown to regulate expression of proteins such as BMP2 and osteopontin [31,32]. Studies using *in vitro* models have demonstrated the important role of mechanical stress, the influence of the matrix and the interaction between VICs, VECs and macrophages in the process of calcification [5,7,33-37]. These studies thereby demonstrated that the absence of the complete valvular structure might prevent drawing accurate conclusions for *in vivo* calcification. *In vivo* mouse models have in turn the advantage of studying the whole aortic valve under native hemodynamic conditions [38]. The induction of calcification, however, is limited in wildtype animals, and requiring dietary and/or genetic modification [38-41]. In addition, in contrast to *in vitro* models, single experimental parameters cannot accurately be controlled and altered.

Because of the *in vitro* and *in vivo* limitations, it is imperative to find more suitable models to study CAVD combining both the preservation of the complex valve structure that characterizes *in vivo* modeling and a mechanically and biochemically controllable system that is facilitated by *in vitro* modeling [42]. We have previously developed the miniature tissue culture system (MTCS), which allows the controllable culture of mouse valves in their natural position in the heart and under specific hemodynamic conditions [43-45]. In this study, we have used the MTCS to develop a calcification model for the intact murine aortic valve. We show that calcification can be induced in the intact aortic valve of wild type mice by exposing the leaflets to increased levels of PI, but not when exposed to OSM. Dexamethasone appeared to be at least partly responsible for the absence of calcification in the OSM condition. Culturing murine valvular cells *in vitro* showed calcification in both OSM and PI conditions, demonstrating clear *in vitro*/*ex vivo* differences. Furthermore, calcification observed in the aortic leaflets was associated with markers of osteogenic differentiation and not of dystrophic calcification. In turn, at the level of the aortic root endochondral differentiation was observed when cultured in both PI and OSM conditions. In conclusion, we developed an *ex vivo* calcification model for murine aortic valves which can facilitate pre-clinical translational studies to further advance our understanding of CAVD.

## Materials and methods

### VIC isolation and culture

Human VICs (hVICs; kindly provided by dr Hjortnaes) were cultured on 0,1% gelatin-coated wells in DMEM supplemented with 10% FBS and PenStrep (100U/ml, Gibco). Mouse VICs (mVICs) were isolated by pooling the aortic, pulmonary, mitral and tricuspid valves per mouse into a 48-wells coated with 0,1% gelatin in 100 $\mu$l dissociation medium (0.125% Trypsin (Serva), 0,125% EDTA (Serva), 1,25 mg/ml Collagenase A (Roche), 46% DMEM high glucose (ThermoFisher), 1% fetal bovine serum (FBS), Insulin-Transferrin-Selenium (ITS; 10 mg/ml insulin, 5,5 mg/ml Transferrin, 6,7 ng/ml sodium selenite; Gibco) and incubated over night at 4 °C. Subsequently, the wells were incubated for 35 minutes at 37 °C and the mixture was gently dissociated using a syringe. Afterwards 300 $\mu$l culture medium (DMEM, 10% FBS, ITS, antibiotics/antimycotics (Sigma)) was added and the cells were grown at 37 °C until confluent. Media was refreshed twice a week. DMEM contains 0,9 mM of phosphate, which is in the range of adult blood phosphate concentrations (0,87-1,45 mM).

### Calcification *in vitro*

Cells were seeded for either visualization of the calcification (48-well size) or RNA isolation (12-well size). Upon confluency, the VICs were treated with calcifying medium OSM (culture medium supplemented with 10 mM β-glycerophosphate (Merck), 100 nM dexamethasone (Merck) and 50 $\mu$g/ml ascorbic acid (Merck)) or PI (culture medium supplemented with 3 mM sodium phosphate (Sigma)) which was replaced twice a week. To quantify the calcification, the cells were fixed after 7 or 21 days using 4% paraformaldehyde solution in phosphate buffered saline (PFA/PBS, pH7.2) for 10 minutes, washed with milli-Q water (MQ) and incubated with 2% Alizarin Red (Sigma, pH 4.2) in MQ for 3 minutes to visualize calcification. The plates were washed twice with MQ and imaged. Finally the alizarin red was dissolved by replacing the MQ with 150 $\mu$l cetylperidiumchloride for 3hr at 37 °C and the absorbance was measured in duplo at 595nm. To study transcriptional activity, RNA was isolated using the ReliaPrep RNA cell miniprep kit (Promega) according to the manufacturer's protocol. RevertAid First Strand cDNA Synthesis (ThermoFisher Scientific) was used to generate cDNA according to the manufacturer's protocol, after which qRT-PCR was performed using GoTaq qPCR Master Mix (Promega, A6001). GAPDH and 28S were used as housekeeping genes. Primer sequences used are detailed in Table 1.

**Table 1.** Primer sequences for qPCR. * 5'end to 3'end

| Gene | Forward* | Reverse* |
|---|---|---|
| GAPDH | AACTTTGGCATTGTGGAAGG | ACACATTGGGGGTAGGAACA |
| 28S | GGCCACTTTTGGTAAGCAGA | GCGGATTCCGACTTCCAT |
| PECAM1 | CAAAGTGGAATCAAACCGTATCT | CTACAGGTGTGCCCGAG |
| ALP | GAACAGACCCTCCCCACGAG | GTCTCTCTCTTTCTCTGGCACA |
| COX2 | AGAAGGAAATGGCTGCAGAA | GCTCGGCTTCCAGTATTGAG |
| PiT1 | TGTGGCAAATGGGCAGAAG | AGAAAGCAGCGGAGAGACGA |
| PiT2 | CCATCGGCTTCTCACTCGT | AAACCAGGAGGCGACAATCT |
| RUNX1 | TCACCTCTTCCTCTGTCCAC | CACCATGGAGAACTGGTAGG |
| RUNX2 | CCACAAGGACAGAGTCAGATTACA | TGGCTCAGATAGGAGGGGTA |
| RUNX3 | CCGGCAATGATGAGAACTAC | GGAGAAGGGGTTCAGGTTTA |
| Aggrecan | TCTACCCCAACCAAACCGG | AGGCATGGTGCTTTGACAGTG |
| Collagen2 | TTCCACTTCAGCTATGGCGA | GACGTTAGCGGTGTTGGGAG |
| αSMA | ACTGGGACGACATGGAAAAG | CATCTCCAGAGTCCAGCACA |

### *Ex vivo* culture of mouse aortic valves

All animal experiments were performed in 2-6 months old mice with a mixed genetic background (B6;129) according to protocols approved by the animal welfare committee of the Leiden University Medical Center and conform the guidelines from Directive 2010/63/EU of the European Parliament on the protection of animals used for scientific purposes. Mouse hearts were cultured in the MTCS as previously described [44]. In summary and with the following modifications: mice were anesthetized with 4% isoflurane and the hearts were *in situ* perfused with salt solutions, removed and transferred to the perfusion chambers. For each heart, the inflow needle of the perfusion chamber was inserted into the aorta and ligated with a suture. Flow (1000 ml/min) was introduced using a pump and medium (control medium, control medium with 100 nM dexamethasone, PI, PI with 100 nM dexamethasone, OSM, OSM without dexamethasone) was directed from the reservoir through the bubble trap and into the perfusion chamber where it flowed through the aorta towards the closed aortic valve into the coronary circulation (Figure 1). The medium exited the heart via the right atrium and recirculated to the reservoir. The medium was replaced one time. After culture for 1 week the hearts were isolated and fixed overnight with 4% PFA/PBS.

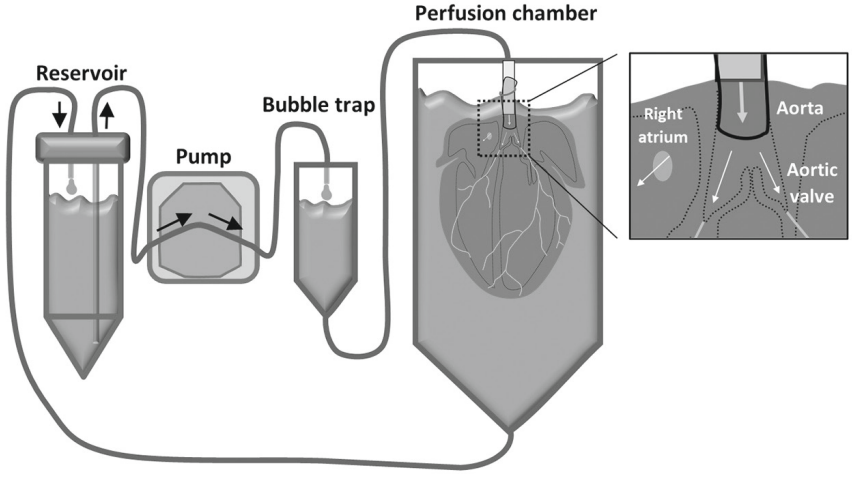


**Figure 1. The *ex vivo* flow system for mouse aortic valves.** The MTCS is a closed flow circuit consisting of a reservoir with medium, a pump, a bubble trap and a perfusion chamber which are connected by tubings. In the perfusion chamber, the mouse heart is ligated to the inflow needle that is inserted into the aorta. The pump directs medium from the reservoir through the bubble trap into the perfusion chamber where it flows from the aorta into the coronary circulation (green lines) thereby closing the aortic valve. The medium exits the heart via the right atrium and flows back to the reservoir (modified from Kruithof et al. 2015[44]).

Fixed mouse hearts were dehydrated through a graded series of ethanol, cleared in xylene, embedded in paraffin, and sectioned at 6mm. The sections were deparaffinized and hydrated before subsequent staining. For visualization of the calcification, alizarin red (Sigma) and von kossa (Sigma) stainings were performed. Sections were stained with Weigert's Resorcin Fuchsin (EMS) to identify elastic fibres, alcian blue (Klinipath) to visualize glycoaminoglycans (GAGs) and counterstained with nuclear-fast red (Sigma). For immunofluorescent staining the slices were boiled for 8 or 35 minutes in Antigen Retrieval Buffer (10 mM Tris (pH9)/1 mM EDTA/0.05% Tween-20) using a pressure cooker. Sections for aggrecan staining were in addition incubated for 1 hour at 37 °C with chondroitinase ABC (Sigma; 200 mU/ml) diluted in 50 mM Tris (pH 8.0; Sigma) with 60 mM sodium acetate (Sigma) and 0.02% bovine serum albumin (BSA; Sigma). After blocking with 1%BSA in 0,1%Tween-PBS, sections were incubated overnight with the primary antibodies directed against RUNX1 + RUNX3 + RUNX2 (RUNX1/2/3; Abcam; [EPR3099] ab92336; 1:100), ALP (R&D; AF2910; 1:250), COX2 (D5H5; Cell Signaling; 12282; 1:200), Platelet Endothelial Cell Adhesion Molecule (PECAM-1; R&D; 1:1000), aSMA (Sigma; A2547; 1:20.000), cleaved caspase-3 (cCasp3; Cell Signaling; #9664; 1:100), aggrecan (Millipore; AB1031; 1:200), collagen II (SouthernBiotech; 1310-01; 1:50) followed by incubation with

alexa-conjugated secondary antibodies (Molecular Probes). Slides are mounted using DAPI containing ProlongGold Antifade reagent (Thermofisher). All slides were scanned with the Pannoramic 250 slide scanner (version1.23, 3DHISTECH Ltd.) and analyzed using Caseviewer (version2.3, 3DHISTECH Ltd.).

**Quantifications**

To quantify the calcification in the aortic valve, the percentage of the alizarin red-positive area of the aortic valve was determined. At least 6 sections with 96 mm interval were used per heart and the measurements were averaged. To determine the alcian blue-positive or elastin-positive area of the aortic root, the surface of the alcian blue-positive or elastin-positive area of the aortic root was determined of at least 4 sections with 96 mm interval per heart and the measurements were averaged. To determine the percentage of RUNX1/2/3-positive cells of the aortic valve, the total number of RUNX1/2/3-positive cells were divided by the total number of nuclei as determined by DAPI-staining. Quantifications were performed using Caseviewer (version2.3, 3DHISTECH Ltd.) and ImageJ.

**Statistics**

Statistical analysis was performed using Graphpad Prism (version 9). Data was tested for significance as indicated in each legend using analysis of variance (ANOVA) with Tukey correction or Kruskal-Wallis with Dunn's correction for multiple groups, and Students t-test or Mann-Whitney test for comparison of 2 groups. Data are reported as means ± SEM. A P-value below 0.05 was considered significant.



## Results

**PI induces calcification in *ex vivo* cultured aortic valves**

In order to induce calcification in intact murine aortic valve leaflets, mouse hearts were cultured in the MTCS in a continuous closed position with medium flowing from the aorta towards the closed aortic valve into the coronary circulation (Figure 1). In this condition, the aortic valve is exposed to continuous hemodynamic stresses at its aortic side and continuous mechanical stresses throughout the valve, which are suggested to be important drivers of aortic valve calcification [22]. Hearts were cultured in the presence of OSM or PI and compared to uncultured mouse hearts and control cultured mouse hearts without OSM or PI (CTRL). Calcification was identified by alizarin red staining (Figure 2A) and confirmed with von kossa staining (not shown). The uncultured and control cultured hearts did not show any calcification (Figure 2A,B). In the presence of

PI, however, calcification was observed in the majority of the hearts (10 out 14) after 7 days of culture with varying densities and located at the tip or body of the leaflet (Figure 2B). In the presence of OSM, on the other hand, no calcification was observed after 7 days (Figure 2A,B). Also after 3 weeks of culture in the presence of OSM no calcification was observed in the aortic valve (n=5; not shown), indicating that the absence of calcification in OSM cultures was not due to a delay in calcification. Therefore, calcification in intact wild type murine aortic valves could efficiently be induced *ex vivo* by PI, but not by OSM.

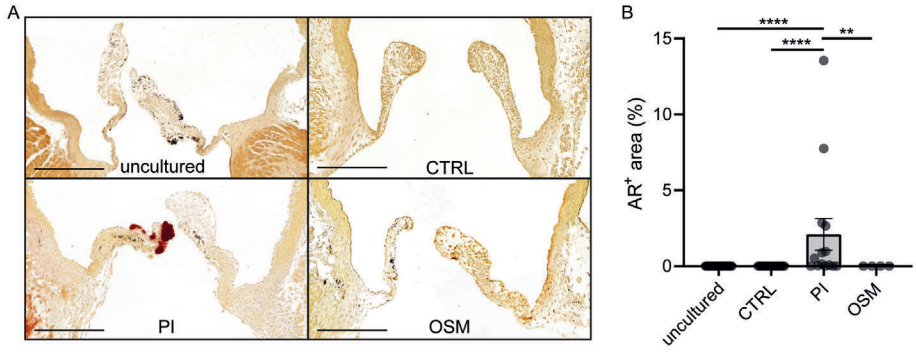


**Figure 2. Calcification of *ex vivo* cultured murine aortic valves.** A. Representative pictures of alizarin red-stained aortic valves cultured for 0 days (uncultured), cultured for 7 days in control medium (CTRL), PI, or OSM. B. Quantification of the percentage of the alizarin red-positive valve area (uncultured: n=27, CTRL: n= 19, PI: n=14, OSM: n=4). Data are presented as means ± SEM. Kruskal-Wallis test followed by Dunn's multiple comparisons test was performed to evaluate significant differences. **:p<0.01, ****:p<0.0001. Scalebar is 250 $\mu$m.

### Both OSM and PI induce calcification *in vitro*

The inability of OSM to induce calcification in the *ex vivo* cultured mouse aortic valve is in contrast with several studies studying the *in vitro* calcification of VICs from different species [7,46-49]. To determine whether this was caused by a species or *in vitro*/*ex vivo* difference, mVICs of cardiac valves were isolated and cultured in PI or OSM and stained using alizarin red. In the first set of experiments (passage 0 and 9), in which mVICs were cultured for 7 days, only PI was able to induce calcification (Figure 3A,C and data not shown). In the second set of experiments, in which mVICs were cultured for 21 days (passage 0 and 13), both PI and OSM were able to induce calcification (Figure 3B,D and data not shown). Similar results were obtained using hVICs (Supplemental figure 1). qPCR analysis of the mVIC cultures of 7 days showed that RUNX2 expression

was significantly higher after culture in PI compared to OSM, whereas COX2 was significantly higher after culture in OSM (Figure 3E,F). qPCR analysis of ALP1, αSMA, aggrecan, collagen II, PiT1 and PiT2 expression did not show significant differences (data not shown). Taken together, PI and OSM could both induce calcification of mVICs and hVICs *in vitro,* although by using different signaling pathways.

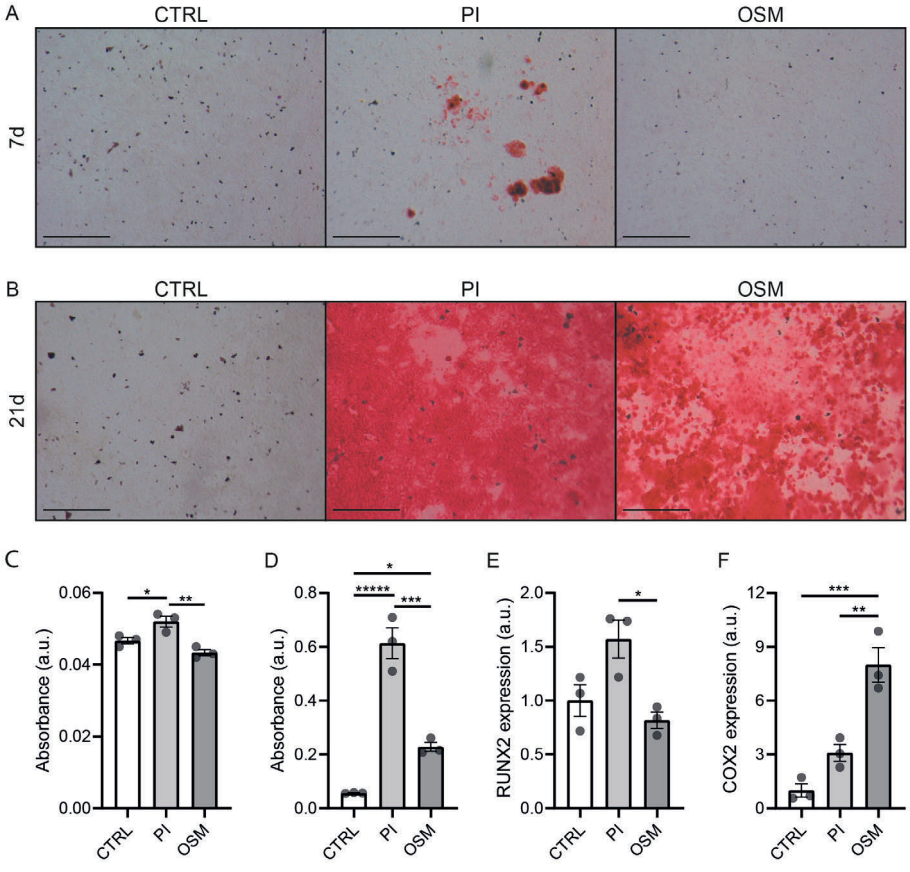


**Figure 3. *In vitro* calcification of mVICs in PI and OSM.** A, B. Representative pictures of alizarin red-stained mVICs after 7 days (passage 9, A) or 21 days (passage 13, B) of culture in control (CTRL), PI or OSM medium. C, D. Quantification of the alizarin red staining in mVICs cultured for 7 (passage 9, C) or 21 days (passage 13, D) by absorbance measurements of dissolved AR staining. Note the different scales for C and D. E,F. Graphs indicating RNA expression of RUNX2 (E) and COX2 (F) in mVICs cultured for 7 days. Data are presented as means ± SEM. One-way ANOVA followed by Tukey's multiple comparisons test was performed to evaluate significant differences. *: $p<0.05$, **:$p<0.01$, ***: $p<0.001$, ****:$p<0.0001$. Scale bar is 250 μm.

**Osteogenic differentiation in cultured aortic valves**

To further characterize the calcification processes in the *ex vivo* cultured aortic valves, stainings were performed for different osteogenic markers. ALP was not expressed in the uncultured valves but was significantly upregulated in the hearts cultured in control medium or in the presence of PI, but not in the presence of OSM (Figure 4A,B). The number of RUNX1/2/3-positive cells was low in uncultured aortic valves and showed a trend towards increase in the hearts cultured with control medium (Figure 4C,D). The number of RUNX1/2/3-positive cells was significantly increased upon culture in PI and OSM compared to uncultured hearts (Figure 4C,D). In PI cultured valves, at the location of the calcification itself, the expression of RUNX1/2/3 and ALP was relatively low (closed arrow in Figure 4E), whereas the expression was higher surrounding these calcifications (open arrow in Figure 4E). COX2 was observed in a subset of VECs in uncultured aortic valves and aortic valves cultured in control medium and OSM. In the calcified region of the valves cultured with PI, COX2 expression was observed in addition to VECs also in non-VECs (see asterisks in Figure 4E). A striking lack of $\alpha$SMA expression was observed at the location of calcification, whereas a low signal of $\alpha$SMA was present in other parts of the valve (Figure 4E). Further, very few cleaved caspase-positive cells were observed in all groups, with no positive cells in the calcification area (data not shown). Altogether, these observations indicate that the calcifications in the aortic leaflets of *ex vivo* cultured mouse hearts are due to osteogenic calcification and not dystrophic calcification. In addition, differential expression of osteogenic markers is observed in PI and OSM cultures.

**OSM and PI induce endochondral differentiation in the aortic root of *ex vivo* cultured mouse hearts**

To assess if chondrogenic differentiation occurs during the *ex vivo* culture of the aortic valves, the expression of glycosaminoglycans (GAGs), elastin, collagen II, aggrecan and RUNX1/2/3, was determined. Alcian blue staining to visualize GAGs demonstrated large round cells surrounded by large amounts of GAGs in the aortic root, near the hinge of valves cultured for 7 days in PI and OSM (Figure 5A,B). These areas were also positive for aggrecan and collagen II (Figure 5A), indicating the presence of cartilage. This was not observed in the leaflets of the aortic valve (Figure 5A and data not shown). Furthermore, culture with OSM induced elastin expression in the cartilage region (Figure 5A,C), indicating the formation of elastic cartilage. RUNX1/2/3 expression was observed mostly surrounding the cartilage, possibly indicating a continuing process of cartilage formation (Figure 5A). To determine whether cartilage formation is followed by

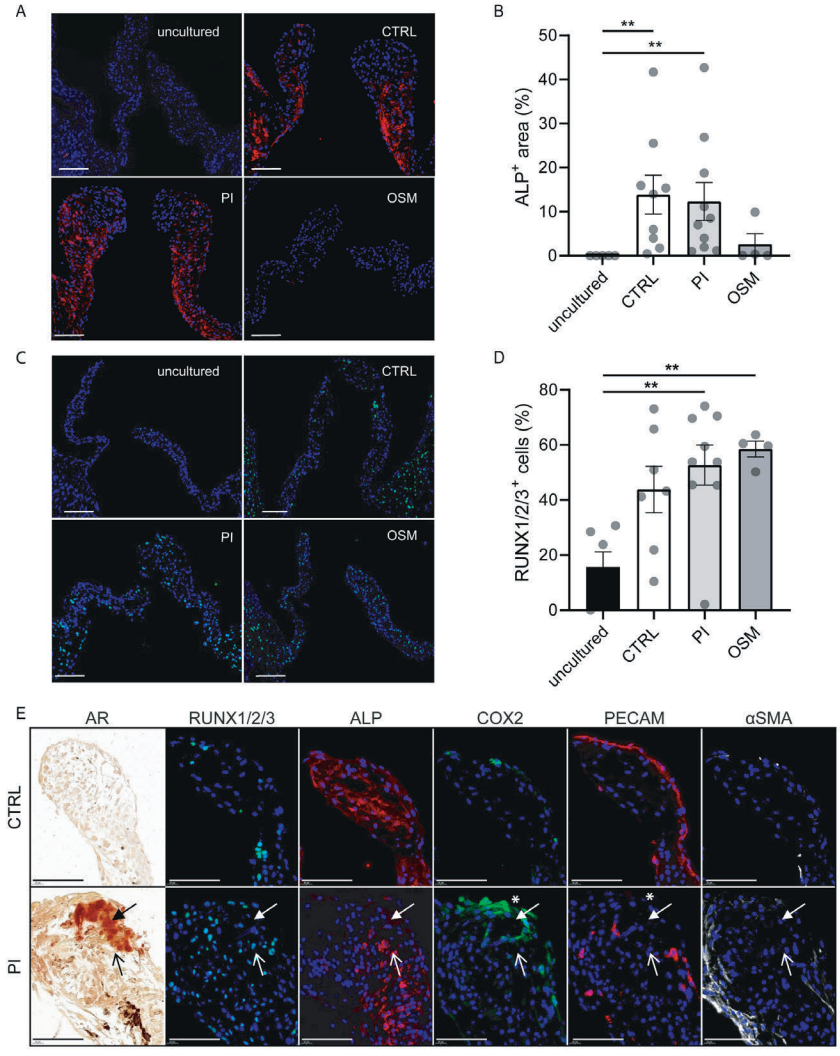


**Figure 4. Osteogenic marker expression in *ex vivo* cultured aortic valves.** A,B. Representative pictures of uncultured and *ex vivo* cultured aortic valves in control medium (CTRL), PI, or OSM stained for ALP (A) and RUNX1/2/3 (B). C,D. Quantification of ALP-positive valve area (B) and percentage of RUNX1/2/3 positive cells in the aortic valve (D). E. Representative pictures of the calcified area in aortic valves cultured in PI and non-calcified aortic valves cultured in control medium (CTRL) showing stainings for alizarin red (AR), RUNX1/2/3, ALP, COX2, PECAM and αSMA. Closed arrows indicate location of calcification. Open arrows indicate area surrounding calcification. Asterisks indicate COX2 expression in PECAM-negative cells. Data are presented as means ± SEM. Kruskal-Wallis test followed by Dunn's multiple comparisons test was performed for the graph in B and One-way ANOVA followed by Tukey's multiple comparisons test was performed for the graph in D to evaluate significant differences. **:p<0.01, ***:p<0.001. Scalebar is 100 μm.

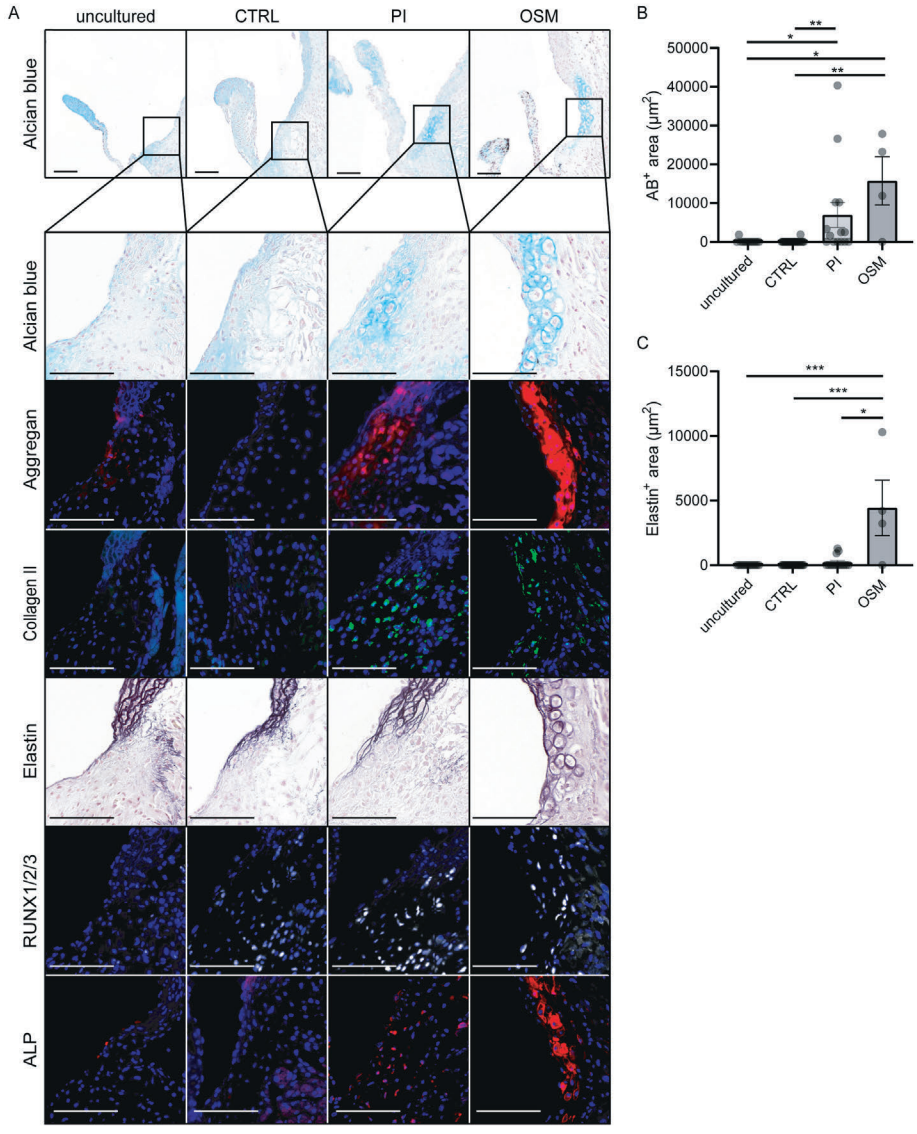


**Figure 5. Endochondral differentiation in the aortic root of *ex vivo* cultured mouse hearts.** A. Representative pictures of uncultured and *ex vivo*-cultured aortic valves in control medium (CTRL), PI, or OSM stained for Alcian blue, aggrecan, collagen II, elastin, RUNX1/2/3 and ALP. The images shown for each condition are from the same heart. B,C. Quantification of the Alcian blue (B)- and elastin (C)-positive area in the aortic root. Kruskal-Wallis test followed by Dunn's multiple comparisons test was performed to evaluate significant differences. *: $p<0.05$, **: $p<0.01$, ***: $p<0.001$. Scalebar is 100 $\mu$m.

ossification as seen in bone formation (endochondral ossification), ALP expression was determined. ALP was found in both PI and OSM cultures although much higher in OSM cultures (Figure 5A). Actual calcification in the aortic root as visualized by alizarin red was not observed after 7 days of culture (not shown and Figure 2A). Together, these observations indicate that endochondral differentiation can be induced in the aortic root of *ex vivo* cultured mouse hearts in the presence of PI and OSM.

**Dexamethasone stimulates endochondral differentiation and inhibits calcification**

The OSM-component dexamethasone is an important inducer of osteogenesis in mesenchymal stem cells [25,26,28], vascular smooth muscle cells [50] and VICs [5] *in vitro*. The effect of dexamethasone on other cell types is less clear and can be contradictory [51,52]. In the *ex vivo* model, all valvular cell types are present in their native environment and it is their interaction that will determine the effect of exposure to dexamethasone. To obtain a better understanding of the effect of dexamethasone on calcification in the aortic valve and aortic root, dexamethasone was added to the control and PI cultures, and omitted from the OSM cultures (Figure 6). In the control cultures, dexamethasone did not change the extent of RUNX1/2/3 expression, whereas ALP expression was abolished in the aortic valve (Figure 6B-D). In the aortic root, cartilage formation was induced as assessed by alcian blue (Figure 6F) and aggrecan expression (Figure 6G,J) and ALP appeared to be slightly induced by dexamethasone addition (Figure 6I,J). In the PI cultures, dexamethasone prevented calcification (Figure 6A) and ALP expression (Figure 6C,D), whereas RUNX1/2/3 expression was not affected (Figure 6B). In the aortic root, dexamethasone slightly increased aggrecan expression (Figure 6G), but inhibited ALP expression (Figure 6I,J). In the OSM cultures, omitting dexamethasone did not result in calcification (Figure 6A) but increased RUNX1/2/3 expression (Figure 6B) and ALP expression (4 out of 4; Figure 6C,D) in the aortic valve. COX2 expression, which was present mostly in the endothelial cells in the control, PI and OSM cultures and in the non-endothelial cells at places of calcification in the PI cultures (Figure 4E, 6E), was present mostly in non-endothelial cells in the OSM cultures where dexamethasone was omitted (Figure 6E). In the aortic root, omission of dexamethasone from the OSM cultures resulted in a decrease of cartilage formation as assessed by alcian blue (Figure 6F), aggrecan (Figure 6G) and elastin expression (Figure 6H), whereas ALP expression did not change (Figure 6I). Together, these observations indicate that in the *ex vivo* cultures of mouse hearts, dexamethasone inhibits calcification in the aortic valve and stimulates endochondral differentiation in the aortic root.

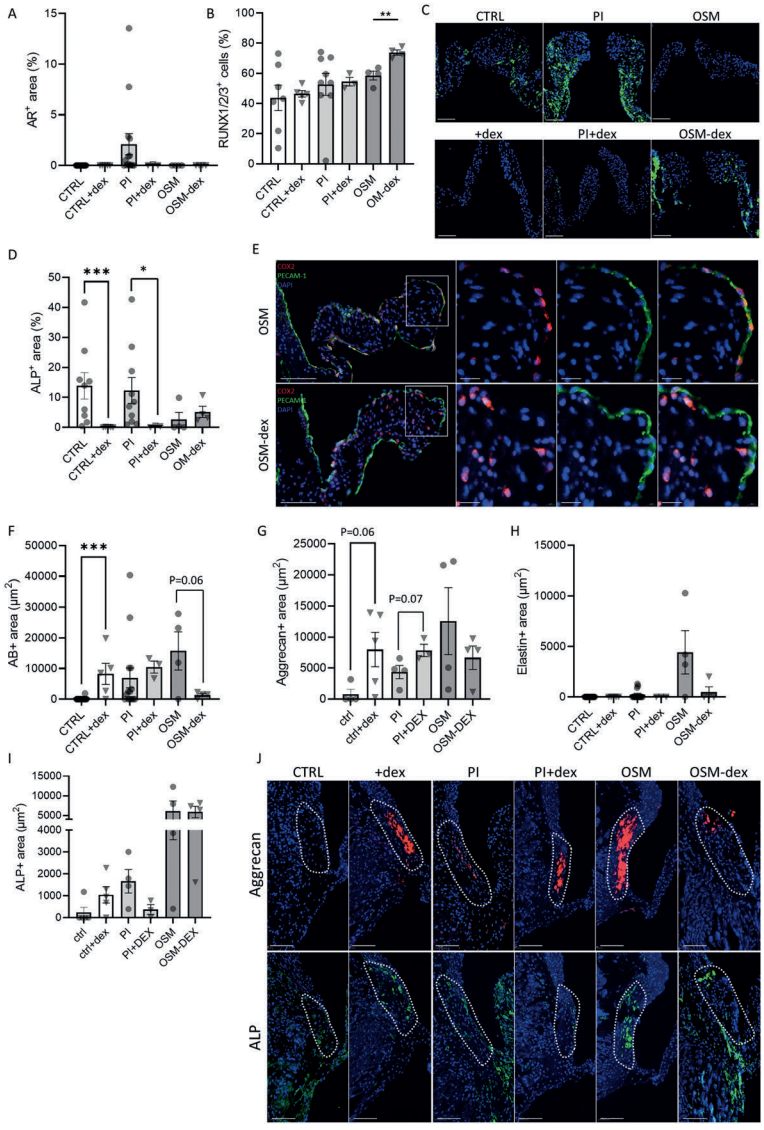


**Figure 6. The role of dexamethasone in osteogenic calcification of the aortic valve and endochondral differentiation in the aortic root of *ex vivo* cultured mouse hearts.** A,B,D,F-I. Quantifications of the alizarin red-positive area (A), the percentage of RUNX1/2/3 positive cells (B) and ALP-positive valve area (D) in the aortic valve and Alcian blue (F)-, aggrecan- (G), elastin- (H) and ALP- (I) positive area in the aortic root of *ex vivo* cultured mouse hearts valves in control medium (CTRL), control medium + dexamethasone (CTRL+dex), PI, PI + dexamethasone (PI+dex), OSM or OSM + dexamethasone (OSM+dex). C,E,J. Representative pictures of *ex vivo* cultured mouse hearts stained for ALP (C), COX2 and PECAM-1 (E) and ALP and aggrecan (J). Mann-Whitney test was performed for the graphs in A,D,F,G,H and I, and an unpaired t-test was performed for the graph in B to evaluate significant differences. *: $p<0.05$, **: $p<0.01$, ***: $p<0.001$. Scalebar is 100 $\mu$m

## Discussion

In this study, we have established a novel *ex vivo* calcification model for intact murine aortic valves. In this model, calcification can be induced in aortic valves of wild type mice that are cultured under flow conditions in their natural position within the heart by the exposure to elevated levels of PI. The commonly used OSM was unable to induce calcification within the aortic valve leaflets in this *ex vivo*-model. In contrast, OSM did induce calcification in *in vitro* cultures of mouse and human valvular cells, indicating clear *in vitro*-*ex vivo* differences. Furthermore, endochondral differentiation was observed in the root of the aorta in both PI and OSM *ex vivo* culture conditions, indicating the presence of different forms and mechanisms of calcification in *ex vivo* cultured aortic valves. Finally, the OSM-component dexamethasone was able to inhibit calcification in the aortic valve and stimulate endochondral differentiation in the aortic root.

A clear understanding of the pathology of valvular calcification has been hampered by insufficient *in vitro* and *in vivo* test-models. *In vitro* models lack the complex valvular structure and the simulation of the hemodynamic condition whereas *in vivo* systems require genetic modification, long incubation times and have limited mechanical and biochemical controllability [5,7,33-35,38]. By culturing the mouse hearts in the MTCS [43] under calcifying conditions, we have created a highly controllable culture model in which calcification can be induced within 1 week in the intact aortic valve. We observed 2 types of aortic valve calcification present at distinct locations, which coincide with the 2 types of calcification found in human aortic leaflets, i.e. the nodular form found on the more distal part of the aortic leaflets and the intrinsic form found at the leaflet hinge [9].

Nodular calcification was only observed in the PI cultures and was mostly present in the body and near the coaptation part of the aortic leaflet characterized by relative low levels of the early osteogenic markers RUNX1/2/3 and ALP and by specific expression of COX2 in the calcified area. The region surrounding the calcification displayed higher levels of RUNX1/2/3 and ALP, indicating ongoing osteogenic differentiation. The absence of $\alpha$SMA within and directly surrounding the calcification area suggests that a transient myofibroblast stage before calcification did not take place, which has been shown for VICs *in vitro* [8] and *in vivo* [16]. The lack of apoptosis in these regions after 7 days of culture further suggested the absence of dystrophic calcification. Calcification in the aortic leaflet was not observed in the OSM cultures. A possible explanation might be the virtual absence of ALP in the aortic valves cultured in OSM as ALP activity is required for OSM induced calcification [48,53]. ALP is present in the cultures without OSM (control cultures), indicating that a component of OSM

inhibits ALP expression. The OSM-component dexamethasone is a synthetic glucocorticoid steroid that has been shown to increase the expression of ALP and other osteogenic marker in cell cultures [7,48,50,54]. Dexamethasone, however, has also been shown to inhibit COX2 expression [55,56], which is required for calcification in the aortic valves of the klotho-deficient mice harboring elevated levels of serum phosphate secondary to kidney failure [16,57]. Whereas we observed non-endothelial COX2 expression in the calcified areas of the aortic valve in the PI cultures, COX2 was mostly absent from the non-endothelial cells, and present in the endothelial cells. To understand the role of dexamethasone in the *ex vivo* cultures of the aortic valve and to find a potential reason for the difference between the effects of PI and OSM, we added dexamethasone to the control and PI cultures and omitted dexamethasone from the OSM cultures. Interestingly, dexamethasone inhibited ALP expression in the control and PI cultures and prevented calcification in the PI cultures, illustrating clear differences between published *in vitro* studies indicating the stimulation of calcification by dexamethasone and our *ex vivo* study showing the inhibition of calcification and calcification pathways by dexamethasone. Omission of dexamethasone did not result in calcification indicating that the presence of dexamethasone in the OSM is not solely responsible for the absence of calcification in the OSM cultures. ALP expression, however was induced and COX2 expression was present in the non-endothelial cells indicating that dexamethasone does inhibit calcification pathways in the OSM cultures. Although calcification was not observed in the control *ex vivo* cultures, RUNX1/2/3 and ALP were found to be upregulated suggesting osteoblastic activity [58]. Since mechanical stresses may play a role in the activation of VICs and propagation of calcification [22], the altered mechanical stress and flow conditions in the *ex vivo* model might have resulted in induction of early osteogenic markers. Subsequent moderately increased levels of phosphates in the PI cultures allowed calcification to take place.

The second type of calcification observed in the *ex vivo* cultured aortic valves is the endochondral differentiation that was observed in the root of the aorta near the hinge of the aortic valve. Cartilage, as evidenced by its morphological features and high alcian blue, collagen II and aggrecan staining, was bordered by the osteogenic markers ALP and RUNX1/2/3. Previously, osteochondrogenic gene expression has been shown to precede calcification in the same region in the klotho-deficient mice [19]. Moreover, cartilage formation was observed in the aortic sinus of an inbred family of Syrian hamster and was suggested to be the result of locally intense mechanical stimulation [59]. These observations suggest that the "intrinsic" calcification found in the human aortic sinus is formed by the process of endochondral calcification and can be recapitulated in wild

type mouse hearts using our *ex vivo* flow model. Interestingly, in contrast to the osteogenic calcification in the aortic leaflets, endochondral differentiation was found both in PI and OSM conditions, although the type of cartilage formed differed with elastic cartilage being present in the OSM cultures. Addition of dexamethasone to the control cultures induced cartilage formation and increased the cartilage formation in the PI cultures. Omission of dexamethasone from the OSM cultures decreased the cartilage formation. Together, these observations show that dexamethasone can induce cartilage formation in the aortic root. PI cultures and OSM without dexamethasone, however, do show cartilage formation indicating that dexamethasone is not solely responsible for the endochondral differentiation process.

Differences between the effects of PI and OSM on VICs are also found in the *in vitro* cultures. After 7 days of *in vitro* culture in OSM, the expression of COX2 was increased, which is in contrast with the PI *in vitro* cultures and the OSM *ex vivo* cultures. Furthermore, RUNX2 expression was increased in PI, but not in OSM *in vitro* cultures. These differences in gene expression between the PI and OSM *in vitro* cultures might explain why PI treatment is more potent in inducing *in vitro* calcification than OSM, showing calcification already after 7 days of culture. Interestingly, in our *in vitro* cultures the valvular cells of aortic, pulmonary, mitral and tricuspid valves were combined and showed after 3 weeks of culture, virtually complete calcification indicating that VICs of all cardiac valves are able to calcify.



The inconsistencies of the observations between the *in vitro* and *ex vivo* experiments are likely caused by the many differences between the culture conditions. First, the hemodynamic condition in the *ex vivo* cultures resembles the diastolic phase of the cardiac cycle and therefore creates similar types of mechanical stresses on the valve as in the *in vivo* situation. Second, the complex valve structure is preserved, including the heterogeneous composition of the matrix and valvular cells whose interactions create multiple levels of regulation, which are lost in cell culture studies [7,33-35,46,49,60]. It is therefore of utmost importance to approach the native environment of the valvular cells as much as possible to obtain the response most representative of the *in vivo* situation. *Ex vivo* systems can fulfill most of these requirements and should be considered an important tool for translational studies.

Some limitations should be mentioned about the culture conditions used in this study. The aortic valves were subjected to flow stress in a continuous closed position, mainly simulating the stresses present during diastole. However, the continuous exposure to retrograde flow from the aorta into the coronary arteries created a mechanical environment favoring calcification to take place already

after 7 days of culture in the presence of PI. Culturing the valve in the open position or in presence of pulsatile flow might give further insight in the mechanical regulation of calcification. Furthermore, the valves are cultured in the absence of blood, which contains multiple cell types and factors potentially crucial in the regulation of calcification. The *ex vivo* flow model, however, provides the possibility to add cells and factors back to the culture medium, allowing the controlled study of the involvement of specific cell types and factors in the regulation of valvular calcification.

In conclusion, with the MTCS we can now study the initiation and progression of osteogenic and endochondral calcification in the intact murine aortic valves and root. This provides the possibility to elucidate the mechanical, cellular and molecular mechanisms underlying CAVD, and therefore may set the stage to identify new targets for effective pharmacological therapies in this common and progressive disease.

**Acknowledgements**

We thank Margreet de Vries for providing mouse hearts and Jesper Hjortnaes for providing the human VICs. This work was supported by grants received from the GE Healthcare, Lantheus medical imaging, St Jude Medical, Medtronic, Boston Scientific, Biotronik, and Edwards Lifesciences, by the Dutch Heart Foundation AHA grant number 2013T093 awarded to the BAV consortium and by the partners of Regenerative Medicine Crossing Borders (www.regmedxb.com).

**Disclosures**

None

## Supplementary figures

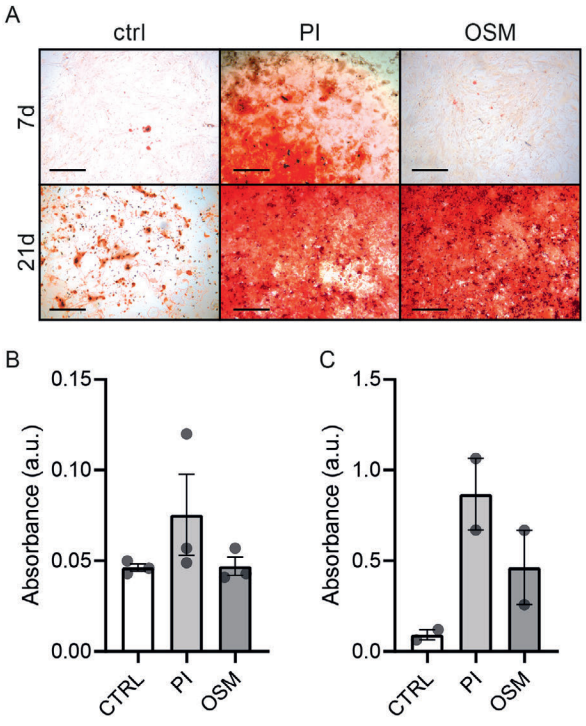


**Supplemental figure 1. hVIC calcification after 7 and 21 days of culture in PI or OSM.** A. Representative pictures of AR staining on hVICs cultured in control medium (CTRL), PI or OSM for 7 or 21 days. B,C. Quantification of the alizarin red stainings in hVICs cultured for 7 (B) and 21 (C) days. Scalebar is 500 $\mu$m.

## References


1. Thaden, JJ, et al. (2014). The global burden of aortic stenosis. *Prog Cardiovasc Dis*
2. Stewart, BF, et al. (1997). Clinical factors associated with calcific aortic valve disease. Cardiovascular health study. *J Am Coll Cardiol*
3. van der Ven, CFT, et al. (2017). In vitro 3d model and mirna drug delivery to target calcific aortic valve disease. *Clinical science (London, England : 1979)*
4. Halevi, R, et al. (2018). A new growth model for aortic valve calcification. *J Biomech Eng*
5. Bowler, MA, et al. (2015). In vitro models of aortic valve calcification: Solidifying a system. *Cardiovasc Pathol*
6. Schoen, FJ. (2008). Evolving concepts of cardiac valve dynamics: The continuum of development, functional structure, pathobiology, and tissue engineering. *Circulation*
7. Yip, CY, et al. (2009). Calcification by valve interstitial cells is regulated by the stiffness of the extracellular matrix. *Arterioscler Thromb Vasc Biol*
8. Monzack, EL, et al. (2011). Can valvular interstitial cells become true osteoblasts? A side-by-side comparison. *J Heart Valve Dis*
9. Gomez-Stallons, MV, et al. (2019). Calcification and extracellular matrix dysregulation in human postmortem and surgical aortic valves. *Heart*
10. Otto, CM, et al. (1994). Characterization of the early lesion of 'degenerative' valvular aortic stenosis. Histological and immunohistochemical studies. *Circulation*
11. Jian, B, et al. (2003). Progression of aortic valve stenosis: Tgf-beta1 is present in calcified aortic valve cusps and promotes aortic valve interstitial cell calcification via apoptosis. *Ann Thorac Surg*
12. Cote, N, et al. (2013). Inflammation is associated with the remodeling of calcific aortic valve disease. *Inflammation*
13. Caira, FC, et al. (2006). Human degenerative valve disease is associated with up-regulation of low-density lipoprotein receptor-related protein 5 receptor-mediated bone formation. *J Am Coll Cardiol*
14. Rosa, M, et al. (2017). Leptin induces osteoblast differentiation of human valvular interstitial cells via the akt and erk pathways. *Acta Diabetol*
15. Cote, N, et al. (2012). Atp acts as a survival signal and prevents the mineralization of aortic valve. *J Mol Cell Cardiol*
16. Wirrig, EE, et al. (2015). Cox2 inhibition reduces aortic valve calcification in vivo. *Arterioscler Thromb Vasc Biol*
17. Bostrom, KI, et al. (2011). The regulation of valvular and vascular sclerosis by osteogenic morphogens. *Circ Res*
18. Rajamannan, NM, et al. (2003). Human aortic valve calcification is associated with an osteoblast phenotype. *Circulation*

19. Gomez-Stallons, MV, et al. (2016). Bone morphogenetic protein signaling is required for aortic valve calcification. *Arterioscler Thromb Vasc Biol*
20. Mohler, ER, 3rd, et al. (2001). Bone formation and inflammation in cardiac valves. *Circulation*
21. O'Brien, KD, et al. (1995). Osteopontin is expressed in human aortic valvular lesions. *Circulation*
22. Gould, ST, et al. (2013). Hemodynamic and cellular response feedback in calcific aortic valve disease. *Circ Res*
23. Thubrikar, MJ, et al. (1986). Patterns of calcific deposits in operatively excised stenotic or purely regurgitant aortic valves and their relation to mechanical stress. *Am J Cardiol*
24. Rutkovskiy, A, et al. (2017). Valve interstitial cells: The key to understanding the pathophysiology of heart valve calcification. *J Am Heart Assoc*
25. Hamidouche, Z, et al. (2008). Fhl2 mediates dexamethasone-induced mesenchymal cell differentiation into osteoblasts by activating wnt/beta-catenin signaling-dependent runx2 expression. *Faseb j*
26. Hong, D, et al. (2009). Osteoblastogenic effects of dexamethasone through upregulation of taz expression in rat mesenchymal stem cells. *J Steroid Biochem Mol Biol*
27. Gaur, T, et al. (2005). Canonical wnt signaling promotes osteogenesis by directly stimulating runx2 gene expression. *J Biol Chem*
28. Langenbach, F, et al. (2013). Effects of dexamethasone, ascorbic acid and beta-glycerophosphate on the osteogenic differentiation of stem cells in vitro. *Stem Cell Res Ther*
29. Bansal, VK. "Serum inorganic phosphorus." *Clinical methods: The history, physical, and laboratory examinations*. Eds., et al. Boston: Butterworths, 1990. Print.
30. Yu, Z, et al. (2019). Warfarin calcifies human aortic valve interstitial cells at high-phosphate conditions via pregnane x receptor. *J Bone Miner Metab*
31. Fatherazi, S, et al. (2009). Phosphate regulates osteopontin gene transcription. *Journal of dental research*
32. Tada, H, et al. (2011). Phosphate increases bone morphogenetic protein-2 expression through camp-dependent protein kinase and erk1/2 pathways in human dental pulp cells. *Bone*
33. Benton, JA, et al. (2008). Substrate properties influence calcification in valvular interstitial cell culture. *J Heart Valve Dis*
34. Butcher, JT, et al. (2004). Unique morphology and focal adhesion development of valvular endothelial cells in static and fluid flow environments. *Arteriosclerosis, Thrombosis, and Vascular Biology*
35. Butcher, JT, et al. (2006). Valvular endothelial cells regulate the phenotype of interstitial cells in co-culture: Effects of steady shear stress. *Tissue Eng*

36. Raddatz, MA, et al. (2020). Macrophages promote aortic valve cell calcification and alter stat3 (signal transducer and activator of transcription 3) splicing. *Arterioscler Thromb Vasc Biol*
37. Rodriguez, KJ, et al. (2009). Regulation of valvular interstitial cell calcification by components of the extracellular matrix. *J Biomed Mater Res A*
38. Sider, KL, et al. (2011). Animal models of calcific aortic valve disease. *International journal of inflammation*
39. Drolet, MC, et al. (2006). A high fat/high carbohydrate diet induces aortic valve disease in c57bl/6j mice. *J Am Coll Cardiol*
40. Awan, Z, et al. (2011). The ldlr deficient mouse as a model for aortic calcification and quantification by micro-computed tomography. *Atherosclerosis*
41. Garg, V, et al. (2005). Mutations in notch1 cause aortic valve disease. *Nature*
42. Ruiz, JL, et al. (2015). Cardiovascular calcification: Current controversies and novel concepts. *Cardiovascular Pathology*
43. Kruithof, BP, et al. (2015). Culturing mouse cardiac valves in the miniature tissue culture system. *J Vis Exp*
44. Kruithof, BPT, et al. (2019). Stress-induced remodelling of the mitral valve: A model for leaflet thickening and superimposed tissue formation in mitral valve disease. *Cardiovasc Res*
45. Lieber, SC, et al. (2010). Design of a miniature tissue culture system to culture mouse heart valves. *Ann Biomed Eng*
46. Schlotter, F, et al. (2018). Spatiotemporal multi-omics mapping generates a molecular atlas of the aortic valve and reveals networks driving disease. *Circulation*
47. Chen, J-H, et al. (2009). Identification and characterization of aortic valve mesenchymal progenitor cells with robust osteogenic calcification potential. *The American journal of pathology*
48. Goto, S, et al. (2019). Standardization of human calcific aortic valve disease in vitro modeling reveals passage-dependent calcification. *Front Cardiovasc Med*
49. Richards, J, et al. (2013). Side-specific endothelial-dependent regulation of aortic valve calcification: Interplay of hemodynamics and nitric oxide signaling. *Am J Pathol*
50. Mori, K, et al. (1999). Dexamethasone enhances in vitro vascular calcification by promoting osteoblastic differentiation of vascular smooth muscle cells. *Arterioscler Thromb Vasc Biol*
51. Ding, Y, et al. (2010). Dexamethasone enhances atp-induced inflammatory responses in endothelial cells. *J Pharmacol Exp Ther*
52. Zielinska, KA, et al. (2016). Endothelial response to glucocorticoids in inflammatory diseases. *Front Immunol*

53. Mathieu, P, et al. (2005). Calcification of human valve interstitial cells is dependent on alkaline phosphatase activity. *J Heart Valve Dis*
54. Mikami, Y, et al. (2010). Bone morphogenetic protein 2 and dexamethasone synergistically increase alkaline phosphatase levels through jak/stat signaling in c3h10t1/2 cells. *J Cell Physiol*
55. Blanco, FJ, et al. (1999). Effect of antiinflammatory drugs on cox-1 and cox-2 activity in human articular chondrocytes. *J Rheumatol*
56. Lasa, M, et al. (2001). Dexamethasone destabilizes cyclooxygenase 2 mrna by inhibiting mitogen-activated protein kinase p38. *Mol Cell Biol*
57. Kuro-o, M. (2010). A potential link between phosphate and aging--lessons from klotho-deficient mice. *Mech Ageing Dev*
58. Aikawa, E, et al. (2007). Multimodality molecular imaging identifies proteolytic and osteogenic activities in early aortic valve disease. *Circulation*
59. Lopez, D, et al. (2004). Formation of cartilage in aortic valves of syrian hamsters. *Ann Anat*
60. Chen, J-H, et al. (2011). Cell–matrix interactions in the pathobiology of calcific aortic valve disease. *Circulation Research*

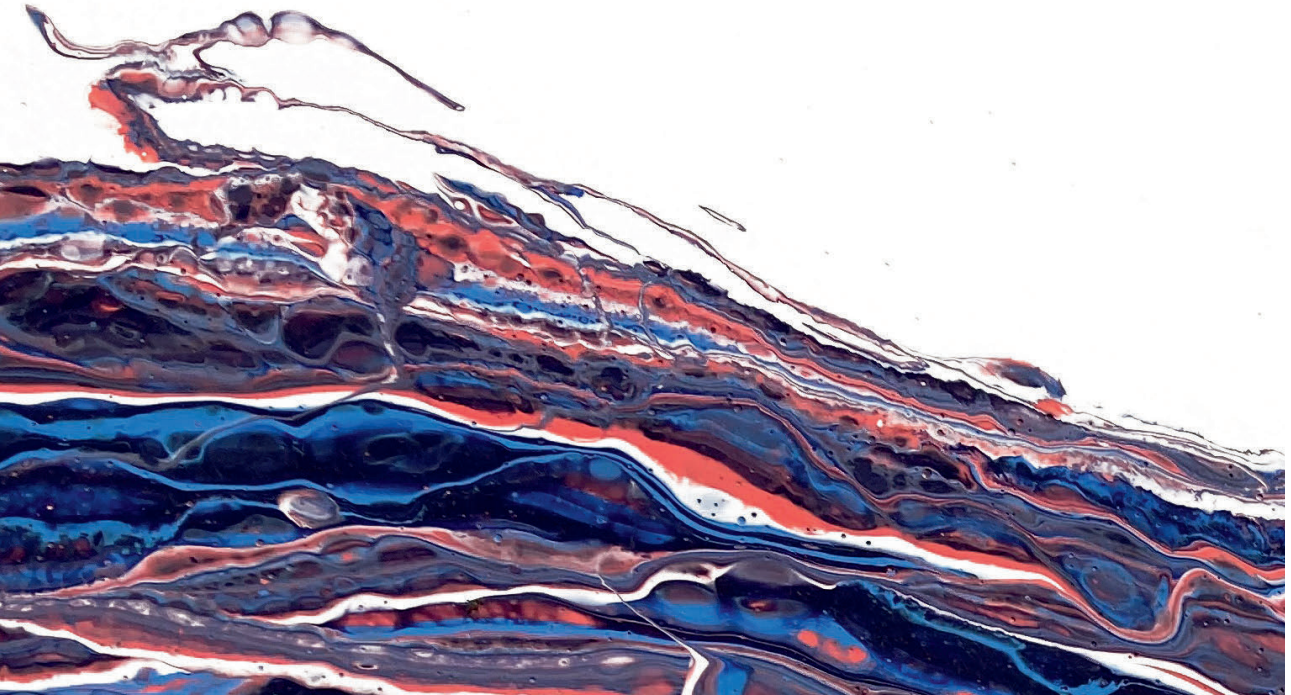

# Chapter 7

## A role for Four-and-a-Half LIM-domain 2 in aortic valve calcification

**Vera van de Pol[1], Boudewijn P.T. Kruithof[1,2,], Konda Babu Kurakula[1], K. Lodder[1], Marco C. DeRuiter[3], Marie-José Goumans[1]**

[1] Department of Cell and Chemical Biology, Leiden University Medical Center, Leiden, The Netherlands
[2] Department of Cardiology, Leiden University Medical Center, Leiden, The Netherlands
[3] Department of Anatomy and Embryology, Leiden University Medical Center, Leiden, The Netherlands

*To be submitted*

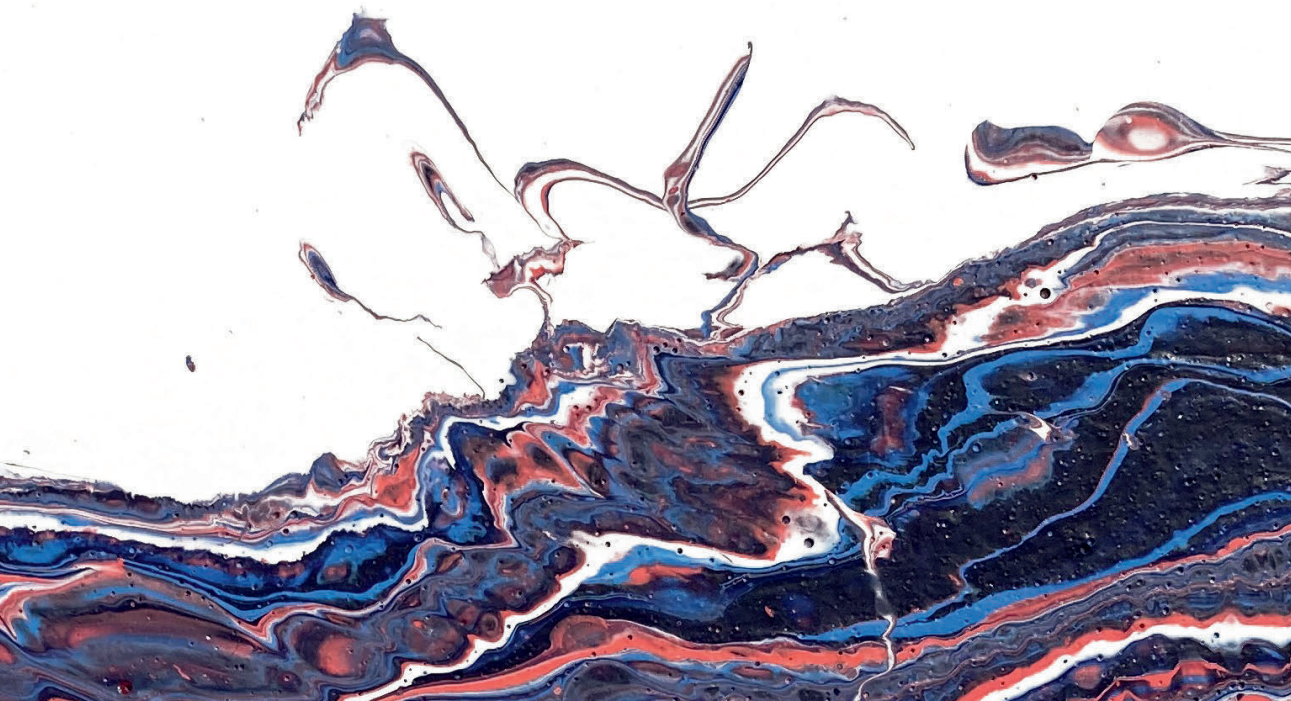

## Abstract

Calcific aortic valve disease (CAVD) is a cardiovascular pathology involving fibrosis, matrix degradation, cell death and mineral accumulation in the aortic valves. CAVD ultimately leads to severely calcified leaflets with impaired motion, requiring valve replacement surgery. Although the protein four-and-a-Half LIM-domain 2 (FHL2) is involved in both osteogenic differentiation processes and cellular responses to alterations in the cardiovascular homeostasis, the role of FHL2 in CAVD has not yet been explored. Therefore, we stained sections of calcified human aortic valves and demonstrated FHL2 expression in valvular interstitial cells (VICs) throughout the leaflets. Interestingly, *ex vivo* tissue culture of whole mouse hearts under calcifying conditions revealed significant differences in the localization of calcification in the aortic valves of FHL2$^{-/-}$ mice compared to valves from WT mice. The calcified areas observed in the FHL2$^{-/-}$ aortic valves were mainly located at the aortic side of the valve whereas in WT hearts the calcification was mostly located at the ventricular side. Our results demonstrate a role for FHL2 in aortic valve calcification and show that the effect of FHL2 on cellular calcification is location dependent.

## Introduction

Calcific aortic valve disease (CAVD) is a common, progressive disease of the aortic valves occurring in approximately 1% of the population by the age of 70 [1]. CAVD progresses from mild valvular thickening without obstruction of blood flow to the final stage of CAVD termed aortic stenosis characterized by severe calcification with impaired leaflet motion. Currently the only treatment option is surgical replacement of the dysfunctional valve. Although the initiation is not known, inflammation and extracellular matrix (ECM) remodeling are related to the valvular fibrosis in CAVD [2-4]. Calcified nodules can arise via osteogenic differentiation of the valvular interstitial cells (VICs), a process which is characterized by the expression of proteins such as osteopontin, osteocalcin and RUNX2 [5-7]. Another process that can cause valvular calcification is dystrophic calcification. Dystrophic calcification involves apoptosis of the VICs and the deposition of minerals in the valve [8].

Four-and-a-Half LIM-domain 2 (FHL2) is a scaffold protein able to bind numerous different proteins, thereby affecting many cellular processes such as proliferation and differentiation. Amongst others, FHL2 has been shown to play a role in the cardiovascular stress response. For example, in the absence of FHL2, β-adrenergic stimulation was reported to cause exaggerated hypertrophy and carotid artery ligation cause increased smooth muscle cell (SMC) proliferation in FHL2$^{-/-}$ mice, resulting in artery occlusion [9,10]. With regard to calcification, FHL2 has been shown to alter transcriptional activity of RUNX2 and increase the expression and activity of alkaline phosphatase [11]. In addition, FHL2 has been reported to stimulate the differentiation of mesenchymal stem cells towards osteoblasts and to reduce osteoclasts activity [12]. As a consequence, mice develop osteopenia when they have a deficiency for FHL2 [13].

Despite the known role of FHL2 in calcification and cardiovascular pathologies, a function for FHL2 in valvular stenosis has not yet been explored. To increase understanding of the process of valvular stenosis and investigate if FHL2 impacts on these processes, we investigated the role of FHL2 in calcification of murine aortic valves in *ex vivo* cultured hearts.

## Results

### FHL2 is present in pre-stenotic and stenotic human aortic valves

We first analyzed the expression of FHL2 and RUNX2 in human aortic valves. Therefore, we collected valves from patients with differing severities of aortic valve stenosis. In total 7 valvular samples were studied (including 3 bicuspid aortic valves). Of these samples, there were 3 samples with an ascending aortic

aneurysm and 2 samples with an aortic root aneurysm. The alizarin red (AR) staining demonstrated that 3 out of 7 samples had calcified nodules. FHL2 and RUNX2 were detected in all samples, independent of the presence of calcified nodules (Figure 1). RUNX123$^{+}$ and FHL2$^{+}$ cells were quantified but there was no significant difference in the percentage of FHL2$^{+}$ or RUNX123$^{+}$ cells between AR$^{+}$ and AR$^{-}$ samples (Figure 1I,J) (AR$^{+}$ mean FHL2=63.63%, SEM:13.62%; AR$^{-}$ mean FHL2=42.40%, SEM=16.45%; p=0.340 | AR$^{+}$ mean RUNX123=77.53%, SEM:5.56%; AR$^{-}$ RUNX123=60.03%, SEM=7.38%; p=0.137). There was no significant correlation between FHL2 and RUNX123 expression (data not shown).

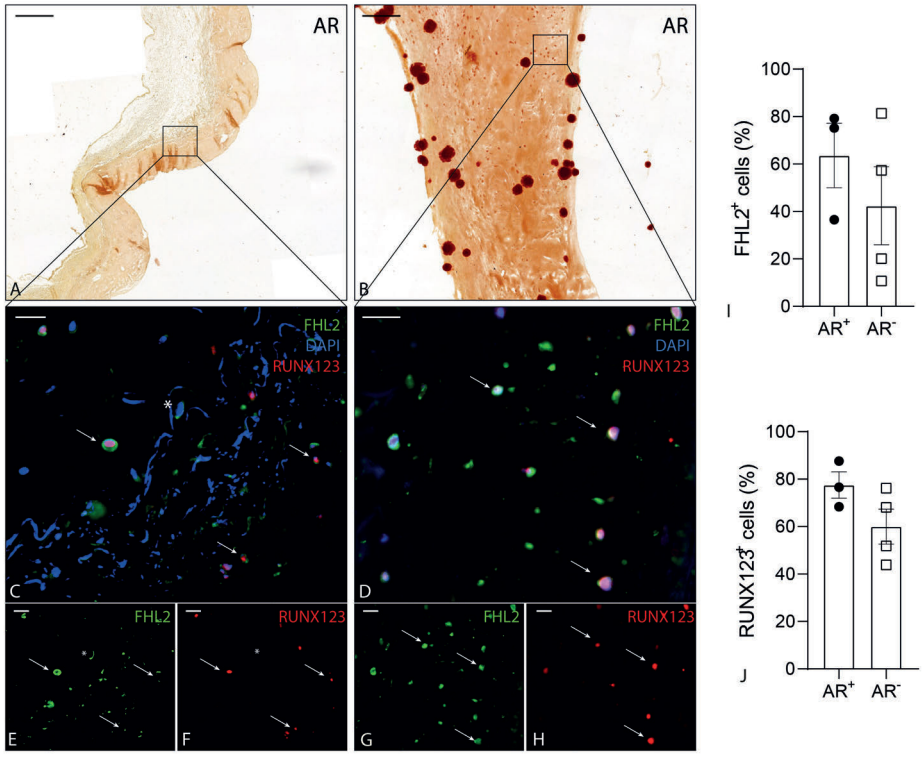


**Figure 1. Images of FHL2 and RUNX123 in aortic valve tissue.** A,B. Overview images of a non-calcified (A) and calcified (B) aortic valve leaflet stained with AR. C,D. Magnifications of locations indicated in images A (C) and B (D) stained with FHL2, DAPI and RUNX123. E-H. Single channel images of image C (E,F) and D (G,H) for FHL2 (E,G) and RUNX2 (F,H). I,J. Graphs of the quantification of FHL2 and RUNX123 in aortic valve tissue with (AR+) or without (AR-) calcifications. Arrows indicate cells positive for DAPI, FHL2 and RUNX123. * indicates FHL2-DAPI positive cells negative for RUNX123. Scalebar in images A+B indicates 200 $\mu$m and in images C-H indicates 20 $\mu$m.

### Altered location of calcification in FHL2$^{-/-}$ *ex vivo* cultured murine valves

Since human valves in the end-stage of CAVD do not provide mechanistic insights of the role of FHL2 in valvular calcification, we used a miniature tissue culture system (MTCS) to study the role of FHL2 in valvular calcification. Ex vivo culture using the MTCS allows the study of valvular calcification in a natural environment, accurately modeling important factors for CAVD development such as tissue stiffness, strain and cellular and ECM contact [14-20]. Therefore, we cultured WT and FHL2$^{-/-}$ murine hearts *ex vivo* for 7 days in medium supplemented with PI. AR staining showed a diverse range in calcification of the aortic valves of both WT (n=10) and FHL2$^{-/-}$ hearts (n=10), ranging from no calcification to severe calcification (Figure 2A).

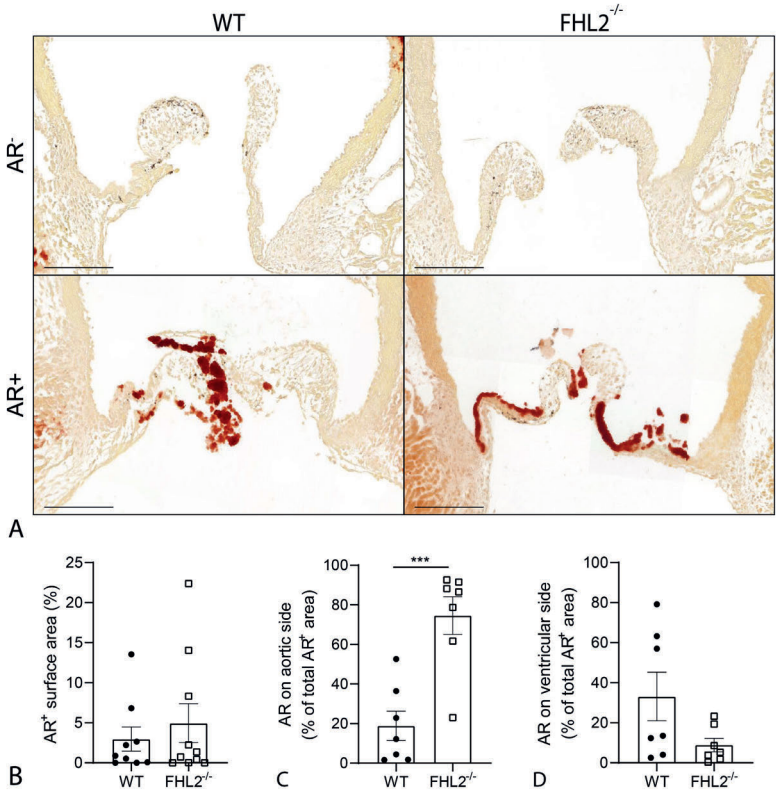


**Figure 2. Calcification assay performed on *ex vivo* cultured WT and FHL2-/- aortic valves.** A. Representative images of valves stained with AR staining after *ex vivo* culture with PI. A range of phenotypes was observed: valves without calcification (AR-) up to high amounts of calcification (AR+) B. Quantification of calcification in aortic valves cultured *ex vivo* with calcifying medium (WT n=9, FHL2-/- n=10). C. Calcification at the aortic side in WT and FHL2-/- valves (N=7). D. Calcification at the ventricular side in WT and FHL2-/- valves (n=7). Scalebar is 200μm, ***=p<0.001.

When analyzing the total amount of $AR^+$ area per valve, there was no significant difference between WT and $FHL2^{-/-}$ valves (WT mean=2.97%, SEM:1.51%; FHL2 mean=4.96%, SEM=2.43%; p=0.508) (Figure 2B). Interestingly, when analyzing the localization of the calcified nodules, $FHL2^{-/-}$ valves showed a significant increase of $AR^+$ surface area at the aortic side of the valves compared to WT aortic valves (WT mean=18.85%, SEM:7.41%; FHL2 mean=74.62%, SEM=9.48%; p=0.0006) (Figure 2C). Complementing this difference is a trend towards a smaller area of calcification at the ventricular side of the valves of $FHL2^{-/-}$ valves compared to WT (WT mean=33.15%, SEM:12.15%; FHL2 mean=8.95%, SEM=3.38%; p=0.079) (Figure 2D). Calcification in the center of the leaflet did not reveal any differences between WT and $FHL2^{-/-}$ valves (data not shown).

## Discussion

Since FHL2 is reported to be involved in calcification and cardiovascular pathology, this study aimed to investigate the role of FHL2 in aortic valve calcification. Our results show that human aortic valves with different types and stages of aortic valve disease express FHL2 independent of the degree of calcification of the valve and the expression of the osteogenic transcription factor RUNX2. In addition, absence of FHL2 did not significantly alter the amount of calcification in the aortic valves after 7 days of ex vivo culture in medium supplemented with PI. However, the location of the calcification nodules was significantly different between WT and FHL2-/- ex vivo cultured aortic valves. The calcification nodules in the FHL2-/- valves were mainly located towards the aortic side whereas in the WT valves they were more located at the ventricular side of the valve.

Despite the relation between FHL2 and RUNX2 that has been described previously, to the best of our knowledge, this is the first study investigating the expression of FHL2 and RUNX2 in human aortic valves [11]. We observed FHL2 and RUNX123 expression in the human valve, but were unable to find a relation between FHL2 and RUNX123 expression in the human aortic valve. This appears to be in contrast with several studies indicating that FHL2 expression increases RUNX2 transcriptional activity and thereby calcification [11,13,21]. This apparent contrast could be due to the limitation of tissue samples in demonstrating cause and consequence and/or a temporal difference between FHL2 and RUNX2 expression. In addition, we were unable to relate FHL2 and runx123 to the presence or absence of calcified nodules in the aortic valve.

Although human tissue is the most accurate study sample when investigating protein expression in relation to a disease, it provides limited opportunities for manipulating and investigating the underlying molecular processes. Therefore, we studied the valves from $FHL2^{-/-}$ mice using the MTCS to culture the valves

*ex vivo*. This allowed us to gain more insight in the role for FHL2 is in valvular calcification whilst keeping the valve in its natural environment [22,23]. Several studies have indicated the importance of the local microenvironment in the calcification process, underscoring the value of maintaining the *in vivo* tissue structure when using the MTCS [14-20]. The results from the *ex vivo* culture experiments demonstrated that not the amount of calcification but the localization is affected by FHL2. The aortic valves of FHL2$^{-/-}$ mice cultured for 7 days in PI showed an increased localization of the calcified area at the aortic side, whereas in the WT valves there is a higher amount of calcification at the ventricular side. The flow on the aortic valves *in vivo* and during *ex vivo* culture is different between the aortic and the ventricular side of the aorta. Similar to diastolic conditions *in vivo*, in *ex vivo* culture the aortic side of the leaflet experiences pressure, the ventricular side is exposed to stretch [23,24]. Interestingly, FHL2 has been shown to translocate to the nucleus upon stretch where FHL2-β-catenin/RUNX2 interactions take place [11,25]. This could explain the differences we observed in the location of calcified nodules between WT and FHL2$^{-/-}$ valves. The FHL2-β-catenin/RUNX2 interactions may be stimulated by the stretch to translocate to the nucleus in WT valves whereas the absence of this translocation and stimulation in FHL2$^{-/-}$ hearts may cause the altered localization of the calcification.

With these experiments we show that FHL2 has the potential to impact on to valvular calcification. To further understand the role FHL2 plays in valvular calcification, it would be interesting to map FHL2 in CAVD in a large patient cohort. Moreover, our data demonstrate an intriguing role for flow and/or strain on FHL2 in the aortic valves requiring research models that accurately mimic the valvular environment.



## Materials and methods

### Staining of the human aortic valves

Seven human aortic valves were obtained from patients undergoing valvular replacement surgery after consent. The aortic valves were fixated in 4%PFA and embedded in paraffin before sectioning (5$\mu$m). To stain for calcification, the sections were deparaffinized and hydrated before the sections were incubated with 2% Alizarin Red. For immunostainings sections were deparaffinized, rehydrated and antigen retrieval was performed by heating the sections to 97°C in sodium citrate buffer (pH 6.0) for 11 minutes. Subsequently, sections were incubated o/n at rt with the primary antibodies (Monoclonal mouse-FHL2 antibody, F4B2-B11 ThermoFisher, 1:250; monoclonal rabbit-RUNX123 antibody; ab92336 Abcam; 1:100) diluted in 1%BSA-PBST before incubating the slides with the secondary

antibodies diluted in 1%BSA-PBST for 40 minutes and 4′,6-Diamidine-2′-phenylindole dihydrochloride (DAPI, D3571 Life Technologies 1:1000) for 5 minutes to stain for nuclei. Sections were mounted using Prolong Gold (Invitrogen, Carlsbad, CA, USA; P36934). Between the staining steps, all sections were rinsed in PBS (2x) and PBST (1x). All slides were scanned with the Panoramic 250 slide scanner (version1.23, 3DHISTECH Ltd.) and visualized using Caseviewer (version2.3, 3DHISTECH Ltd.). FHL2 and RUNX2 positive and negative cells were manually quantified in at least three images from different locations per valve. These quantifications were correlated to the presence or absence of local calcification.

### *Ex vivo* culture of mouse aortic valves

All animal experiments were performed in 2-6 months old mice with a mixed genetic background (B6;129) according to protocols approved by the animal welfare committee of the Leiden University Medical Center and conform the guidelines from Directive 2010/63/EU of the European Parliament on the protection of animals used for scientific purposes. Mouse hearts were cultured in the MTCS as previously described [22,23]. In short and with the following modifications; mice were anesthetized with 4% isoflurane and the heart was removed and transferred to the perfusion chamber. The inflow needle of the perfusion chamber was inserted into the aorta and ligated with a suture. Flow (1000 ml/min) was introduced using a pump and PI medium (growth medium supplemented with 3mM sodium phosphate (Sigma)) was directed through the aorta towards the closed aortic valve into the coronary circulation. The medium exited the heart via the right atrium and recirculated to the reservoir. The medium was replaced twice a week. After culture for 1 week the hearts were isolated and fixed overnight with 4% PFA/PBS. Fixed mouse hearts were dehydrated through a graded series of ethanol, cleared in xylene, embedded in paraffin, and sectioned at 6mm. The sections were deparaffinized and hydrated before subsequent staining. For visualization of the calcification, the sections were incubated with 2% Alizarin Red.

### Quantification calcification of the *ex vivo* cultured valves

The surface area of the murine *ex vivo* cultured valves positive for AR was measured manually. To calculate the percentage of AR-positive area, the AR positive surface area was divided by the total surface area of the valve leaflets. At least 6 sections with 96 mm interval were used per heart and the measurements were averaged. The location of the calcification was determined by measuring the area of calcification bordering the leaflet edge at the ventricular side of the leaflet, the aortic side of the leaflet or neither (center calcification).

### Statistics

Statistical analysis was performed using Graphpad Prism (version 8). Data was tested for significance using Students t-test for unpaired data. Data are reported as mean±SEM. P-value ≤ 0.05 was considered significant.

### Acknowledgements

We gratefully thank Judith M.A. Verhagen for collecting the human aortic valve samples. We are also very grateful for the help of Mariska Vos and with the isolation of the murine hearts and Carlie J.M. de Vries for providing the mice.

## References


1. Nkomo, VT, et al. (2006). Burden of valvular heart diseases: A population-based study. *Lancet*
2. Cote, N, et al. (2013). Inflammation is associated with the remodeling of calcific aortic valve disease. *Inflammation*
3. Otto, CM, et al. (1994). Characterization of the early lesion of 'degenerative' valvular aortic stenosis. Histological and immunohistochemical studies. *Circulation*
4. Gomez-Stallons, MV, et al. (2019). Calcification and extracellular matrix dysregulation in human postmortem and surgical aortic valves. *Heart*
5. Bostrom, KI, et al. (2011). The regulation of valvular and vascular sclerosis by osteogenic morphogens. *Circ Res*
6. Rajamannan, NM, et al. (2003). Human aortic valve calcification is associated with an osteoblast phenotype. *Circulation*
7. Caira, FC, et al. (2006). Human degenerative valve disease is associated with up-regulation of low-density lipoprotein receptor-related protein 5 receptor-mediated bone formation. *J Am Coll Cardiol*
8. Jian, B, et al. (2003). Progression of aortic valve stenosis: Tgf-beta1 is present in calcified aortic valve cusps and promotes aortic valve interstitial cell calcification via apoptosis. *Ann Thorac Surg*
9. Kurakula, K, et al. (2014). The lim-only protein fhl2 reduces vascular lesion formation involving inhibition of proliferation and migration of smooth muscle cells. *PLoS One*
10. Kong, Y, et al. (2001). Cardiac-specific lim protein fhl2 modifies the hypertrophic response to beta-adrenergic stimulation. *Circulation*
11. Hamidouche, Z, et al. (2008). Fhl2 mediates dexamethasone-induced mesenchymal cell differentiation into osteoblasts by activating wnt/beta-catenin signaling-dependent runx2 expression. *Faseb j*
12. Lai, CF, et al. (2006). Four and half lim protein 2 (fhl2) stimulates osteoblast differentiation. *J Bone Miner Res*
13. Gunther, T, et al. (2005). Fhl2 deficiency results in osteopenia due to decreased activity of osteoblasts. *Embo j*
14. Yip, CY, et al. (2009). Calcification by valve interstitial cells is regulated by the stiffness of the extracellular matrix. *Arterioscler Thromb Vasc Biol*
15. Benton, JA, et al. (2008). Substrate properties influence calcification in valvular interstitial cell culture. *J Heart Valve Dis*
16. Butcher, JT, et al. (2004). Unique morphology and focal adhesion development of valvular endothelial cells in static and fluid flow environments. *Arteriosclerosis, Thrombosis, and Vascular Biology*
17. Butcher, JT, et al. (2006). Valvular endothelial cells regulate the phenotype of interstitial cells in co-culture: Effects of steady shear stress. *Tissue Eng*

18. Bowler, MA, et al. (2015). In vitro models of aortic valve calcification: Solidifying a system. *Cardiovasc Pathol*
19. Raddatz, MA, et al. (2020). Macrophages promote aortic valve cell calcification and alter stat3 (signal transducer and activator of transcription 3) splicing. *Arterioscler Thromb Vasc Biol*
20. Rodriguez, KJ, et al. (2009). Regulation of valvular interstitial cell calcification by components of the extracellular matrix. *J Biomed Mater Res A*
21. Langenbach, F, et al. (2013). Effects of dexamethasone, ascorbic acid and beta-glycerophosphate on the osteogenic differentiation of stem cells in vitro. *Stem Cell Res Ther*
22. Kruithof, BPT, et al. (2019). Stress-induced remodelling of the mitral valve: A model for leaflet thickening and superimposed tissue formation in mitral valve disease. *Cardiovasc Res*
23. Kruithof, BPT, et al. (2015). Culturing mouse cardiac valves in the miniature tissue culture system. *JoVE*
24. Balachandran, K, et al. (2011). Hemodynamics and mechanobiology of aortic valve inflammation and calcification. *Int J Inflam*
25. Nakazawa, N, et al. (2016). Matrix mechanics controls fhl2 movement to the nucleus to activate p21 expression. *Proceedings of the National Academy of Sciences of the United States of America*

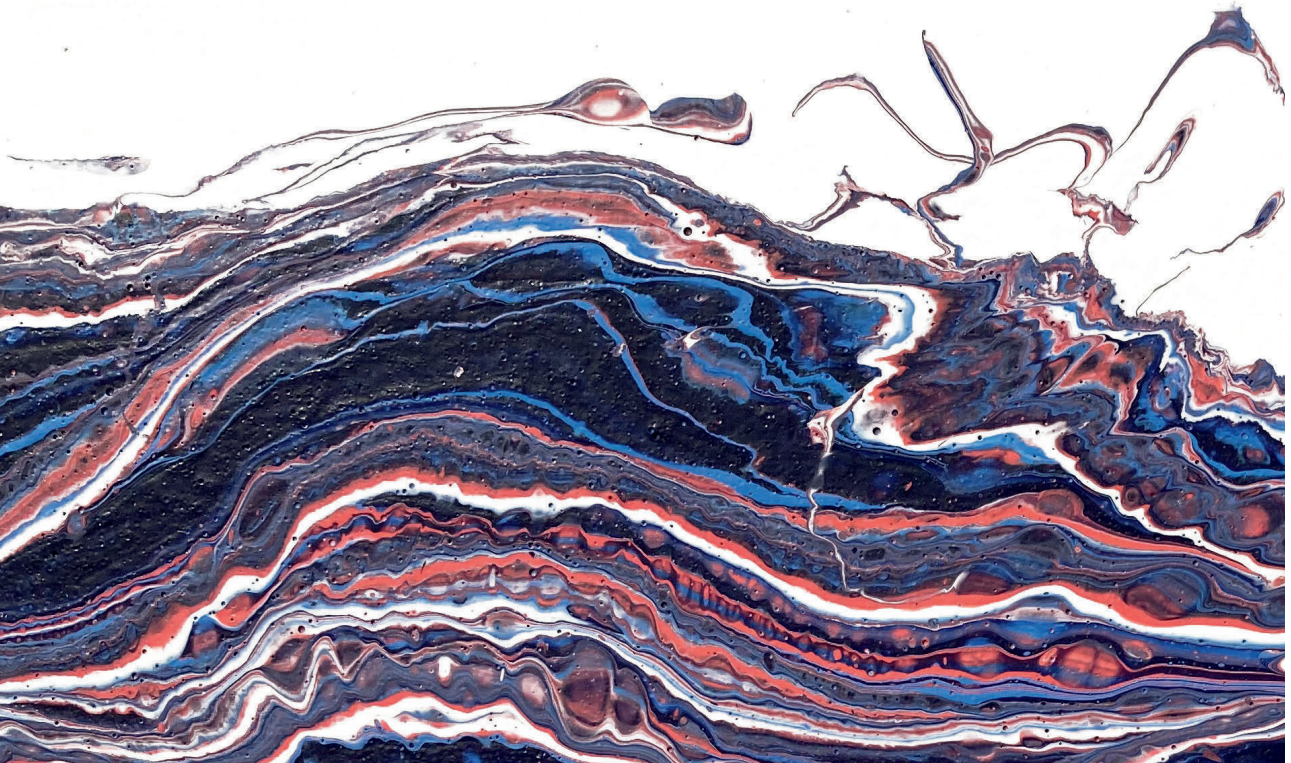

# Chapter 8

## A role for FHL2 in aortic dilation in BAV patients

**Vera van de Pol[1], Lidia R. Bons[2], Tiago Guimaraes Ferraz[1], Jan Lindeman[3], Thomas J. van Brakel[4], Carlie J. de Vries[5], Jolien W. Roos[2], Marco C. DeRuiter[6], Konda Babu Kurakula[1], Marie-José Goumans[1]**

[1] Department of Cell and Chemical Biology, Leiden University Medical Center, Leiden, The Netherlands
[2] Department of Cardiology, Erasmus Medical Center, Rotterdam, The Netherlands
[3] Department of Surgery, Leiden University Medical Center, Leiden, The Netherlands
[4] Heart Lung Center, Leiden University Medical Center, Leiden, The Netherlands
[5] Department of Medical Biochemistry, University Medical Center Amsterdam, The Netherlands
[6] Department of Anatomy and Embryology, Leiden University Medical Center, Leiden, The Netherlands

*To be submitted*

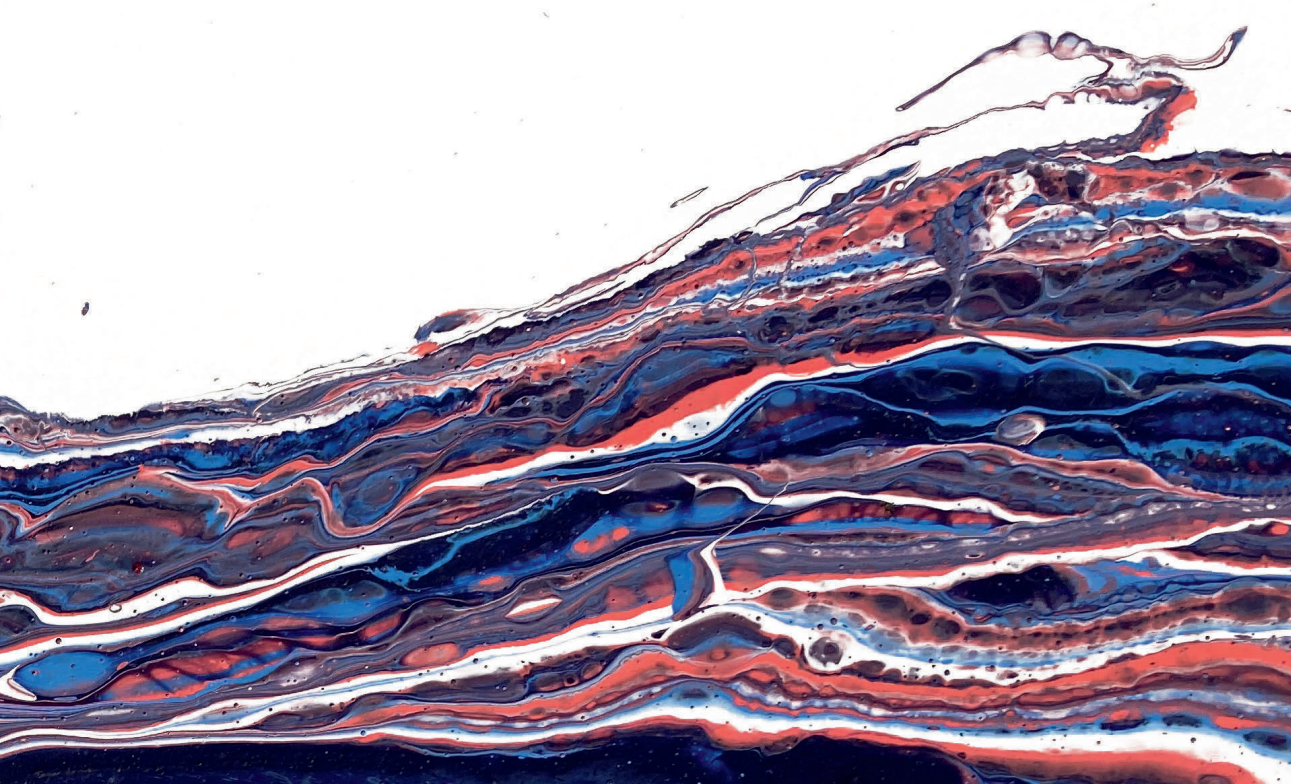

## Abstract

Bicuspid aortic valve is the most common congenital heart defect and is associated with increased prevalence of thoracic aortic aneurysm and rupture. During aortic dilation, the structure of the vessel wall is weakened by degeneration of the extracellular matrix and phenotypic switching of the vascular smooth muscle cells (vSMCs) from a contractile to synthetic phenotype. Four-and-a-Half LIM-domain 2 (FHL2) is involved in vSMC phenotypic switching in carotid artery lesions. To investigate whether FHL2 also plays a role in the phenotypic switching of vSMCs in thoracic aortic dilation, we studied the expression of FHL2 in the non-dilated and dilated thoracic aorta of patients with a tricuspid (TAV) and bicuspid aortic valve (BAV). Moreover, we studied the behaviour of aortic vSMCs isolated from FHL2$^{-/-}$ mice and the levels of FHL2 in the conditioned medium of these cells. Finally, FHL2 levels were investigated in plasma from BAV patients with and without dilation.

Immunofluorescent analysis revealed different expression patterns of FHL2 protein in the aortic wall of BAV and TAV patients. While FHL2 was expressed in the vSMCs in the intima, inner media and adventitia, a different pattern was observed in the middle of the media where FHL2 was mainly present in the extracellular space. Areas lacking nuclei and $\alpha$-smooth muscle actin ($\alpha$SMA) expression, contained high amounts of extracellular FHL2. Furthermore, our *in vitro* studies showed that FHL2$^{-/-}$ vSMCs lose their contractile phenotype faster than WT vSMCs and that vSMCs secrete extracellular vesicles containing FHL2. Moreover, we showed that FHL2 is present in human plasma. However, because FHL2 plasma levels were highly variable between patients, no relation between FHL2 levels and aortic dilation or other patient characteristics was observed. In summary, we identified an inverse relationship between FHL2 and $\alpha$SMA as a new and interesting role for FHL2 in vSMC contractility in aortic dilation. Moreover, the presence of FHL2 in extracellular vesicles and peripheral blood suggests a potential extracellular signaling role for this protein.

## Introduction

The most common congenital heart defect is bicuspid aortic valve (BAV) in which, instead of the usual 3 leaflets, the aortic valve consists of 2 leaflets [1]. Although a BAV can function normally throughout life, people with BAV have an increased risk of developing an ascending aortic aneurysm, potentially leading to rupture of the aorta [2]. Aortic dilation is caused by degeneration of the extracellular matrix (ECM), the elastic lamellae and phenotypic switching of vascular smooth muscle cells (vSMCs) from a contractile to a synthetic phenotype [3-5].

In a healthy aortic wall, vSMCs have a contractile phenotype; a state in which they express high levels of contractile proteins such as $\alpha$-smooth muscle actin ($\alpha$ SMA) and SM22$\alpha$ [6,7]. When homeostasis is altered, e.g. after vessel wall damage, vSMCs can undergo a phenotypic switch from a contractile state to a synthetic state [8,9]. Synthetic vSMCs are characterised by a high proliferative and migratory potential and express less contractile proteins than contractile vSMCs [7,10]. Serum response factor (SRF) plays a central and crucial role in vSMC phenotypic switching by regulating both contractile and synthetic gene transcription [7,11-13]. SRF also promotes the expression of the scaffold protein Four-and-a-Half LIM-domain protein 2 (FHL2). Interaction between FHL2 and SRF has been shown to inhibit transcription of SRF-responsive smooth muscle genes and knockdown of FHL2 increased the contractility of vSMCs in a collagen matrix contractile assay [14,15]. FHL2 is reported to modulate the cardiovascular stress response and impact on vSMC contractility in carotid artery lesions [16-19]. However, the role of FHL2 in aortic dilation has not yet been studied. Therefore, this study aims to investigate the role of FHL2 in thoracic aortic dilation in TAV and BAV patients.



## Results

FHL2 is expressed throughout the intima, media and adventitia of dilated aorta

To determine the expression of FHL2 in the ascending aortic wall, a staining for $\alpha$SMA and FHL2 was performed on aortic tissues with a range of different phenotypes from healthy to dilated and severely remodeled. In all samples FHL2 protein was detected, however the pattern and cellular localization differs within the media, adventitia and in the intima depending on the degree of remodeling observed in the aortic wall. In the remodeled intima/inner media, FHL2 was mainly present in vSMCs as indicated by the co-localization of $\alpha$SMA and FHL2 (Figure 1A). FHL2 and $\alpha$SMA expression were present at different locations within the cells in the inner media, whereas the expression of FHL2 in $\alpha$SMA$^+$ cells co-localized with $\alpha$SMA expression within the vSMCs in severely remodeled intimal tissue (Figure 1A,B). In the media, FHL2 was mainly found extra-

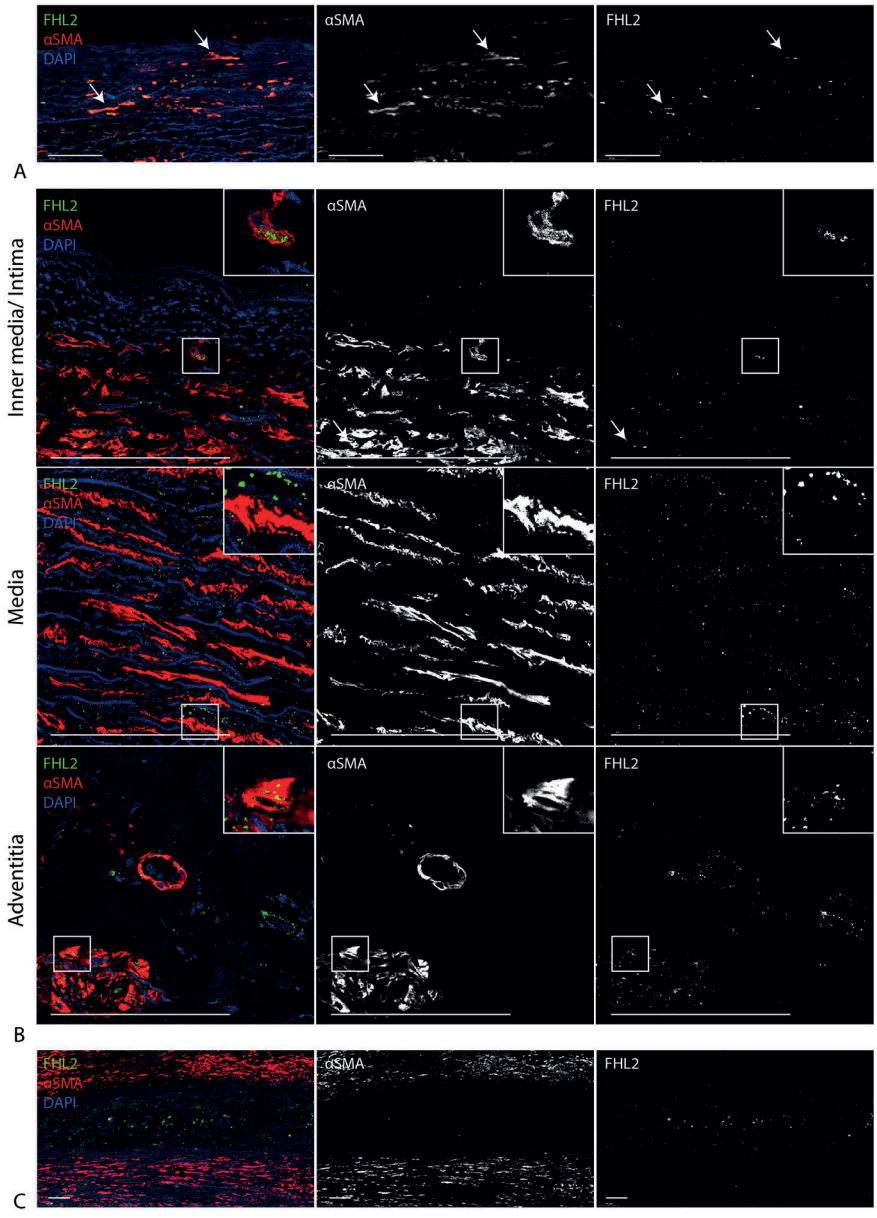


**Figure 1. FHL2 expression in the thoracic aortic wall.** A. Representative image of a remodeled intima. Arrows indicate areas where αSMA and FHL2 overlap. B. Representative images showing FHL2 and αSMA expression in the inner media, media and adventitia of the vessel. C. Representative image showing a medial area with decreased αSMA and increased FHL2 expression. Bars indicate 100 μm.

cellularly in a speckled pattern. Only very little FHL2 expression was observed within the medial vSMCs. In the adventitia both intracellular and extracellular expression of FHL2 was clearly present. Interestingly, in areas in the middle of the aortic wall with clear medial degeneration (indicated by the absence of αSMA expression, nuclei and elastic lamellae) high expression of FHL2 protein was observed (Figure 1C).

**FHL2 is increased in dilated TAV aorta**

Large variation in the expression of FHL2 staining could be observed between different aortic samples (Figure 2A). To determine if the amount of FHL2 could be related to specific patient characteristics, we performed a WB analysis on aortic samples from TAV and BAV patients with (D) and without (N) aortic dilation (TAV N n=7, TAV D n=11, BAV N n=8, BAV D n=14). We observed that FHL2 in the aorta of TAV samples with dilation was significantly increased compared to all other groups ($F(3, 36) = 0.355$, $p=0.0155$ ($R^2=0.25$), TAV N $t(16)=2.886$, $p=0.011$, $r=0.34$, BAV N $t(17)=3.486$, $p=0.0028$, $r=0.42$ and BAV D $t(23)=2.362$, $p=0.027$, $r=0.20$).

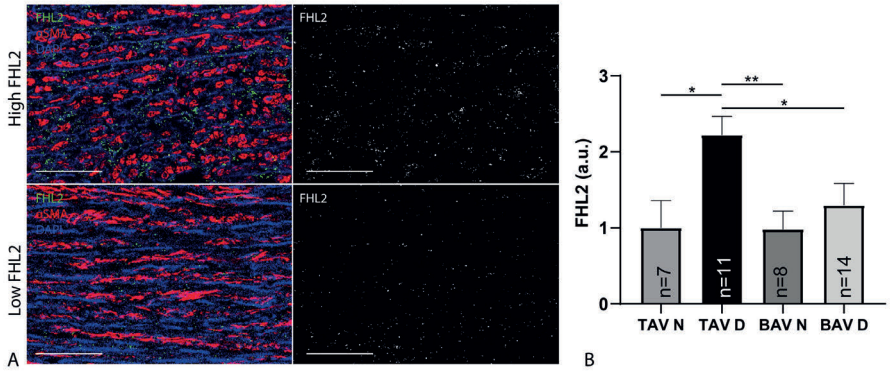


**Figure 2. FHL2 is increased in TAV dilated aorta.** A. Images showing high and low amount of FHL2 in the media. B. Quantification of FHL2 in aortic patient samples. N= non-dilated, D=dilated. Bars indicate 50 μm. *, P<0.05 **, P<0.01.

**FHL2$^{-/-}$ smooth muscle cells lose their contractile phenotype *in vitro***

To explore the relation between FHL2 and the contractility of vSMCs, we cultured aortic vSMCs isolated from FHL2$^{-/-}$ and WT mice. After the first passage, vSMCs from both WT and FHL2$^{-/-}$ mice showed the same elongated morphology (Figure 3A) and expressed αSMA (data not shown). During culture the FHL2$^{-/-}$ vSMCs lost their contractile morphology and became cobble shaped (Figure

3A). qPCR analysis confirmed a significant decrease in αSMA in the FHL2$^{-/-}$ (M=0.0996, SD=0.095) compared to the WT vSMCs (M=1, SD=0.13) (p<0.0001) (Figure 3B).

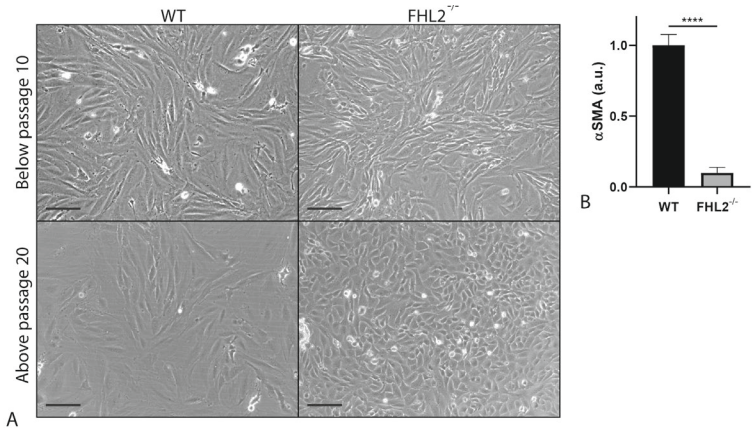


**Figure 3. FHL2$^{-/-}$ SMCs lose contractile morphology quicker than WT.** A. Representative images of early (below p10) and late passage (above p20) WT and FHL2$^{-/-}$ SMCs. B. qPCR results of αSMA in late passage WT and FHL2$^{-/-}$ SMCs. Bars indicate 200 μm. ****, P<0.001.

**FHL2 is secreted in conditioned medium and plasma**

As mentioned, FHL2 staining shows a speckled pattern in the aortic media. To determine if FHL2 was secreted extracellularly, WB was performed on extracellular vesicles isolated from vSMC conditioned medium. This confirmed that FHL2 is present in the extracellular fraction (Figure 4A). Moreover, manipulation of the intracellular FHL2 levels by knocking down or overexpressing FHL2 in the vSMCs indicated that the amount of FHL2 in the conditioned medium could be altered (Figure 4B,C).

As FHL2 can be secreted, we determined whether FHL2 was present in plasma from BAV patients and control subjects. Indeed, FHL2 could be detected in human plasma. Moreover, a large variation in the amount of FHL2 between the different samples was observed (Figure 4D). To determine if FHL2 may serve as a biomarker to detect aortic dilation, we determined the levels of FHL2 in plasma of 3 groups: TAV without aortic dilation, BAV patients without aortic dilation and BAV patients with aortic dilation (Table 1). No correlation was observed between the FHL2 plasma levels and aortic dilation or BAV ($H(2) = 0.72$, $p = 0.65$) (Figure 4E). Analysing the data in more detail we observed two distinct groups; one group with a high FHL2 in plasma and another group with a low amount of FHL2 in plasma. However, we were unable to identify which factors, such

as gender, age, height, weight or medication use of the patients, discriminates between the high or low FHL2 plasma levels.

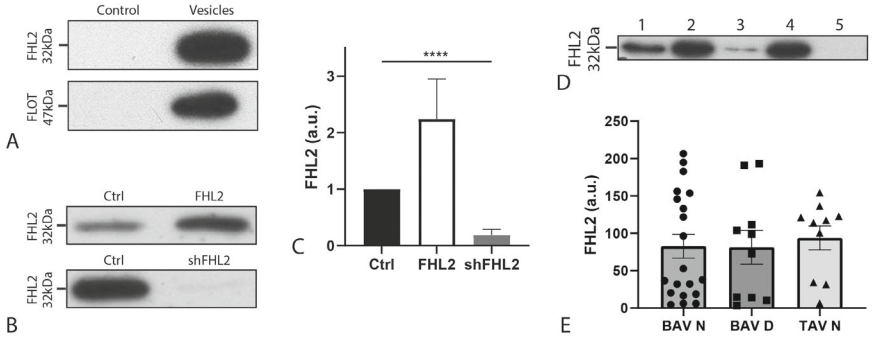


**Figure 4. FHL2 in CM and extracellular vesicles.** A. WB for FHL2 and FLOT on vesicles and vesicle deprived medium (control) conditioned by haSMCs. B. WB for FHL2 on haSMC conditioned medium with overexpression and knockdown of FHL2. C. Quantification of WB results for FHL2 on medium conditioned by SMCs. D. Representative image of WB for FHL2 on patient plasma samples. E. Quantification of WB for FHL2 on patient plasma samples. N=non-dilated, D=dilated, a.u.= arbitrary units. ****, P<0.001.

**Table 1.** Patient characteristics

| Group (N) | Age (mean,SD) | Height (mean cm,SD) | Weight (mean,SD) | Gender (male%) |
|---|---|---|---|---|
| TAV N (10) | 37.6, 9.6 | 176.0, 7.1 | 77.4, 13.6 | 50 |
| BAV N (20) | 35.7, 12.9 | 171.6 , 13.1 | 70.0, 10.6 | 45 |
| BAV D (10) | 51.0, 7.0 | 187.2, 8.1 | 91.1,16.7 | 100 |

## Discussion

In the present study, we determined if the scaffold protein FHL2 is involved in aorta dilation by analyzing the expression of FHL2 in vSMCs in relation with αSMA, vSMC contractility and the dilating aorta. We detected FHL2 throughout the aortic wall either in vSMCs or in the extracellular space. Interestingly, especially in areas of severe medial degeneration, the expression level of FHL2 was very high. Although all aortic walls showed FHL2 expression, the amount of FHL2 was significantly higher in the dilated TAV aorta compared to non-dilated TAV aorta, dilated and non-dilated BAV aorta. Furthermore, FHL2 was secreted by the vSMCs in extracellular vesicles and present in human plasma.

We found increased FHL2 protein levels in dilated TAV aortas compared to non-dilated TAV aortas. Interestingly, this increase was not found in BAV dilated aorta compared to non-dilated BAV aorta samples. Since FHL2 is involved in a wide variety of processes, a difference in expression could be related to or caused by one of the multiple differences known between TAV and BAV aortas. For example; FHL2 impacts smooth muscle cell contractility and it is known that BAV aortic tissue contains less αSMA than TAV aortas [14,15,20]. Furthermore, FHL2 can influence the proliferation of cells and, in dilated aortas, the gene expression profile of TAV vSMCs indicate a more proliferative phenotype than BAV vSMCs [21,22]. In line with previous studies on carotid artery vSMCs, our *in vitro* studies suggest that increased levels of FHL2 stimulate a contractile phenotype in aortic vSMCs [17]. Therefore, the increased expression of FHL2 in the dilated TAV aorta could be an attempt of vSMCs to maintain or regain a contractile phenotype. The lack of an increased FHL2 expression in BAV dilated aortas could therefore play a role in the increased prevalence of aortic aneurysms in BAV patients. [15,17].

Not only the amount, but also the expression pattern of FHL2 showed interesting differences. FHL2 in the aorta was expressed intracellularly in vSMCs in the inner media and adventitia while in the middle media and adventitia FHL2 was expressed extracellularly. Our finding that FHL2 can be secreted by vSMCs could explain the speckled FHL2 expression pattern in the media and adventitia of the dilated aorta. Interestingly, the expression of intracellular FHL2 in the intima and adventitia may also be stimulated by different mechanisms and have different effects than the extracellular FHL2 in the media. FHL2 secretion has also been reported for other cell types such as myoblasts and mesenchymal cells [23,24]. Since vSMCs can secrete FHL2 and FHL2 expression is increased in the dilated TAV aorta, we hypothesized that plasmic FHL2 levels could serve as a biomarker for aortic dilation. Therefore, we compared FHL2 plasma levels of TAV controls to BAV patients with and without aortic dilation. Unfortunately, we were unable to correlate the level of FHL2 in plasma to the degree of aortic dilation, which might be due to the number of patient samples analysed. Increasing the number of patients might improve sensitivity. However, the presence of two distinct groups in the data (high and low plasmic FHL2 levels) would imply that plasmic FHL2 levels are related to a common factor. We were unable to relate the plasmic FHL2 levels to factors such as gender, weight, height, age or use of medication. For future research we aim to include TAV patients with a dilating aorta, as we found an increased expression of aortic FHL2 in this group. Unfortunately, we were unable to include plasma samples of these patients into our study.

In conclusion, FHL2 is secreted by vSMCs into the aortic extracellular space and into the circulation In local areas with severe medial degeneration and in TAV aortic dilation, FHL2 expression is increased. These results highlight the intricate interaction FHL2 has with vSMC contractility.

## Material and methods

### Aortic samples

Ascending aortic wall sample collection and handling was carried out according to the official guidelines of the Medical Ethical Committee of Leiden University Medical Center (LUMC), Leiden, and the code of conduct of the Dutch Federation of Biomedical Scientific Societies (www.FMWV.nl).

In short, material was collected during surgery from TAV and BAV patients with and without aortic dilation (defined by > 44mm). After 24hr fixation in 4% formalin, samples were decalcified in a formic acid buffer (120hr), embedded in paraffin and sectioned transversally (5$\mu$m).

### Cell culture

Human aortic vSMCs were isolated from aortic tissue as described previously [25]. Informed consent was obtained according to the protocols of the Medical Ethical Committee of the Academic Medical Center (Amsterdam). The cells were cultured in DMEM:F12 supplemented with 10% fetal bovine serum (FBS) and PenStrep (100U/ml, Gibco). Cells were transduced with lentivirus containing FHL2-CMV overexpression construct [26], GFP-CMV control, shFHL2 [27] or PLKO1 control (Mission Library, Sigma) via o/n incubation and refreshing the medium the next day. Cells were refreshed at least 3 times before starting the experiments. To condition medium, cells were incubated with DMEM:F12 for 24 hours after which the medium was collected and used for WB or extracellular vesicle isolation. Mouse aortic vSMCs were isolated from WT and FHL2$^{-/-}$ mice via collagenase digestion and dissociation as described previously and approved by an independent animal ethic committee of the Amsterdam Medical Center (Amsterdam, permit number DBC102226) [17]. Cells were cultured in DMEM supplemented with 20% FBS and PenStrep. Expression of $\alpha$SMA was confirmed at P1 via qPCR.

### Plasma samples

Venous blood samples were collected from patients after informed consent at the Erasmus University Medical Center (Rotterdam). The study has been approved by the local Medical Ethical committee (MEC14-225). We included adult patients

with BAV and with and without aortic dilation defined by sinus of Valsalva ≥40 mm and/or aortic size index ≥2.1 cm/m$^2$ (ascending aorta). TAV control samples were isolated from people without known cardiovascular diseases. Exclusion criteria were: age <18 years, previous valve or aortic replacement, pregnancy or not capable of understanding or signing informed consent. Peripheral blood was collected in EDTA coated tubes and plasma was isolated by centrifuge for 10 min at 2000G. Afterwards it was stored at -80 °C within two hours after withdrawal.

**Extracellular vesicle isolation**

Conditioned medium (approximately 80 ml) was spun for 15 min at 2000G, 4°C. The supernatant was carefully isolated without disturbing the pellet and subsequently spun at 10.000G, 4°C for 30 min to further clear debris. To isolate the vesicles the debris-free supernatant was spun 70 min ultracentrifuge at 100.000G, 4°C. The pellet containing the vesicles was washed by adding PBS and isolated by centrifugation for 70 min using the ultracentrifuge at 100.000G, 4°C. Finally, the pellet was resuspended in PBS.

**Immunohistochemistry**

Sections were deparaffinised, rehydrated and antigen retrieval was performed by heating the sections to 97°C in sodium citrate buffer (pH 6.0) for 11 minutes. Subsequently, sections were incubated o/n at room temperature with the primary antibodies (Monoclonal mouse-FHL2 antibody, F4B2-B11ThermoFisher, 1:250; Rabbit-αSMA, ab5694, Abcam, 1:500) diluted in 1%BSA-PBST before incubating the samples with the secondary antibodies diluted in 1%BSA-PBST for 40 minutes and 4',6-Diamidine-2'-phenylindole dihydrochloride (DAPI, D3571 Life Technologies 1:1000) for 5 minutes to stain for nuclei. Sections were mounted using Prolong Gold (Invitrogen, Carlsbad, CA, USA; P36934) Between the staining steps, all sections were rinsed in PBS (2x) and PBST (1x).

**Protein isolation and Western blot**

To isolate protein from the aortic samples and cells, a lysis step was used. Both crushed aortic samples and cells were lysed in cold radio immunoprecipitation (RIPA) lysis buffer supplemented with protease inhibitors (Complete protease inhibitor cocktail, 11697498001, Roche Diagnostics, Basel, Switzerland). Protein concentration was determined using BCA protein assay (23225, ThermoFisher Scientific, Waltham, MA, USA). Equal amounts of protein were diluted using 5x sample buffer. To perform WB on (the extracellular fraction of) conditioned medium and plasma the lysis step was not required. For these samples, equal volumes were supplemented with 5x sample buffer (CM cleared from debris by

centrifugation step, plasma 1:1000 diluted in 1x SB). Ponceau staining was performed to check for equal loading. From this point, all samples follow the same protocol. After 5 minutes at 98°C, the samples were loaded onto and separated by SDS-PAGE and transferred to Immobilon-P PVDF membranes (IPVH00010, Merck). Membranes were blocked in Tris-buffered saline, 0.2% Tween-20 (TBST) containing 10% dry milk and incubated overnight with primary antibodies (FHL2: Abcam, ab202584, 1:2000; FLOT: Santa Cruz, SC-25506, 1:1000; αSMA: Sigma, A2547, 1:10.000) diluted in 5% BSA in TBST. Membranes were washed 3 times with TBST and incubated with a horseradish peroxidase-conjugated goat-anti-rabbit antibody (31458, ThermoFisher Scientific) diluted 1:10.000 in 10% dry milk in TBST. Membranes were washed with TBST again after which protein expression was detected using enhanced chemiluminescence (WesternBright Quantum, Advanstra) and visualized on x-ray film (Fuji film).

**mRNA isolation and quantitative RT-PCR**

RNA was isolated using the ReliaPrep RNA cell miniprep kit (Z6012, Promega) according to the manufacturer's protocol. RevertAid First Strand cDNA Synthesis (K1622, ThermoFisher Scientific) was used to generate cDNA according to the manufacturer's protocol, after which qRT-PCR was performed using GoTaq qPCR Master Mix (A6001, Promega).

**Table 2.** Primers

| | | |
|---|---|---|
| αSMA | FW: 5′-TCGGTGGCTCCATCCTGGCT-3′ | RV: 5′-TGCTAGAGGCAGAGCAGGGGG-3′ |
| GAPDH | FW: 5′-AGCCACATCGCTCAGACAC-3′ | RV: 5′-GCCCAATACGACCAAATCC-3′ |
| ARP | FW: 5′-CACCATTGAAATCCTGAGTGATGT-3′ | RV: 5′-TGACCAGCCGAAAGGAGAAG-3′ |

**Statistical analysis**

All results were obtained in 3 independent experiments, unless otherwise mentioned. Statistical assays were performed using Graph Pad Prism (version 7). Correlations were tested using One-Way ANOVA (WB aortic FHL2) or Kruskal-Wallis test (patient plasma FHL2) when required. All other statistical tests were performed using Students t-test for unpaired samples. P-values $< 0.05$ were considered significantly different.

## References


1. Ward, C. (2000). Clinical significance of the bicuspid aortic valve. *Heart*
2. Nistri, S, et al. (1999). Aortic root dilatation in young men with normally functioning bicuspid aortic valves. *Heart*
3. Serhatli, M, et al. (2014). Proteomic study of the microdissected aortic media in human thoracic aortic aneurysms. *J Proteome Res*
4. Nataatmadja, M, et al. (2003). Abnormal extracellular matrix protein transport associated with increased apoptosis of vascular smooth muscle cells in marfan syndrome and bicuspid aortic valve thoracic aortic aneurysm. *Circulation*
5. Halushka, MK, et al. (2016). Consensus statement on surgical pathology of the aorta from the society for cardiovascular pathology and the association for european cardiovascular pathology: Ii. Noninflammatory degenerative diseases - nomenclature and diagnostic criteria. *Cardiovasc Pathol*
6. Rensen, SS, et al. (2007). Regulation and characteristics of vascular smooth muscle cell phenotypic diversity. *Neth Heart J*
7. Owens, GK, et al. (2004). Molecular regulation of vascular smooth muscle cell differentiation in development and disease. *Physiol Rev*
8. Gomez, D, et al. (2012). Smooth muscle cell phenotypic switching in atherosclerosis. *Cardiovasc Res*
9. Chaabane, C, et al. (2014). Smooth muscle cell phenotypic switch: Implications for foam cell formation. *Curr Opin Lipidol*
10. Frismantiene, A, et al. (2018). Smooth muscle cell-driven vascular diseases and molecular mechanisms of vsmc plasticity. *Cell Signal*
11. Wang, D, et al. (2001). Activation of cardiac gene expression by myocardin, a transcriptional cofactor for serum response factor. *Cell*
12. Yoshida, T, et al. (2003). Myocardin is a key regulator of carg-dependent transcription of multiple smooth muscle marker genes. *Circ Res*
13. Wang, Z, et al. (2004). Myocardin and ternary complex factors compete for srf to control smooth muscle gene expression. *Nature*
14. Philippar, U, et al. (2004). The srf target gene fhl2 antagonizes rhoa/mal-dependent activation of srf. *Mol Cell*
15. Neuman, NA, et al. (2009). The four-and-a-half lim domain protein 2 regulates vascular smooth muscle phenotype and vascular tone. *J Biol Chem*
16. Tran, MK, et al. (2016). Protein-protein interactions of the lim-only protein fhl2 and functional implication of the interactions relevant in cardiovascular disease. *Biochim Biophys Acta*
17. Kurakula, K, et al. (2014). The lim-only protein fhl2 reduces vascular lesion formation involving inhibition of proliferation and migration of smooth muscle cells. *PLoS One*

18. Friedrich, FW, et al. (2014). Fhl2 expression and variants in hypertrophic cardiomyopathy. *Basic Res Cardiol*
19. Huang, PH, et al. (2013). Deletion of fhl2 gene impaired ischemia-induced blood flow recovery by modulating circulating proangiogenic cells. *Arterioscler Thromb Vasc Biol*
20. Grewal, N, et al. (2014). Ascending aorta dilation in association with bicuspid aortic valve: A maturation defect of the aortic wall. *J Thorac Cardiovasc Surg*
21. Blunder, S, et al. (2018). Targeted gene expression analyses and immunohistology suggest a pro-proliferative state in tricuspid aortic valve-, and senescence and viral infections in bicuspid aortic valve-associated thoracic aortic aneurysms. *Atherosclerosis*
22. Charlotte, L, et al. (2008). The lim-only protein fhl2 regulates cyclin d1 expression and cell proliferation. *The Journal of biological chemistry*
23. Martin, SF, et al. (2012). Proteome turnover in the green alga ostreococcus tauri by time course 15n metabolic labeling mass spectrometry. *J Proteome Res*
24. Kim, HS, et al. (2012). Proteomic analysis of microvesicles derived from human mesenchymal stem cells. *J Proteome Res*
25. de Vries, CJ, et al. (2000). Differential display identification of 40 genes with altered expression in activated human smooth muscle cells. Local expression in atherosclerotic lesions of smags, smooth muscle activation-specific genes. *J Biol Chem*
26. Kurakula, K, et al. (2011). Fhl2 protein is a novel co-repressor of nuclear receptor nur77. *J Biol Chem*
27. Kurakula, K, et al. (2015). Lim-only protein fhl2 is a positive regulator of liver x receptors in smooth muscle cells involved in lipid homeostasis. *Molecular and cellular biology*

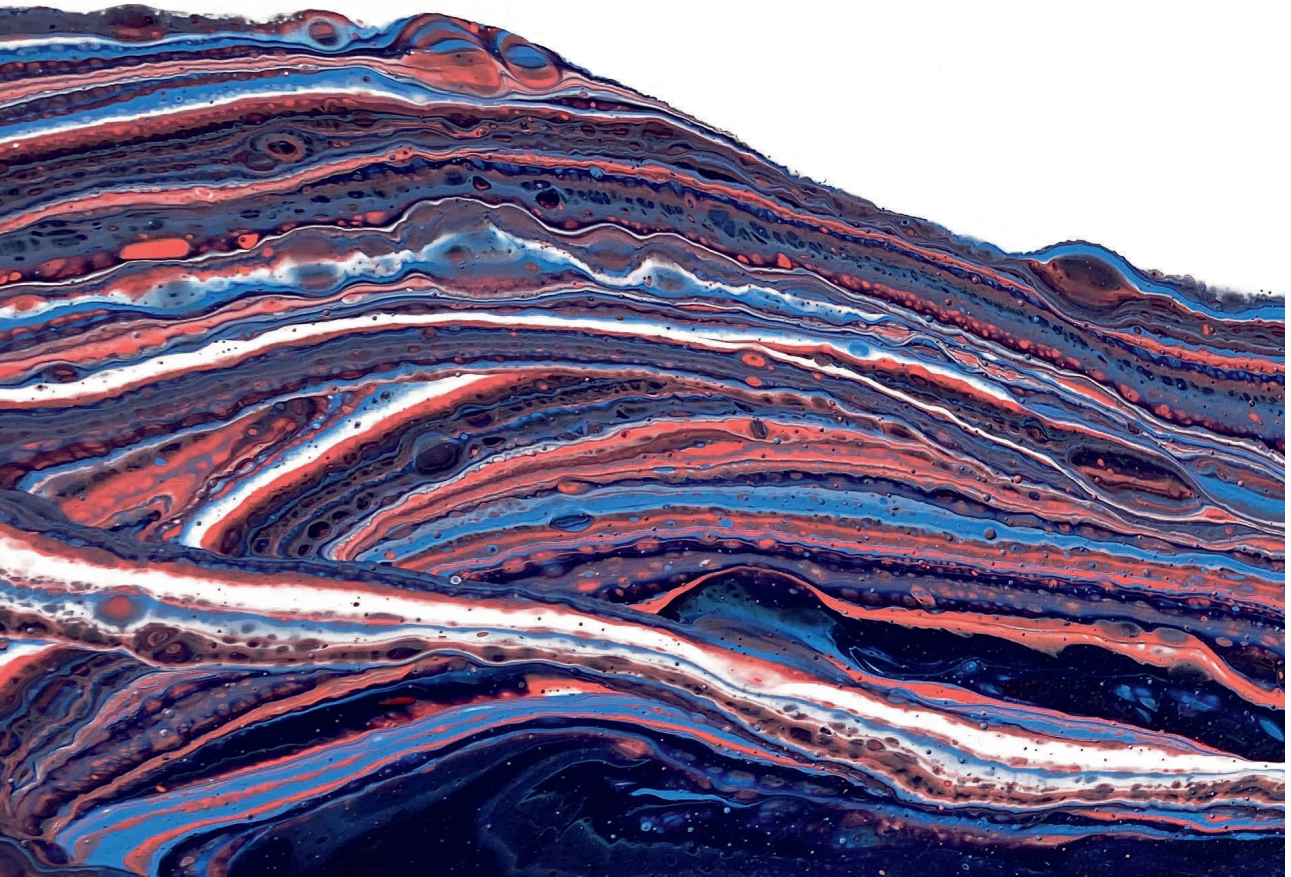

# Chapter 9

## LIM-only protein FHL2 attenuates inflammation in vascular smooth muscle cells through inhibition of the NFκB pathway

**Vera van de Pol[1], Mariska Vos[2], Marco C. DeRuiter[3], Marie-josé Goumans[1], Carlie J.M. de Vries[2], Konda Babu Kurakula[1]**

[1]Department of Cell and Chemical Biology, Leiden University Medical Center, Leiden, The Netherlands
[2]Department of Medical Biochemistry, Amsterdam Cardiovascular Sciences, Amsterdam UMC, University of Amsterdam, Amsterdam, The Netherlands
[3]Department of Anatomy and Embryology, Leiden University Medical Center, Leiden, The Netherlands

*Published: Vascular pharmacology, 2019 | 125-126:106634*

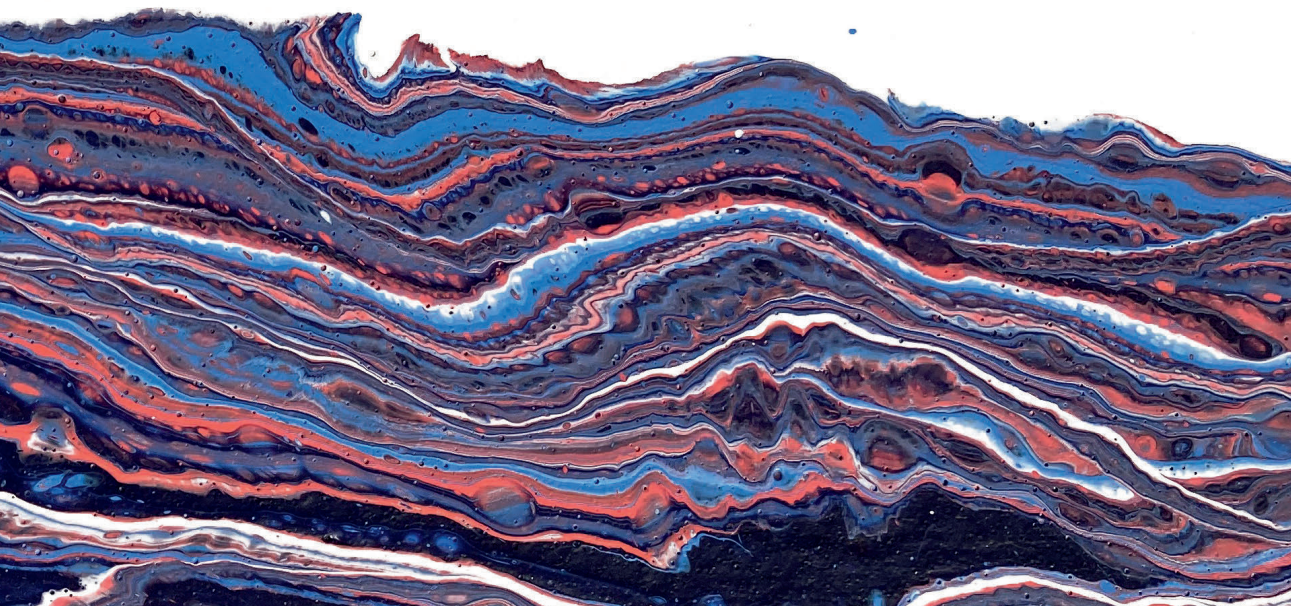

## Abstract

Despite the advent of new-generation drug-eluting stents, in-stent restenosis remains a significant problem in patients with coronary artery disease. In- stent restenosis is defined as the gradual re-narrowing of a stented coronary artery lesion due to arterial damage with subsequent local inflammation of the vessel wall and excessive growth of the vascular smooth muscle cells (vSMCs). Four-and-a-half LIM-domain protein 2 (FHL2) is a scaffold protein involved in regulating vSMC function and inflammation. Previously we have demonstrated that FHL2 prevents vSMC proliferation in a murine carotid artery ligation model. However, the effect of FHL2 on the inflammatory response of the vSMCs is not investigated. Therefore, we studied the inflammatory response in the vessel wall of FHL2-deficient (-KO) mice after carotid artery ligation. We found that circulating cytokines and local macrophage infiltration in the ligated carotid vessels were increased in FHL2-KO mice after carotid artery ligation. Moreover, FHL2-KO vSMCs showed increased secretion of cytokines such as SDF-1$\alpha$ and RANTES, and enhanced activation of the NFκB pathway. Finally, we found that blocking the NFκB signaling pathway abrogated this pro-inflammatory state in FHL2-KO vSMCs. Taken together, our results demonstrate that FHL2 decreases the inflammatory response of vSMCs through inhibition of the NFkB-signaling pathway.

## Introduction

With age, atherosclerotic plaques build up inside the human cardiovascular system, preferentially at sides with disturbed flow. Especially when occurring inside coronary arteries, these plaques can be life-threatening when reaching a point when the vessel is too narrow to supply the heart with sufficient blood. Furthermore, rupture of instable plaques can cause acute vessel occlusion and can lead to myocardial infarction. In many cases, a bare-metal stent is placed to widen the lumen of the narrowed artery and restore blood flow. Unfortunately, a large number of the patients (± 6-43%) develop in-stent restenosis due to growth of the intima/media into the lumen of the stent, which can already occur within 1 month after stent placement [1,2].

Placing a stent causes de-endothelialization of the underlying surface, initiating a wound healing response [3]. Due to the arterial damage, endothelial cells become dysfunctional and secrete several growth factors, cytokines and chemokines which in turn promote recruitment of inflammatory cells such as leukocytes and neutrophils into the injury site [4]. Furthermore, the release of chemokines such as stromal cell derived factor-1$\alpha$ (SDF-1$\alpha$/CXCL12) induces a smooth muscle cell (SMC) phenotypic switch from contractile to synthetic phenotype allowing proliferation and migration of SMCs towards the damaged intima [5]. Moreover, macrophage infiltration and lipid deposition can create neoatherosclerosis within the restenotic tissue [3]. With time, these processes narrow the lumen of the artery requiring another intervention. Although it is well established that inflammation plays a pivotal role in the pathogenesis of in-stent restenosis [6,7], the factors that regulate the inflammatory process are still largely unknown.



Four-and-a-half LIM-domain 2 (FHL2) is a LIM-only protein that can act as a scaffold protein. By binding other proteins, it can affect signaling of pathways controlling many cellular processes such as inflammation, apoptosis and migration [8,9]. FHL2 has been shown to act as a cofactor for several transcription factors including Nur77, androgen receptor, LXR and NFκB [9-11]. FHL2-KO mice do not present with cardiovascular pathologies, but when triggered by for example a Western-Type diet, adrenergic stimulation or carotid artery ligation, the importance of FHL2 for homeostasis of the cardiovascular system becomes very apparent [12-14]. Carotid artery ligation in mice induces a vascular healing response similar to in-stent restenosis, involving intimal thickening, inflammation and extensive SMC proliferation [15]. We demonstrated previously that SMC proliferation and the formation of SMC-rich lesions are increased in FHL2-KO mice after carotid artery ligation, demonstrating that absence of FHL2 enhances disease progression [12].

As a scaffolding protein, FHL2 interacts with various proteins and modulates several pathways in a cell- and context-dependent fashion. For example, FHL2 has been shown to induce expression of IL-6 and IL-8 via activation of the NFκB signaling pathway in liver and muscle cells [16]. In line with this, bone marrow derived macrophages from FHL2-KO mice exhibited decreased levels of IL-6 and TNFα in response to LPS [16]. In contrast, bone marrow derived macrophages from FHL2-KO also showed increased expression of TNFα, MCP-1 and SDF-1α following LPS stimulation [17]. Interestingly, peritoneal macrophages from FHL2-KO mice displayed no change in pro-inflammatory cytokine expression following LPS stimulation [18]. However, under basal conditions, FHL2-KO mice exhibited higher serum protein levels of S100A8/A9, a well-established pro-inflammatory marker [18,19]. Taken together, these data suggests that FHL2 regulates the inflammatory response in a highly context- and tissue-dependent manner. Therefore, we investigated the role of FHL2 in the inflammatory response of vascular SMCs *in vitro* and in a murine carotid artery ligation model. In this study, we found that both systemic and local vascular inflammation is increased in FHL2-KO mice after carotid artery ligation. In addition, FHL2 deficient SMCs secreted increased amounts of chemokines and cytokines, which was decreased to baseline when FHL2 levels were exogenously increased. Finally, we show that pharmacological inhibition of the NFκB pathway significantly attenuated the increased inflammatory status of FHL2 deficient SMCs signifying that FHL2 interferes with this specific signaling pathway.

## Results

### FHL deficiency increases inflammation in carotid artery ligation

Previous studies showed that carotid artery ligation causes an increase in SMC-rich lesion area in FHL2-deficient mice compared to control mice [12]. Since inflammation is an important trigger for intimal hyperplasia, we determined the plasma levels of the pro-inflammatory cytokine SDF-1α in FHL2-KO and WT mice 4 weeks after ligation. We found a significant increase of SDF-1α in plasma of FHL2-KO mice compared to WT control (Figure 1A). In addition, baseline plasma levels of SDF-1α were elevated in FHL2-KO mice compared to WT animals (Figure 1B). An increase in plasma SDF-1α levels reflects a systemic increase in inflammation that may drive monocyte recruitment from the bone-marrow [4,20].

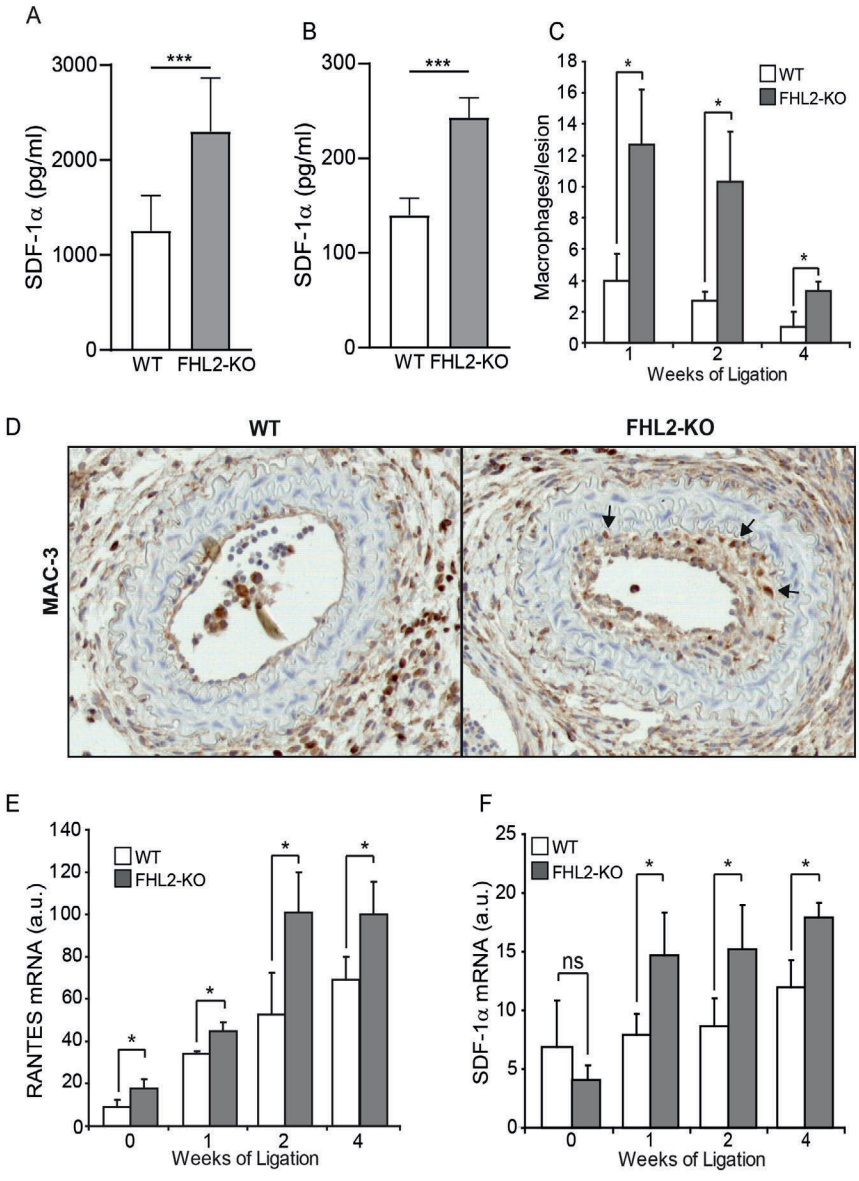


**Figure 1. FHL2 deficiency increases inflammatory protein expression.** A. Plasma levels of SDF-1α in the WT and FHL2-KO mice after 4 weeks of carotid artery ligation. B. Plasma levels of SDF-1α in the WT and FHL2-KO mice at baseline. C. Quantification of MAC-3 immunostaining on WT and FHL2-KO carotid arteries ligated for 1,2 or 3 weeks. D. Representative images of MAC-3 staining of WT and FHL2-KO carotid arteries ligated for 2 weeks. Arrows indicate positive cells. E,F. Graphs showing results of qRT-PCR for mRNA expression of RANTES (E) and SDF-1α (F) in the ligated vessels from WT and FHL2-KO mice for the indicated time periods. Data represent means±SD, *p<0.05, ***p<0.005.

To determine if there was an influx of macrophages in the local microenvironment, we stained carotid lesions for MAC-3, a protein present on differentiating and activated macrophages, allowing the number of macrophages in the vessel to be quantified. In the first week after ligation the number of macrophages were the highest, and decreased over time in both WT and FHL2-KO mice (Figure 1C,D). However, at all timepoints analysed (1, 2 and 4 weeks after ligation), the number of macrophages was significantly increased in the FHL2-KO mice compared to WT animals. Next we determined mRNA levels of RANTES and SDF-1$\alpha$ in ligated carotid artery tissue at these different timepoints. Both inflammatory mediators showed increasing expression over time in FHL2-KO and WT mice (Figure 1E-F), but the expression levels of RANTES were significantly higher in FHL2-KO mice compared to WT animals under both basal and ligated conditions. Although SDF-1$\alpha$ levels were unchanged at baseline in FHL2-KO mice, carotid artery ligation resulted in significantly higher the levels of SDF-1$\alpha$ in FHL2-KO mice compared to WT counter parts.

**FHL2-KO SMCs express increased inflammatory markers in vitro**

Activated SMCs can produce an array of inflammatory cytokines that are instrumental in progression of vascular diseases, including restenosis [21,22]. Therefore, to further substantiate our *in vivo* observations, we isolated aortic SMCs from FHL-KO and WT mice. Upon serum-starvation, we measured the mRNA levels of SDF-1$\alpha$ in cells and protein levels in the supernatants of WT and FHL2-KO SMCs. Consistent with the *in vivo* findings, both mRNA expression and protein levels of SDF-1$\alpha$ were significantly increased in FHL2-KO SMCs compared to WT SMCs (Figure 2A,B). Moreover, FHL2-
KO SMCs showed a significant increase in expression of several other proinflammatory cytokines, namely protein expression of IL-6 and MCP-1, and mRNA expression of RANTES and CXCL-1 compared to WT SMCs (Figure 2C-D). Altogether, FHL2-KO SMCs exhibit a pro-inflammatory phenotype *in vitro*.

**FHL2 attenuates inflammation via inhibition of the NFκB pathway**

Previous reports showed that activation of NFκB pathway plays a crucial role in neointima formation and cytokine production [6,23,24]. Since FHL2 can act as a cofactor for NFκB in different cell types, we determined mRNA levels of the inhibitor of NFκB signal transduction, IκB$\alpha$, and found that IκB$\alpha$ levels were slightly decreased in serum-starved FHL2-KO SMCs compared to WT cells. Interestingly, stimulation with serum decreased IκB$\alpha$ expression only in FHL2-KO SMCs, suggesting that the pro-inflammatory phenotype of the FHL2-KO SMCs is regulated via activation of the NFκB pathway (Figure 3A). To further study

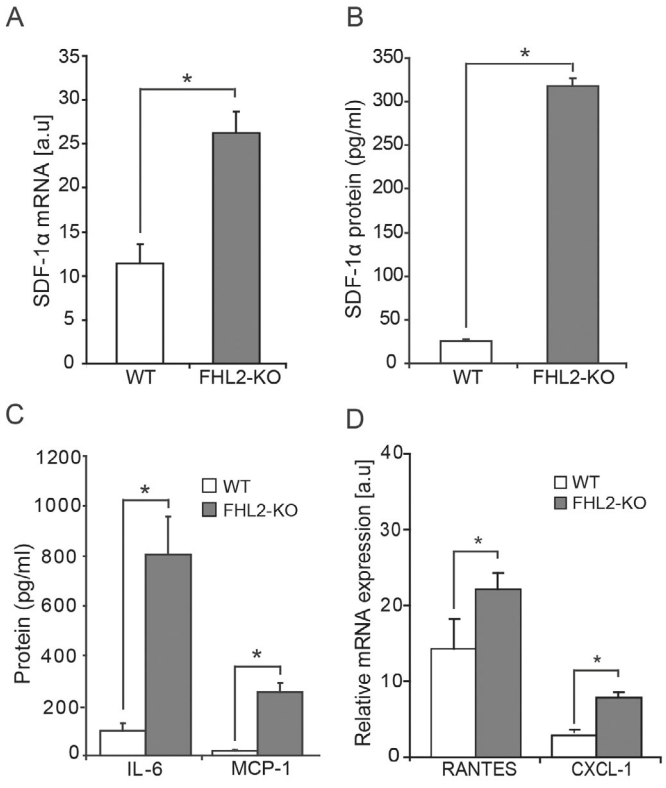


**Figure 2. FHL2-KO smooth muscle cells show increased inflammatory markers in FHL2-KO *in vitro*.** A. Semiquantitative RT-PCR was performed to assess mRNA expression of SDF-1α in serum-starved SMCs (n=2). B. Protein levels in supernatants of serum-starved SMCs measured by ELISA (n=3). C. Graph showing ELISA results of IL-6 and MCP-1 protein expression (C) or semi-quantitative RT-PCR for mRNA of RANTES and CXCL1 (D) of serum-starved SMCs stimulated with FCS for 8h (n=2). Data represent means±SD, *p<0.05.



the effect of FHL2 on the NFκB signaling pathway, we determined NFκB transcription in FHL2-deficient SMCs by using two distinct NFκB luciferase-reporter constructs. As expected, in normal culture conditions, NFκB transcription was significantly higher in FHL2-KO SMCs versus WT SMCs (Figure 3B). Moreover, NFκB activity is markedly higher in FHL2-KO SMCs under TNFα stimulated conditions as demonstrated by both NFκB reporter plasmids (Figure 3C). To further elucidate the effect of FHL2 on NFκB signaling in SMCs, we made use of a pharmacological inhibitor of NFκB, BAY11-7085, which inhibits of IκBα phosphorylation, thereby keeping the NFκB dimer sequestered in the cytoplasm [25]. Inhibition of NFκB with BAY11-7085 decreased mRNA expression of IL6, MCP-1, RANTES and SDF-1α significantly in the FHL2-KO SMCs (Figure 3D).

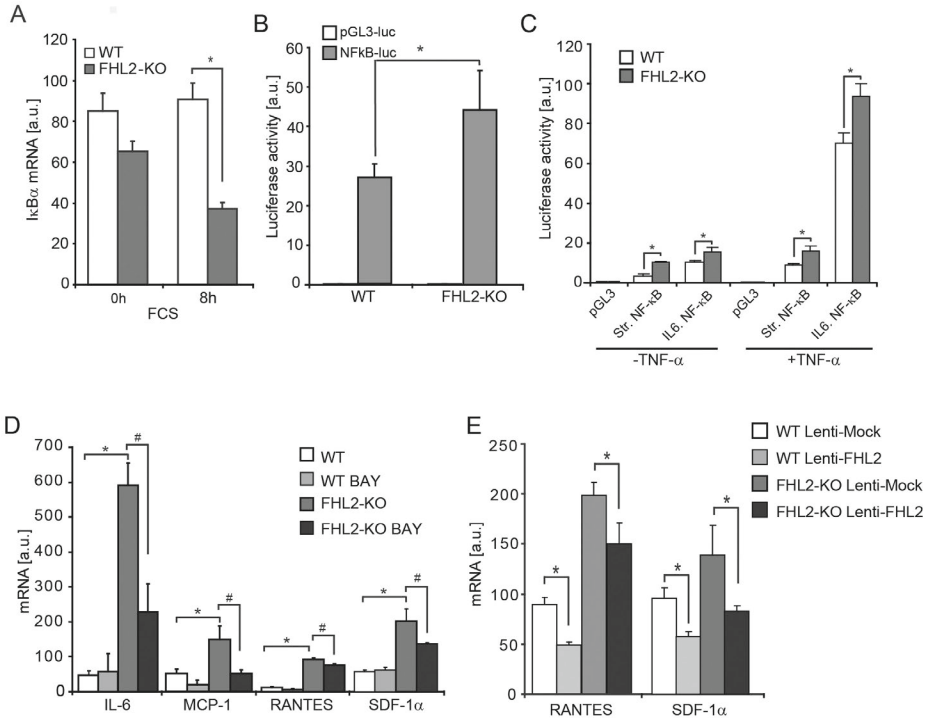


**Figure 3. FHL2 attenuates inflammation via the NFκB-pathway.** A. Graph showing qRT-PCR results for mRNA expression of IκBα in serum-starved SMCs stimulated with FCS. B. Graph showing NFκB-response element reporter-plasmid luciferase activity in serum-starved SMCs stimulated with TNF-α. C. Graphs showing the activity of NF-κB was monitored in serum-starved SMCs transfected with a construct containing the NF-κB response element of the Stratagene (Str.) or IL-6 promoter stimulated with or without TNF-α. D. Graph showing qRT-PCR results for mRNA expression of IL-6, MCP-1, RANTES and SDF1-α in serum-starved SMCs treated with or without BAY11-7085. E. Graph showing qRT-PCR results of mRNA expression of RANTES and SDF1-α, in WT and FHL2-KO SMCs transduced with FHL2-lentivirus. Data represent means±SD. *p<0.05 for FHL2-KO versus WT. #p<0.05 for BAY or PD versus control.

Finally, when FHL2 levels were restored in FHL2-KO SMCs using FHL2 lentivirus, the expression levels of RANTES and SDF-1α were significantly decreased (Figure 3E). Taken together, these data support that FHL2-KO SMCs exhibit a high pro-inflammatory phenotype via sustained activation of the NFκB pathway. In Figure 4 we summarized our data in a schematic representations.

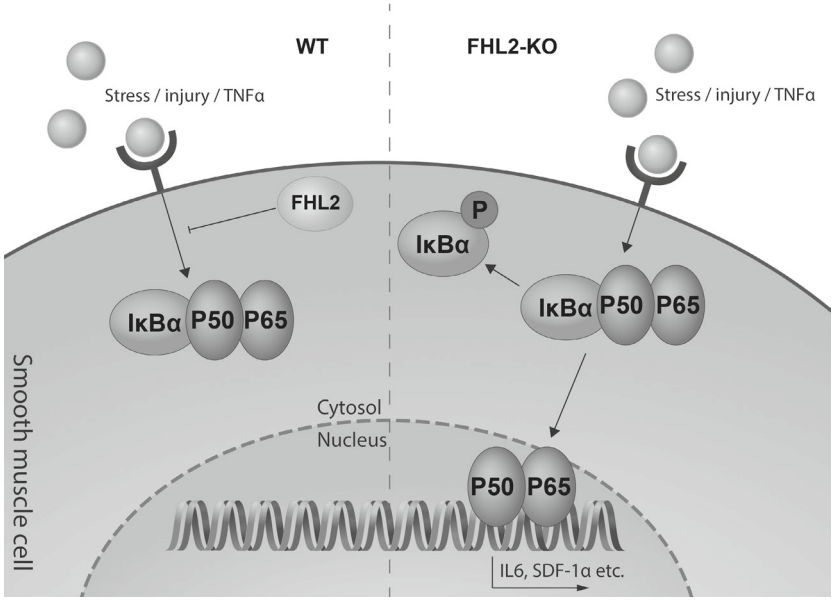


**Figure 4. FHL2 regulates inflammation in vascular smooth muscle cells through inhibition of NFkB pathway.** The left panel shows the normal situation where FHL2 inhibits NFkB pathway in the cytosol, whereas the right panel represents the effect of FHL2 deficiency resulting in enhanced activity of NFkB pathway.

## Discussion

Numerous studies have demonstrated that neointima formation is associated with increased cytokine and chemokine production by SMCs [26-28]. In this study we found that FHL2 deficiency increases both local and systemic inflammation after ligation of the carotid artery. Moreover, FHL2-deficiency induces the secretion of multiple inflammatory cytokines by SMCs, among which IL-6, MCP-1, CXCL1, RANTES and SDF-1$\alpha$. Furthermore, we show that blocking the NFκB pathway, the inflammatory phenotype of FHL2-KO SMCs is reverted.

The NFκB signaling pathway is a central regulator of inflammatory events associated with neointima formation. FHL2 has previously been shown to modulate NFκB activity in osteoclasts, even though FHL2 does not directly interact with NFκB [29]. We found that NFκB transcriptional activity is also constitutively enhanced in FHL2 depleted SMCs and consistent with this, we observed diminished IκB$\alpha$ expression in FHL2-KO SMCs. These data indicate that the function of endogenous FHL2 involves inhibition of the inflammatory response of SMCs. It has been shown that FHL2-KO mice show higher levels of inflammation in the serum under basal conditions [18]. In the current study, we also found that higher

levels of SDF-1α in the serum of FHL2-KO mice compared to WT mice under basal conditions. Furthermore, we demonstrated that FHL2 deficient SMCs exhibit a proinflammatory phenotype compared to WT SMCs through a sustained activation of NFκB pathway.

Previously it has been reported that FHL2 can induce or attenuate inflammation depending on the cell type involved in various disease models [16-19]. Therefore, FHL2 as a scaffold protein,

can regulate inflammatory responses of multiple cell types in a cell-and context-dependent manner. Further research is warranted to delineate the molecular mechanism of FHL2 on inflammation in various cell types in different disease contexts.

We have reported previously that FHL-KO mice showed an increased SMC-rich lesion area in the ligated vessels *in vivo*, and increased proliferation of FHL2-KO SMCs was also observed *in vitro* [12]. Interestingly, our results concerning SDF-1α complement the explanation for increased lesion area upon FHL2-deficiency. It has been shown that SDF-1α is abundantly expressed after vascular injury and was identified in a genome-wide association study of myocardial infarction [30] and also associates with carotid artery disease [4,31]. After vascular injury, platelets account for short-term SDF-1α release whereas SMCs mediate long-term SDF-1α release to contribute to the process of vascular remodeling and repair [32-34]. SDF-1α is also known to recruit circulating SMC progenitor cells into the vessel wall, but this aspect has not been addressed in the current study [33]. We show SDF-1α expression is markedly higher in the plasma of FHL2-KO mice than of WT mice. Furthermore, FHL2-KO SMCs displayed higher levels of SDF-1α expression and overexpression of FHL2 restored SDF-1α expression in FHL2-KO SMCs. Hence, we propose that enhanced SDF-1α levels along with other inflammatory cytokines in FHL2-KO mice may contribute to neointima formation by promoting platelet activation, possibly by recruiting SM-progenitor cells, and by enhancing proliferation and migration of SMCs.

Previous research on ApoE-/- mice showed a decrease in atherosclerotic lesion size in absence of FHL2 [13]. Moreover, FHL2-/- mice on a cholesterol-enriched diet show the same decrease [35]. Atherosclerosis is primarily initiated by lipid accumulation and activation of mononuclear cells whereas carotid artery ligation induces a SMC based pathology. This might be at the root of the differences in vascular pathogenesis in $FHL2^{-/-}$ mice.

In conclusion, FHL2 deficiency causes an increased inflammatory response after carotid artery ligation. *In vitro*, FHL2-KO SMCs secrete increased amounts of cytokines and show enhanced activation of NFκB pathway. Exogenous FHL2 efficiently blocked the production of these cytokines. These results indicate that

FHL2 inhibits the inflammatory response of vascular SMCs through attenuating NFkB-signaling.

## Methods

### Animals and Left carotid artery ligation

All mice experiments were approved by the local animal ethic committee of the Amsterdam Medical Center, University of Amsterdam, The Netherlands (DBC102226) and were carried out according to the guidelines issued by the Dutch government. The procedure of murine left carotid artery ligation has been described previously [12].

### Isolation and culturing of mouse aortic SMCs

Aortas from age and sex-matched WT and FHL2-KO mice were harvested and aortic SMCs were prepared as described previously [12].

### Lentiviral transduction and Luciferase reporter assays in SMCs

Recombinant lentiviral particles encoding FHL2 were produced, concentrated, and titrated as described previously [11,12]. Transduction of SMCs was described previously [11,12]. Transient transfection and reporter assays were carried out in serum starved SMCs with the NFκB luciferase reporter plasmids using Fugene6 transfection reagent (Roche) according to the manufacturer's protocol and described previously [12].

### Cytokines measurement by ELISA

Cytokine levels in mouse serum and cell supernatants were measured using the Cytometric Bead Array mouse inflammation kit (BD Biosciences, San Diego, CA). SDF-1$\alpha$ secretion was measured by ELISA (RayBiotech).

### qPCR

RNA was isolated from cells using the Total RNA mini kit (Bio-Rad) and from tissue using Trizol reagent (Invitrogen) according to the manufacturer's instructions. cDNA was made using the iScript cDNA synthesis kit (Bio-Rad). Real-time reverse transcription PCR was performed using the MyIQ system (Bio-Rad) and the following mouse primers: SDF-1$\alpha$ forw: 5'-CCTCGGTGTCCTCTTGCTGTCC-3', SDF-1$\alpha$ rev: 5'-GGCTCTGGCGATGTGGCTCTC-3', IL6 forw: 5'-GTTCTCTGGGAAATCGTGGA -3', IL6 rev: 5'-GGAAATTGGGGTAGGAAGGA-3', MCP-1 forw: 5'-AGCAGGTGTCCCAAAGAAGC-3', MCP-1

rev: 5′-TGAAGACCTTAGGGCAGATGC-3′. RANTES forw: 5′-TCGTGCCCACGTCAAGGAGTATTT-3′,, RANTES rev: 5′-TCTTCTCTGGGTTGGCACACACTT-3′,; CXCL-1 forw: 5′-GCTGGGATTCACCTCAAGAA-3′, CXCL-1 rev: 5′- AGGTGCCATCAGAGCAGTCT-3′. As an internal control for cDNA content of the samples, acidic ribosomal phosphoprotein P0 was measured (P0 forw: 5′-GGACCCGAGAAGACCTCCTT-3′, P0 rev: 5′-GCACATCACTCAGAATTTCAATGG-3′).

**Immunostaining**

Mouse carotid sections were fixed and stained as previously described [12]. Briefly, Paraffin sections were deparaffinized and rehydrated. Sections were boiled and blocked with 1% BSA in 0.1% Tween-PBS. Then sections were incubated overnight at 4°C with primary antibodies directed against MAC3 (1:1000;M3/84, BD Pharmingen) followed by an HRP-conjugated secondary goat anti-rabbit antibody. DAB substrate was used for detection. After counterstaining with hematoxylin all the sections were embedded in pertex (HistoLab).

**Statistical analysis**

Statistical assays were performed using Graph Pad Prism (version 7). All tests were analyzed using Students t-test. Data are reported as mean±SD unless otherwise specified. P values $<0.05$ were considered as statistically significant.

**Funding**

This work was supported by the Netherlands CardioVascular Research Initiative: the Dutch Heart Foundation, Dutch Federation of University Medical Centers, the Netherlands Organization for Health Research and Development, and the Royal Netherlands Academy of Sciences Grant 2012-08 and 2018-29 awarded to the Phaedra consortium (http://www.phaedraresearch.nl) and GENIUS consortium (CVON2011-19). This research is also supported by the Dutch Heart Foundation (BAV consortium grant 31190). We also acknowledge support for KK by the Dutch Lung Foundation (Longfonds) grant number-5.2.17.198J0 and by the Leiden University Foundation grant (W18378-2-32).

**Declaration of interest**

The authors declare that they have no known competing financial interests or personal relationships that could have appeared to influence the work reported in this paper.

## References


1. Solinas, E, et al. (2007). Gender-specific outcomes after sirolimus-eluting stent implantation. *J Am Coll Cardiol*
2. Serruys, PW, et al. (1988). Incidence of restenosis after successful coronary angioplasty: A time-related phenomenon. A quantitative angiographic study in 342 consecutive patients at 1, 2, 3, and 4 months. *Circulation*
3. Chaabane, C, et al. (2013). Biological responses in stented arteries. *Cardiovasc Res*
4. Sjaarda, J, et al. (2018). Blood csf1 and cxcl12 as causal mediators of coronary artery disease. *J Am Coll Cardiol*
5. Mazin, I, et al. (2019). Neoatherosclerosis - from basic concept to clinical implication. *Thromb Res*
6. Welt, FG, et al. (2002). Inflammation and restenosis in the stent era. *Arterioscler Thromb Vasc Biol*
7. Paiva, MS, et al. (2008). Differences in the inflammatory response between patients with and those without diabetes mellitus after coronary stenting. *J Interv Cardiol*
8. Wixler, V. (2019). The role of fhl2 in wound healing and inflammation. *Faseb j*
9. Tran, MK, et al. (2016). Protein-protein interactions of the lim-only protein fhl2 and functional implication of the interactions relevant in cardiovascular disease. *Biochim Biophys Acta*
10. Kurakula, K, et al. (2011). Fhl2 protein is a novel co-repressor of nuclear receptor nur77. *J Biol Chem*
11. Kurakula, K, et al. (2015). Lim-only protein fhl2 is a positive regulator of liver x receptors in smooth muscle cells involved in lipid homeostasis. *Mol Cell Biol*
12. Kurakula, K, et al. (2014). The lim-only protein fhl2 reduces vascular lesion formation involving inhibition of proliferation and migration of smooth muscle cells. *PLoS One*
13. Ebrahimian, T, et al. (2015). Absence of four-and-a-half lim domain protein 2 decreases atherosclerosis in apoe-/- mice. *Arterioscler Thromb Vasc Biol*
14. Kong, Y, et al. (2001). Cardiac-specific lim protein fhl2 modifies the hypertrophic response to beta-adrenergic stimulation. *Circulation*
15. Holt, AW, et al. (2013). Experimental rat and mouse carotid artery surgery: Injury & remodeling studies. *ISRN Minim Invasive Surg*
16. Dahan, J, et al. (2013). Lim-only protein fhl2 activates nf-κb signaling in the control of liver regeneration and hepatocarcinogenesis. *Mol Cell Biol*
17. Kurakula, K, et al. (2015). Lim-only protein fhl2 regulates experimental pulmonary schistosoma mansoni egg granuloma formation. *Eur J Immunol*
18. Alnajar, A, et al. (2013). The lim-only protein fhl2 attenuates lung inflammation during bleomycin-induced fibrosis. *PLoS One*
19. Wang, S, et al. (2018). S100a8/a9 in inflammation. *Front Immunol*

20. Hill, WD, et al. (2004). Sdf-1 (cxcl12) is upregulated in the ischemic penumbra following stroke: Association with bone marrow cell homing to injury. *J Neuropathol Exp Neurol*
21. Barath, P, et al. (1990). Tumor necrosis factor gene expression in human vascular intimal smooth muscle cells detected by in situ hybridization. *Am J Pathol*
22. Clinton, SK, et al. (1991). Interleukin-1 gene expression in rabbit vascular tissue in vivo. *Am J Pathol*
23. Yoshida, T, et al. (2013). Smooth muscle-selective inhibition of nuclear factor-kappab attenuates smooth muscle phenotypic switching and neointima formation following vascular injury. *J Am Heart Assoc*
24. Blackwell, TS, et al. (1997). The role of nuclear factor-kappa b in cytokine gene regulation. *Am J Respir Cell Mol Biol*
25. Tang, JR, et al. (2013). The nf-κb inhibitory proteins iκbα and iκbβ mediate disparate responses to inflammation in fetal pulmonary endothelial cells. *J Immunol*
26. Clausell, N, et al. (1995). Expression of tumour necrosis factor alpha and accumulation of fibronectin in coronary artery restenotic lesions retrieved by atherectomy. *Br Heart J*
27. Kornowski, R, et al. (1998). In-stent restenosis: Contributions of inflammatory responses and arterial injury to neointimal hyperplasia. *J Am Coll Cardiol*
28. Wasser, K, et al. (2011). Inflammation and in-stent restenosis: The role of serum markers and stent characteristics in carotid artery stenting. *PLoS One*
29. Bai, S, et al. (2008). Tumor necrosis factor receptor-associated factor 6 is an intranuclear transcriptional coactivator in osteoclasts. *J Biol Chem*
30. Subramanian, S, et al. (2014). Stromal cell-derived factor 1 as a biomarker of heart failure and mortality risk. *Arteriosclerosis, thrombosis, and vascular biology*
31. Borghini, A, et al. (2014). Stromal cell-derived factor-1-3'a polymorphism is associated with decreased risk of myocardial infarction and early endothelial disturbance. *J Cardiovasc Med (Hagerstown)*
32. Schober, A, et al. (2003). Crucial role of stromal cell-derived factor-1alpha in neointima formation after vascular injury in apolipoprotein e-deficient mice. *Circulation*
33. Zernecke, A, et al. (2005). Sdf-1alpha/cxcr4 axis is instrumental in neointimal hyperplasia and recruitment of smooth muscle progenitor cells. *Circ Res*
34. Chatterjee, M, et al. (2013). Platelet-derived cxcl12 (sdf-1α): Basic mechanisms and clinical implications. *Journal of Thrombosis and Haemostasis*
35. Chu, PH, et al. (2010). Deletion of the fhl2 gene attenuates the formation of atherosclerotic lesions after a cholesterol-enriched diet. *Life Sci*

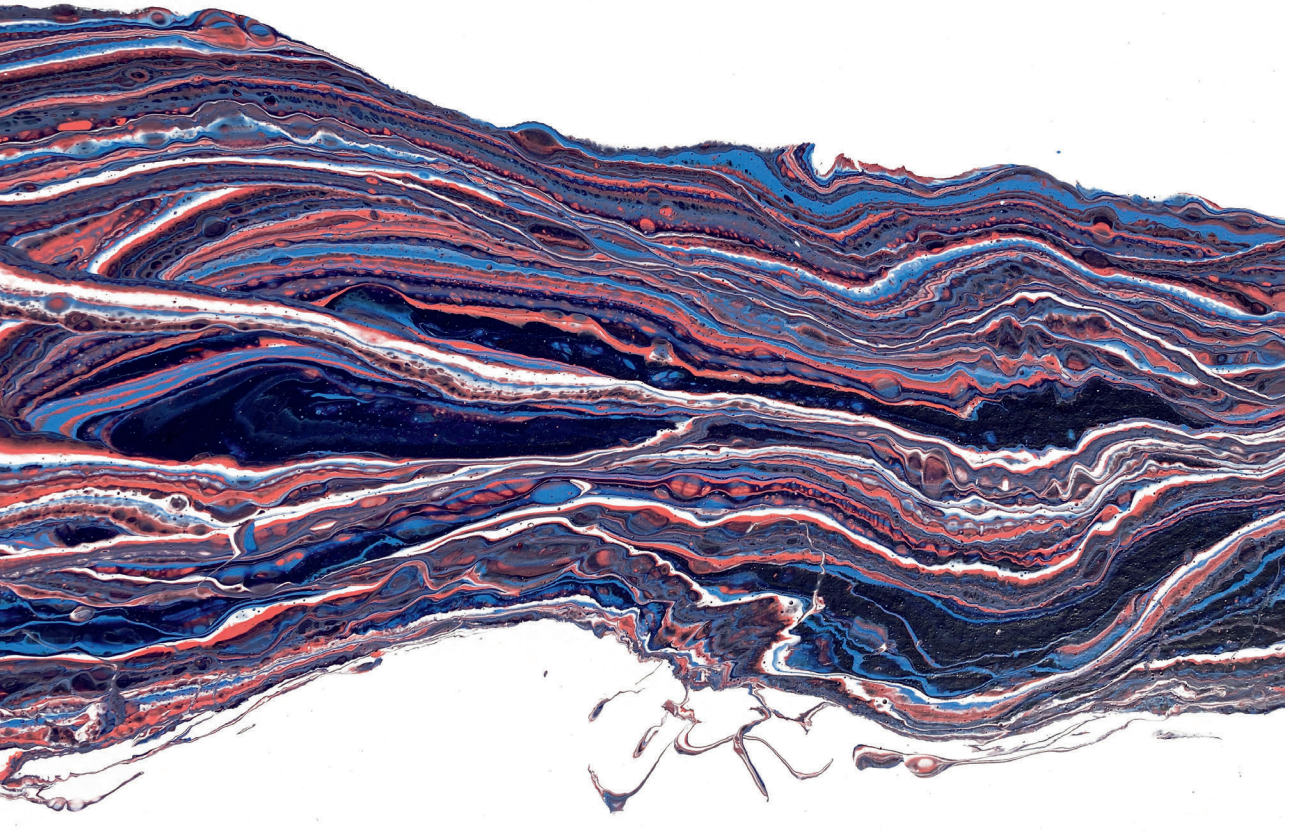

# Chapter 10

## General discussion

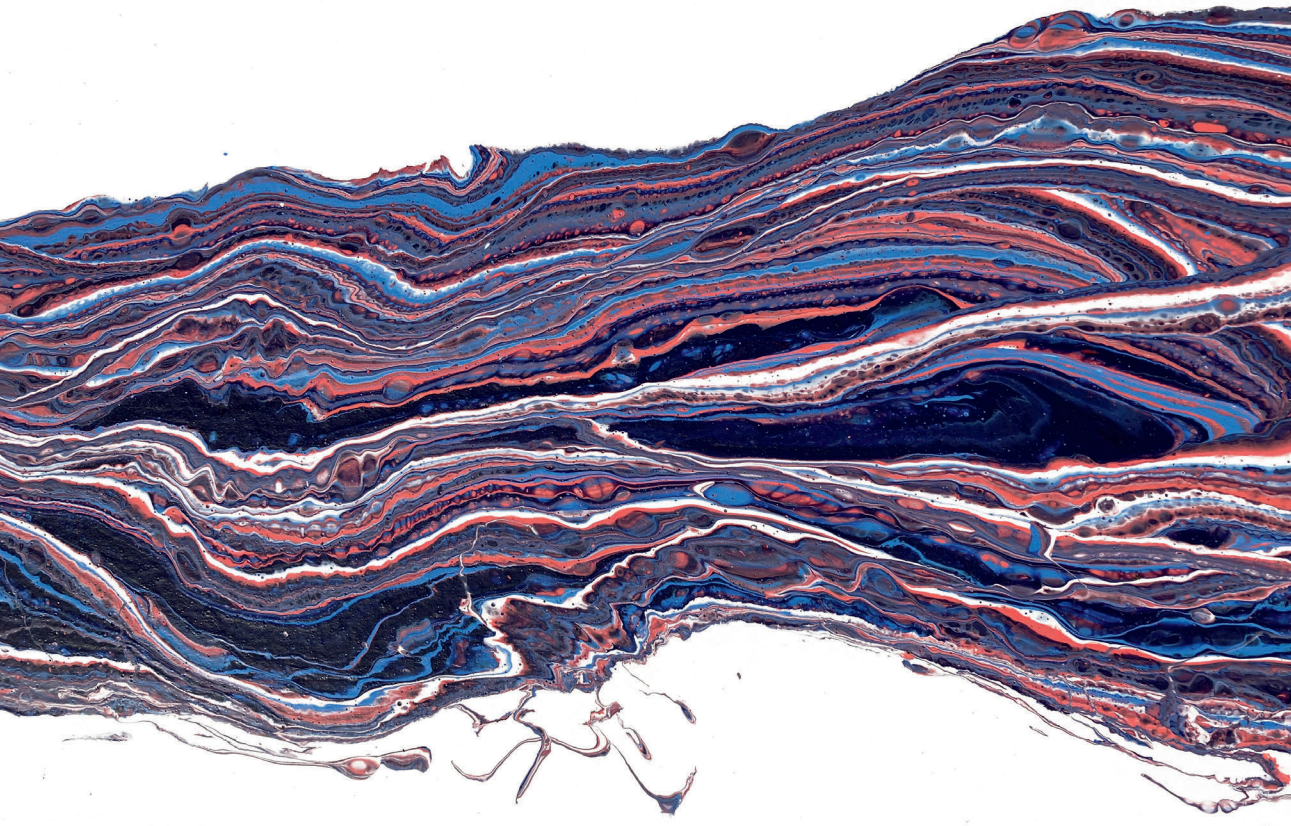

Bicuspid aortic valve (BAV) is the most common congenital heart defect and in patients with a BAV the prevalence of calcific aortic valve disease (CAVD) and thoracic aortic aneurysms is increased [1,2]. To date, the pathogenesis of BAV as well as the associated CAVD and aneurysm formation are not fully understood. Currently, the only available treatment options for CAVD or aortic aneurysm are to replace or repair the malfunctioning aortic valves and/or the ascending aorta/aortic root. Therefore, there is an urgent need to develop a treatment that will delay, prevent and possibly even reverse CAVD and aortic aneurysm formation. This requires an increase in our understanding of the mechanisms behind BAV and the related pathologies.

Different factors have hampered research aiming to understand the pathogenesis of BAV and disease progression of CAVD and aortic aneurysm in BAV patients. BAV is usually only diagnosed after patients experience health problems related to the aortic dilation or CAVD. Therefore, the initiation of the dilation or CAVD as well as the formation of the BAV itself is difficult to study in humans. Moreover, tissue biopsies from the aortic valves or the aortic wall are not available unless the patient receives valvular and/or aortic replacement surgery. Finally, although genetic studies have identified multiple gene mutations and genetic variants associated with BAV, there is not (yet) one common genetic profile associated with all BAV patients. All these factors make research on the aetiology of BAV rely heavily on experimental models and end-stage materials.

Much of the research on BAV aneurysm formation is focussed on the media and the function of smooth muscle cells (SMCs), because the most obvious pathological remodeling in aortic dilation often occurs in the media. The endothelial cells (ECs) lining the aortic wall form only a small fraction of the cells present in the vessel wall and, consequently, the role ECs play in the development of BAV and the associated pathologies is rarely studied. Although the endothelial layer is thin, multiple cardiovascular diseases have been shown to start with EC dysfunction and many disease models show the impact EC dysfunction can have on the vessel wall.



Therefore, the aim of this thesis was to study the underlying pathogenesis of aortic valve calcification and aortic dilation in BAV patients using different (novel) disease models and increase understanding of the role of ECs in these processes.

**Novel models for development of CAVD; the potential for BAV research**

Aortic stenosis, the most severe stage of CAVD, can lead to cardiac hypertrophy and often requires aortic valve replacement surgery to prevent heart failure. But even after valve replacement surgery, patients may still require life-long medi-

cation and monitoring. BAV CAVD patients require valve replacement surgery at a younger age than TAV CAVD patients, increasing the possibility that BAV patients require a second replacement surgery later in life. To prevent this lifelong impact of valve replacement surgery, CAVD disease progression should be halted or even reversed or prevented. To achieve this a detailed knowledge of the pathological mechanisms of CAVD from initiation until the end is required.

To study the initial stages of CAVD we described an *ex vivo* calcification model to study CAVD in the native configuration of the valves (chapter 6). We adapted the culture protocol of the previously developed miniature tissue culture system (MTCS), in which mouse aortic valves maintain their natural position in the heart in a controlled setting [3]. We were able to model different forms of calcification in the aortic valve using two different media, inorganic phosphates (PI) or osteogenic medium (OSM), in the MTCS. Most strikingly, our data showed that when using medium containing PI, but not when containing OSM, calcification can be induced in the aortic valves of wild-type (WT) mice when cultured *ex vivo*, while both OSM and PI induced calcification *in vitro.* These differences between *in vitro* and *ex vivo* calcification and between PI or OSM induced calcification reiterate the importance of the complex, local environment of the valves in the development of CAVD.

The *ex vivo* cultured leaflets expressed markers of osteogenic differentiation such as COX2 and RUNX2. Especially COX2 colocalized with calcified nodules in the valves of PI cultured hearts. In addition, cartilage formation was observed in the root of the aorta in both PI and OSM *ex vivo* culture conditions, indicating the presence of different forms and mechanisms of calcification in the *ex vivo* cultured aortic valves demonstrating the value of 3D modelling [4,5]. Interestingly, in contrast to previously published findings, the addition of dexamethasone abrogated the formation of calcification induced by the PI treatment [6]. Moreover, alkaline phosphatase (ALP) expression in the valves was also prevented in all conditions by the addition of dexamethasone. In addition, dexamethasone has been widely used as an adjuvant in mesenchymal cell culture medium to induce calcification in many different cells including valvular interstitial cells (VICs) [7,8]. The observed discrepancy with our study could be due to the use of different type of cells, distinct protocols, and differences between *in vitro* versus *ex vivo cultures.*

Tissue stiffness, extracellular matrix (ECM) and cellular composition of the aortic valves as well as the flow and blood composition to which they are exposed are important determinants in the valvular calcification process [9-12]. The culture model described in chapter 6 offers a novel method to study the initial stages of valvular calcification in the native environment of the aortic valve.

It is one of the very few methods allowing to study CAVD in an environment closely resembling the aortic valves *in vivo*. Complementing this model to unravel disease progression is a diet-based-method (high cholesterol, phosphate and calcium, low vitamin D3) that is able to induce calcification in the valvular commissures in WT mice [13]. Moreover, two-photon excited fluorescence (TPEF) microscopy allows early detection of CAVD progression by providing quantitative measurements that correlate with calcium deposition, collagen remodeling and osteogenic differentiation [13]. This new *in vivo* model has great potential for the progression research of CAVD in BAV if the pro-calcific diet can also induce calcification in different genetic mouse models for BAV [14-17]. The main differences between the *ex vivo* MTCS and the diet-induced mouse models are the method of induction of CAVD and the type of flow the valves are exposed to. While the diet-induced CAVD animal model makes use of mice and the physiological valvular flow, the MTCS culture model allows the study of different types of flow on the aorta and aortic valves. Furthermore, *ex vivo* modelling allows for more manipulation compared to (ethically acceptable in) live animal models.

In addition, an interesting abstract was recently published demonstrating organ-on-a-chip modelling of CAVD in a complex co-culture of VICs and valvular endothelial cells (VECs) [18]. Innovations like this will greatly increase the suitability of cell culture in research towards CAVD in the future. If cells from BAV patients would be used in this model, the underlying mechanisms in CAVD pathogenesis in BAV may be further elucidated.

**A role for FHL2 in CAVD and BAV associated aortic dilation**

FHL2 is a scaffold protein known to be involved in the cardiovascular response to changes in homeostasis and other triggers. For example, FHL2$^{-/-}$ mice have an exaggerated cardiac hypertrophic response to β-adrenergic stimulation and an increased SMC proliferation rate after carotid artery ligation, exacerbating vascular lesion formation [19,20]. Moreover, FHL2 is known, amongst others, for its involvement in calcification processes [21,22]. Interestingly, dexamethasone was shown to induce osteogenic differentiation of stem cells in vitro via FHL2/β-catenin-mediated transcriptional activation of RUNX2 [7].



**FHL2 in CAVD**

To investigate the role of FHL2 in cardiovascular calcification, we studied the role of FHL2 in calcification of the aortic valves *ex vivo* (chapter 7). *Ex vivo* cultured valves from FHL2$^{-/-}$ mice with PI did not show a significant difference in the amount of calcification. However, the location of the calcified nodules

was significantly different between FHL2$^{-/-}$ and WT aortic valves. In the FHL2$^{-/-}$ valves, the calcification nodules located more towards the aortic side whereas in the WT valves the calcification was located mostly at the ventricular side of the valve. Our data shows that FHL2 has the potential to impact valvular calcification. These spatial specific results could not have been discovered with *in vitro* modelling nor in human aortic valve tissues obtained during valve replacement surgery, demonstrating the unique results that can be achieved with this model.

Our results demonstrate that the effect of FHL2 on formation of calcified nodules is different between the aortic and ventricular side of the leaflet. Since FHL2 is expressed by different cell populations throughout the body and is involved in many different processes, targeting FHL2 systemically would likely have numerous side-effects [19,20]. One study reported that it is possible to deliver a drug in specifically the aortic valves using a drug-eluting balloon during valvuloplasty [23]. Further development of similar procedures may allow targeting of FHL2, or other possible targets such as miRNA's, specifically in the aortic valves and can provide innovative treatment options for CAVD in the future [24]. However, our results suggest that targeting of FHL2 may require not only a delivery method that is valve specific, but also one that is specific for one side of the leaflet. Therefore, miRNA's that target multiple proteins involved in CAVD may be a more realistic treatment option.

**FHL2 and the aorta**

Because FHL2 plays a role in the differentiation status and proliferation rate of SMCs, we hypothesized that FHL2 plays a role in the aortic medial degeneration that occurs in aortic aneurysm formation (chapter 8) [19,25,26]. We found that FHL2 is increased in dilated compared to non-dilated TAV aortas but not in dilated compared to non-dilated BAV aortas. Especially in the middle of the media, in the pathological absence of $\alpha$SMA, FHL2 expression was high. Furthermore, we found large variations between patient samples in the amount of FHL2 present in the aortic wall, reiterating significant heterogeneity in patients with a BAV. Moreover, we found that FHL2 is secreted by SMCs in extracellular vesicles (EVs) and is present in human plasma as demonstrated by Western blotting. The secretion of FHL2 into plasma increase its usefulness as potential biomarker. However, to date, we were unable to find a difference in plasma FHL2 levels between TAV controls and BAV patients with and without aortic dilation. Although our data illustrates that aortic remodeling is a local response, it may be possible to monitor these local processes from a distance. It has been shown that EVs secreted by SMCs with a contractile phenotype have a distinctly different content from EVs secreted by synthetic SMCs [27]. If these EVs can be isolated

and analysed from plasma, using SMC specific markers, similar to the way in which cancer specific EVs are studied in plasma, FHL2 in these EVs may prove to be suitable as a marker for aortic dilation in TAV [28].

To further understand the role of FHL2 in the vasculature and because FHL2 is also involved in inflammation, we studied the role of FHL2 in SMCs and vascular inflammation (chapter 9). We found that both systemic and local vascular inflammation is increased in FHL2$^{-/-}$ mice after carotid artery ligation. In addition, FHL2$^{-/-}$ SMCs secreted increased amounts of chemokines and cytokines, which was brought back to baseline when FHL2 levels were exogenously increased. Finally, we show that blocking the NFκB pathway reverts the inflammatory phenotype of FHL2$^{-/-}$ SMCs. These results indicate that FHL2 inhibits the inflammatory response of vascular SMCs through attenuating NFkB-signaling.

We found that FHL2 decreases inflammation in aortic SMCs and that there is an increase in FHL2 expression in dilated TAV aortas. Moreover, TAV dilated aortas have an increased inflammatory state compared to dilated aortas of BAV patients [29]. Possibly, FHL2 is present in the TAV dilated aortic tissue to dampen the inflammatory signaling cascade. However, the effect of FHl2 expression in TAV and BAV aortic wall remains to be discovered. Since FHL2 is a scaffolding protein, it affects many pathways simply by bringing different proteins together, and its function is largely context and cell type dependent. Therefore, the proteins FHL2 interacts with in TAV or BAV aortas will determine the downstream signaling. Furthermore, localization and expression levels of FHL2 might determine the outcome in specific cell type in different diseases (demonstrated by multiple seemingly contradicting articles [30-33] and our own results on the locally different effects in response to PI during *ex vivo* culture in FHL2$^{-/-}$ valves). Many proteins are differently expressed between TAV and BAV (dilated) aorta [29,34,35]. Therefore, the signaling pathways in which FHL2 is involved might be very different between TAV and BAV, even if the amount of FHL2 expression is similar. Of course, this holds true for all comparisons in which FHL2 is not the only protein that is differently expressed, hampering direct conclusions from patient-control experiments. Keeping this in mind whilst studying FHL2 will lead to a better understanding of how FHL2 affects which pathways in different contexts. Future research will hopefully allow completion of the equation and help to understand 1) why FHL2 expression is increased in TAV aortic dilation but not in BAV aortic dilation, and 2) what the effects are of this increase.



**Endothelial cells in BAV and aortic dilation**

Most research to understand BAV related aortic dilation is focussed on the SMCs and medial degeneration, as the media is the location of the major pathology.

However, the vessel wall is more than only SMCs. As detailed in Chapter 2, ECs play a major role in vascular integrity and remodeling and are under-investigated in the pathogenesis of BAV. Consequently, there are only few experimental models available to study EC function of BAV patients. Patient derived endothelial cells would be a suitable model to gain more insight in the role of the endothelium in BAV. One of the major advantages of patient specific ECs is that the (epi)genetics and resulting altered mechanisms can be studied *in vitro*. This is especially relevant for modelling diseases in which not one gene is responsible for the pathology, and genetically manipulated mouse and cell models are not able to fully model the genetic background, such as BAV [36].

**An in vitro model of BAV patient ECs: ECFCs**

Isolating aortic endothelial cells relies on the availability of aortic tissue. Endothelial colony forming cells (ECFCs) are cells that can be isolated from the mononuclear cell fraction of blood and have been used as a patient specific *in vitro* model for a range of different diseases involving the cardiovascular system such as vasculitis, pulmonary arterial hypertension, and diabetes, providing insights in disease development and mechanism [37-40]. Given the important role of EC function in vascular homeostasis, we aimed to investigate EC function in BAV in Chapter 4. Therefore, we isolated and characterised ECFCs from BAV patients and healthy controls. Relating the outgrowth and proliferation of ECFCs to patient characteristics, we observed a striking decrease in efficiency of successful ECFC isolation in BAV patients with a dilated aorta. In the ECFCs that were successfully isolated, proliferation rate and cell size were similar but there was a decrease in migratory behaviour of ECFCs from BAV patients when compared to TAV controls. A recent study shows that, besides a smaller amount of calcification in CAVD between younger BAV females and older TAV males, there is no difference between the amount of calcification in CAVD between TAV and BAV patients [41]. However, the increased prevalence of CAVD in BAV patients lead us to hypothesize that the calcification experiment would show an increased amount of calcification in BAV ECFCs compared to TAV ECFCs. Although BAV ECFCs were able to spontaneously develop calcified nodules, the calcification response to osteogenic medium was higher in TAV ECFCs than BAV ECFCs. It is possible that ECs are not involved in the increased prevalence of CAVD in BAV or that ECFCs do not accurately reflect the BAV EC response to osteogenic stimulation. Another possibility, however, is that the used method of calcification is not suitable to study the differences between BAV and TAV calcification processes. Both PI and the OSM medium used for mVICS and the MTCS-CAVD model were not able to induce calcification in the ECFCs. This also relates to the observation

in chapter 6 that different protocols stimulate calcification in different ways and will thereby lead to different conclusions. Unfortunately, protocols inducing a calcification process in ECFCs are sparse, limiting the study of this phenomenon in current patient-specific experimental models. Therefore, further optimization of protocols (e.g.: longer incubation, higher concentration, etc.) using PI, OSM or similar is needed to study calcification in ECFCs to further understand the role of ECs in CAVD development in BAV patients.

Our results in chapter 5 show that inflammatory stimuli IL-1β and TNF-α induce endothelial to mesenchymal transition (EndoMT) in primary ECs, which become prone to undergo osteogenic differentiation in response to BMP-9, a potent ligand of the BMPR2 receptor in ECs. We identified BMPR2 downregulation as a key event in this process, which leads to decreased JNK activation, thereby enhancing BMP-9-induced mineralization. Interestingly, BMP9 can bind ALK2 and deficient signaling via ALK2 has been shown to cause BAV in mice [42]. Therefore, it may be possible and interesting to further understand the BAV EC calcification by pre-treating the ECFCs with an inflammatory stimulus. This is further supported by our result showing that PiT2, a type III sodium-dependent phosphate transporter is increased in TAV but not in BAV ECFCs after TNFα stimulation.

The translation of *in vitro* results to *in vivo* effects is often difficult and this certainly applies to ECFCs as well, caused by, amongst others, the difference between the simple environment of a culture dish compared to the complex *in vivo* homeostasis. The results of the *in vitro* migration assay are an example of this complex issue. Although the *in vitro* scratch migration assay is meant to mimic a wound healing response, there was no correlation between migration of ECFCs *in vitro* to the decreased wound healing observed *in vivo* in patients with diabetes [38]. Therefore, although we observed an increase in the *in vitro* migration rate of BAV ECFCs compared to TAV ECFCs, we are unable to conclude what effect this may have on *in vivo* ECFC or EC behaviour. More research will increase knowledge on the association between disease phenotypes with specific altered responses of ECFCs and improve the interpretation of ECFC *in vitro* response to *in vivo* functioning.

Intriguingly, resident ECFCs have recently been found in the developing, neonatal lungs, and ECFC dysfunction was related to the development of congenital lung diseases [43-46]. Although the role of ECs in aortic valve formation is well-known, the involvement of ECFCs is not explored. One might speculate that ECFCs are also involved in valvulogenesis and therefore ECFC dysfunction is potentially involved in the formation of congenital valvular diseases, such as BAV, during development.

**Aortic ECs of BAV patients**

The limitations of 2D cell culture in modelling a complex environment also affects research involving ECs. In their native environment, aortic ECs are exposed to amongst others flow, immune cells and vascular SMCs [47]. To increase our understanding of EC functioning in BAV we studied aortic ECs in their complex, natural environment by histologically characterizing ECs in aortic samples from BAV patients (chapter 3). The tissue samples were obtained from the aortic wall at two locations: the 'jet' side and the 'non-jet' side. This allowed a study of the effect caused by different flow patterns in the BAV aorta on endothelial activation. One of the strengths of this approach is that ECs from different aortic locations can be compared within one patient. Therefore each patient is its own control, minimizing patient variabilities and taking confounding factors out of the equation that may occur by grouping BAV patients together, such as different genetic causes, pathogenic mechanisms, and disease progression. Histological analysis demonstrated that ECs at the non-jet side of the aorta showed a trend towards higher expression of inflammatory, EndoMT and proliferation pathways compared to the ECs on the jet side, indicating a more active EC phenotype at the non-jet side. These data are in line with research showing that the non-jet side of the BAV aorta is exposed to oscillatory flow and studies demonstrating that ECs are activated by oscillatory flow [48-51].

Although this study makes use of a unique set of samples, one aspect that would be interesting to study, but is limited in this dataset, is the comparison of EC activation to a healthy control. Mouse models of BAV could be used for this comparison, allowing the study of flow on ECs and compare BAV to TAV [15,52]. In addition, mouse models would allow the study of ECs in a less diseased aorta compared to the end-stage disease tissues obtained after surgery. Especially since many mouse models of BAV do not show a 100% penetrance of the phenotype, the TAV mutant mice could serve as a genetic control. Unfortunately and intriguingly, in literature we could not confirm whether BAV in mice alters the aortic flow similarly to BAV in humans, indicating that there may be untapped potential in the use of these models. Since flow can be manipulated in the MTCS, this *ex vivo* model may also provide interesting insights into the relation between BAV, flow and aortic remodeling.

In addition, we found that there are large variations in histological morphology in diseased human aortic tissues. Chapter 3 briefly describes the local differences of vWF expression, but also stainings for $\alpha$SMA showed great diversity within one tissue sample. Figure 1 shows data from three locations in one tissue sample. Strikingly different conclusions can be drawn from these three graphs and will be drawn if the localized diversity of the aorta is not taken

into consideration. This does not count for all proteins as can be appreciated for our vWF expression showing the same average expression level differences between patient groups as when measured at one specific location. Local differences should be taken into consideration when designing experiments and the methods used and should fit the research question. Depending on the research question a certain characteristic can be measured at multiple locations within one sample (studying the general quality of the tissue) or a specific location can be studied for all samples (studying local processes).

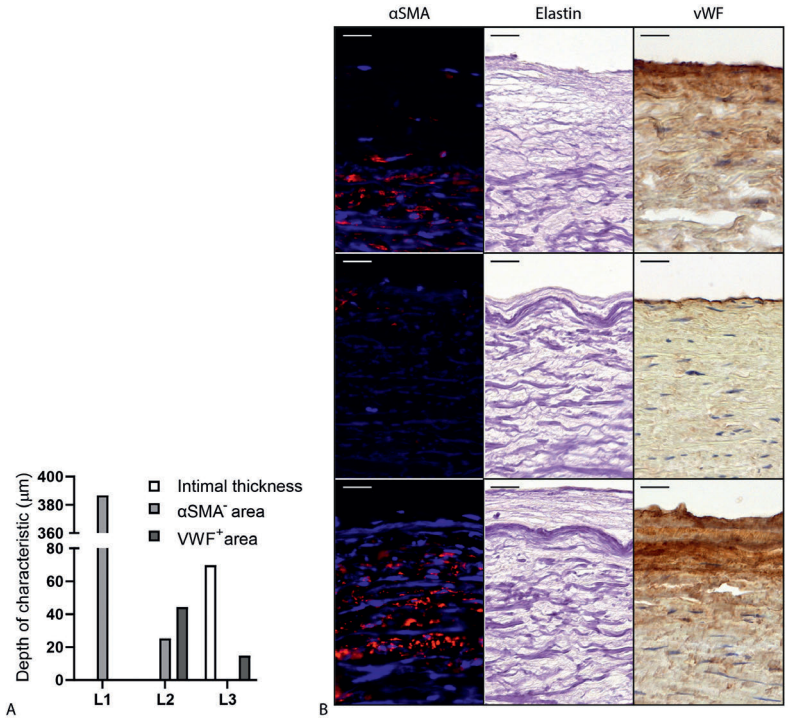


**Figure 1. Variation within aortic tissue samples.** Illustrative graph (A) and images (B) of one single patient sample in vWF and $\alpha$SMA expression and intimal thickness. Scalebar is 20 $\mu$m.

## Future perspectives

The ultimate aim of BAV research is the development of a non-invasive treatment preventing or reversing CAVD and aortic dilation. Moreover, this needs to be combined with a method to detect CAVD and aortic dilation in an early stage of the disease. To be able to develop these treatment options, the initiating and

progression occurring in these pathologies need to be well understood. The difficulty of BAV is that the initiation and development of a BAV can hardly be studied in humans. Furthermore, the molecular characteristics of the valves and the aorta can hardly be studied in the early stages of CAVD and aortic dilation. Therefore, accurate experimental models are required.

The MTCS is an interesting new model to study the role of flow on the valves and aorta in BAV and TAV mouse models. Future studies using the MTCS may help in understanding the role of flow, specific proteins and treatments in BAV and TAV aortic remodeling and CAVD, in addition to the other diseases that can be studied in the MTCS.

To understand the cellular functioning of BAV ECs, VICs and SMCs, another model that could be used is a combination of *in vitro* models such as valve- and vessel-on-a-chip with patient specific cells such as ECFCs and iPSCs derived vascular cells [18,53]. These models allow detailed analysis of the different molecular pathways involved in processes such as SMC phenotype, ECM maintenance and calcification. Moreover, patient-specific models can be used to study different treatments targeting these processes.

ECFCs provide a novel patient-specific cell model to study pathological processes in BAV. While iPSCs can also be differentiated towards ECs, ECFC culture does not require a differentiation stage. This may be preferred in studying BAV EC characteristics since many mutations found in BAV are involved in cellular differentiation, possibly affecting the EC phenotype of differentiated BAV but not TAV iPSCs. It has already been shown that BAV iPSCs have a defect in differentiation towards a SMC [54]. This does illustrate that iPSCs can provide valuable information on the differentiation of BAV ECs and thereby aid in understanding of the formation of BAV during valvulogenesis.

The use of patient-specific material in BAV research should, however, be accompanied by the awareness that BAV is not one disease but a pathology which can be caused by a myriad of pathogenic mechanisms [17,55]. In our study using ECFCs we were able to generate significant results with a small sample size, however, future studies likely require a larger sample size to generate more detailed results due to the non-homogenous population that characterizes BAV.

All research in experimental models requires translation to patients. Because of the lack of tissue samples in BAV during the early pathogenesis, the patients can be monitored using advanced imaging techniques and detection of key factors in the blood. To detect CAVD and aortic dilation in an early stage of the disease, biomarkers are and should be studied. Understanding the pathological processes will help targeting the search for a biomarker. FHL2 may have some potential to serve as a biomarker. Especially in TAV dilation FHL2 in SMC spe-

cific EVs may be used to monitor the local aortic medial degeneration. Although the study of correlations between plasma samples and the aortic histology of patients may provide interesting results, long-term follow-up studies are required to validate plasma samples or EVs as a biomarker predicting aortic pathology. Furthermore, FHL2 is an interesting protein to increase understanding of CAVD, flow and tissue stiffness. To understand the role of FHL2 under regular flow conditions the diet-induced CAVD mouse model may provide interesting insights [13]. To understand the role of FHL2 in aortic dilation, BAV and TAV, patient specific cells in different co-culture and flow experiments, such as the valve- and vessel-on-a-chip models can be used.

The combination of new insights using accurate experimental models with patient samples and data will increase the understanding of the BAV pathogenesis that will, over time, turn into new and better treatment options for BAV patients.

## References


1. Roberts, WC, et al. (2005). Frequency by decades of unicuspid, bicuspid, and tricuspid aortic valves in adults having isolated aortic valve replacement for aortic stenosis, with or without associated aortic regurgitation. *Circ*
2. Michelena, HI, et al. (2011). Incidence of aortic complications in patients with bicuspid aortic valves. *Jama*
3. Kruithof, BP, et al. (2015). Culturing mouse cardiac valves in the miniature tissue culture system. *J Vis Exp*
4. Mohler, ER, 3rd, et al. (2001). Bone formation and inflammation in cardiac valves. *Circulation*
5. Otto, CM, et al. (1994). Characterization of the early lesion of 'degenerative' valvular aortic stenosis. Histological and immunohistochemical studies. *Circulation*
6. Li, Q-x, et al. (2020). Dexamethasone causes calcium deposition and degeneration in human anterior cruciate ligament cells through endoplasmic reticulum stress. *Biochemical Pharmacology*
7. Langenbach, F, et al. (2013). Effects of dexamethasone, ascorbic acid and beta-glycerophosphate on the osteogenic differentiation of stem cells in vitro. *Stem Cell Res Ther*
8. Goto, S, et al. (2019). Standardization of human calcific aortic valve disease in vitro modeling reveals passage-dependent calcification. *Front Cardiovasc Med*
9. Bowler, MA, et al. (2015). In vitro models of aortic valve calcification: Solidifying a system. *Cardiovasc Pathol*
10. Chen, J-H, et al. (2011). Cell-matrix interactions in the pathobiology of calcific aortic valve disease.
11. Yip, CY, et al. (2009). Calcification by valve interstitial cells is regulated by the stiffness of the extracellular matrix. *Arterioscler Thromb Vasc Biol*
12. Butcher, JT, et al. (2006). Valvular endothelial cells regulate the phenotype of interstitial cells in co-culture: Effects of steady shear stress. *Tissue Eng*
13. Tandon, I, et al. (2020). Label-free optical biomarkers detect early calcific aortic valve disease in a wild-type mouse model. *BMC Cardiovascular Disorders*
14. Fernández, B, et al. (2020). Bicuspid aortic valve in 2 model species and review of the literature. *Vet Pathol*
15. Laforest, B, et al. (2011). Loss of gata5 in mice leads to bicuspid aortic valve. *J Clin Invest*
16. Lee, TC, et al. (2000). Abnormal aortic valve development in mice lacking endothelial nitric oxide synthase. *Circulation*
17. Sievers, HH, et al. (2014). Toward individualized management of the ascending aorta in bicuspid aortic valve surgery: The role of valve phenotype in 1362 patients. *J Thorac Cardiovasc Surg*

18. Tandon, I, et al. (2020). Abstract 16123: *in vitro* valve-on-chip platform to assess the effects of hemodynamic and mechanical stimuli on early calcific disease progression. *Circulation*
19. Kurakula, K, et al. (2014). The lim-only protein fhl2 reduces vascular lesion formation involving inhibition of proliferation and migration of smooth muscle cells. *PLoS One*
20. Kong, Y, et al. (2001). Cardiac-specific lim protein fhl2 modifies the hypertrophic response to beta-adrenergic stimulation. *Circulation*
21. Gunther, T, et al. (2005). Fhl2 deficiency results in osteopenia due to decreased activity of osteoblasts. *Embo j*
22. Lai, CF, et al. (2006). Four and half lim protein 2 (fhl2) stimulates osteoblast differentiation. *J Bone Miner Res*
23. Spargias, K, et al. (2009). Drug delivery at the aortic valve tissues of healthy domestic pigs with a paclitaxel-eluting valvuloplasty balloon. *J Interv Cardiol*
24. van der Ven, CF, et al. (2017). In vitro 3d model and mirna drug delivery to target calcific aortic valve disease. *Clin Sci (Lond)*
25. Tran, MK, et al. (2016). Protein-protein interactions of the lim-only protein fhl2 and functional implication of the interactions relevant in cardiovascular disease. *Biochim Biophys Acta*
26. Halushka, MK, et al. (2016). Consensus statement on surgical pathology of the aorta from the society for cardiovascular pathology and the association for european cardiovascular pathology: Ii. Noninflammatory degenerative diseases - nomenclature and diagnostic criteria. *Cardiovasc Pathol*
27. Comelli, L, et al. (2014). Characterization of secreted vesicles from vascular smooth muscle cells. *Molecular bioSystems*
28. Zhao, Z, et al. (2019). Extracellular vesicles as cancer liquid biopsies: From discovery, validation, to clinical application. *Lab on a Chip*
29. Grewal, N, et al. (2014). Ascending aorta dilation in association with bicuspid aortic valve: A maturation defect of the aortic wall. *J Thorac Cardiovasc Surg*
30. Hubbi, ME, et al. (2012). Four-and-a-half lim domain proteins inhibit transactivation by hypoxia-inducible factor 1*. *Journal of Biological Chemistry*
31. Hinson, JS, et al. (2008). Regulation of myocardin factor protein stability by the lim-only protein fhl2. *Am J Physiol Heart Circ Physiol*
32. Philippar, U, et al. (2004). The srf target gene fhl2 antagonizes rhoa/mal-dependent activation of srf. *Molecular Cell*
33. Chu, P-H, et al. (2008). Deletion of the fhl2 gene attenuating neovascularization after corneal injury. *Investigative Ophthalmology & Visual Science*
34. Grewal, N, et al. (2014). Bicuspid aortic valve: Phosphorylation of c-kit and downstream targets are prognostic for future aortopathy. *Eur J Cardiothorac Surg*

35. Maleki, S, et al. (2016). Mesenchymal state of intimal cells may explain higher propensity to ascending aortic aneurysm in bicuspid aortic valves. *Sci Rep*
36. Prakash, SK, et al. (2014). A roadmap to investigate the genetic basis of bicuspid aortic valve and its complications: Insights from the international bavcon (bicuspid aortic valve consortium). *Journal of the American College of Cardiology*
37. Ingram, DA, et al. (2004). Identification of a novel hierarchy of endothelial progenitor cells using human peripheral and umbilical cord blood. *Blood*
38. Langford-Smith, AWW, et al. (2019). Diabetic endothelial colony forming cells have the potential for restoration with glycomimetics. *Sci Rep*
39. Smits, J, et al. (2018). Blood outgrowth and proliferation of endothelial colony forming cells are related to markers of disease severity in patients with pulmonary arterial hypertension. *Int J Mol Sci*
40. Wilde, B, et al. (2016). Endothelial progenitor cells are differentially impaired in anca-associated vasculitis compared to healthy controls. *Arthritis Res Ther*
41. Voisine, M, et al. (2020). Age, sex, and valve phenotype differences in fibro-calcific remodeling of calcified aortic valve. *Journal of the American Heart Association*
42. Thomas, PS, et al. (2012). Deficient signaling via alk2 (acvr1) leads to bicuspid aortic valve development. *PLoS One*
43. Alphonse, RS, et al. (2014). Existence, functional impairment, and lung repair potential of endothelial colony-forming cells in oxygen-induced arrested alveolar growth. *Circulation*
44. Baker, CD, et al. (2012). Cord blood angiogenic progenitor cells are decreased in bronchopulmonary dysplasia. *Eur Respir J*
45. Fujinaga, H, et al. (2016). Cord blood-derived endothelial colony-forming cell function is disrupted in congenital diaphragmatic hernia. *Am J Physiol Lung Cell Mol Physiol*
46. Alphonse, RS, et al. (2015). The isolation and culture of endothelial colony-forming cells from human and rat lungs. *Nat Protoc*
47. van Buul-Wortelboer, MF, et al. (1986). Reconstitution of the vascular wall in vitro: A novel model to study interactions between endothelial and smooth muscle cells. *Experimental Cell Research*
48. Zhou, J, et al. (2014). Shear stress-initiated signaling and its regulation of endothelial function. *Arterioscler Thromb Vasc Biol*
49. Krüger-Genge, A, et al. (2019). Vascular endothelial cell biology: An update. *International journal of molecular sciences*
50. Nerem, RM, et al. (1998). The study of the influence of flow on vascular endothelial biology. *Am J Med Sci*
51. Chien, S. (2008). Effects of disturbed flow on endothelial cells. *Ann Biomed Eng*

52. Fernández, B, et al. (2009). Bicuspid aortic valves with different spatial orientations of the leaflets are distinct etiological entities. *Journal of the American College of Cardiology*
53. Pollet, AMAO, et al. (2020). Recapitulating the vasculature using organ-on-chip technology. *Bioengineering (Basel, Switzerland)*
54. Jiao, J, et al. (2016). Differentiation defect in neural crest-derived smooth muscle cells in patients with aortopathy associated with bicuspid aortic valves. *EBioMedicine*
55. Buchner, S, et al. (2010). Variable phenotypes of bicuspid aortic valve disease: Classification by cardiovascular magnetic resonance. *Heart*

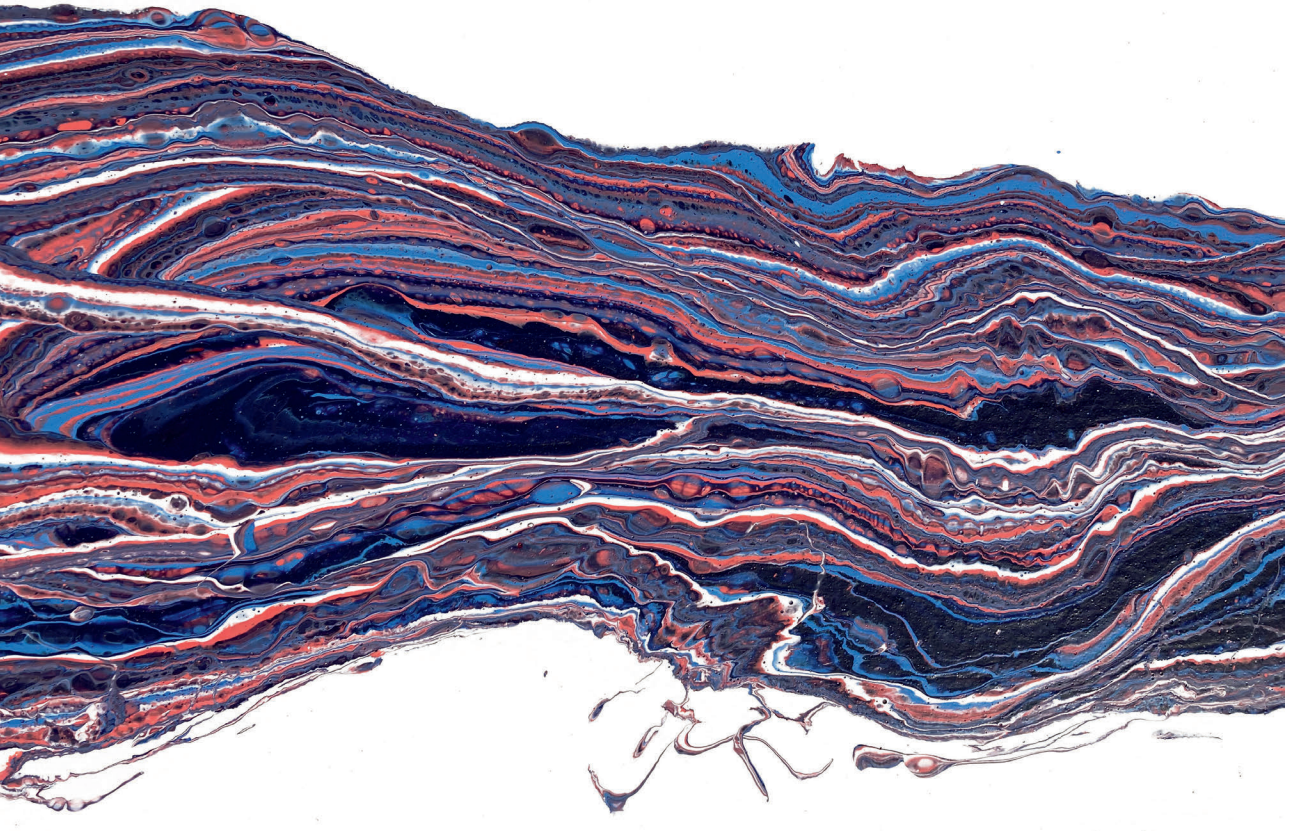

Nederlandse samenvatting

Curriculum Vitea

Dankwoord

List of publications

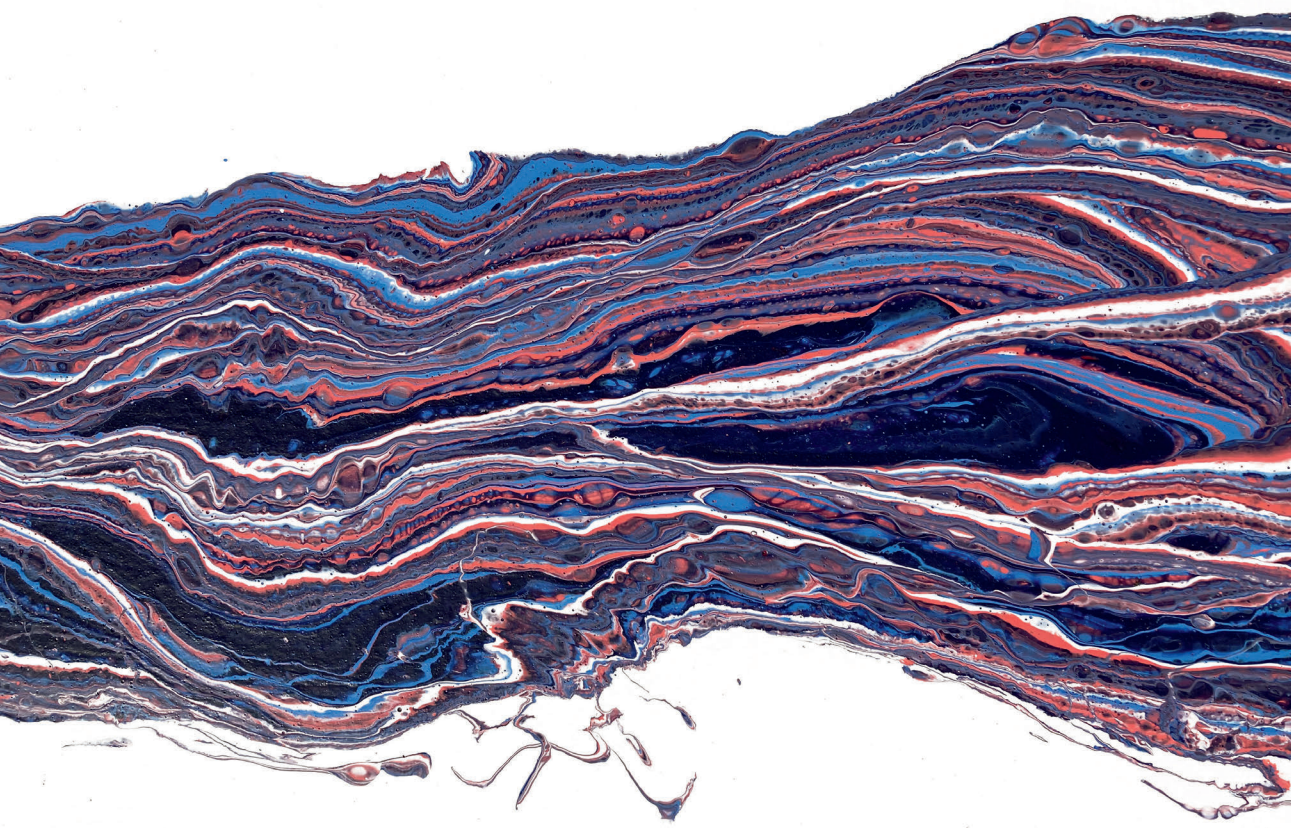

# Nederlandse samenvatting

**Achtergrond**

Een bicuspide aortaklep (bicuspid aortic valve - BAV) is een aangeboren hartafwijking waarbij de hartklep tussen de linker hartkamer en de grote lichaamsslagader, de aorta, uit twee in plaats van de normale drie klepslipjes bestaat (tricuspid aortic valve - TAV). Hoewel een BAV goed kan functioneren, treedt er bij een groot deel van de mensen met een BAV al vroeg in het leven verkalking van de hartkleppen op of ontstaat er een verwijding van de aorta. Beide complicaties zijn levensgevaarlijk; omdat het hart harder moet werken om bloed langs verkalkte hartkleppen te pompen kan dit leiden tot hartfalen en een verwijde aorta kan op een gegeven moment scheuren. Er is geen andere behandeling beschikbaar dan een hartoperatie om de klep en/of aorta te vervangen. Hoewel er meerdere theorieën zijn waarom een BAV tot deze problemen kan leiden, is het nog niet duidelijk waarom patiënten met een BAV gevoelig zijn voor het ontwikkelen van hartklepverkalking en aortaverwijding. Ook is het niet duidelijk waarom sommige BAV patiënten hun gehele leven zonder complicaties blijven en andere patiënten al op jonge leeftijd ernstige problemen ervaren.

De vaatwand en hartkleppen bestaan uit verschillende celtypes die een rol spelen bij de vorming en het onderhoud van een gezonde weefselstructuur. De wand van de aorta bestaat voor het grootste deel uit gladde spiercellen. Aan de binnenkant is deze laag spiercellen met een dunne laag endotheelcellen bekleed. De hartkleppen bestaan voor een groot deel uit fibroblasten, die ook bedekt zijn met een laag endotheelcellen. Endotheelcellen vormen niet alleen een fysieke barrière tussen het bloed en het onderliggende weefsel, maar ze hebben ook een regulerende functie voor de gezonde balans van de gladde spiercellen en fibroblasten in de aorta en hartkleppen. Het belang van deze regulerende functie wordt duidelijk wanneer endotheelcellen niet goed functioneren. Als de endotheelcellen niet goed functioneren leidt dit in veel gevallen tot structurele veranderingen in de vaatwand en hartkleppen. De functie van het endotheel in relatie tot de ontwikkeling van aortaverwijding en hartklepverkalking is nog niet goed bestudeerd. Dit komt mede omdat het isoleren van endotheelcellen lastig is, maar ook omdat het moeilijk is om deze ziekten te bestuderen in de vroege beginfase van de verwijding en verkalking. Immers kan je niet zomaar een stukje uit een prima functionerende hartklep halen om te bestuderen. Daarnaast ondergaat de laag spiercellen een overduidelijke veranderingen in aortaverwijding, waarbij ze overgaan van een rustig (contractiele) staat naar een actieve (synthetische) staat. Hierdoor is veel aandacht besteed aan het bestuderen van deze veranderingen in de gladde spiercellen. Wel zijn BAV en

endotheelcellen los van elkaar uitvoerig bestudeerd. **Hoofdstuk 2** beschrijft, op basis van recent onderzoek naar BAV, aorta verwijding en endotheelcellen, hoe endotheelcellen een effect kunnen hebben op BAV en de geassocieerde aorta verwijding en klepverkalking.

**Doel**

Het doel van het onderzoek beschreven in dit proefschrift is om het ziekteproces van aortaklepverkalking en aortaverwijding bij BAV-patiënten te bestuderen met een speciale aandacht voor de rol van endotheelcellen in deze processen.

**De rol van endotheelcellen in BAV**

Bij een normale hartklep wordt het bloed vanuit het hart door het midden van de klepslippen naar buiten gepompt. Het bloed volgt een vloeiende lijn om efficiënt door het lichaam te worden verspreid. Een BAV heeft een afwijkende vorm, waardoor het bloed niet in een vloeiende lijn, maar met wat turbulentie door de aorta heen vloeit. Hierdoor wordt één zijde van de aortawand blootgesteld aan een verhoogde bloedstroomsnelheid ("jet kant") terwijl de tegenoverliggende zijde te maken heeft met een onregelmatige (oscillerende) stroming ("niet-jet kant"). Endotheelcellen kunnen de stroming van het bloed voelen, en reageren wanneer de stroming verandert. Hierdoor worden endotheelcellen geactiveerd en geven signalen door aan de gladde spiercellen. Zo kunnen de bloedvaten reageren op de veranderende bloedstroom. Wanneer de bloedstroming te turbulent of oscillerend is, kunnen de geactiveerde endotheelcellen echter ontstekingen en afbraak in het gladde spierweefsel veroorzaken.

Het is nog niet bekend of de veranderde bloedstroom in BAV activatie van endotheelcellen in de aortawand veroorzaakt. Daarom hebben wij in **hoofdstuk 3** onderzocht of deze stromingsverschillen bij BAV-patiënten de activatie van het endotheel beïnvloedt door de weefselstructuur op microscopisch niveau te bekijken aan twee kanten van de aorta: de jet kant en de niet-jet kant. Hoewel er geen waarneembare verschillen zijn in de hoeveelheid van elastisch bindweefsel (elastine) tussen de jet en niet-jet kant, is er wel een significant grotere hoeveelheid van het eiwit von Willebrand Factor aan de jet kant van de aorta van BAV-patiënten vergeleken met de niet-jet kant. De aanwezigheid van Von Willebrandfactor is een aanwijzing dat endotheelcellen meer geactiveerd zijn, maar het is wel een indirecte relatie. Daarom hebben we ook gekeken naar directe kenmerken van activatie in de aanwezige endotheelcellen zelf. De endotheelcellen vertonen een trend naar een hogere expressie van activatie markers van endotheel-naar-mesenchymale overgang, celdeling en ontsteking aan de

niet-jet kant vergeleken met de jet kant. Dit wijst op een verhoogde endotheel activatie aan de niet-jet kant.

Omdat het lastig is om endotheelcellen van de aorta uit patiënten te isoleren hebben wij in **hoofdstuk 4** endotheel voorlopercellen uit het bloed van patiënten geïsoleerd. Deze cellen hebben in kweeksituaties dezelfde eigenschappen als endotheelcellen die de vaatwand bekleden. Met deze cellen hebben we de eigenschappen van de endotheelcellen van BAV patiënten bestudeerd. We ontdekten dat het niet mogelijk is om deze cellen te kweken van BAV patiënten die een verwijding hebben van de aorta. Er zitten geen verschillen in de snelheid van celdeling, celgrootte en de aanwezigheid van markers voor endotheel-naar-mesenchymale overgang (EndoMT) tussen de cellen geïsoleerd van mensen met een TAV en van patiënten met een BAV zonder aortaverwijding. De bewegelijkheid (migratie) van de BAV patiënt cellen is wel hoger dan de cellen van mensen met een TAV. Daarnaast is de verkalking van de endotheel voorlopercellen verminderd in BAV in vergelijking met TAV endotheel voorlopercellen.

In **hoofdstuk 5** beschrijven we het onderzoek waarin we de rol van ontsteking in EndoMT en verkalking van de vaatwand bestuderen. Dit onderzoek laat zien dat de pro-inflammatoire signaalmoleculen (cytokines) tumornecrosefactor (TNF)-$\alpha$ en interleukine-1$\beta$ EndoMT veroorzaakt in aorta endotheelcellen. Hierdoor zijn de cellen gevoelig geworden voor verkalking door de groeifactor bone morphogenetic protein (BMP)-9.

### Een kweekmodel van muis-hartkleppen en het eiwit Four-and-a-Half-LIM domain 2

Om hartklepverkalking te kunnen begrijpen, zijn naast goede celmodellen, ook weefselkweek en diermodellen noodzakelijk. In **hoofdstuk 6** wordt het onderzoek beschreven waarin we twee verschillende verkalkingsmethoden met elkaar hebben vergeleken met behulp van cel- en weefselkweek modellen. Er zijn namelijk meerdere manieren waarop verkalking kan optreden. Endochondrale verkalking is een manier van verkalken zoals ook bij het vormen van bot gebeurt, waarbij er eerst kraakbeen ontstaat wat daarna vervangen wordt door bot. Dystrofe verkalking is een vorm van verkalking waarbij ontsteking en celdood een belangrijke rol speelt. Om de complexe klepstructuur te behouden hebben we een miniatuur weefselkweeksysteem (MTCS) gebruikt waarin we hele muisharten kunnen kweken. Aortakleppen en aortaklepcellen werden blootgesteld aan twee verschillende verkalkende kweekvloeistoffen (OSM en PI). We hebben bestudeerd of met beide methoden verkalking van de hartkleppen optreedt en, zo ja, op welke manier dan. In de aortaklepcelkweek treedt verkalking op bij blootstelling aan OSM én PI, maar in de aortakleppen tijdens

weefselkweek treedt alleen dystrofe verkalking op bij blootstelling aan PI. De intacte weefselstructuur van de hartkleppen, aorta en het hart stelde ons in staat om daarnaast endochondrale differentiatie te detecteren in zowel PI- als OSM-omstandigheden in de wand van de aorta. Beide vormen van verkalking lijken sterk op verkalking die wordt gevonden in menselijke hartklepverkalking, qua locatie van verkalking en type verkalking.

Omdat het ex vivo hartkweeksysteem een goede weergave geeft van menselijke hartklepverkalking gebruikten we dit systeem om verkalking te bestuderen in een diermodel. Dit is beschreven in **hoofdstuk 7**. De harten van de muizen die we hebben onderzocht, missen het eiwit Four-and-a-Half-LIM domain 2 (FHL2). FHL2 is een eiwit dat onder andere een grote rol speelt in botvorming. Nadat we in coupes van verkalkte menselijke aortakleppen FHL2 hebben aangetoond, onthulde de weefselkweek significante verschillen in de locatie van verkalking in de aortakleppen van FHL2 deficiënte muizen vergeleken met kleppen van controle muizen. De verkalkte gebieden in de FHL2 deficiënte aortakleppen bevinden zich voornamelijk aan de aortazijde van de klep, terwijl in de controle harten de verkalking zich met name aan de kant van de hartkamer bevindt.

FHL2 is niet alleen betrokken bij botvorming maar ook bij de overgang van een rustige, contractiele naar geactiveerde staat van gladde spiercellen. Daarom beschrijven we in **hoofdstuk 8** de studie waarin is gekeken naar de aanwezigheid van FHL2 in aortaweefsel van verwijde en niet-verwijde aorta van patiënten met een TAV of BAV. Wanneer we FHL2 zichtbaar maken met kleuringen laat FHL2 in het midden van de aortawand een ander patroon zien (voornamelijk aanwezig buiten de cellen, in het extracellulaire ruimte) dan in de binnenste en buitenste lagen van de aorta (waar het zich met name in de cel bevindt). Ook is FHL2 in grote hoeveelheden aanwezig in gebieden zonder kernen en $\alpha$-gladde spiercelactine. In de celkweek hebben we ontdekt dat FHL2 deficiënte gladde spiercellen hun contractiele eigenschappen sneller verliezen dan gladde spiercellen met FHL2. Cellen scheiden kleine blaasjes uit, en in dit onderzoek hebben we ook ontdekt dat gladde spiercellen FHL2 uitscheiden in deze blaasjes. Deze blaasje komen ook voor in het bloed, en hoewel we hebben aangetoond dat FHL2 aanwezig is in deze blaasjes in bloed, is er geen relatie gevonden tussen de hoeveelheid FHL2 in de blaasjes in het bloed en een BAV en/of een verwijde aorta.

Tot slot beschrijven we in **hoofdstuk 9** de studie naar hoe FHL2 de ontstekingsreactie van gladde spiercellen in de vaatwand beïnvloedt. We hebben ontdekt dat zowel de cytokinen in het bloed als de hoeveelheid ontstekingscellen verhoogd zijn in FHL2 deficiënte vaatwanden vergeleken met controle vaatwanden wanneer de bloedstroom wordt afgesloten met een hechting. Bovendien scheiden FHL2 deficiënte gladde spiercellen meer cytokinen uit en is de

activering van de inflammatoire (NFκB-)signalering versterkt. De inflammatoire toestand in FHL2 deficiënte gladde spiercellen kan worden genormaliseerd door het blokkeren van de NFκB-signalering.

Met het onderzoek beschreven in dit proefschrift hebben we onder andere aangetoond dat endotheelcellen van BAV patiënten anders reageren dan cellen van mensen met een TAV. Ook is de endotheelcel activatie in de vaatwand van BAV patiënten anders en afhankelijk van de bloedstroom. We hebben twee goede weefselkweekmethoden gevonden waarmee verkalking van de hartkleppen kan worden bestudeerd en hebben deze gebruikt om de rol van het eiwit FHL2 te bestuderen in dit proces. Het blijkt dat FHL2 een rol speelt in de signalering waardoor verkalking op een andere locatie kan optreden. Daarnaast is FHL2 aanwezig in de verwijde aortavaatwand en beïnvloedt het de contractiele eigenschappen en ontstekingsreactie van gladde spiercellen.

## Curriculum Vitae

Vera van de Pol is geboren in het Culemborg in 1991. Na het afronden van het vwo aan het Koningin Wilhelmina College in 2003, startte ze met de bachelor Biomedische wetenschappen in Leiden. Ze rondde deze af met een stage gericht op atherosclerose. Hierbij werden muismodellen gebruikt. Vera vervolgde haar opleiding met de master Biomedical sciences in 2012, ook aan de Universiteit Leiden, en rondde deze succesvol af in 2014 met twee stages, allebei gericht op cardiovasculaire ziekten. Bij de eerste stage werd het hartslagritme van mensen onderzocht en bij de tweede stage leerde ze uitgebreid celkweken met stamcellen en hartspiercellen. Het promotie onderzoek bij Marie-José Goumans en Marco de Ruiter, waarbij met celkweekmodellen, muismodellen en patiënt-onderzoek de aangeboren hartafwijking bicuspide aortakleppen verder bestudeerd werd, sloot dus niet alleen inhoudelijk maar ook qua onderzoekstechnieken goed aan bij de tot dan toe opgedane ervaring van Vera. De mogelijkheid om tijdens het promotieonderzoek de ziekte te bestuderen op cel en weefsel niveau gecombineerd met het patiëntcontact zorgden voor een compleet perspectief op de hartafwijking.

In de afrondende fase van het proefschrift is Vera bij het NWO gaan werken. Hier ondersteunt ze onderzoek en onderzoekers vanaf een afstandje, waar ze haar ervaringen binnen de universiteit waardevol kan inzetten.

## Dankwoord

Ik ben iedereen dankbaar die door de jaren heen direct of indirect heeft bijgedragen aan de totstandkoming van dit proefschrift. Collega's en patiënten maar ook zeker vrienden en familie hebben mij allemaal geholpen om tot dit punt te komen. Hoewel deze dankbaarheid te groot is om in woorden te vatten, ga ik het toch proberen.

Marie-José, door jouw begeleiding heb ik naast mijn onderzoeksvaardigheden ook mezelf kunnen ontwikkelen. Hoewel ik zelf niet met het BAV onderzoek verder ga, hoop ik dat het voor jou nog veel goeds gaat brengen.

Marco, voor besprekingen over de voortgang van het onderzoek kon ik altijd bij jou terecht. Dit is een belangrijke steun geweest, die ik erg waardeer.

Babu, I appreciate you and all your help, enthusiasm and fun! Aside from your scientific drive and optimism, I will remember your successful efforts in the social bonding of the STAR-group (by organizing drinks!).

During my PhD I was fortunate to be involved in the departments Molecular Cell Biology and Anatomy and Embryology. As a result, I had a huge group of kind and diverse colleagues who not only helped me with questions, but with whom I could also have a beer. Willem, Berend, Viola and all others, many thanks!

All colleagues of the STAR-group; Tiago, Karien, Calinda, Kirsten, Annemarie, Esther, Anke, Tessa, Gonzalo, Tom, Boudewijn and José thank you for giving input on my experiments and results, asking the critical questions and the fun. Karien, Calinda and Tiago, my roommates, I enjoyed chatting about the weekend and discussing scientific questions with you. It was 'gezellig'!

Kirsten, je steunde mij niet alleen mentaal bij de verschillende aspecten van het promotietraject maar hebt ook vele uren naast mij gezeten in de celkweek bij het isoleren en kweken van cellen. Hartelijk bedankt voor de gezelligheid in het lab én daarbuiten.

Ook bedank ik graag alle leden van de CarVer-group: Mary, Tim, Sjoerd, Adri, Margot, Bert, Conny, Monique en Rob. De donderdagochtenden waren vaak genieten!

Daarnaast heb ik mogen genieten van mooie samenwerkingen binnen het BAV-Consortium. Graag bedank ik alle collega's binnen dit consortium voor de inspirerende gesprekken. In het bijzonder wil ik graag Lidia Bons bedanken. Lidia, dankjewel dat je mij regelmatig en op een zeer gezellige manier hebt geholpen met het vinden van deelnemers voor het onderzoek. Ik kon altijd bij je terecht, ook met bijzondere verzoeken zoals een slaapplek voor een vroege vlucht vanuit Rotterdam.

Lieve Anneloes, mijn 'scientific soulmate', ik heb veel van jou geleerd. Dankjewel voor alle gezelligheid en de inspiratie dat het leven bovenal leuk moet zijn.

Joshua, we zijn ongeveer tegelijk begonnen en hebben het traject met verschillende onderzoeken en afdelingen samen doorlopen. Iedere woensdagochtend konden we sparren over de verschillende onderzoeken, bedankt voor je input.

Bij mijn nieuwe werk heb ik ook het geluk om omringd te zijn met veel fantastische collega's. Liesbet, Nina, Ruud en alle andere NRO-collega's: bedankt voor alle gezelligheid én interesse in mijn onderzoek tijdens deze afgelopen twee jaar.

Daarnaast is de steun en gezelligheid van mijn vrienden en familie onmisbaar geweest bij het doorzetten tijdens en de afronding van dit project. Rozet, Anne, Ruth, Marit, Carla, Loes, Mariëlle Peter en Mariëtte en alle anderen: enorm bedankt. Ik kijk ernaar uit om hier met jullie allen op te proosten!

Jenna and Julien, thank you for being with me in the empty labs and the long hours behind the computer. Your funny and interesting conversations and crazy stunts entertained and distracted me during tedious work.

Lieve Ramses, grote vriend, mijn thuiswerk collega. Dankjewel voor al je uren gezelschap tijdens het schrijven van dit boekje. En dankjewel voor het zorgen voor een geschikte opvolger, Benny, die mij hartelijk laat lachen, zelfs op de minder zonnige dagen.

Lieve Rosanne, dankjewel voor de gezelligheid en afleiding, begrip en motivatie. Al vanaf de middelbare school begrijpen we elkaar. Helaas kunnen we ons ook allebei inleven in de moeilijkheden die een promotietraject met zich mee kan brengen. Je bent een fijne vriendin en ik weet zeker dat we binnenkort ook op de afronding van jouw promotie kunnen proosten!

Lieve familie: mam en pap, Iris en Jeroen maar ook zeker Peggy, Ronald en Guy, vanaf het begin hebben jullie mij door dit proces zien gaan. Bedankt dat jullie altijd geïnteresseerd zijn geweest en met mij naar dit moment hebben toegeleefd. Het is gelukt!

Tot slot, Rob, mijn lieve man, zonder jou had ik dit niet kunnen doen. Bedankt voor de niet-aflatende steun, het luisterende oor, het advies, de afleiding in moeilijke tijden en het meevieren van de mooie momenten. Mijn rots en rust, dankjewel.

## List of publications


1. **van de Pol, V.**, Kruithof, B. P. T., Los, T., Lodder, K., Gourabi, B. M., DeRuiter, M. C., . . . Ajmone Marsan, N. (2021). New calcification model for intact murine aortic valves. J Mol Cell Cardiol, 156, 95-104. doi:10.1016/j.yjmcc.2021.03.003
2. **van de Pol, V.**, Vos, M., DeRuiter, M. C., Goumans, M. J., de Vries, C. J. M., & Kurakula, K. (2020). LIM-only protein FHL2 attenuates inflammation in vascular smooth muscle cells through inhibition of the NFκB pathway. Vascul Pharmacol, 125-126, 106634. doi:10.1016/j.vph.2019.106634
3. **van de Pol, V.**, Bons, L. R., Lodder, K., Kurakula, K. B., Sanchez-Duffhues, G., Siebelink, H. J., ... Goumans, M. J. (2019). Endothelial Colony Forming Cells as an Autologous Model to Study Endothelial Dysfunction in Patients with a Bicuspid Aortic Valve. Int J Mol Sci, 20(13). doi:10.3390/ijms20133251
4. **van de Pol, V.**, Kurakula, K., DeRuiter, M. C., & Goumans, M. J. (2017). Thoracic Aortic Aneurysm Development in Patients with Bicuspid Aortic Valve: What Is the Role of Endothelial Cells? Front Physiol, 8, 938. doi:10.3389/fphys.2017.00938
5. Sánchez-Duffhues, G., García de Vinuesa, A., **van de Pol, V.,** Geerts, M. E., de Vries, M. R., Janson, S. G., . . . Ten Dijke, P. (2019). Inflammation induces endothelial-to-mesenchymal transition and promotes vascular calcification through downregulation of BMPR2. J Pathol, 247(3), 333-346. doi:10.1002/path.5193
6. Akintola, A. A., **van de Pol, V.**, Bimmel, D., Maan, A. C., & van Heemst, D. (2016). Comparative Analysis of the Equivital EQ02 Lifemonitor with Holter Ambulatory ECG Device for Continuous Measurement of ECG, Heart Rate, and Heart Rate Variability: A Validation Study for Precision and Accuracy. Front Physiol, 7, 391. doi:10.3389/fphys.2016.00391
7. Birket, M. J., Ribeiro, M. C., Kosmidis, G., Ward, D., Leitoguinho, A. R., **van de Pol, V.**, . . . Mummery, C. L. (2015). Contractile Defect Caused by Mutation in MYBPC3 Revealed under Conditions Optimized for Human PSC-Cardiomyocyte Function. Cell Rep, 13(4), 733-745. doi:10.1016/j.celrep.2015.09.025
8. Kooijman, S., Boon, M. R., Parlevliet, E. T., Geerling, J. J., **van de Pol, V.**, Romijn, J. A., . . . Rensen, P. C. (2014). Inhibition of the central melanocortin system decreases brown adipose tissue activity. J Lipid Res, 55(10), 2022-2032. doi:10.1194/jlr.M045989